STRATIGRAPHY AND SEDIMENTOLOGY OF THE AREA AROUND BIDA, NIGER STATE

BY

OLUFEMI ROBINSON OLUGBEMIRO
B.Sc. Geology (A.B.U, 1995)

A THESIS SUBMITTED IN PARTIAL FULFILLMENT OF THE REQUIREMENTS
FOR THE AWARD OF THE MASTER OF SCIENCE IN GEOLOGY

DEPARTMENT OF GEOLOGY
FACULTY OF SCIENCE
AHMADU BELLO UNIVERSITY, ZARIA

JANUARY, 1989

DECLARATION

I declare that this thesis is based on the result of research carried out by me; that it is my own composition and that it has not been previously presented for a higher degree at any University or Institution.

Information derived from published and unpublished work has been duly acknowledged.

Femi-Robinson 20/12/89

OLUGBEMIRO, Robinson OLufemi — Date

CERTIFICATION

This Thesis entitled *"Stratigraphy and Sedimentology of the Area Around Bida, Niger State"* by Olufemi Robinson Olugbemiro meets the regulations governing the award of the degree of Master of Science in Geology (Sedimentology) of Ahmadu Bello University, and is approved for its contribution to knowledge and literary presentation.

Chairman, Supervisory Committee	Date
Member, Supervisory Committee	Date
Head of Department	Date
Dean, Postgraduate School	Date

DEDICATION

This project is dedicated to

Nelson Mandela

and the oppressed people of South Africa

ACKNOWLEDGEMENTS

I wish to acknowledge the support and assistance of my Supervisors; Drs C.S Nwajide (Geological Survey of Nigeria, Kaduna); S.I. Abaa and E.C. Ike. Much thanks and gratitude goes to Dr Nwajide who initiated the project and whose criticisms and suggestions, both on the field and in the laboratory are extremely invaluable. My immense appreciation to Dr S.I. Abaa for critically going through the thesis and offering useful and valuable comments and Dr E.C. Ike whose guidance and suggestions, saw the completion of the thesis.

Other members of staff's contribution are acknowledged especially Messrs M. Woakes, E.M. Sakoma, N. Obaje and Mrs Adetunji for not only making necessary literature available when needed but also for their useful suggestions and assistance. My colleagues in the M.Sc. class: Messrs I.I. Funtua, I. Adamu, J. el-Naffaty, A. Chup, R. Danladi, P. Agbata, and I. Adoke, have given me all the encouragements. To them I am most grateful.

Moral assistance from friends especially Abiola Banwo is deeply appreciated. I thank Mallam Baba Bobai for processing the photographs, Emmanuel Duro for the cartography work and James Bale of NAPRI for typing the thesis.

The moral and financial assistance from my parents are deeply appreciated. Everybody's assistance would forever remain memorable.

ABSTRACT

The Bida Basin in the Middle Niger is a shallow trough filled with Campanian – Maastrichian marine to fluviatile sediments. Four lithostratigraphic units which belong to the Nupe Group have been identifed in the area of study: Aranaceous, Argillaceous Ironstones and Laterits. These have been grouped under the Bida Formation, Sakpe Ironstone Formation, Enagi Formation and Batati Ironstone Formation. The laterite unit which is Quartenary to Recent in age, is derived from the Ironstone facies.

The Ironstone Formations are oolitic and pisolitic and occur at summits of stratigraphic sections while the laterite unit is a product of the ironstone Formation. By field observations a cyclic fining upward and local coarsening upward mode of lithologic succession are deduced for the Argillaceous and Arenaceous unit (Bida Formation and Enagi Formation)-

Investigations of the textural properties of sediments in the area of study show that sandstones in the Bida Basin are poorly sorted, positively skewed and leptokurtic. The use of bivariate plots for environmental discrimination indicates an environment of deposition that range from fluvial to transitional for pebbles, while for sandstones a more distinct fluvial environment is discernible in the area. Analysis of assemblages of heavy mineral indicates an Igneous-Metamorphic provenance for sands within the studied area, in addition to classification of sandstones, by framework, matrix and cement composition which indicate a moderate degree of maturity.

Sedimentary structures display characteristic bias towards a relatively shallow regime of deposition. Assemblages of sedimentary trace fossil range between Thaiassinoides, Ophiomorpha, Giossifungites, Cruziana to Zoophycas indicating a rather shallow environment of deposition, while types and occurrence of sedimentary structures suggests a fluvial environments for the non-ironstone facies units. The ironstone units are distinctive with typical trough cross-bedding, broken shells, and oolitic—pisolitic texture supporting a high energy possibly tidal environment of deposition. Paleocurrent analysis indicates a northerly direction of paleoflow with a mean azimuth value of 359. from cross bedding azimuth measurement.

Finally, a general inference can be drawn for a subsidence origin for the Bida Basin, based on sediment composition, nan—occurrence of rift or volcanic related features within the basin and similarity of sediments with that of the Iullemeden Basin. Although origin of the Bida Basin seems related to tectonic activities in adjacent basement areas: South—western Nigeria, and the Younger arenite Province, but with clastic contribution mainly from the Igneous and Metamorphic basement complex of South—Western Nigeria. An Al1uvial—Fluvial model of deposition is inferred for the Aranaceoous and Argillaceous units while a shallow marine (lagoon, tidal inlet, or barrier island) environment is inferred for the Ironstone facies probably related to the Tethys transgression into Nigeria during the Tertiary,

TABLE OF CONTENTS

		Page
Title page		i
Declaration		ii
Certification		iii
Dedication		iv
Acknowledgements		v
Abstract		vi
Table of contents		viii
List of Tables		xi
List of Figures		xii
List of Plates		xiv
List of Appendices		xvi
Abbreviations, Definitions, Glossaries and Symbols		xvii
CHAPTER 1	**INTRODUCTION**	
1.1	Location, Extent and Accessibility	1
1.2	Previous Work	1
1.3	Present Work	3
1.4	Physiography	4
1.4.1	Relief and Drainage	4
1.4.2	Climate	6
1.4.3	Vegetation and Soils	7
1.5	People and Occupations	8
CHAPTER 2	**GEOLOGY AND STRATIGRAPHY**	
2.1	Synopsis of Geology and Stratigraphy	10
2.2	Local Stratigraphical Succession	15
2.2.1	Stratigraphic profile A	16
2.2.2	Stratigraphic profile B	19
2.2.3	Stratigraphic profile C	19
2.2.4	Stratigraphic profile D	22
2.2.5	Stratigraphic profile E	27
2.2.6	Stratigraphic profile F	30
2.2.7	Stratigraphic profile G	3
2.3	Regional Facies Relationship	32
2.3.1	Laterite Lithotype	34
2.3.2	Ironstone Lithotype	38
2.3.3	Argillaceous Lithotype	40

2.3.4 Arenaceous Lithotype 43
2.3.5 Interpretation 44

CHAPTER 3 SEDIMENTARY STRUCTURES AND PALEOCURRENTS

3.1 Types of Sedimentary Structures 46
3.1.1 Cross-Bedding 46
3.1.2 Ichnofossils 53
3.1.3 Mudcracks and Load casts 55
3.1.4 Graded Bedding 57
3.1.5 Calcrete 58
3.2 Hydrodynamics 59
3.3 Paleocurrent Indicators and Reconstrution 61

CHAPTER 4 MINERALOGY AND GRAIN SIZE ANALYSIS

4.1 Introduction 67
4.1.1 Framework Components 67
4.1.1.1 Quartz 67
4.1.1.2 Feldspar 68
4.1.1.3 Rock Fragments 72
4.1.2 Matrix 73
4.1.3 Cement 73
4.2 Fabric 77
4.2.1 Grain sizes 77
4.2.2 Grain Relation 77
4.2.3 Grain Orientation 80
4.2.4 Grain Shape and Roundness 80
4.3 Heavy Mineral Analysis 82
4.3.1 Results 83
4.3.2 Environmental Implications 88
4.4 Pebble Morphometry 91
4.4.1 Introduction 91
4.4.2 Method of Study 92
4.4.3 Results and Environmental Implication 108
4.5 Sieve Analysis 113
4.5.1 Method of Analysis 113
4.5.2 Results and Environmental Implication 117
4.5.2.1 Mean Grain size 117
4.5.2.2 Standard Deviation or Sorting 126
4.5.2.3 Skewness 127

4.5.2.4 Kurtosis 128
4.6 Bivariate Plots 129
4.7 Classification and Maturity 129

CHAPTER 5 BASIN SYNTHESIS

5.1 Depositional Environments 135
5.1.1 Stratigraphy 135
5.1.2 Mineralogy and Size Analysis 137
5.1.3 Sedimentary Structures and Paleocurrents 141
5.2 Provenance 146

CHAPTER 6 DISCUSSIONS AND CONCLUSIONS 149

REFERENCES 153

APPENDICES 161

LIST OF TABLES

Table 2.1 Generalized Sequence of the Geologic History of the Middle Niger Area 11

3.1 Dip, Strike and Azimuth measurements of Cross-beddings from locations 1, 2, 3, 4, 5, 7, 8 and 9 49

3.2 Statistical Analysis of Azimuth readings to obtain resultant vectors for locations 1, 2, 3, 4, 7, 8 and 9 63

4.1 Weight Percentages of Light and Heavy Minerals in the facies studied 84

4.2 Detrital mineral suites characteristic of source rock types 89

4.3 Calculation of pebble parameters based on short, Intermediate and Long axes and estimation of roundness 93

4.4 Pebble Morphometry results used in Enviro-mental Diagnosis 109

4.5 Size Parameters and their formulae 115

4.6 Size Parameters (by moment and graphic measures) of sediments derived from Sieving and their Interpretations 118

4.7 Classification of sedimantary rocks in study area based on micro and macroscopic observations 133

LIST OF FIGURES

Figure 1 Location Map of Study Area 2

2 Generalized Stratigraphical Correlation of the Campanian-Maestrichian strata of the Middle Niger Valley 14

3 Geological Map of study Area (Behind in the folder)

4 Stratigraphic profile A (In Location 1) 17

5 Stratigraphic profile B (In Location 2) 20

6 Stratigraphic profile C (In Location 3) 21

7 Stratigraphic profile D (In Location 4) 23

8 Stratigraphic profile E (In Location 7) 28

9 Stratigraphic profile F (In Location 8) 31

10 Stratigraphic profile G (In Location 9) 33

12 Paleocurrent Map for the study area 52

11 Relationship of bed Forms to stream power and grain size (Simons *et al.*, 1965 and Allen 1968a) 51

13 Estimation of pebble roundness (After Shepard and Young, 1961) 81

Figure 14 Bivariate plots used in pebble Morphometry after (Dobkins and Folk, 1970; and Sames, 1966)
I) Pebbles from unit $1FR_3$ 101
II) Pebbles from unit $1FR_4$ 102
III) Pebbles from unit $3FR_2$ 103
IV) Pebbles from unit $4FR_1$ 104
V) Pebbles from unit $4FR_3$ 105
VI) Pebbles from unit $4FR_4$ 106
VII) Pebbles from unit $4FR_4$ 107

15 Bivariate plots used in Environmental Diagnosis after (Friedman, 1979)
I) Scatter plot, simple skewness measure versus Sorting Measure 120
II) Plot of skewness and standard deviation for Nearshore Dune (NDS) and River sands (RS) 121
III) Plot of simple skewness measure and simple Sorting measure, for NSD and RS 122
IV) Plot of 1st percentile and standard deviation for Inland Dune (IDS) and River Sands (RS) 123
V) Plot of mean and standard deviation for Inland Dune (IDS) and River Sands (RS) 124
VI) Plot of 1st percentile and mean, for Inland Dunes (IDS) and River Sands (RS) 125

16 Classification of Sandstone 130

17 Paleographical map of Nigeria during the depositional phase of the Lower Ironstone 152

LIST OF PLATES

Plate 1 Flat topped ("mesa" shaped) conical lateritic residual hill 10 km Northwest of Bida 5

2 Fine sand overlying a clay-shale unit both of the Bida Formation with interstrata bioturbation 18

3 Cross-bedded, medium grained sandstone unit of the Bida Formation. 25

4 Trough cross-bedded ironstone unit of the Batati Formation 26

5 Thinly laminated Ferruginous sandstone unit of the Enagi Formation 29

6 Intrastratal facies boundary in the Bida Formation. 35

7 Primary laterite capping a residual hill 37

8 Oolites occurring in the Ironstone unit 39

9 Laminated Ironstone exhibiting sharp basal contact with medium grained ferruginous sandstone 41

10 Planar cross-bedded sandstone unit 47

11 Load casts depicted by a coarse sandstone unit overlying a fine sandstone 56

12 Composite quartz crystals (thin section) in a basal sandstone unit 69

13 Quartz crystal (in thin section) with zircon, and biotite inclusions 70

14 Partially decomposed feldspar (in thin section) displaying Albite twinning 71

LIST OF PLATES

Plate 15 Kaolinite (in thin section) occurring as the dominantly, cloudy matrix in a siltstone unit 74

16 Goethite (in thin section) occurring as cement mineral in a basal sandstone unit 76

17 Poorly sorted basal sandstone in thin section 78

18 Floating grain fabric of ironstone, with equi-granular well sorted quartz crystals (thin setion) 79

19 Hematite (as a heavy mineral) occurring as sub-angular-subrounded grains (Mounted on slide) constituent of Oolites 85

20 Zircon (as a heavy mineral), showing a high degree of roundness with etched or pitted surface (Mounted on slide) 86

21 Tourmaline (as a heavy mineral) occurring as prismatic, subhedral grains (mounted on slide) 87

LIST OF APPENDICES

Appendix 1 Sieve analysis results tabulated into columns for the 33 samples analysed

Appendix 2 Cumulative frequency graphs on a probability graph scale for the 33 samples analysed

Appendix 3 Smoothed frequency curves on an arithmetic graph scale.

ABBREVIATIONS, DEFINITIONS AND SYMBOLS

°C	Degree Centigrade
Cm	Centimeter
Cm/Sec	Centimeter per second
Cos	Cosine
ENE	East-North-East
ESE	East-South-East
et al.,	and others
Fig	Figure
gm	Gram
Km	Kilometer
Km^2	Squared kilometer
m	meter
mm	millimeter
M^3/sec	Cubed meter per second
N	North
NNE	North-North-East
NNW	North-North-West
Sin	Sine
SSE	South-South-East
SSW	South-South-West
$\tan^{-1}$	Arc tan
WSW	West-South-West
$\bar{X}$	Mean
%	Percentage
$\longrightarrow$	Transition to
$\rightleftharpoons$	Reversible Transition
$\sum$	Summation
<	Less than
>	Greater than

CHAPTER ONE

INTRODUCTION

1.1 Location, Extent and Accessibility

The project area is located in Niger State of Nigeria and covers an area of 3,731 km² (Fig 1). The area is bounded by longitudes 5° 46′ 57" and 6° 15′ E and latitudes 8° 55′ 27" and 9° 28′ 58" N covering portions of 1:100,000 Sheets 183, 184, 204, and 205. The area is traversed by River Kaduna (and its tributaries) and by the tributaries of River Niger (River Gbako, River Chanchaga). Accessibility within the area of study is good, by various modes of transport. Bida, which is the major town in the area of study is linked westward (to Batati), eastwards (to Agaie) and northwards (to Lemu) by Trunk 'A' roads. River navigation is also a mode of transportation along River Kaduna by the use of canoes. Apart from roads (Trunk 'A') and rivers, numerous footpaths exist and allow accessibility into remote corners of the study area.

1.2 Previous Work

Relatively fewer geological studies have been carried out within the Bida Basin compared to other sedimentary basins of Nigeria. Studies in this area include accounts of the geology of the area by Falconer (1911) and Russ (1957). Du Preez (1949) studied the occurrence of oolites and pisolites in Nigerian laterites, while Pullan (1967) gave a morphological classification of lateritic ironstones and ferruginised rocks in Northern Nigeria, including present area of study.

More recently Adeleye (1971) and Adeleye and Dessauvagie (1972) studied the stratigraphy and sedimentation in the

KASHIM IBRAHIM LIBRARY

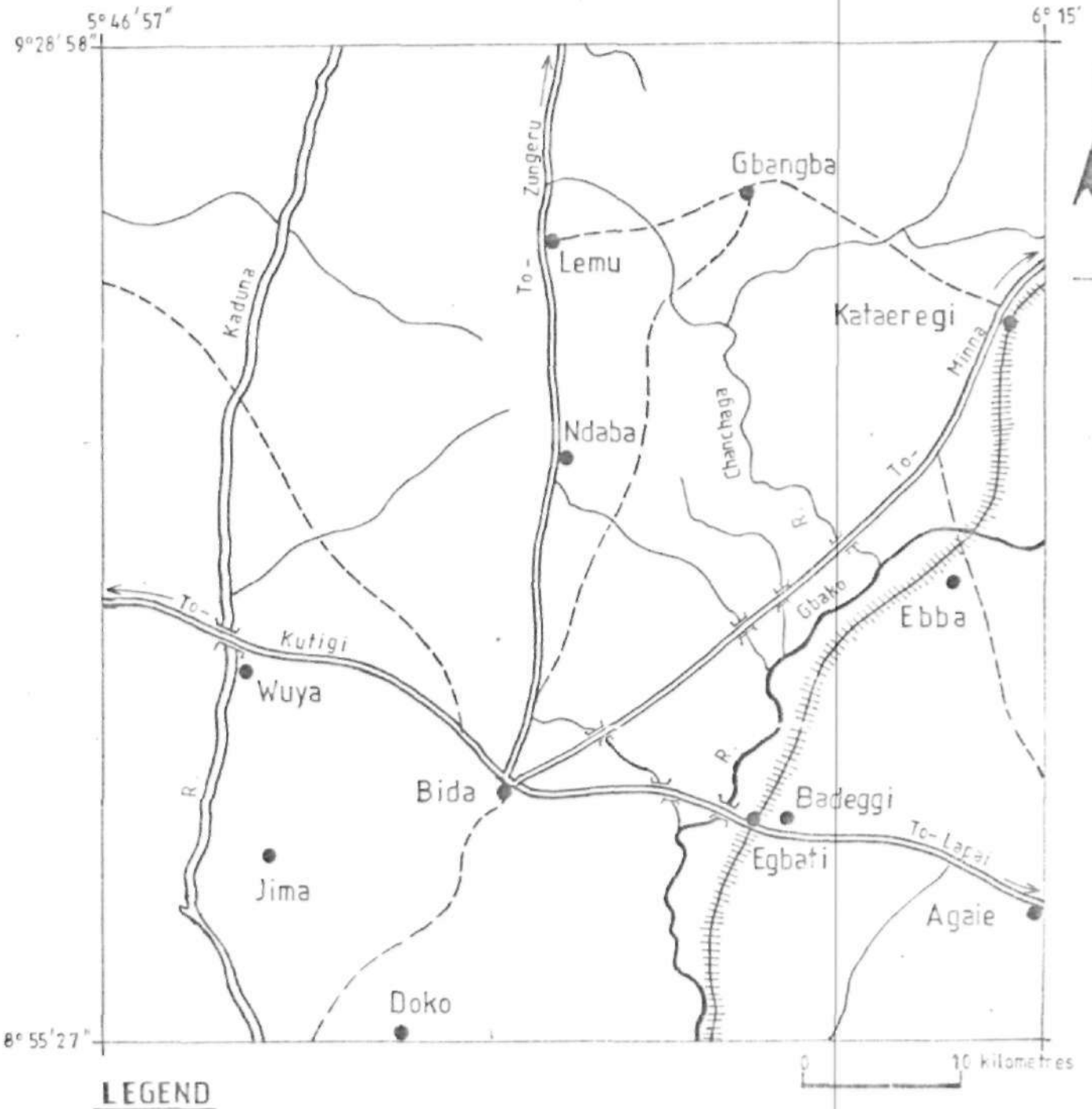


Fig. 1. Location Map of Study Area

Middle Niger (Bida) Basin. Ojo and Ajakaiye (1974) used a gravity survey of the area to establish the sediment thickness and to suggest that the basin originated by subsidence. Several hydrogeological studies have been carried out in the basin: Shekwolo (1983) evaluated the groundwater potentials of the River Gbako catchment area; Kehinde (1988) investigated the groundwater potential in Niger State. Much earlier, hydrogeological work within Bida was carried out by the Geological Survey of Nigeria (Jones, 1953).

1.3 Present Work

The aim of the present study is to evaluate the stratigraphy and determine the conditions of sedimantation of the sedimentary fill of the Bida Basin. Like other sedimentary basins in Nigeria, various sources of basin fill have been postulated using as a basis various parameters normally applied in environmental reconstruction. In this project, the mode of succession of basin fill, mineralogy and size analysis of sediments and sedimentary structures have been studied to evaluate the stratigraphy and conditions of sedimentation in the Bida Basin.

A systematic mapping of the area was carried out to measure the regional disposition of rock types and their relationships. Sections were also logged to determine facies succession mode. Samples were collected (pebbles and sedimentary rocks) for granulometric, heavy minerals and petrographic analysis. For paleocurrent analysis, dip, strike and azimuth measurements of cross beddings were taken.

The field work lasted about 2 months while the subsequent laboratory studies took 3 months.

1.4 Physiography

1.4.1 Relief and Drainage

The dominant topographical features of the study area relate to the River Niger and its major tributaries: River Kaduna, River Chanchaga and River Gbako (Fig 1). Away from the rivers are the flood plains most of which consist of gently undulating alluvium. The hills occuring here are mostly conically shaped or flat topped ("mesa" shaped) with complete laterite or lateritic ironstones, rising to 40-45 m above the surrounding country. An example of such is the Kochikota hill (Plate 1), about 10 km northwest of Bida. Thin soils characterize the lateritized areas, but in the non-lateritic plains, the soils are reddish brown and have a deep profile, which according to Nwajide (Personal Communication) are actually lateritic soils too.

Practically all hills are fringed by prominent scarps. Many of these "mesas" have been stripped of their original ironstone cap to varying degrees, and have accordingly been transformed into irregular or rounded hills.

The drainage pattern is generally dendritic (Fig 1), this is a reflection of the uniformity of the geology of the area. The major rivers draining the area are River Kaduna and River Gbako, and their distributaries, with the main watershed running parallel to these major rivers. The area is traversed more or less diagonally by River Gbako, while to the west, River Kaduna flows almost parallel. The Gbako river flows for about 50 km on the Bida sandstone before joining the River Niger in the south. Its direction of flow, like other major rivers around Bida is north-south (N-S). According to Shekwolo (1983), River Gbako has an average discharge of 60 m^3/sec during the rainy season and 3 m^3/sec in dry season and the average rise of water in the



Plate 1: Flat topped ("mesa" shaped) conical laterite residual hill (10 km North-west of Bida.)

rainy season is about 4 m and in the dry season, the river guage reads about 1 m. Drainage density in the study area is low, which Nye (1954) postulates, probably reflects the widespread occurrence of deep regoliths, with infiltration capacities high enough to absorb a large proportion of precipitation. Such regoliths have been found to extend well into the savannahs of Nigeria and they possibly reduce any tendency for drainage densities to increase even as precipitation intensity and the length of dry season increase , and vegetation cover become reduced (Thomas 1966a). Although Fournier (1962, Fig 26, p. 115) predicted for this zone high denudation rates. But these do not appear to be the case on terrains of low relief (Thomas, 1974), like the study area is.

1.4.2 Climate

The climate of Nigeria is controlled by the interaction of two widely different air masses and the movement of the zone of convergence of these two air masses relative to the ground. The zone of convergence is referred to as the Inter Tropical Convergence Zone (I.T.C.Z). In the months of November to March the dry north-easterly air stream (Tropical Continental Air Mass), often laden with fine red dust from the Sahara (Harmattan dust), dominates and leads to low relative humidity, high daytime temperatures (about 38°C), northeast winds and virtually zero rainfall. At this time the I.T.C.Z is considered to be located to the south of the area under investigation. The subsequent northward movement of the I.T.C.Z increases the influence of the moisture laden south-westerly air mass (Equatorial Maritime) which becomes dominant in Niger State from April. As a result, day time temperatures are lower. There is relatively high humidity

due to winds from the southwest and the greater part of the annual rainfall occurs when the south-west wind is dominant.

Applying the parameter of a worldwide system, the climate of the area under study can be classified as "moist-dry Equatorial Tropical" with maximum temperature above 35.5°C (Shekwolo, 1983). The seasonal rainfall regime of this area give rise to a longer wet season of about 7 months, with an average rainfall of 250 mm and a shorter dry season of 5 months, with little or no rain. In general, the rainfall distribution can be said to be bimodal; that is possessing two rainfall peaks. The mean annual rainfall shows a general decrease westwards within the Bida Basin, with high variability of monthly total rainfall. The rainfall regime confirms the view that Bida Basin is a zone of transition between the forested south of Nigeria and the Sudan savannah (Udoh, 1978; p. 11), while the occurrence of extensive swamps during the rainy season is common.

1.4.3 Vegetation and Soils

The area under study lies in the geographic belt of Nigeria termed the Middle Belt. It falls in the Southern Guinea zone of transitional woodland of savannah vegetation. Marked differences which occur at close intervals both in floristic composition and the open character of the vegetation are often caused by variation in soil types, topography, groundwater situation and human interference (Udoh, 1968; p. 119). The large rivers (Kaduna, Gbako, and Chanchaga) support open savannah with occasional trees, but the valleys of the smaller and seasonal streams are covered with dense woodlands or gallery forests. The area is mostly under grass vegetation with tussocky grasses 1.6-3.5 m high and short-

boled broad leaved trees up to 16.6m in height.

Parent material as well as topography are the main factors influencing soils in this region. Fine to coarse grained sands are common along the river valleys, and in the Fadamas, the soils are usually hard when dry. Lateritic ironstones are common except on the alluvium of the river flood plains. Thus, generally, the soil types can be classified into fine to medium grained Nupe Sandstone soils, river alluvial soils and ironstone mineral soils. A vast expanse of the areas is covered by fine to medium grained Nupe Sandstone soils. They give rise to swampy grasslsands or forest vegetation in places. This soil type occurs at Baddeggi, along Gbako river course and Baddeggi Rice Research Station. The other kind of soil type found along "mesa landscapes" are termed raw mineral soils (Maxlock, 1979). They are made of ferrugionous capping and some very shallow lithosols over ironpan. In more advanced stages of the weathering of the ironpan, the lithosols become more common. Where finally the ironpan is about to be removed completely by erosion, outcrops of sandstones (Raw mineral soils), very shallow soils covered by transported rubbles (which may comprise of boulders of ironpan) or both predominate.

1.5 People and Occupation

The people of the Middle Niger (around Bida) region fall into 3 groups namely: the Riverine tribes such as the Gunga was, Lopawa and Nupes, the Upland tribes like the Kamberis, Gwaris and Yorubas and the Hausa-Fulani tribes, scattered over wide areas. In the areas of study the main occupation is farming (especially rice) along the Fadama beds

close to the river valleys, petty trading and migration labour. There is abundant farmland, especially the ferruginous tropical soils for other crops like guinea corn, maize, groundnut, cotton and tobacco. Fishing is also actively practised here along the rivers especially kaduna, Gbako and Chanchaga

CHAPTER TWO.

GEOLOGY AND STRATIGRAPHY

2.1. Synopsis of Geology and Stratigraphy

The Middle Niger (Bida) Basin is a gently downwarped trough by local subsidence (Ojo and Ajakaiye, 1974). The buried basement complex probably has a high relief (Jones, 1955), which is made of many different rock types, often of a medium to high grade metamorphism (Russ, 1957). The Precambrian to probably Paleozoic basement complex is overlain by sediments of the Nupe Group (Table 2.1.). It is clear that the basement complex on which these sediments were laid, occur deep in the earth's crust and considerable erosion took place before the Upper Cretaceous (Nupe Group) rocks were laid down (Adeleye, 1971; Adeleye and Dessavagie, 1972).

The basement complex is directly overlain by rounded to sub-rounded coarse conglomerates, clay-sand-pebble admixtures and cross stratified sandstones, locally with scattered pebbles, cobbles, and boulders. These basal sediments may be of alluvial fan origin (Adeleye, 1974a). They are conformably overlain by a lithology comprising mainly sandstones, and subsidiary claystones, fine conglomerates, and siltstones. Both these beds and underlying ones are probably about 300 m thick (Adeleye, 1974b)and are known by various names, Bida Sandstones around Bida and Lokoja Basal Sandstone around the Niger/Benue confluence. The sandstones are generally angular to subangular, well to poorly sorted and very fine to very coarse grained and pebbly. Arkoses and feldspartic sandstones are common in the basal areas, while quartzose sandstones dominate the upper parts.

Table 2.1 Generalized Sequence of the Geologic History of the Middle Niger Area (Russ, 1957)

Age	Succession	Rock Type
Recent and Tertiary	Superficial deposits	Laterite, alluvium, terrace and terrestrial gravels and sand
Upper Cretaceous	Nupe Group	Sandstones
	Older Granite Cycle	Quartz Veins dolerite intrusions pegmatitic, aplitic and granite dykes. Granites and related rocks
PreCambrian	Orogenic phase	Formation of schists folding, faulting and (?) intrusions of auriferous quartz veins
	Sedimentary cycle	Mudstones, siltstones, quartzites, etc. later converted to paraschists
	Earlier period of sedimentation, intrusion and metamorphism	Orthogneisses, orthoschists paragneises and schists quartzites quartz schists etc.

KASHIM [illegible]

The basal beds are succeeded by dominantly goethitic, oolitic and pisolitic ironstones of about 5 m maximum thickness. The ironstones form a prominent break of slope along the "mesa"-walls in the Bida area. They are called the Sakpe Ironstone Formation (Adeleye, 1971). Laminations and thin to thick flat bedding are the most common structures of these ironstones (Adeleye, 1973). The oolites commonly vary from 1-2 mm, they are well formed, and spherical to spheroidal. The pisolites are restricted to the Bida area where they occur in the middle area of the Lower Ironstones. The Lower Ironstones are overlain by predominantly argillaceous strata dominated by siltstone. Where the Lower Ironstones are absent, the argillaceous beds conformably overlie basal sandstone beds. The siltstones are commonly thinly laminated or massive. These argillaceous members are referred to as the Enagi Siltstone Formation (Adeleye, 1971). Another ironstone horizon, the Upper Ironstones succeeds the argillaceous strata. Around Bida, they are referred to as the Batati Ironstone Formation (Adeleye, 1971). The maximum thickness is about 15 m. They cap the "mesas" of the Middle Niger under a layer of lateritic bodies of variable thickness. The beds are dominantly oolitic and show irregular lithologic changes. Very subsidiary ferruginous clay-stones, sandstones and shelly beds occur locally. The beds are generally massive although thin to thick flat bedding and laminations are locally well developed (Adeleye, 1973). Occasionally the rocks show concretions in which fresh looking goethitic oolites and whitish kaolinitic clays and quartz silts are present.

Two principal sub-facies of oolitic ironstones are present:

(1) Coarse grained oolitic subfacies which is dominant around

the Niger/Benue confluence

(2) Fine grained oolitic subfacies, known as "Unweathered oolites" around Lokoja, Dekina Interbedded Oolites around Dekina (Jones, 1955) and the Kutigi Oolitic subfacies around Bida (Adeleye, 1971). The terms "coarse" and "fine" are relative and carry no definite grain size. According to Adeleye (1973), where the two subfacies occur together, the former overlies the latter with a shelly bed and/or erosional surface in between. Altogether, the marine to fluviatile strata that fill the Middle Niger Valley, have been dated as Campanian - Maastrichtian in age by plant and animal remains (Adeleye, 1974b; Jan. Du Chene, et al., 1978). This has led to a generalized stratigraphic correlation of the Campanian Maastrichtian strata of the Middle Niger Valley as shown in Fig. 2. The stratigraphic correlation extends from Sokoto and Illo in the Iullemeden Basin through Bida, Lokoja, and Dekina, in the Middle Niger Valley. The Bida Sandstones may be correlated with the crosse bedded coarse sandstones in the Illo and Lokoja areas. The pisolitic clay horizon at Illo may possibly be correlated with the Lower (Sakpe) Oolitic Ironstones around Bida which may continue into the interbedded ironstones at Lokoja. The pisolitic and oolitic (Middle Illo, and Sakpe Ironstone Formation) are regionally overlain by dominantly argillaceous beds (Fig.2.), with subsidiary fine-grained sandstones and lignite (Adeleye, 1973). This argillaceous bed represents the Enagi Siltstone, which may be a lateral equivalent of the Patti Formation at Lokoja but a facies change must be accepted if the

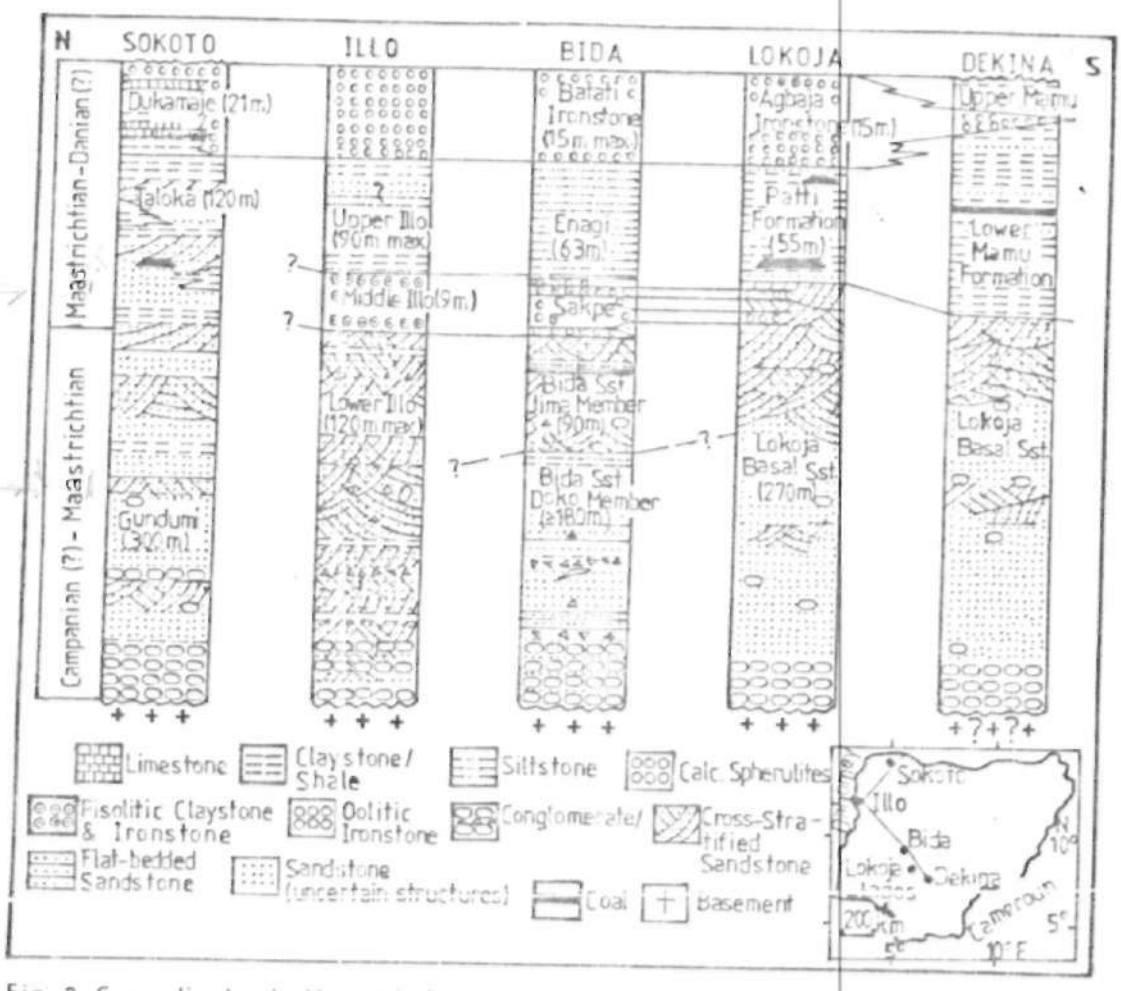


Fig. 2. Generalised stratigraphical correlation of the Campanian-Maastrichtian Strata of the Middle Niger Valley. (Adeleye, 1973)

siltstones are to be compared with the coarse clastics overlying the pisolitic clay at Illo. The Batati Ironstone Formation may be compared with the Agbaja Formation (Adeleye, 1973), though the Agbaja Formation was formerly grouped with the underlying, argillaceous Patti and Mamu Formations (Jones, 1958). In the north around Sokoto, the ironstones show a lateral facies change into the marine Dukamaje Formation (Fig. 2). The Dukamaje Formation is overlain by younger Maastrichtian and Cenozoic strata, whereas in Bida area the ironstones form resistant cappings to the Campanian-Maastrichtian beds present.

A geological map of the study area is presented in Fig. 3. showing the occurence of the most predominant Bida Sandstone Formation, overlain by the Sakpe (Ironstone), Enagi (Siltstone) and Batati (Ironstone) Formations. A complete succession of formations was recorded in one location only (Jima village), that is, Bida, Sakpe, Enagi, and Batati formations. In other locations the Sakpe Ironstone Formation is absent. The undifferentiated laterite hills forming "mesas" that form topographic peaks (Spot heights) in this area remnants of ironstones that have been lateritized and no other formations are recognized along their slopes.

2.2 Local Stratigraphic Succession

Altogether, a total of seven (7) sections were logged. In all descriptions and terminologies applied, the nomenclature is that of the American Commission on Stratigraphic Nomenclature (A.A.P.G., 1961).

2.2.1. Stratigraphic Profile A (Location I).

This section is shown in Fig. 4. A total of 5 lithologic units can be recognised. The basal unit (IFR1.) is clay. Bioturbation occurs as branching and continuous burrows, trails and tracks. Burrow linings have a fairly uniform diameter of about 0.5cm. The unit has a thickness of 1m. The unit is well sorted, greyish and has polygonal mudcracks.

Directly overlying IFR, is a 40 cm thick, very fine sand unit (1FR2). The boundary separating this unit from the basal unit is gradational (not well defined.) This unit is also bioturbated (Plate 2), well sorted, greyish to brownish. This unit is cross-bedded (Plate 2) on a small scale (small scale cross-stratification).

On top of this unit rests a pebbly sandstone unit (1FR3). which is poorly sorted with extremes of grain sizes, trough cross-bedded and about 120 cm thick. There is no preferred orientation of pebble direction. The unit is reddish brown.

Next is a conglomerate unit (1FR4) which consists almost completely of pebble, cobble and boulder sized clastics, with little or no sediment matrix. The unit is 15 cm thick and fairly continuous. The clastics are predominantly quartz, while the matrix is made of decomposed feldspar and broken quartz grains. This unit is capped by a lateritic ironstone horizon which is dark brown, nodular, and indurated. This is the topmost unit exposed aerially. Generally a coarsening upward sequence can be diagnosed from this profile (1FR1 -1FR4). This section is located at 22 km outside Bida on the Minna - Bida road.

GRID: LONG. 6° 11' 13" E
LAT. 9° 11' 40" N

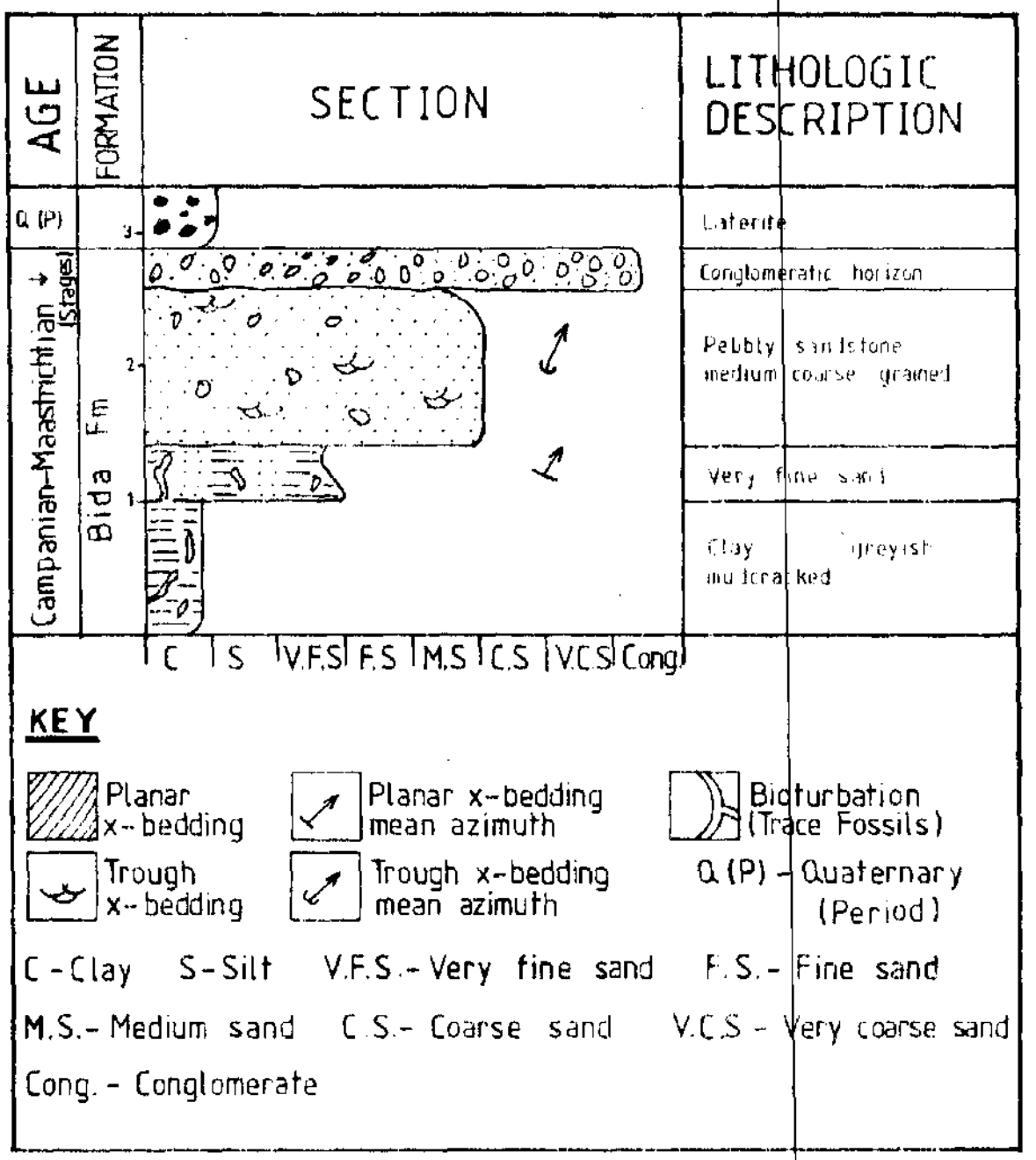


Fig. 4. Stratigraphic Profile A (22 km to Bida, Bida - Minna road)



Plate 2: Fine sand overlying a clayshale unit (both of the Bida formation) with interstratal bioturbation.

2.2.2 Stratigraphic Profile B (Location 2)

This section is shown in Fig. 5. A total of 5 lithologic units are recognised. The basal unit (2 FR1) is a very fine sand unit. The unit is 30 cm thick, whitish to yellowish and friable. The unit is well sorted with narrow size range.

Overlying unit 2FR1 is a partially ferruginized clayey unit (2FR2) of 140 cm thickness. It is reddish to yellowish in colour; bioturbation burrows are prominent. The clay is massive and moderately sorted with polygonal mudcracks. The third lithologic unit in vertical sucession is a siltsontone (2RF3) which is 50 cm thick, with tabular and trough cross stratification. The unit is yelowish to reddish, displays bioturbation and moderately well sorted.

Overlying the third unit in vertical succession is a clayey unit (2FR4) of 130 cm thickness. The unit is reddish, massive and less intensi ely bioturbated (than the unit above), with good grain sorting. Large scaled trough cross-strastification is well displayed.

Forming a capping above 2FR4 unit is a lateritic ironstone horizon which is thinly laminated, fine-grained, dark brown with occasional lateritic nodlules where laterization is at an advanced stage. This ironstone unit also shows trough cross-bedding.

Generally, a repetitive fining upward sequence can be deduced from section B (2FR1 - 2FR4). This section is located 7 km outside Bida on the Bida - Zungeru road.

2.2.3 Stratigraphic Profile C (Location 3)

This section is shown in Fig. 6. A total of 3 lithologic units are recognised. The basal unit (3 FR1) is clay; greyish, plastic with

GRID: LONG. 6° 01' 43" E
LAT. 9° 09' 10" N

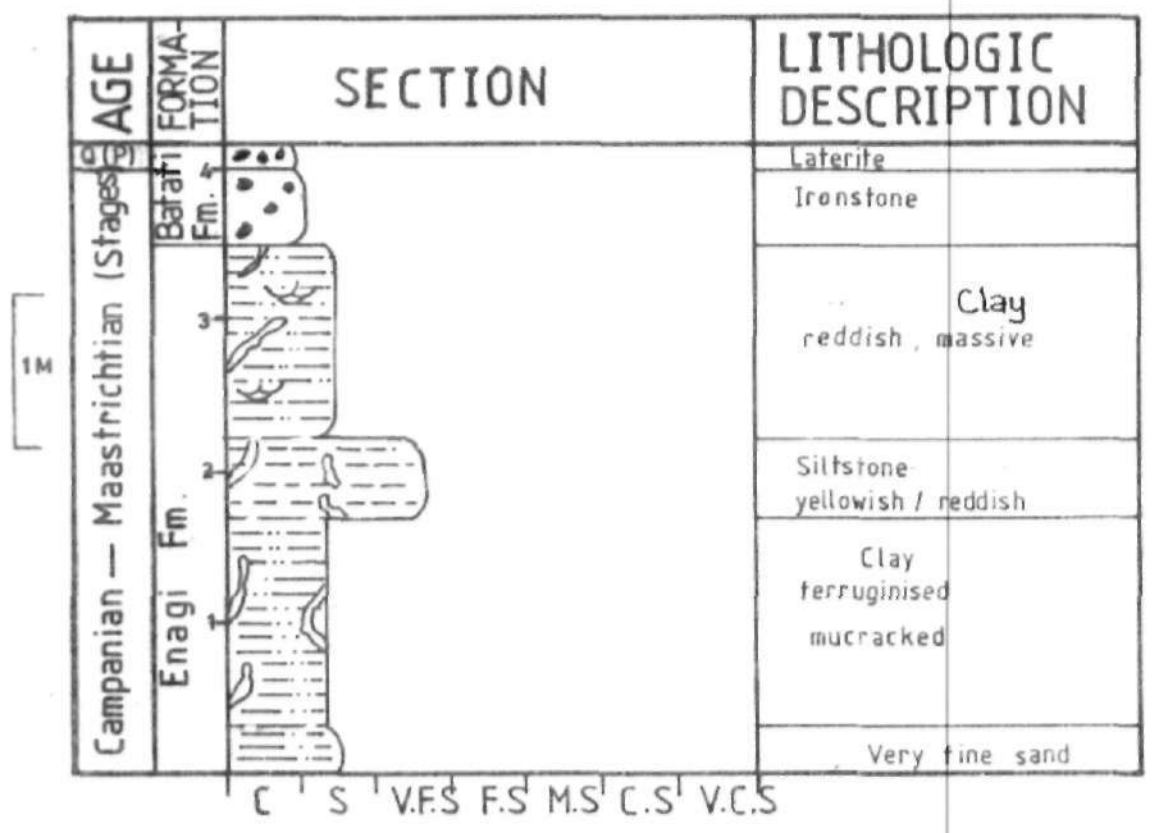


Fig. 5. Stratigraphic Profile B (7 km outside Bida, Bida - Zungeru road)

GRID: LONG. 6° 01' 44" E
LAT. 9° 24' 10" N

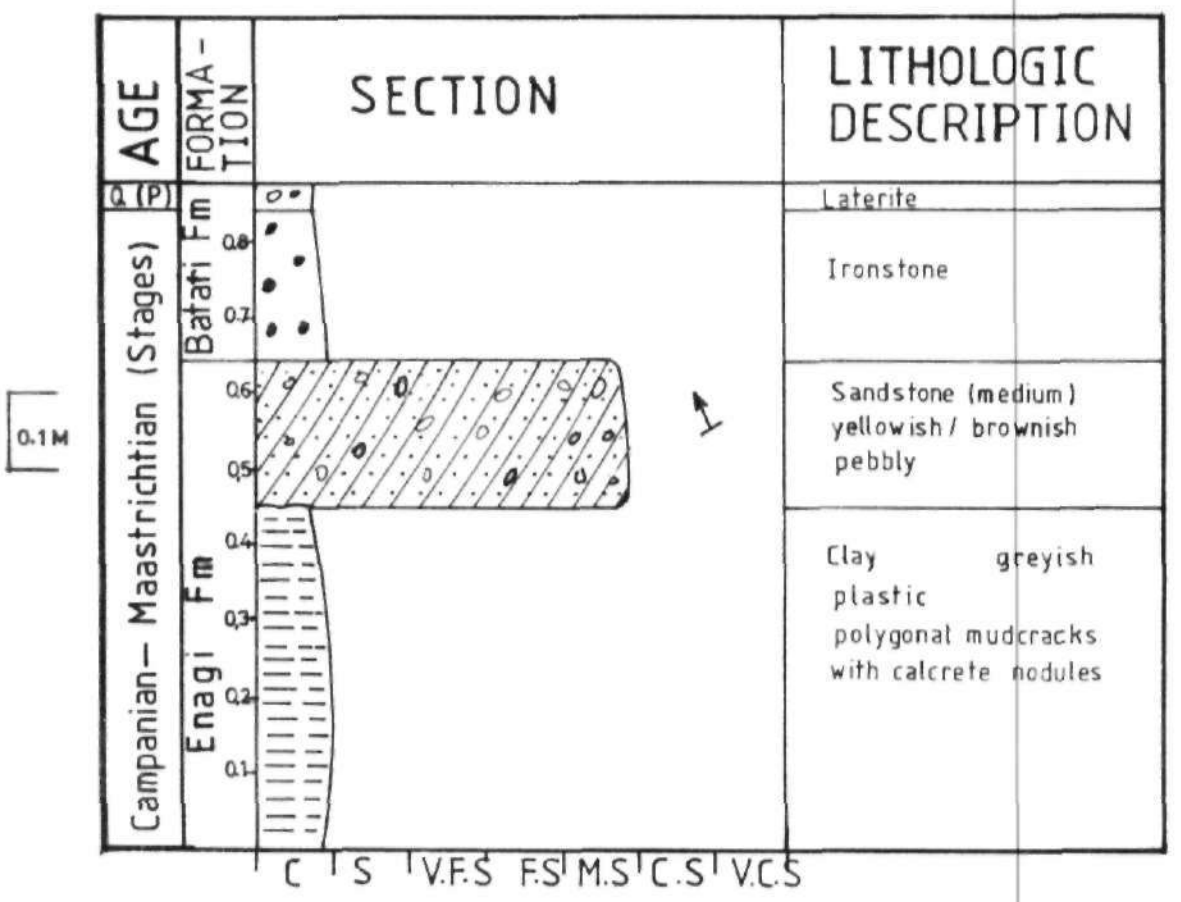


Fig. 6. Stratigraphic Profile C (2 km outside Lemu village, Lemu - Zungeru road)

polygonal mudcracks. The unit is 45cm thick. Occurring within this unit is a calcrete (CaCO3 bearing rock) horizon, which is whitish, loose with rounded nodules. The calcrete horizon has a thickness of 5 cm. This unit (3FR1) has no observable bioturbation burrows, but plant rootlets (probably the taproots of plant from the superficial cover) are common. The unit is well sorted.

Overlying the 3FR1 unit is a medium grained sandstone (3FR2) about 10 cm maximum thicknes, which is yellowish to brownish and pebbly. The pebbles wich is predominatly quartz, are rounded to subangular, and held together by a sandstone matrix. This unit is cross-bedded without bioturbation, and poorly sorted (reflected as wide grain size range).

Forming a capping above this sandsto unit (3FR2) is an ironstone horizon (3FR3), that is fine-grained with a limonite (yellowish) matrix which appears friable and rusty.

On the whole the lithologic sequence exhibited in this section is coarsening upward (3FR1 - 3FR2). This section is found at about 2 km outside Lemu village (Bida - Lemu - Zungeru road).

2.2.4 Stratigraphic Profile D (Location 4).

This section is shown in Fig. 7. There are a total of 9 lighologic units exposed. There is a rapid and distinct facies changes in this section. The basal unit (4FR1) appears arkosic (felspartic sandstone). The unit is poorly sorted, medium to coarse grained with quartz and feldspar peebles. It has a thickness of 6 m; the unit is brownish to yellowish. There is no bioturbation and no cross-bedding.

Lying above the basal unit is a fine-grained, yelowish sandstone (4FR2), which is about 9 m thick, with evidence of organic activity as

GRID: LONG. 5° 56' 32"E

LAT. 8° 55' 50"N

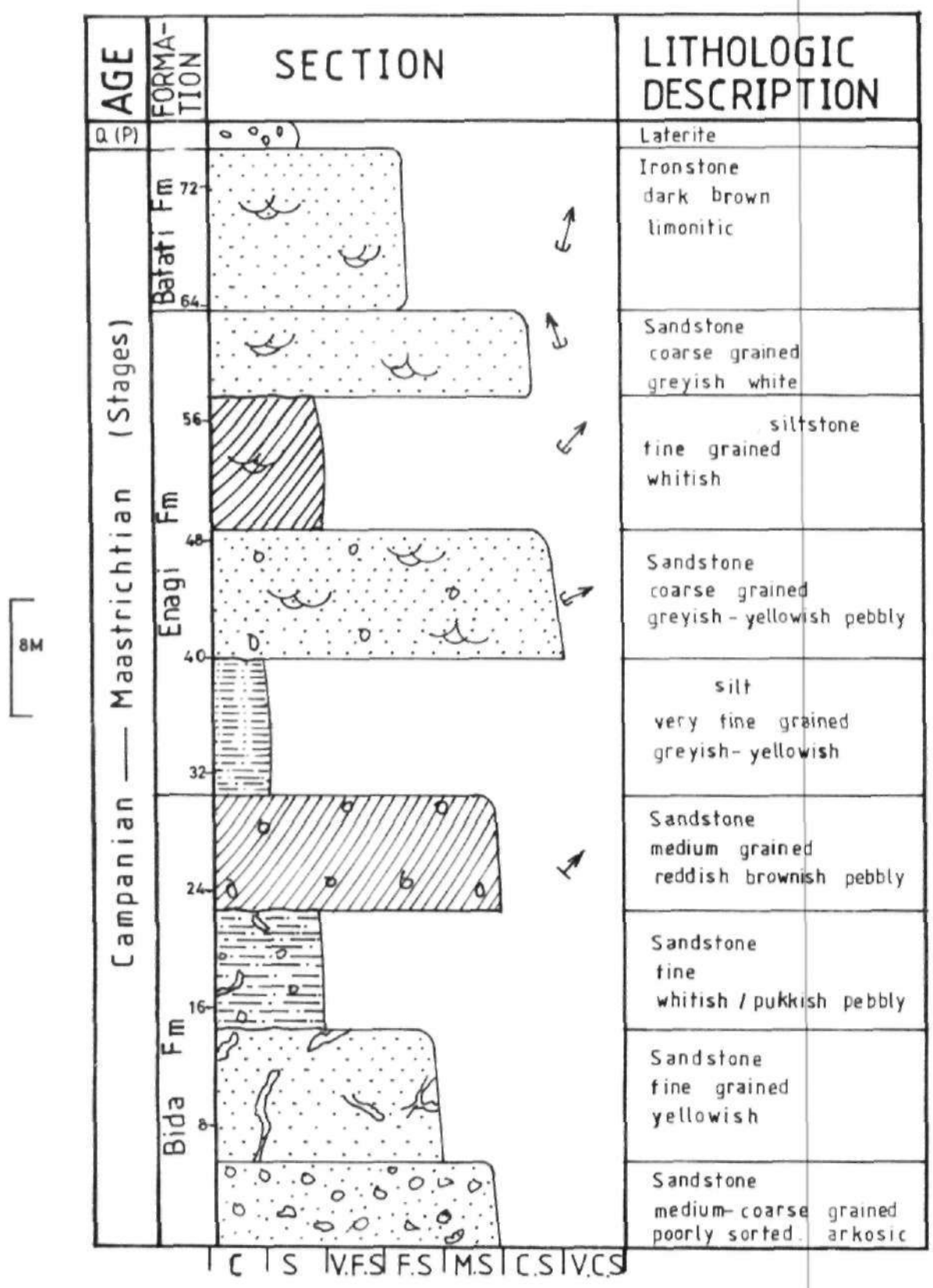


Fig. 7. Stratigraphic Profile D (Doko village)

bioturbation structures. The unit is finer than the basal unit (4FR1) with a distinct boundary.

The next unit in vertical succession is a fine sandstone unit (4FR3). This unit has fossil evidience as tracks, trails and burrows, Whitish to pinkish, and is about 8 m thickness. The unit is pebbly and transition from lower sandstone (4FR2) is sharp and well defined.

The fourth unit (4FR4) in vertical succession is a cross-bedded, moderately sorted, pebbly, reddish to brownish, medium grained sandstone (Plate 3). It has a thickness of 8m.

The fifth lithologic unit (4FR5) in vertical succession is siltstone, that is greyish to yellowish and very fine-grained. It has thickness of 9m, well sorted and massive. The unit is non-bioturbated.

The four remaining lithologic units in this section (D) are 4FR6, 4FR7, 4FR8, and 4FR9 which are coarse sandstone, siltstone, coarse sandstone and limonite-rich ironstone respectively. All the four lithologic units are tabular and trough cross-bedded especially the ironstone unit (4FR9) which displays perfect examples of trough cross-stratification (plate 4). The siltstone unit (4FR7) is greyish to white and friable. The coarse sandstone unit (4FR6) is however pebbly. The four lithologic units have thicknesses of 9m, 9m, 6m, and 11m respectively. the lighologic units in this section have relatively close thicknesses; the least being 6m while the maximum is 11m.

This section (D), displays a repetitive fining upward sequence. The section is located at Doko village, in the southernmost portion of the study area.



Plate 3: Cross-bedded, medium grained sandstone unit of the Bida Formation.



Plate 4: Trough cross-bedded ironstone unit of the Batati formation.

2.2.5 Stratigraphic Profile E (Location 7

This section is shown in Fig. 8. There are a total of 9 lithologic units. The basal unit (7RF1) is clayey sandstone (arkosic) to feldspartic sandstone, with angular to subangulalr, quartz and feldspar pebbles in a sandstone matrix. The unit is poorly sorted, brownish to yellowish, medium grained, and with a thickness of 7m. There is no bioturbation and cross-bedding.

The next unit in vertical succession, is a fine grained sandstone (7FR2), reddish, mottled, moderately well sorted, with a thickness of 8m. The unit is ferruginized and massive. No bioturbation is observable and cross-bedding is absent.

The third unit (7FR3) is a cross-bedded very fine grained, ferruginized (limonitic?) sandstone. Greyish to yellowish the unit is mottled, well sorted with bioturbation (burrows, tracks and trails). The unit is 8m thick.

The fourth unit (7FR4) is a pinkish, coarse-grained, moderately sorted and trough cross-bedded sandstone. The unit is 9m thick and bioturbated.

The fifth unit (7FR5), which is the thickest in this section (15m), is a poorly sorted, reddish, bioturbated and trough cross-bedded sandstone, which is friable and coarse grained.

The sixth unit is also sandstone (medium to coarse grained), mottled, reddish to brownish, well sorted, trough cross-bedded and has a thickness of 9m.

Lighologic units 7FR7 (7m) and 7FR8 (9m) are ferruginous sandstone and ironstone respectively. Both are thinly laminated (Plate 5), trough cross-bedded and brownish to reddish. The unit 7FR8 is mottled and

GRID: LONG. 5° 52' 14"E
LAT. 9° 02' 30"N

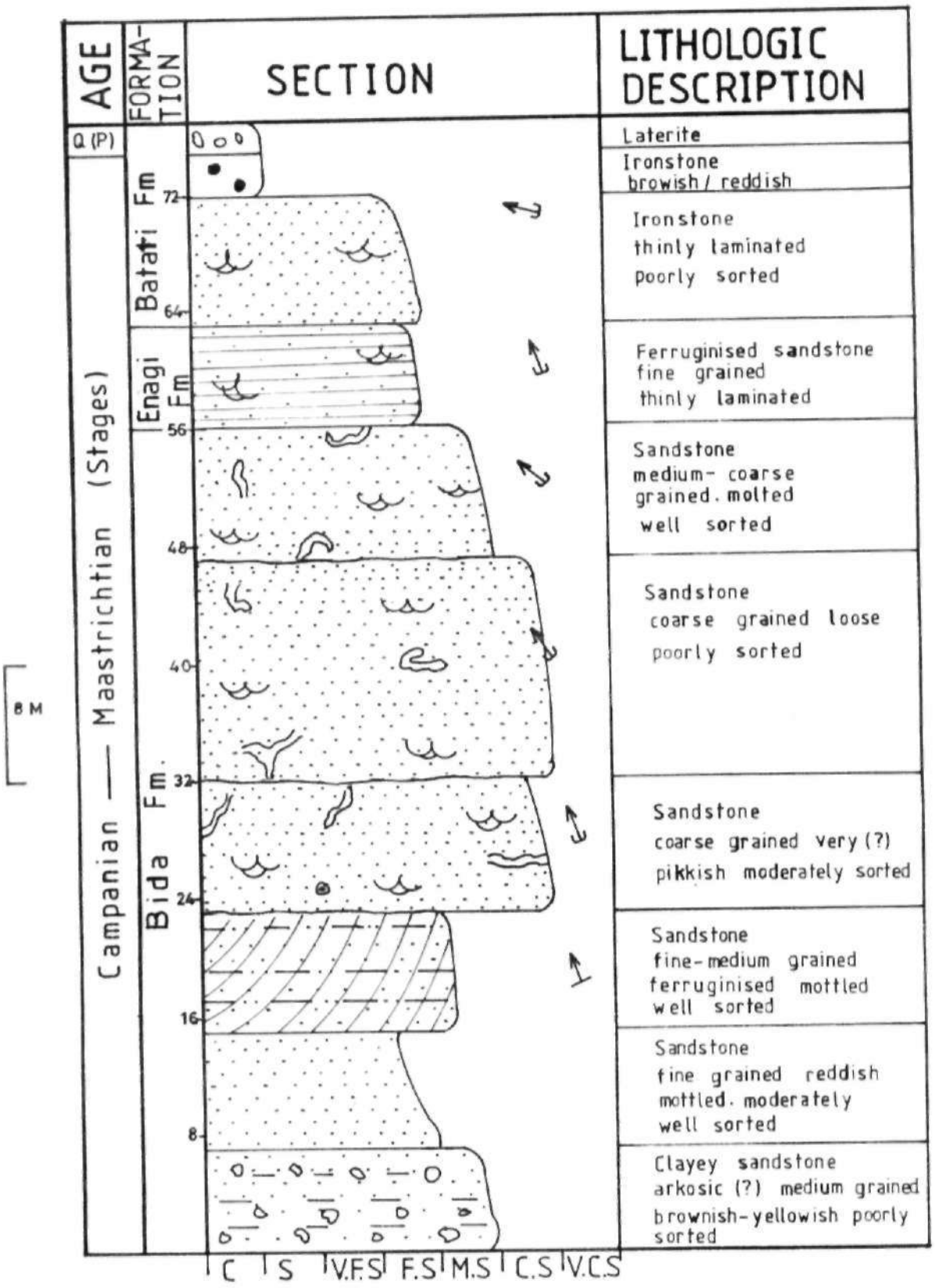


Fig. 8. Stratigraphic Profile E (2km to Jima village)



Plate 5: Thinly laminated Ferruginous Sandstone unit of the Enagi Formation.

poorly sorted, while the topmost unit (7FR9) forms a lateritic capping that is nodular, reddish to dark brown and also mottled. The unit is 3m thick.

The section in location 7 shows a generally fining upward sequence that is repetitive. This is located at about 2km outside Jima village.

2.2.6 Stratigraphic Profile F (Location 8).

This section is shown in Fig. 9. There are a total of 6 lithologic units. All lithologic units in this section except the topmost lateritic capping are cross-bedded. The basal unit (8FR1) is a fine-grained sandstone, that appears mottled. Bioturbation (burrows) is prominent with small scale cross-bedding. This unit is 5m thick and well sorted.

Above this unit (8FR1) is a coarse grained sandstone (8FR2) which is 6m thick, mottled, bioturbated, trough cross-bedded, reddish to brownish and well sorted. The burrow linings are clean.

The next unit in vertical succession is a medium to coarse grained sandstone (8FR3) that is reddish to brownish, trough cross-bedded, and poorly sorted having a thickness of 8m.

The fourth unit (8FR4) is a fine sandstone unit which is reddish, bioturbated, trough cross-bedded, well-sorted, having a thickness of 4m.

The fifth unit (8FR5) which is 7 m thick is a coarse sandstone (arkosic), poorly sorted, with bioturbation structures. The unit is cross-bedded, reddish and massive.

The topmost unit (8FR6) is a lateritic horizon that is brownish and powdery. The unit is about 3m in thickness.

GRID: LONG. 6°E

LAT. 9° 4' 59"N

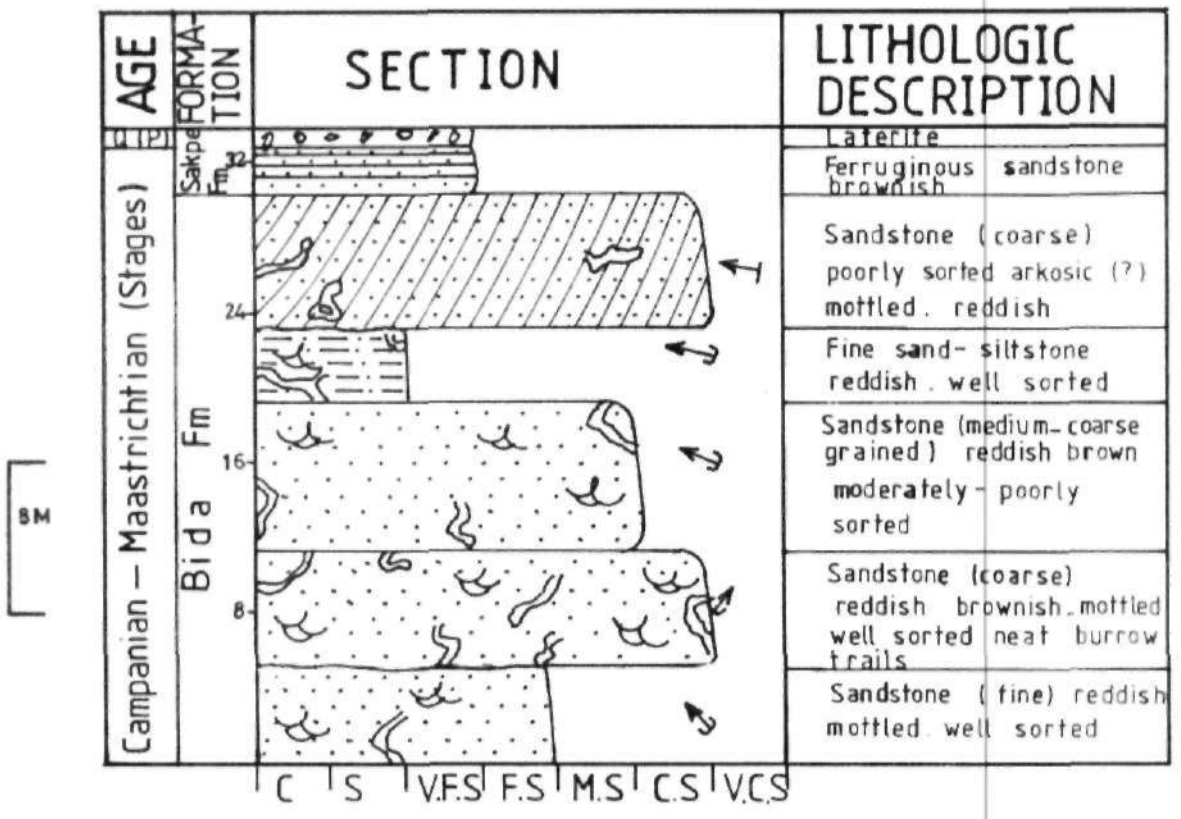


Fig. 9. Stratigraphic Profile F (Bida Town, behind Govt. Girls Sec. Sch.)

Generally, this section displays a sequence that is fining upward. The section is located in the heart of Bida, behind the Government Girls Secondary School.

2.2.7 Stratigraphic Profile G (Location 9)

This section is shown in Fig.10. There are a total of 4 lithologic units in this section. The basal unit (9FR1) is a very fine grained sandstone, that is dark brown and friable with shiny flakes of muscovite. It has a thickness of 2.5m and is well sorted.

The second unit (9FR2) in vertical succession is a fine sandstone, that is brownish, friable and cross-bedded. It is well sorted with a thickness of 2 m.

The third unit (9FR3) is a repetition of the basal unit in all characteristics, with a thickness of 2.5.m.

The fourth unit (9FR4) is another fine grained sandstone which is a replica of 9FR2 except that it is lighter brown in colour, and has a thickness of 1.m.

This section (G) is also repetitive but coarsens upward. The lithologic units occurring here are however friable in texture with no bioturbation. This section is located on the bank of River Kaduna, about 2 km North of Wuya village.

2.3. Regional Facies Relationship.

A facies state is a recurring lithotype which is distinct from others and is consistently recognizable through many different stratigraphic sections (Hoque and Ewajide, 1985). Lithostratigraphic units recognised in this study are defined by dominant lithologic types

GRID: LONG. 5° 49' 38"E
LAT. 9° 11' 40" N

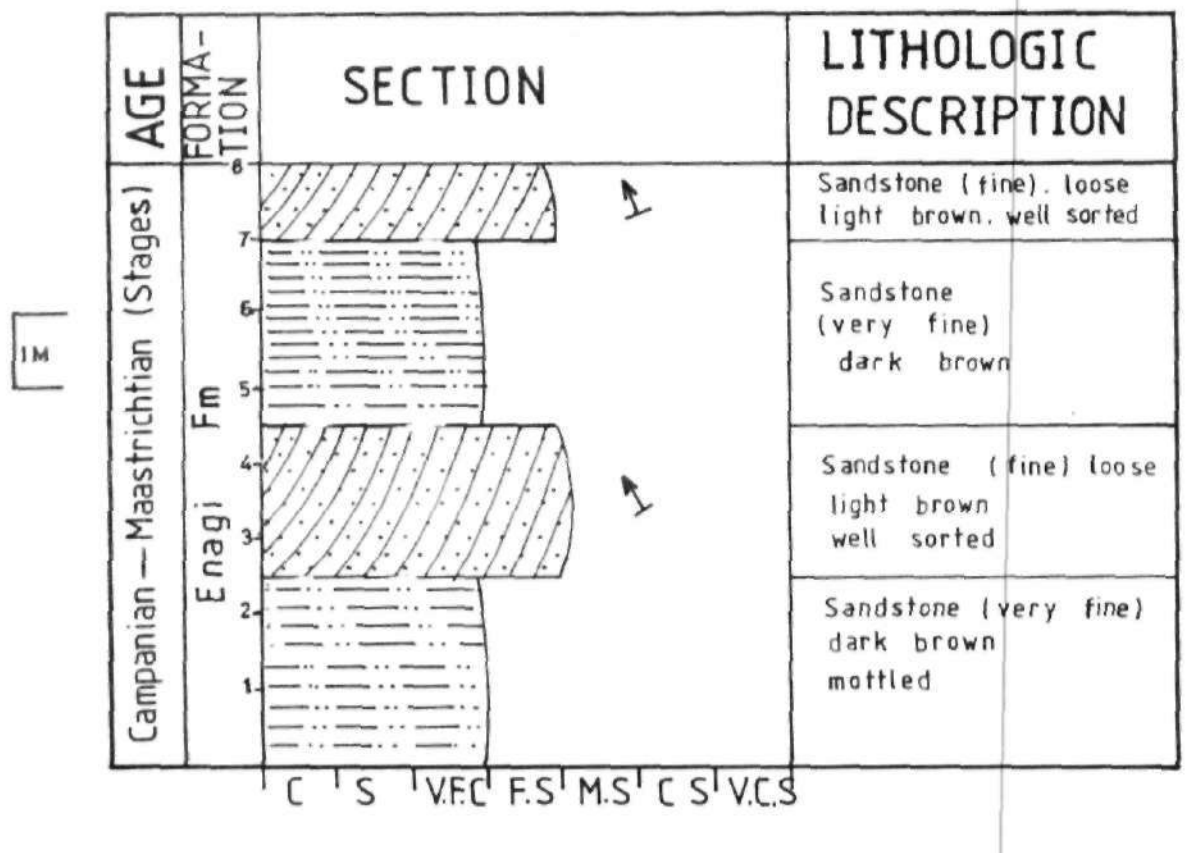


Fig. 10. Stratigraphic Profile G (Bank of River Kaduna, 2 km North of Wuya village)

and texture (especially grain size) with diverse kinds of primary sedimentary structures. Boundaries in the sections logged are of two types; the intra stratigraphic boundaries, and inter stratigraphic boundarises. The intra stratigraphic boundaries are mostly gradational (not sharply defined) depicting not a complete break in deposition (non-deposition) or erosion but a change in hydrodynnamic regime (or energy) of depositional medium. The inter stratigraphic boundaries and in some cases the boundaries between two different but vertically successive beds of the same facies state (multistory lithology) are either clear breaks (observed by distinct changes in lithology) in deposition or erosion surfaces, or scoured surfaces. Examples of intra and inter stratigraphic boundaries are shown in Plate 6 and 9 respectively.

A total of four lithostratigraphic units were observed in the 7 sections logged: (1) Laterite unit (2) Ironstone unit (3) Argillaceous (clay-shale-siltstone) unit and (4) Aranaceous (Pebbly - coarse - medium - fine sandstone) unit.

2.3.1. Laterite Lithotype

Laterite lithotype occurring within the area of study are of two major types. They are the primary and secondary types which correlate with those of Du Preez, (1949) and Pullan (1967), or types A or B and C of Thomas (1974).

Primary laterites (Type A or B) occur as oolitic and pisolitic concretions with concentric laminations, usually nodular and indurated. They occur along summits and usually as cappings of ironstone units (source of iron for laterilization). They are continuous and often vesicular. On the other hand, secondary laterites (Type C) are

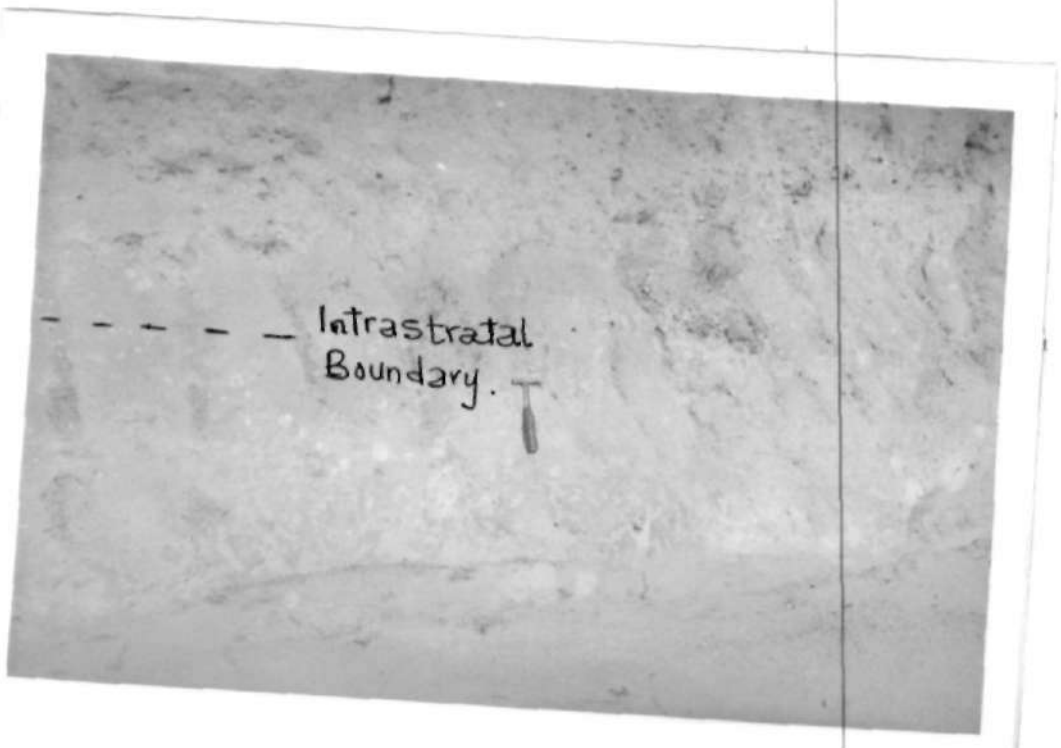


Plate 6: Intrastratal facies boundary in the Bida Formation.

concretionary or detrital and occur as fragments, though occasionally locally indurated. They are considered to be secondary because they are not in-situ products but washed down to their positions by denudation, as products of primary laterites. The mineralogy of both primary and secondary laterites are the same; quartz, feldspars and oxides of iron and aluminium, with quartz and felspars usually occurring as nuclei with oxides of iron and aluminium occuring as coatings. Where indurated, the matrix is made up of clay minerals (Kaolinite). Laterite occuping in location 1 (Fig 4) is a good exmaple of Secondary laterite. While sections from locations 2, 3, 4, 7, 8 and 9 display good occurences of primayry laterite (Plate 7), being products of the laterization of ironstone units.,

Occurrences of laterites (Primary especially) within the area of study have been enhanced due to favourable climatic and relief conditions. According to Thomas (1974) conditions critical to laterite formation include.

(1) Source of iron (Fe^{2+} and Fe^{3+})

(2) Persistence of a steady state of low relief during a prolonged period of uplift and denudation.

(3) Moderate precipitation.

(4) Mobility of iron as a result of presence of a reducing environment (particularly due to praesence of organic acids).

(5) Wetting and drying under subaerial conditions to bring about hardening.



Plate 7: Primary laterite capping a residual hill

2.3.2. Ironstone Lithotype

The occurence of ironstone within the area of study is distinct and regionally distributed. They occur as the topmost beds in all the seven(7) profiles logged. Although Adeleye (1971) recognised two Ironstone Formations (Sakpe and Batati) separated by the argillaceous Enagi Formation. this has not been very well definedwithin the area of study. Sakpe Ironstone Formation occurs in only one location (8), succeeding the Bida Formation; while the Batati Ironstone Formation occurs in four locations (2, 3, 4 and 7), that is, there was no complete stratigraphic succession within the study are

The closest to such complete stratigraphic succession was observed in Location 7, where yellowish to dark brown ferruginous sandstone (7FR3) occurs within the clastic unit but this cannot be referred to as ironstone since the proportion of iron within the unit is not enough to merit such a name (ironstone). Moreover, the beds succeeding this ferruginous sandstone in Location 7 are not argillaceous which does not possibly correlate them as Sakpe Ironstone Formation.

Description: The ironstone beds are generally massive, thin to thick flat bedded, with locally developed laminations (Plate 5). There is a predominance of trough cross-bedding with occurrences of trace fossils and shelly beds (Locations 4 and 7). The beds are dominantly oolitic with subsidiary ferrugionous claystones. The oolites vary in diameter ranging between 0.8 and 1.3 mm (Plate 8). They are spherical to subspherical with poorly defined outline. Occasionally oolites appear as moderately flattened ellipsoidal structures having sharp contact with the groundmass, and pisolites having diameters ranging between 1.5-1.7 mm. The beds are usually fine grained, yellowish to

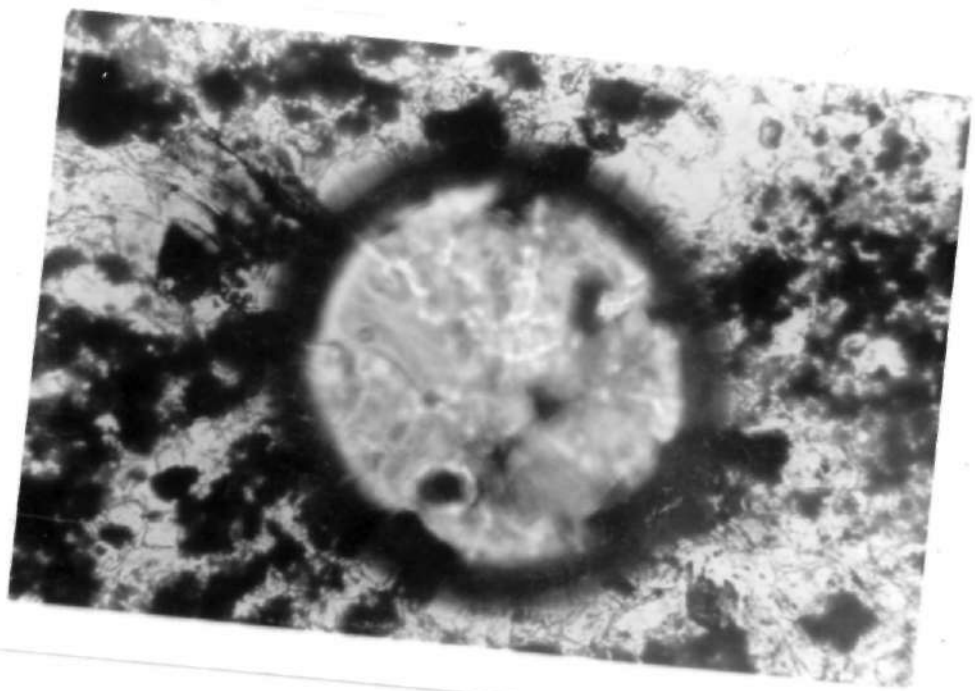


Plate 8: Oolite occuring in the ironstone facies. (Mag x16)

brownish, dominantly goethitic and kaolinitic, with vesicles filled by white probably kaolinitic matter. The basal contact of the ironstone units with the underlying units are sharp and well defined (Plate 9) depicting an erosional surface.

2.3.3 Argillaceous Lithotype.

Argillaceous lithotypes (clay, silt, very fine sandstone) observed within the area of study mostly occur interbedded with the aranaceous lithotypes. Adeleye (1971) recognised the predominantly argillaceous lithotypes of the Middle Niger Valley as belonging to the Enagi Formation describing them as dominated by siltstone with subsidiary fine-grained sandstones and lignite. Though the occurence of lignite has not been observed in this work, clay, siltstone and very fine sandstone beds were observed with considerable thicknesses that can be considered as the Enagi Formation . Two sections, Location 4 (Fig 7) and Location 7 (Fig 8), display the occurences of Enagi Formation conformably overlying the Basal Bida Formation without the intervening Lower (Sakpe) Ironstone Formation.

Description: The beds occuring as the argillaceous lithotypes are typically fine-grained, ranging from clay size to fine sandstone, with characteristic trace fossils. Boundaries with precceding units are not prominent, closely representing more of an event of reduced deposition or non-deposition rather than erosional surfaces, but contact with succeeding beds are sharp. Argillaceous beds are greyish to yellowish or whitish, massive and hard or soft and friable with occasional claystone nodules. Planar cross-stratification (small scale) is predominant in the clays and siltstones. The siltstones are locally



Plate 9: Laminated ironstone exhibiting sharp basal contact with medium grained ferruginous sandstone.

well sorted and occasionally ferruginized, with a thickness ranging from a few centimetres to 2 m, the ferruginized units being fractions of centimetres thick. Two basic types of the argillaceous lithotype (facies) can be identified. One is well sorted, medium to coarse, micaceous, massive siltstone while the other is poorly sorted, sandy and clayey. The first type is found in Locations 2, 3, 4, and 7 while the second type is found in location (9) Polygonal mudcracks are common within the clay units of this lithotype as seen in locations 1 and 3, signifying subaerial exposure (Reineck and Singh, 1978).

The argillaceous lithotype commonly form near the top of mesas and near tops of residual hills, especially the sandy and clayey units, and usually appear weathered.

In assigning the units within the argillaceous lithotypes into any particular formation (Bida or Enagi) care must be taken Adeleye (1971) recognised the occurence of an argillaceous subfacies within the Bida (aranaceous) Sandstone Formation; he distinguished between the argillaceous facies that makes up the Enagi Siltstone Formation from the argillaceous subfacies of the Bida Sandstone Formation on the basis of ferruginization and lamination of beds. While the siltstone facies of Enagi Formation are occasionally ferruginized and massive, the argillaceous subfacies of the Bida Formation are typically non-ferruginous and commonly soft and friable. Based on field observations in this work this distinction based on ferruginization and lamination is confirmed and seems plausible. A typical section of argillaceous facies units belonging to the Enagi Siltstone Formation which is recognised in this project occurs in Location (9) (Fig. 10) capped by lateritic ironstone. This belongs to the well-sorted, medium to coarse, micaceous

and massive sub-facies identified earlier in this chapter, while the poorly sorted, sandy and clayey subfacies occurs in Location (2) (Fig. 5)

2.3.4. Aranaceous Lithotype.

Aranaceous (Sandstone) lithotypes observed within the area of study are of great vertical and aerial extent. Subsidiary lithofacies are coarse-medium-fine sandstone, conglomerates, pebbly sandstones, siltstones and claystones.

Description: Lithologic units belonging to this lithotype ranges from cross-stratified to massive sandstones with extremely poor sorting at the base containing pebbles, cobbles, and boulder sized clastic grains, with sorting becoming moderate to good at higher horizons. Contacts of beds with preceeding and succeeding beds are sharp (erosional surfaces). The sandstones of this lithotype are generally angular to subangular, very fine to very coarse. Arkoses and feldspartic sandstone are common in the basal parts, while quartose sandstone dominate the upper parts. Massive appearance and flat beds are most common in the basal portions of the sandstones in the Bida area. The upper parts display large scale cross-stratification. The beds generally fine upwards with occasionaly cyclothemic fining upward, the type described by Allen (1965) and Visher (1965).

A type Aranaceous lithotype which belong to the Bida Formation is shown in locations 4 (Fig 7) and 7 (Fig. 8). The aranaceous lithotype also have trace fossils profusely dispersed in the upper well to moderately sorted parts.

2.3.5. Interpretation.

By visual examinations of lithostratigraphic units described above, a cyclic fining upward and local coarsening upward of facies transition can be deciphered. Many cyclic patterns suggesting different stages and hydrodynamic conditions of deposition can be interpreted. Miall (173) suggested that most fining upward cycles originated by debris flow sweeping across pediment surface and creating new channels in a fluvial environment. He also noted that conglomerate beds could not be fitted into a fining upward cycle and he interpreted them as deposits of debris flood that did not result in the establishment of new channel systems, so that once the flood has passed, the original fluvial pattern re-established itself. Miall (1973) suggested that pebbly sandstones may not be of different genetic origin to the conglomerates, the latter are debris flow deposits, whereas sandstone with scattered pebbles may represent non-violent run-off, the pebbles being carried as traction load than in suspension., The presence of cross-bedding in some pebbly sandstones confirms this interpretation. It is possible to apply Allen's (1970) sedimentation model for fluvial cycles to the present study area except that the study area has a paucity of sedimentary structures which suggest the predominance of upper regime, plane-bed flow (Harms and Fahnestock, 1965) during the deposition of the coarse to medium sandstone.

The siltstones which are often interbedded with this relatively fine grained sandstones, overlying suncracked surfaces are probably flood plain topstratum deposits resprectively, levee, backswamp, and crevasse-splay environments. The oolitic ironstones suggests deposition in a

shoreline high energy environment. This is supported most importantly by the oolites which ressemble products of some oceanographic conditions similar to the calcareous oolites of Tricial coastline (Shearman et al., 1970).

CHAPTER THREE

SEDIMENTARY STRCUTRES AND PALEOCURRENT

3.1Types of Sedimentary Structures

Sedimentary structures are very important indicators of depositional environment. They give some indication of the depth and energy level of the environment and of the velocity, hydraulics, and direction of the currents which flowed across it.

Sedimentary structures occuring in the are of study are widely varied, ranging from primary (inorganic and organic) to secondary types. Examples of sedimentary strctures found include cross-bedding, inchnofossils (trace fossiles, or leben-spurren), mud cracks, load casts, graded beddings and calcrete.

3.1.1Cross-Bedding

Cross-bedding is abundant within the various lighostratigraphic units logged from the basal member of the Bida Sandstone Formation to the topmost Batati Ironstone formation. Both large (>5 cm thickness) scale of Reineck and Singh (1978) are observed. Planar and trough cross-bedding are found although there seems to be a preponderance of trough over planar cross-beds. Planar cross-bedding consists of tabular cross units, with diagonal or sendibly planar contacts to the adjacent sedimentation unit (Plae 10) while the trough shaped types of cross-bedding have curved basal contacts which are generally concave in shape at base, and are more common within the Ironstone Facies (Plate 4) that is, occurence of Planar cross-bedding



Plate 10: Planar cross-bedded sandstone unit.

decreases with increase in stratigrahic position of lithofacies. The thickness of individual cross-bedded units vary from 3 cm (at Location 2) to about 2 m (at Doko, Location 4). The boundary surface between the adjacent cross-bedded units are predominatly erosional and less frequently non-erosional. Where the boundary is erosional, pebbles accumulate at the base of bedding planes or facies change becomes rapid with abrupt change in character; non-erosional surfaces have radational boundaries.

Planar (tabular) cross-bedding which consist of planar beds have angular contact with the basal surface of the set (or with the dpreceeding bed) ranging from as flow as 11° in location 1 to a maximum of 45° in Location 7, while trough-shaped cross-bedding consists of scoop shaped beds with tangential bases and higher dip angles ranging from a minimum of 20° (in Location 7) to a maximum of 40° (in Location 4). Table 3.1 shows the dip, strike and azimuth measurements for cross-beddings obtained from each location. Measurements show little variation in readings, with all clustering within the 19° - 45° range. The basis for the recognition of these two (Planar and trough) types of cross-bedding is hinged on the definition of Mckee and Weir (1953), that a set of cross-beds is a group of essentially conformable cross-strata separated from other sedimentary units by surfaces of erosion, non-deposition or abrupt change in character. On the other hand cross-stratification hence bedding, is a product of down-stream migration of ripple, sand waves and dunnes which themselves (ripples, sand waves and dunes) are downstreame-migrating bed forms produced by unidirectional aqueous flow, their formation depends on stream power and grain size (Fig. 11).

By plotting the raw uncorrected azimuthal measurements of cross-beddings on a rose diagram, a preferred northerly direction (NNW - SSE) of plaeflow is indicated over the area studied as shown in Fig. 12.

Table 3.1 Dip, Strike and Azimuth measurements of cross bedded units from locations 1,2,3,4,7,8 and 9, within the study area

Location	Dip Degrees	Strike (Degrees)	Azimuth (Degrees)
Location 1	36 4 24 18	335 NNW 340 NNW 336 NNW	50 56 37
	19 11 30 25	20 NNE 352 NNW 339 NNW	55 12 32
	20 21 30 33	278 WNW 23 NNE 325 NNW	41 19 316
	22 28 39	334 NNW 330 NNW 330 NNW	33 33 340
Location 2	22 30		
	32 42	330 NNW 315 WNW 280 WNW	180 33 25
	22 50	320 NNW	16 60 300
	38 25	326 NNW 353 WNW	358 80 280
	26 28	340 NNW 305 WNW	52 87 310
	24 25	352 NNW 301 WNW 342 NNW	348 189
	23 38	353 NNW 279 WNW	100 8
	30	310 WNW 290 WNW	90 303
Location 3	20 36	289 WNW 230 WSW	285 300
	35 40	279 W 190 SSW	24 20
	20	141 SSE	6
	25 33	95 ESE	350
	30	121 ESE	341 189
		272 WNW	
Location 4	30 28 24	330 NNW 373 NNW	60 342 30
	38 21 21	338 NNW 354 NNW	252 33 34
	20 24 29	290 WNW 320 NNW	355 91 44
	40 36 27	280 WNW 311 WNW	61 85 84
	27 38 37	315 NW 313 WNW	74 300 270
	20 22 40	360 N 314 WNW	130 53 66
	25 29	40 NNE 285 WNW	90 60 38
	43 27 25	38 NNE 278 WNW	355 62 320
	38 25 13	335 NNW 290 WNW	352 66 284
	35 20 18	331 NNW 15 NNE	64 72 270
	28 20 18	333 NNW 1 NNE	66 311 180
	26 21 22	336 NNW 327 NNW	68 53 270
	45 40 33	327 NNW 79 ENE	67 52 49
	14 32 22	300 WNW 60 ENE	140 251 349
		3 NNE 290 WNW	90 55 36
		10 NNE 330 NNW	175 310 288
		23 NNE	273 5 130
		283 NNW	66 318 342
		300 WNW	64 32
		333 NNW	36 350
		87 ENE	331 348
		333 NNW	
		335 NNW	

Table 3.1 (cont'd)

Location 1	Dip Degrees	Strike (Degrees)	Azimuth (Degrees)
	20 24 29		
Location 7	25 21 33	280 WNW 260 WSW 312 WNW	334 301 146
	24 29	243 SSW 190 SSW 308 WNW	52 44 197
	27 24	300 WNW 199 SSW	298 173
	45 38	331 NNW 201 SSW	326 9 197
	30 27	290 WNW 105 ESE	5 345
	23 33	270 WNW 168 SSE	10 33 286
		283 WNW 213 SSW	345 288 312
			350 300 316
			328 336 308
			10 341 294
			15 338 356
			280 320
			348 284
			358 273
	35 26 39	189 SSW 200 SSW	330 49 189
Location 8	43 28	268 WSW 316 NNW 312 WNW	346 56 200
			89 215
	30 20	300 WNW 258 WSW	289 21 329
	25 41	211 SSW 309 WNW	310 5 300
		190 SSW	300 323 308
			300 265 275
			305 280 210
			270 347 350
Location 9	26 25	290 WNW 305 NNW	330 5 6
	35 30	300 WNW 310 WNW	315 16 10
	40 25	189 SSW 294 WNW	305 348 12
			284 295 347
			15 300 350

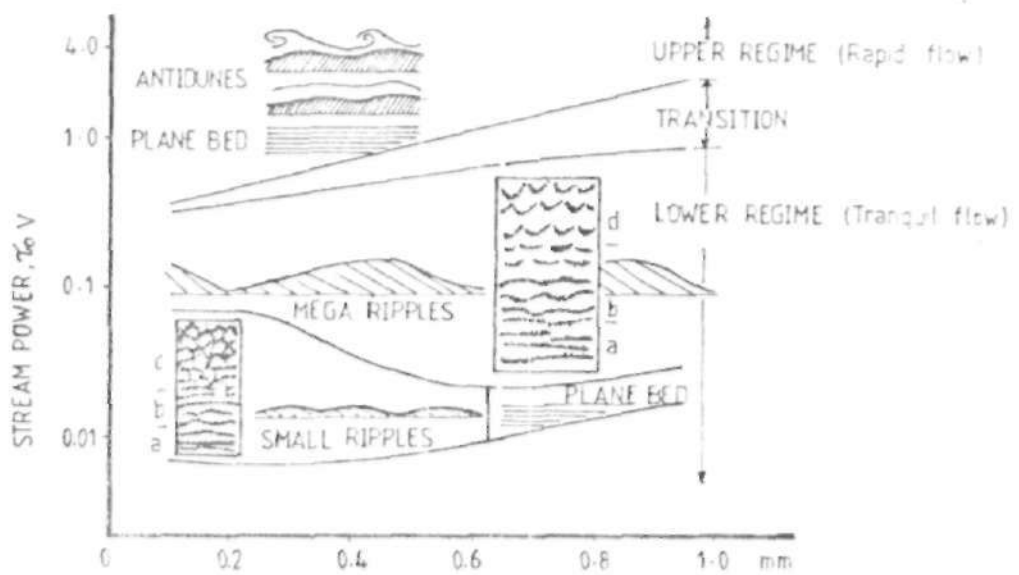


Fig.11. Schematic representation of various bedforms and their relationship to grain size and stream power. Based on SIMONS et al (1965) and ALLEN (1968a): a Straight-crested ripples, b Undulatory ripples, c Linguoid ripples; d Lunate ripples. For both small ripples and megacurrent ripples, ripple crests tend to become discontinuous with increasing stream power.

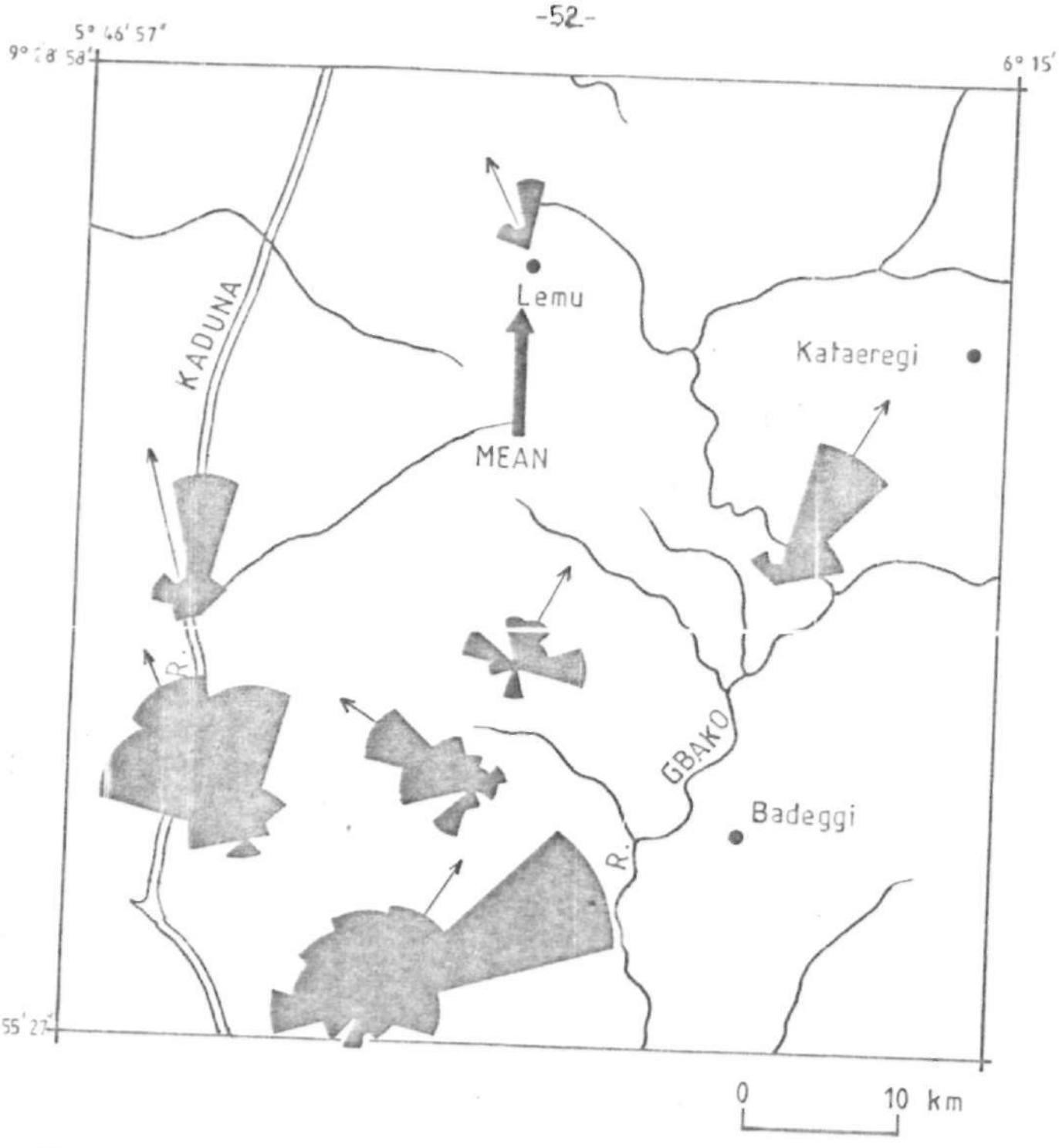


Figure 12. Regional Paleocurrent Map (Area of Study)

3.1.2 Ichnofossils

Ichnofossils, trace fossils, lebenspuren and bioturbation structures (Richter, 1936, 1937, 1952) denote the structures formed by the activity of living animals within or on the sediment surface. Reineck and Singh (1978) classified them as organic primary sedimentary structures, while Greensmith, (1978) and Tucker (1982) classified them as biogenic structures.

The occurrences of trace fossils within the study area are varied and occasionally profuse. Plate 2 shows trace fossils occuring essentially in the clayey-siltstone unit in Location 1. Occasional mottling of sandstone and ironstone units are observable. The traces vary in orientation and position of occurence. Some traces are epistratal (located on the bedding surface), coiled, curved and occasionally radiating furrows occur formed by organisms systematically ingesting sediment for food usually by mobile deposit feeding epibenthic organisms (Seilacher, 1964). Some trace fossils typically consists of a network of filled burrows, branching and unbranched, these trace fossils are intrastratal (found below sediment surface) formed by epibenthic and endobenthic deposit feeders which live within a burrow system. Also some burrows are simple vertical tubes, U-Shaped and sometimes complicated. Many dwelling burrows are lined by pellets which indicate dwelling position. Borings are also types of trace fossils with bore linings. Another important structure noticed is mottling. Mottling which is also good indicator of animal activity (Reineck and Singh, 1978), appears as irregular distribution of sandy nests in clay and sandstone - siltstone units. Mottling in ironstone can be seen as whitish pellets in a vertical, horizontal or irregular sometimes rounded holes or cavities.

Trace fossils (burrows especially) are fairly continuous and strech interstrata; that is burrows originating from within a unit can extend to the overlying or underlying unit (Plate 2). Diameter of burrows ranges from as little as 5 mm to a maximum of 5 cm, though trace fossil length (grazing trails) are as much as 30 cm, while resting traces which are usually rounded have a diameter range of 5 mm - 3 cm with a central depression. The interpretation of these trace fossils is based on Seilacher's (1953a and 1967). Seilacher (1953a), based on some ecological factors, suggested a classification which distinguishes five groups of trace fossils - (1) Resting traces (2) Crawling traces (3) Feeding or Browsing traces (4) Feeding structures (5) Dwelling traces. Seilacher (1967) gave a bathymetry based on the form and patterns of burrows, and concluded there is a general gradation from vertical burrows in deep water deposits, thus recognising five ichnofacies namely Skolithos, Glossifungites, Cruziana, Zoophycos and Nereites with increasing depths from the littoral sands to pelagic muds of marine setting.

Illustration of common trace fossils occuring in the study area thus shows that they are essentially feeding, resting, and dwelling traces, especially in situation where pellet remains are observed. Based on bathymery, there is a preponderance of vertical and branching traces over horizontal traces, hence a shallow-water setting can be said to predominate over deep water, with characteristic Thalassinoides and Ophimorpha trace fossils (Tucker, 1982) occuring frequently. Hence ichnofacies assemblages based on characteristic properties can be seen to vary from Skolithos (which has typical dwelling traces) through Glossifungites and Cruziana to Zoophycos (which consist typically of feeding and resting

traces) but Nereites assemblage is not discrernible.

3.1.3 Mudcracks and Load Casts

Occurrence of mudcracks in the study area is restricted to the fine to very fine grained, clayey, well consolidated, sandstone and clay. The cracks are both radially and concentrically disposed, with wide and deep principal fissures. The fissures are V-shaped, measuring about 2 cm deep and 2 cm wide. A good occurence of mudcracks was recorded in Locations 1 and 3 in the clay units. Mudcracks or shrinkage cracks (Reineck and Singh, 1978) orininage by dessication and compaction of water saturated muddy sediments, and also originate subaqueously as a result of synearesis (Jungst, 1934). They signify intermittent subaerial exposures of surfaces of dried-up ponds, coastal and inland sabkas, lakes and lagoons, abandoned river channels, flood plains and intertidal zones (Reineck and Singh, 1978).

On the other hand load casts are sole structures. they occur as bulbous, downward - directed protuberances of a sandstone bed into underlying sedimentns are hydroplastic hence unstable, creating inverted density gradient (Nwajide, 1987). Loadcasts have limited facies restriction, occuring within fine sandstone, siltstone, and clay units. They occur as mammilarly mounds and as rounded inviduals sometimes tapering out at the ends. Usually the more dense unit (mostly sand) overlies a less dense clay or siltstone. Plate 11 is a load cast structure showing coarse sandstone unit overlying a finer sandstone. The base of the loadcasts are usually concave upwards, with size diameter ranging from 5 mm to 8cm. Load casts like mudcracks are classified by Nwajide (1987) as irregular physically formed

KAS...



Plate 11: Load cast depicted by a coarse sandstone unit overlying a fine sandstone.

sedimentary structures. The origin of loadcast is thought to depend mostly on gravitational adjustment of a diapiric nature, causing sinking of a denser unit into an underlying less dense unit, in an unstable gravity field. This is termed Rayleigh - Taylor instability (Leeder, 1982, p. 114; Allen, 1982, p. 354) and such adjustment might need a triggering mechanism.

3.1.4 Graded Bedding

Two types of grading have been observed within the area of study which are the types of normal grading described by Tucker, (1982); (1) a gradual decrease in the whole grain size up through the bed (2) a gradual upward decrease in size of the coarsest grains within a bed. Grading was observed mainly in the sandstone-siltstone units most especially arkosic (feldspartic sandstone) and poorly sorted units. Most common is the first type (gradual decrease in whole grain size up through the bed) of grading, and particularly in Locations 4 and 7 (Figs 7 and 8), although differentiation between the two types of grading mentioned earlier in the field is difficult. Reverse or inverse grading is another common type in the study area (though interstratal, across facies) showing a coarsening upward of grain size up across facies. This is particularly noticeable in location 1, 3 and 8 (Figs 4, 5, and 9). Such intrastratal and interstratal grading reflects changes in energy and hydrodynamic regime of depositing medium.

According to Reineck and Singh (1978), origin of graded bedding has been attributed to turbidity currents, but occasionally graded bedding is observed in shallow water sediments, where however they don't make thick sequences. Graded beddings can also be produced by sedimentation of

suspension clouds, deposition in the last phases of heavy flood, by periodic silting of delta distributaries and by settling of volcanic ash after an eruption. Locally on intertidal flats and beaches reverse grading is found, but usually thin. Observed graded beddings in this project are probably a result of fluvial processes with fluctuating energy regimes. It should however be noted that sections logged are usually a fraction of a complete facies succession representing various environments, hence a regional fining or coarsening upward tendency can be determined by application of statistics

3.1.5 Calcrete

The occurrence of pedogenic carbonate deposits is not normally considered to be a type of sedimentary structure (Nwajide 1987), but carbonate nodules and concretions may be taken as irregular structures since they originate post-depositionally and invariably tend to deform the original bedding (Collinson and Thompson, 1982), hence its disruptive tendency makes it a defomational structure (chemically induced).

In the study area, the occurence of calcrete nodules in a horizon was observed in Location 3 (Fig 6), within a clay-unit having a maximum thickness of about 5 cm.

The nodules are discontinous, the calcrete horizon having a total length of about 3 m. Nodule sizes increase from the edges to the central portion of the horizon, occuring within a greyish clay unit with cracks.

Macroscopically, the calcrete appears whitish to greyish, highly indurated, breaking into rounded nodules and dery matrix. In thin section, calcrete contains corrided, poorly sorted, subangular - angular quartz

grains (nuclei) coated with calcite, minor feldspar, and iron minerals. There is no contact between quartz grains and the groundmass which is microcrystalline calcite.

The origin of calcretes in soil profiles has had considerable attention from sedimentologists and pedologists (Reeves, 1970; Steel, 1974; Allen, 1974; Arakel, 1982, etc). Since the calcrete found within the area of study occurs in clastic beds, the main mode of origin may be reasonably assumed to be by precipitation (Collinson and Thompson, 1982). Reeves (1970) and James (1972) observed that the ideal environment for calcrete formation is neither too arid nor too humid, and as such calcrete does not characterise any particular climatic regime . They contend that too little moisture allows only surface accumulation of carbonate while excessive moisture and relief causes regional leaching of soil solubles. Nwajide (1987) believes an alternating periods of rainfall and intense evaporation is necessary for calcrete formation. Hence the occurence of calcrete in the study area can be easily explained with the low relief, alternating wet and dry climate and moderate moisture. The most probable source of carbonate is likely to be the carbonate rich loess and wind blown calcium sulphate from gypsum which Nwajide (1987) postulates is contained in the well known saharan dust known as the Northeast trade wind. Other surface sources of carbonate are decay of leaf litter and other vegetable matter (Goudie, 1973, p. 136).

3.2 Hydrodynamics

Hydrodynamic control is important in the formation of physical syn-depositional sedimentary structures, examples of which are cross-bedding and graded bedding discussed above. Their hydrodynamic control is essential to understand the

regime most favourable for their origin.

The downstream migration of ripples, sand waves, and dunes under conditions of net sedimentation give rise to cross-stratification. The interaction of a fluid with a non-cohesive material such as sand produces features like ripples and antidunes. Current ripples, sand waves and dunes are downstream - migrating bedforms produced by unidirectional Aqueous flows, their formation depends on the flow strength and the sediment grain size (Fig 11). There are small scale ripples and large scale ripples (megaripples). Small scale ripples are small bedforms with gentle upstream slopes and steep downstream slopes. The lowest velocity capable of producing small ripples (hence small scale cross-bedding) in fine sand is about 20 cm/sec (Reineck and Singh, 1978) while Rees (1966) gives current velocities of 8 - 15 cm/sec for producing ripples (hence cross-beds) in clay free silt. Bagnold (1956) states that small ripples cannot exist in quartz sands of mean diameter greater than about 0.67-0.71 mm, while Simons *et al.*, (1965) accepts a mean diameter of 0.6 mm for the upper limit of small ripples. Generally flow conditions under which ripples, sandwaves and dunes are formed are referred to as lower flow regime (that is, Froude number < 1) where Froude number, F

$$= V/(gh)^{1/2}$$

where V = flow velocity

g = acceleration due to gravity

h depth of flow

F < 1 characterises tranquil flow at which bedforms of lower flow regime are stable while F > 1 characterises rapid flow in which bedforms of upper flow regime are stable.

Graded bedding could result from either (1)

sedimentation from a current gradually decreasing in velocity and competency, or (2) sedimentation from a suspension in which all sizes are carried and out of which they settle. Hence graded bedding is not flow regime restricted.

3.3 Paleocurrent Indicators and Reconstruction

Various structures and components occur in sedimentary rocks which permit some inferences regarding paleoflow directions of ancient streams, regional paleoslope patterns, strand line configuration and other paleogeographic features (Royce, 1970). These are vectorial properties which include cross-bedding, current lineation, ripples marks, oriented fossils, sole markings and grain fabric. The concern in the present study in determining paleoflow is with cross-bedding. This is very ubiquitous within the area of study with a 3-dimensional geometry with specific azimuths of maximum dip direction, dip angle and strike of bedding. Table 3.1 shows readings of azimuths, strike and dips obtained from each location, obtained by the use of Bruton compass. The method of Royce (1970) was used for grouping the readings into classes of 30°

According to Potter and Pettijohn (1977) the vector mean of grouped data for an individual outcrop is obtained as

$$X = \tan^{-1} W/V$$

where $$W = \sum_{i=1}^{n} n_i \text{ Sin } X_i$$

where $V = \sum_{i=1}^{n} n_i \text{ Cos } X_i$

where X_i = midpoint azimuth of the i^{th} class interval

X = azimuth of resultant vector

n_i = number of observations in the i_{th} class

n = total number of observations.

The magnitude or length of the resultant vector is

$$R = (V^2 + W^2)^{1/2}$$

while magnitude of resultant vector in percent is

$$L = (R/n)100$$

Table 3.2 below depicts statistical analysis of azimuth readings for each location. Based on values, (resultant vector, magnitude of the resultant, and standard deviation) rose diagrams were prepared for each location, which gives the regional paleocurrent map a preferred northerly paleoflow direction (Fig 12), with a regional vector mean of 359° (NNW). Current roses for most locations show strong unimodal trends (locations 1, 3, 4 and 9) while polymodal roses were obtained for locations 2, 7 and 8, although the polymodality are still marked by strong modes.

According to Potter and Pettijohn (1977) virtually all alluvial, eolian and deltaic environments have unimodal current roses, while tidal environments characteristically have bipolar roses whereas some marine shelf sandstones may in addition have polymodal as well as unimodal cross-bedding orientation, but tidal environments cannot be completely ruled out as a possible depositional setting for sediments of the study area.

The strong unimodality of our current roses and supporting evidence given by results of paleoenvironmental discrimination carried out in chapter 4 gives support to an alluvial setting coupled with the thick sequences recorded.

Table 3.2 Statistical analysis of azimuth readings to obtain resultant vectors (azimuth) for locations 1,2,3,4,7,8 and 9

Class	ni	xi	niSinxi	niCosxi	
				Location 1	$X_v = \tan_{-1}$ (7.464/13.392)
I	1	0	0	1	
II	10	30	5.000	8.660	
III	4	60	3.464	2.000	= 29° 8'
IV	–	90	0	0	$R = (7.464^2 + 13.392^2)^{1/2}$
V	–	120	0	0	= 15.332
VI	–	150	0	0	L = (R/n).100
VII	–	180	0	0	
VIII	–	210	0	0	= (15.332/17) x 100
IX	–	240	0	0	
X	–	270	0	0	= 90.188 %
XI	–	300	0	0	
XII	2	330	– 1.000	1.732	
	17		7.464	13.392	
				Location 2	$X_v = \tan_{-1}$ (3.634/6.098)
I	3	0	0	3.000	
II	3	30	1.500	2.598	
III	2	60	1.732	1.000	= 30° 48'
IV	4	90	4.000	0	$R = (3.634^2 + 6.098^2)^{1/2}$
V	–	120	0	0	= 7.099
VI	–	150	0	0	L = (R/n).100
VII	2	180	0	–2.000	
VIII	–	210	0	0	= (7.099/18) x 100
IX	–	240	0	0	
X	1	270	–1.000	0	= 39.439 %
XI	3	300	–2.598	1.500	
XII	–	330	0.000	0	
	18		3.634	6.098	

Table 3.2 (Cont'd)

Class	ni	xi	niSinxi	niCosxi	
			Location 3		
					$X_{\circ} = \tan^{-1}(-2.232/4.866)$
I	4	0	0	4.000	
II	–	30	0		
III	–	60	0		$= 335° 22'$
IV	–	90	0		$R = (-2.232^2 + 4.866^2)^{1/2}$
V	–	120	0		$= 5.354$
VI	–	150	0		$L = (R/n).100$
VII	1	180	0	-1.000	
VIII	–	210	0		$= (5.354/8) \times 100$
IX	–	240	0		
X	–	270	0		$= 66.925\ \%$
XI	2	300	-1.732	1.000	
XII	1	330	-0.500	0.866	
	8		-2.232	4.866	
			Location 4		
					$X_{\circ} = \tan^{-1}(14.990/24.892)$
I	7	0	0	7.000	
II	8	30	4.000	6.928	
III	19	60	16.454	9.500	$= 31° 3'$
IV	5	90	5.000	0	$R = (14.990^2 + 24.892^2)^{1/2}$
V	2	120	1.732	-1.000	$= 29.057$
VI	1	150	0.500	-0.866	$L = (R/n).100$
VII	2	180	0	-2.000	
VIII	–	210	0	0	$= (29.057/60) \times 100$
IX	2	240	-1.732	-1.000	
X	5	270	-5.000	0	$= 48.428\ \%$
XI	4	300	-3.464	2.000	
XII	5	330	-2.500	4.330	
	60		14.990	24.892	

Table 3.2 (Cont'd)

Class	ni	xi	niSinxi	niCosxi	
					Location 7
					$X_{\sim} = \tan^{-1}(-12.062/22.160)$
I	10	0	0	10.000	
II	3	30	1.500	2.598	
III	1	60	0.866	0.500	$= 331^{\circ}\ 26'$
IV	-	90	0	0	$R = (-12.062^2 + 22.160^2)^{1/2}$
V	-	120	0	0	$= 25.230$
VI	1	150	0.500	-0.866	$L = (R/n).100$
VII	1	180	0	-1.000	
VIII	1	210	-0.500	-0.866	$= (25.230/37) \times 100$
IX	-	240	0	0	
X	3	270	-3.000	0	$= 68.189\ \%$
XI	8	300	-6.928	4.000	
XII	9	330	-4.500	7.794	
	37		-12.062	22.160	
					Location 8
					$X_{\sim} = \tan^{-1}(-9.830/6.366)$
I	2	0	0	2.000	
II	1	30	0.500	0.866	
III	2	60	1.732	1.000	$= 302^{\circ}\ 56'$
IV	1	90	1.000	0	$R = (-9.830^2 + 6.366^2)^{1/2}$
V	0	120	0	0	$= 11.711$
VI	0	150	0	0	$L = (R/n).100$
VII	1	180	0	-1.000	
VIII	3	210	-1.500	-2.598	$= (11.711/24) \times 100$
IX	0	240	0	0	
X	4	270	-4.000	0	$= 48.796\ \%$
XI	7	300	-6.062	3.500	
XII	3	330	-1.500	2.598	
	24		-9.830	6.366	

Table 3.2 (Cont'd)

Class	ni	xi	niSinxi	niCosxi	
					Location 9
					$X_{\circ} = \tan^{-1}(-3.598/11.964)$
I	7	0	1.000	7.000	
II	2	30	0	1.732	
III	-	60	0	0	$= 343^{\circ}\ 15'$
IV	-	90	0	0	$R = (-3.598^2 + 11.964^2)^{1/2}$
V	-	120	0	0	$= 12.493$
VI	-	150	0	0	$L = (R/n).100$
VII	-	180	0	0	
VIII	-	210	0	0	$= (12.493/15) \times 100$
IX	-	240	-1.000	0	
X	1	270	-2.598	0	$= 83.287\ \%$
XI	3	300	-1.000	1.500	
XII	2	330	-3.598	1.732	
	15		-2.232	11.964	

CHAPTER FOUR

MINERALOGY AND SIZE ANALYSIS

4.1 Scope of Work

This chapter involves the microscopic examination of the mineralogic characteristics of the various facies states present in the area of study (in contrast to description given in Chapter 2, which are essentially macroscopic), by the study of the framework elements (Quartz, Feldspar and rock fragments), matrix and cement composition, which would be used in the classification of sandstones especially. The fabric of the facies states are also studied, based on grain relations, orientation, shape and roundness. Analysis of heavy minerals has been undertaken, to study occurences of heavy minerals within the various facies for possible provenance evaluation.

The next stage in this chapter is size analysis, which involves pebble morphometry and sieve analysis for paleoenvironmental diagnosis.

4.1.1 Framework Elements

4.1.1.1 Quartz

This is the predominant framework mineral in all facies units studied. Percentage of quartz by volume varies from greater than 95 per cent in the sandstone-siltstone facies to about 75 per cent in ironstone facies where iron-oxide cement has been introduced diminishing the percentage of quartz. Both mono and polycrystalline varieties of quartz are observed, with monocrystalline: polycrystalline ratio as high as 4:1. Quartz crytals constituting polycrystalline types seldom exceed 5, mostly between 2 - 5 range, which according

to Folk (1980) are typical of schists or recrystallized metamorphic terrain and to a small extent in granites. Quartz of the sandstone, siltstone and clay units are fractured (Plate 12) with a single quartz crystal, having as much as 8 crystal units; this is however not observed in quartz of the ironstone facies. The mono-crystalline: polycrystalline quartz ratio in the ironstone facies is even higher than in other facies. Undulatory extenction is common in most quartz crystals in all facies units, an indication of stress in environment of derivation of such quartz (Folk, 1980). Undulose and straight extinction are commonly displayed by quartz. Quartz are generally euhedral and less often subhedral. Vacuoles are also abundnat in some quartz grain giving a bubbly appearance. Composite and semi-composite quartz grains are abundant in all facies except the ironstone occurring as equant interlocking grains with straight boundaries, but not always in optical continuity. Commong mineral inclusions in quartz are zircon (most abundant), rutile and biotite (Plate 13). Overgrowths in quartz are displayed in closely packed units usually in optical continuity with the original quartz grain, sometimes separated by hematite or clay and without inclusions.

4.1.1.2 Feldspar

Feldspars observed have been mostly altered into clay minerals. Feldspar identified are in an alteration transition stage into clay minerals hence their composition cannot be easily determined. They are usually cloudy and with distinct twining (kPlate 14). Feldspar has been

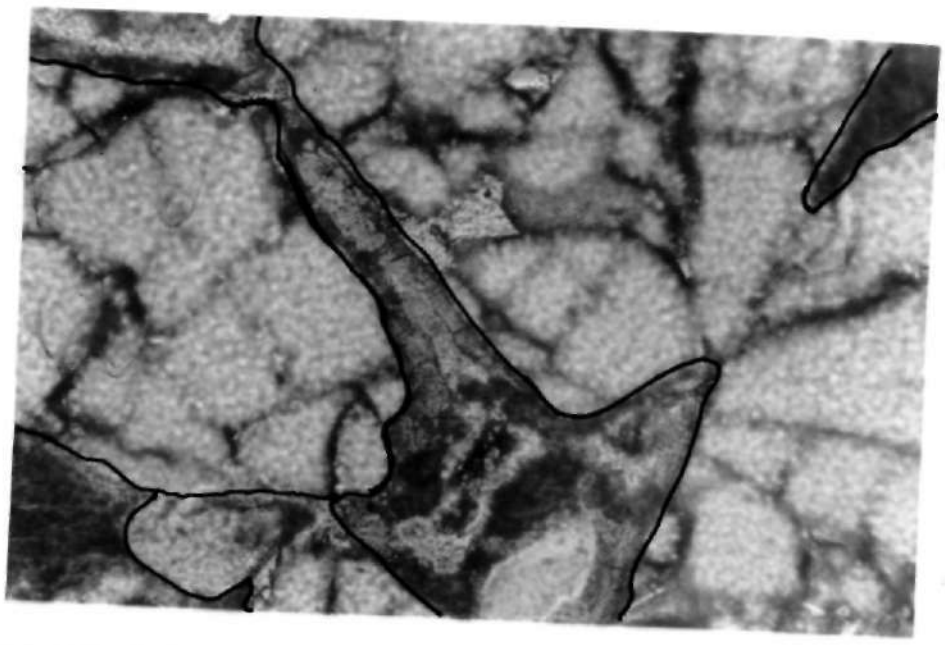


Plate 12: Composite (fractured) Quartz crystals within a Basal Sandstone unit. (Magnification x 16).

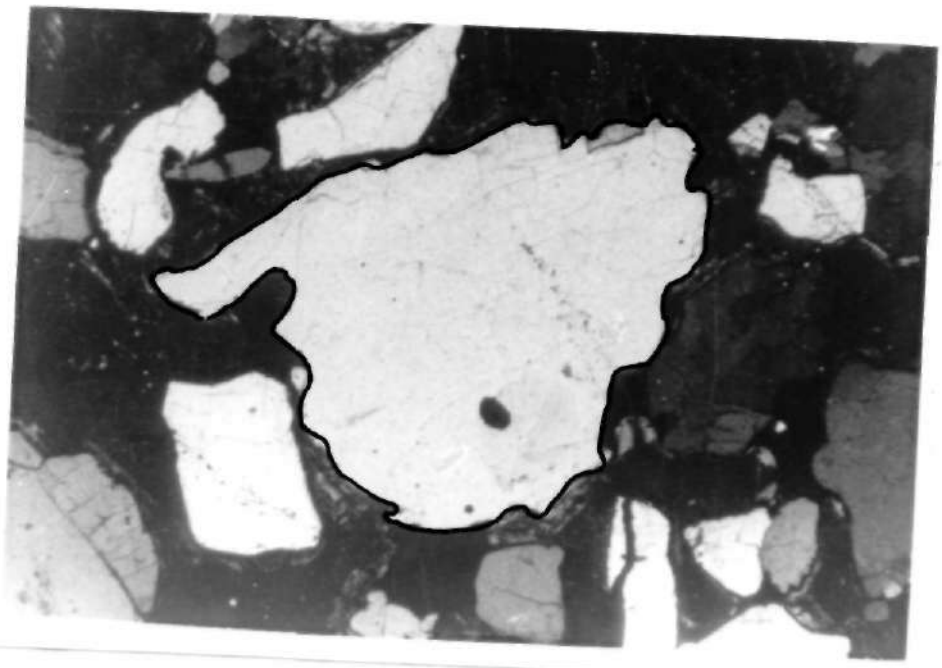


Plate 13: Quartz crystal with zircon and biotite inclusions. (Magnification x 6.3)

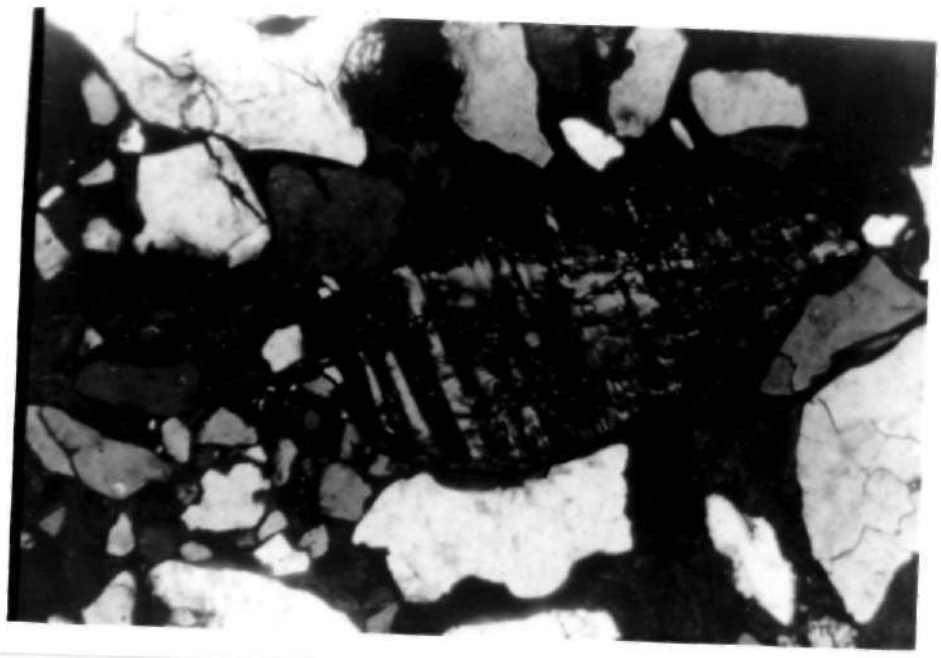


Plate: 14 Partially decomposed feldspar displaying albite twinning (Magnification x 6.3).

identified within sandstone, silstone and ironstone units, apprearing colourless in plane polarized light and brownish to yellowish under crossed nicols with albite twining, (Plate 14). They comprise less than 0.5 per cent of total composition of the thin sections (2FR1, 8FR2) where they occur, and in most cases do not exist at all either in fresh or altered forms. Feldspar commonly occurs embedded within clay mineral matrix or iron oxide cement giving rise to little or no contact with quartz. The sparse occurrence of feldspar can easily be explained as due to its susceptibility to destruction by transportation, erosion and weathering.

4.1.1.3 Rock Fragments

Common rock fragments observed are foliated fragments of older rocks (metamorphic). They are commonly found in all facies units but to a lesser extent in the ironstone. Foliated rock fragments exhibiting distinct cleavage and platy characterisitics are interpreted by Blatt et al., (1980) as metamorphic rock fragments precisely of gneiss migmatite or schistose origin. Rock fragments make up about 10 per cent of the volume of sandstone, and stilstone units.

4.1.2 Matrix

Matrix is made up of clay minerals and iron hydroxides in all lithofacies studied. Clay mineral types include: kaolinite (most abundant), gibbsite, and chlorite. The sandstone, siltstone and clay units are characterised by kaolinite and chlorite minerals while the ironstone facies matrix is made up of predominantly kaolinite and less commonly gibbsite.

Kaolinite occurs as colourless to weakly coloured fine grained agregates appearing as dusty alteration of feldspar (Plate 15) or as cloudy aggregates, with weak to nil birefringence (White or grey). Chlorite appears coloureless to pale green and yellow, and as tiny flakes (fibrous), foliated, fine grained, and pleochroic. On the other hand gibbsite is coloureless to pale brown occuring as whorls or botryoidal or stalactitic forms. Gibbsite is fibrous and fine grained too.

In as much as the occurence of other clay mineral types (montomorillinite, illite, etc) have not been observed their occurence if any, would be negligible. Generally the matrix of the various facies units make up between 20 - 30 per cent of the entire volume of the lithofacies with a higher matrix percentage in the sandstone, siltstone and clay units than in the ironstone unit.

4.1.3 Cement

Cement is the chemically precipitated mineral material that occurs in the spaces among the individual grains of a consolidated sedeimentary rock (Gary et al., 1974). Within all units studied (sandstone, siltstone, clay and ironstone) the cement is made up of

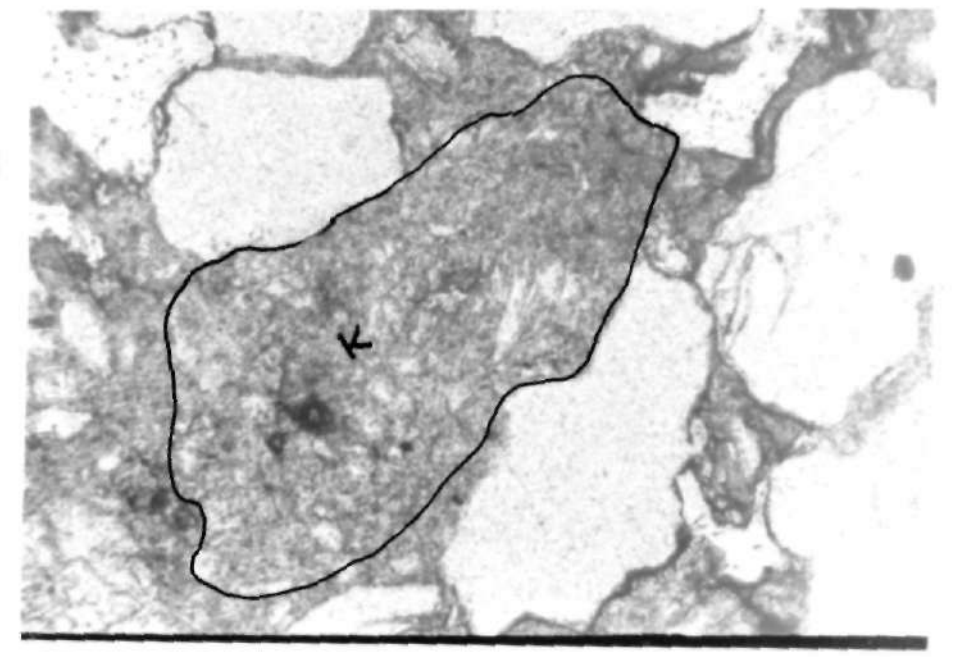


Plate 15: Kaolinite (in thin Section) occuring as the dominantly, cloudy clay mineral matrix in a Siltstone unit.
(Magnification x 6.3)

oxides and hydroxides of iron. These include in order of abundance hematite, geothite, limonite and very rarely siderite, pyrite and magnetite. The hematite cement cuts across facies boundaries while limonite, siderite and magnetite are observed only in the ironstone facies units.

Hematite is distinguished from other iron oxide minerals and most opaque minerals by red internal reflections in reflected light and blood red colour. Hematite occurs as cement within the interstices of framework elements. Reniform or botryoidal forms are common and are the major components of the Oolites in the Oolitic Ironstone unit (Plate 8.) It is the most abundant (by volume) of all ironoxide cement present. Goethite occurs as fibrous, highly colour yellow to brown, acicular or botryoidal forms, with distinct colour banding (Plate 16), can be distinguished from hematite by the opaque or distinctly reddish colour of hematite. Limonite, on the other hand apears yellow to yellowish brown showing colloform structure, resulting in an indistinct boundnary with co-existing geothite (which can also be classified as cement). Siderite, pyrite and magnetite are observed only as local occurences, with pyrite occuring opaque and yellowish in surface relfection, siderite appears as colourless to pale yellow, oolitic with isochromatic rings, while magnetite ocfurs opaque in section and grey in relfected light.

Percentage of cement by volume increases from the basal sandstone facies units upwards becoming most predominant in the ironstone facies. The upper level ironstone facies units might have been responsible for the introduction of ironoxide cement into the lower sandstone, siltstone

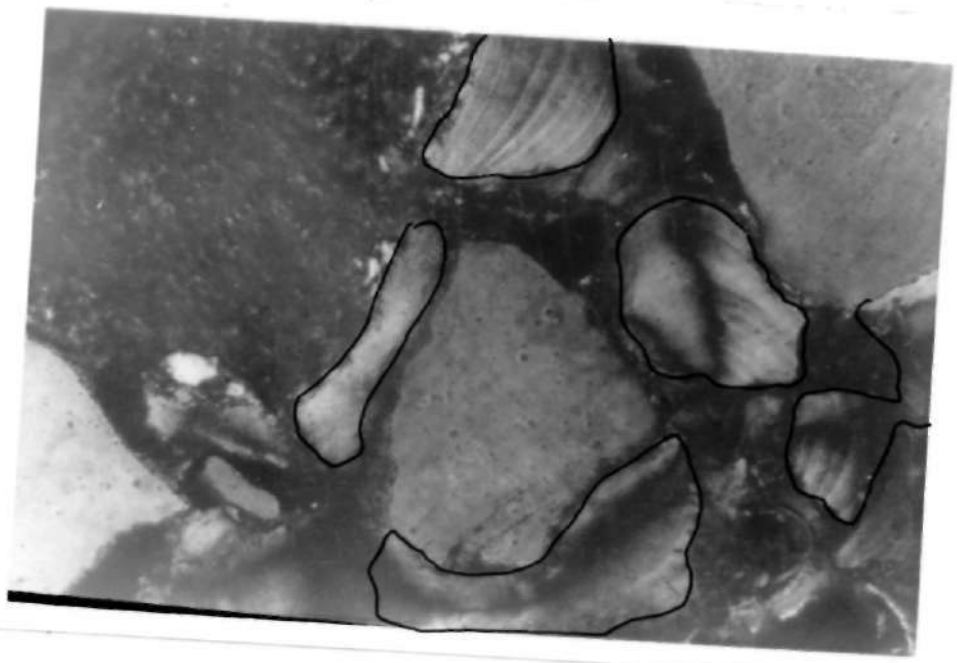


Plate 16: Goethite occuring as matrix element in a basal sand-stone unit. (Magnification x 16)

4.2 Fabric

According to Friedman and Sanders (1978), the fabric of a sediment refers to the arrangement of particles (or crystals) in terms of their (1) Orientation of shape and size (2) Mineral composition (3) Packing and (4) Sorting.

Another factor considered in this work under fabric is roundness of grains, while the second factor above (mineral composition) has already been discussed in the previous section (4.1.1), hence would not be repeated.

4.2.1 Grain Sizes

There is a general decrease in grain size from the basal sandstone units upwards through the siltstone, claystone units with the smallest framework and matrix grain sizes in the ironstone units, this could be due to increased reworking, hence a fining upward sequence, or an increased distance of transportation or could even reflect differential intensity of weathering of framework and matrix elements. Basal sandstone are generally poorly sorted with both coarse and fine grain sizes coexisting (Plate 17) while the siltstone facies units display uniform medium sized grains and the claystone units are fine grained. The ironstone units are of equigranular grains (well sorted) with grain sizes in the fine - medium range (Plate 18).

4.2.2 Grain Relation

This factor expresses the type of relationship existing between grains, that is, types of grain contact. Type of contact exhibited by any rock type would depend on degree of packing or post depositional distruption of fabric (or previous packing). There is no clear preference of grain relationship between different facies studied. All units

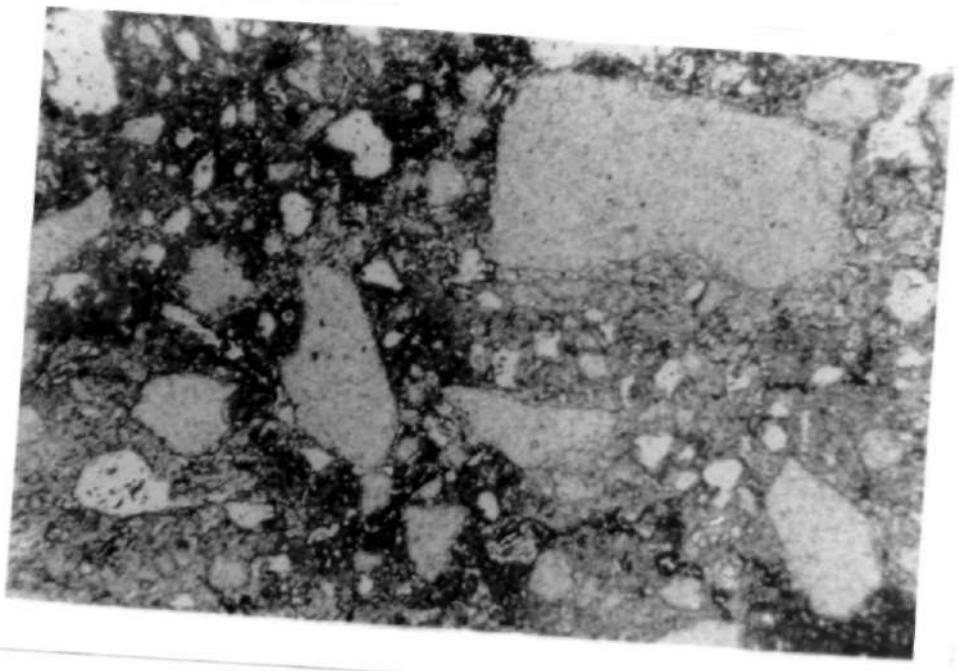


Plate 17: Poorly sorted Basal Sandstone
(Magnification x 6.3)

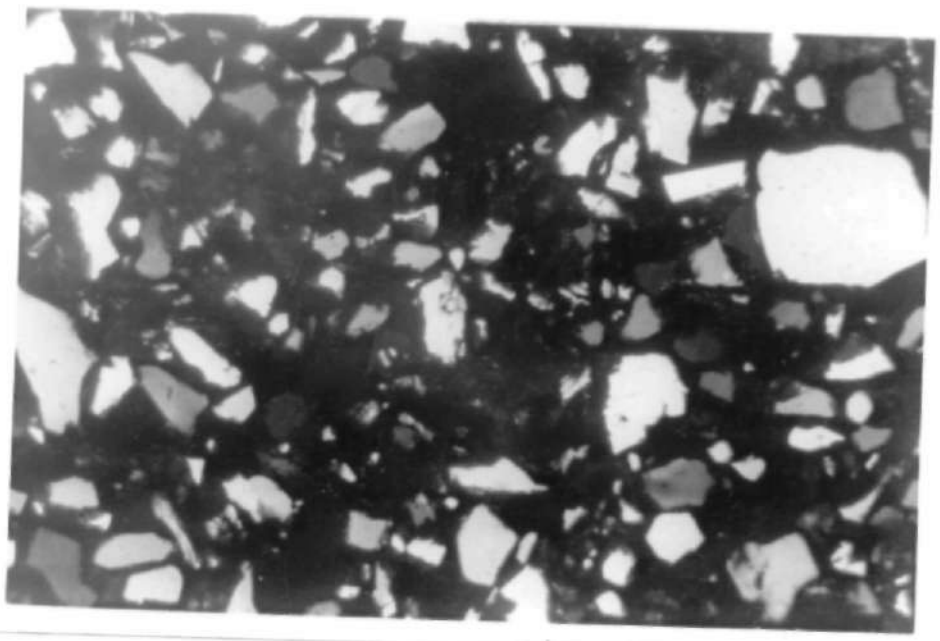


Plate 18: Floating grain fabric of ironstone, with equiangular well sorted quartz crystals

(Magnification x 6.3)

and clay units by groundwater migration, that is, introduced by downward migration of iron oxide minerals.

display point, line, sutured and concavo-convex contracts. Packing within the ironstone units is relatively loose compared to the sandstone, siltstone, and claystone units. In the sandstone, siltstone and claystone units, grain contacts are hindered by the presence of abundant matrix, while in the ironstone units grain contacts are hindered mainly by iron-oxide cement. However, it was observed that the degree of grain contact is directly related to the amount of matrix and cement present, that is the higher the amount of cement and matrix, the lower the number of grains having contacts. "Floating" grain fabrics are also common, especially in the sandstone, and ironstone units (Plate 17 and 18), although compact arrangement of grains also occur in Basal sandstone.

4.2.3 Grain Orientation

There is no preferred orientation of framework elements within any of the units studied. This is equally significant in itself, as the preferred orientation of framework grains indicates the direction of depositing currents, while the non-preference of a direction could also be indicative of multidirectional current or post-depositional distruption of iriginal orientation (Nwajide, Personal Communication).

4.2.4 Grain Shape and Roundness

Classification of shape and roundness is based on the format of Shepard and Young (1961 Fig. 1), presented in Fig. 13. Generally the sandstone, siltstone, claystone units, have average grains that are subangular to subrounded (3 - 4) while the ironstone units are more rounded with average of subrounded to rounded (5 - 6). Table 4.7 shows mean grain.....

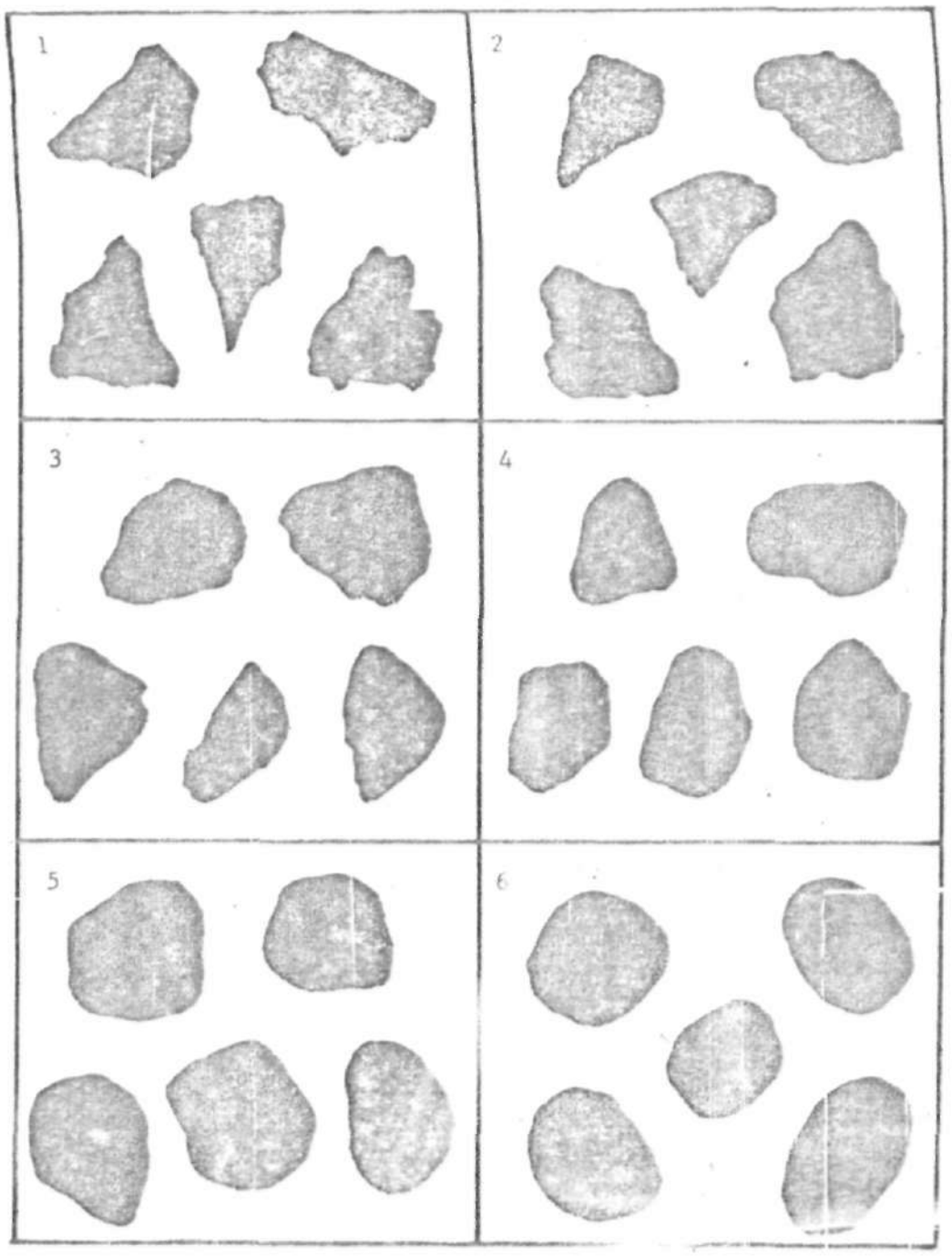


Fig. 13. - Six classes for visual estimation of particle roundness. Redrawn from Shepard and Young (1961, Fig. 1). 1 = very angular; 2 = angular; 3 = sub-angular; 4 = sub-rounded; 5 = rounded; 6 = well-rounded.

shape and roundness values from thin section and binocular studies for all 4 units studied.

4.3 Heavy Mineral Analysis

Minerals with specific gravities greater than 2.85 are defined as "heavy" whereas those of lesser specific gravity are referred to as "light" (Royce, 1970).

Procedure

In this study, solution of tetrabromethane ($CHBr_3$) is used as the separating medium. Having sieved all 33 samples (Refer 4.4), a 5 gm portion of the 355 - 500 microns interval (mixed) samples were introduced into tetrabromethane in a separating funnel and stirred well, after which they are left for maximum separation to be achieved (when no discernible grain movement occurs). The "Sinks"(heavy) fractions were separated into labelled filter papers, and the float (light) fractions in other labelled filter papers. Excess bromoform was drained off into beaakers for reuse. The separating funnels were washed with acetone, and also the filter papers, removing any remaining tetrabromethane with the acetone at the completion of separation of each sample. These procedures were carried out in a fume cupboard, as a safety precaution.

The samples on filter papers were placed under infra-red lamps, for both sinks and floats to dry. Once dried each fraction was weighed and labelled, using the sample reference number. The dried sink samples were then mounted on slides, for identification by a petrographic microscope.

4.3.1 Result

The heavy mineral population are dominated by the opaques (between 80 - 95 per cent with an estimated average of 90 per cent), zircon, tourmaline,and ritile. Sillimanite, topaz, hornblende,kyanite, garnet, and staurolite are present in accessory amounts. Table 4.1 shows percentages of light and heavy minerals present in samples analysed.

Close study by reflected light shows that the opaques comprise ilmenite, hematite, limonite, magnetite (?) and traces of leucoxene. The grains are commonly anhedral and angular. Many sub angular to subrounded grains also occur. Plate 20 shows hematite grain occuring as subangular, while rounded grains are rare.

Zircon is next to the opaques in the order of abundance. It forms between 3 to 20 per cent of the total heavy mineral populations, with an estimated average of 10 per cent. The most common forms are angular, prismatic, enhedral to subhedral. Zircon shows a higher degree of roundness than other heavy minerals with etched or pitted surfaces and probably gas bubbles as inclusions (Plate 21).

The next major mineral, tourmaline forms from 0.1 to 9 per cent of the heavy mineral population, with an estimated average of 3 per cent. Both angular, small to medium size, prismatic, enhedral to subhedral forms and large grains are present. The bluish and black varieties of tourmaline are mostly present (Plate 22).

Rutile may be entirely absent or make up about one per cent (1%) of the heavy mineral population with an estimated average of 0.5 per cent. The dark red and black varieties are present, usually anherdal and needle like (Plate 23).

Topaz, hornblende and sillimanite occur as large angular grains. Topaz appear · irregular, or as cleavage fragments.

Table 4.1 Weight Percentages of Light and Heavy Minerals

Sample No.	Light Minerals		Heavy Minerals	
	Wt (gm)	Percentages (%)	Wt (gm)	Percentages (%)
$1FR_1$	4.90	97.96	0.10	2.04
$1FR_2$	4.92	98.37	0.08	1.63
$1FR_3$	4.85	96.91	0.15	3.09
$2FR_1$	4.85	96.91	0.15	3.09
$2FR_2$	4.82	96.27	0.18	3.73
$2FR_3$	4.88	97.55	0.12	2.45
$2FR_4$	4.90	97.96	0.10	2.04
$3FR_1$	4.90	97.96	0.10	2.04
$3FR_2$	4.95	98.99	0.05	1.01
$4FR_1$	4.95	98.99	0.05	1.01
$4FR_2$	4.89	97.75	0.11	2.25
$4FR_3$	4.85	96.91	0.15	3.09
$4FR_4$	4.89	97.75	0.11	2.25
$4FR_5$	4.84	96.69	0.16	3.31
$4FR_6$	4.81	96.05	0.19	3.95
$4FR_7$	4.87	97.33	0.13	2.67
$4FR_8$	4.92	98.37	0.08	1.63
$7FR_1$	4.81	96.05	0.19	3.95
$7FR_2$	4.83	96.60	0.17	3.40
$7FR_3$	4.88	97.55	0.12	2.45
$7FR_4$	4.91	98.20	0.09	1.80
$7FR_5$	4.83	96.60	0.17	3.40
$7FR_6$	4.86	97.20	0.14	2.80
$7FR_7$	3.98	79.60	1.02	20.40
$8FR_1$	4.80	96.00	0.20	4.00
$8FR_2$	4.95	98.99	0.05	1.01
$8FR_3$	4.83	96.60	0.17	3.40
$8FR_4$	4.87	97.33	0.13	2.67
$8FR_5$	4.82	96.27	0.18	3.73
$9FR_1$	4.83	96.60	0.17	3.40
$9FR_2$	4.85	96.91	0.15	3.09
$9FR_3$	4.81	96.05	0.19	3.95
$9FR_4$	4.80	96.00	0.20	4.00
MEAN	4.838	96.705	0.162	3.295

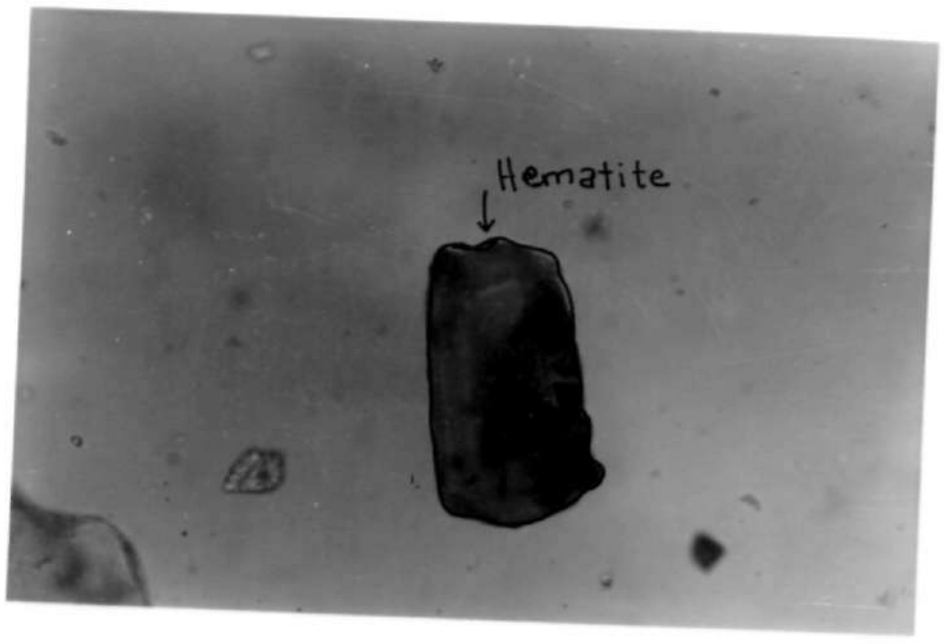


Plate 19: Hematite 'as a heavy mineral) occurring as subangular - sub rounded grains.

(Magnification x 16)

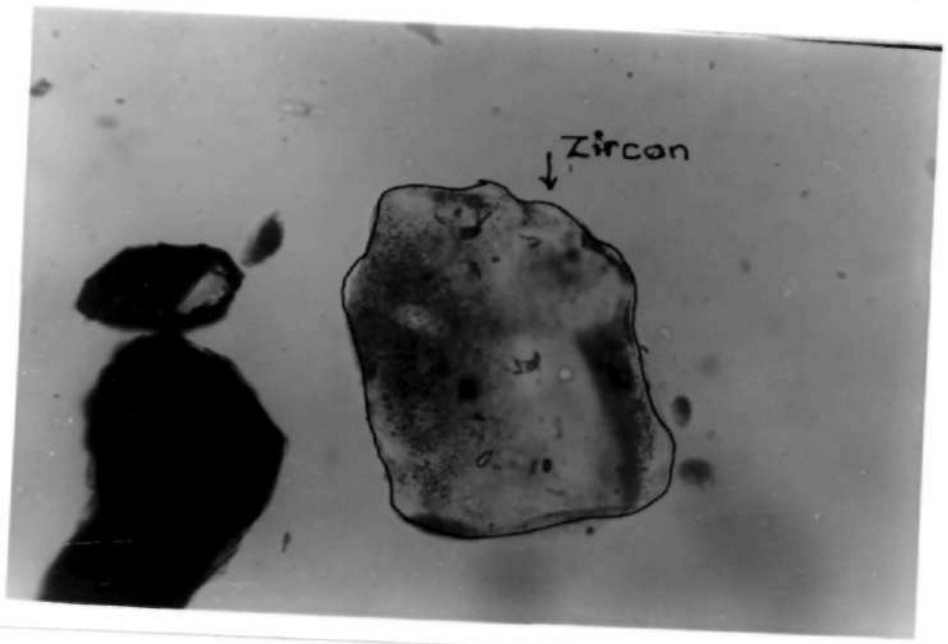


Plate 20: Zircon (as a heavy mineral), showing a high degree of roundness, with etched and pitted surface. (Magnification x 16).

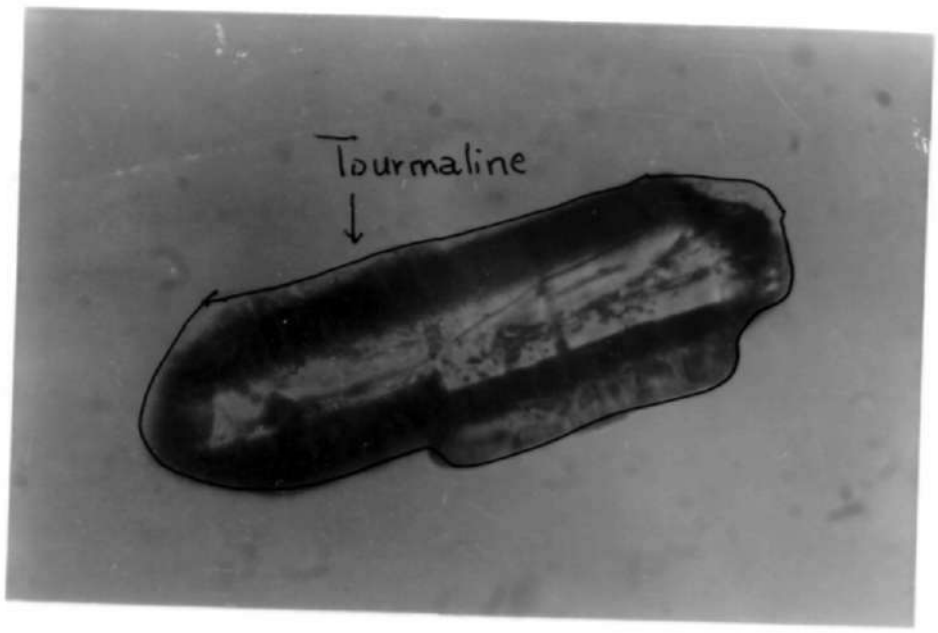


Plate 21: Tourmaline (as a heavy mineral) occuring as prismatic, subhedral grain. (Magnification x 16).

Hornblende occurs as cleavage fragment with ragged ends appearing very dark to pale green displaying distinct colour zoning while sillimanite occurs as flattened or slender grain, colourless with high birenfringence. Kyanite occurs as pale blue bladed to columnar fibrous to splintery fragments. Garnet occurs characteristically reddish without cleavage but conchoidal fracture. Lastly, staurolite occurs as dark to reddish brown, rectangular to prismatic and irregular fragments (sometimes yellowish brown).

These accesory "heavies" make up a negligible percentage (about 0.05 per cent) of the entire heavy mineral population.

4.3.2 Environmental Implication

The heavy mineral content is a function of five very complex variables. The five variables are (Folk, 1980)

(1) Lithology of the source area
(2) Differential stability of minerals to weathering in source area.
(3) Durability of mineral to long continued abrasion
(4) Hydraulic factor - differential transportation of minerals based on shape and specific gravity leading to changes in mineral ratio
(5) Post-depositional survival factor; or intrastratal solution or surficial weathering of less stable minerals.

Of all the five variables stated above the first (lithology of source area) is the most important variable to which heavy mineral analysis is used in inferring, and which this work is most particular in determining.

Pettijohn (1975) gave characteristic suites of detrital mineral for different source rocks (Table 4.2). The table displays detrital suites for 6 source rock types, with overlaps of detrital minerals recorded consistently. Inference

Table 4.2 Detrital mineral suites characteristic of source rock types

Reworked Sediments	
Barite	*Leucoxene*
Glauconite	*Rutile*
Quartz (especially)	*Tourmaline*, rounded
with worm overgrowth)	*Zircon* rounded
Chert	
Quartzi te fragments (ortho-	
quartzite type)	
Low-rank Metamorphic	
Slate and phyllite fragments	*Quartz* and quartzite frag-
Biotite and *muscovite*	ments (metaquartzite type)
Feldspars generally absent	*Tourmaline* (small pale
Leucoxene	brown euhedra carbonate
	inclusions)
High-rank Metamorphic	
Garnet	*Quartz* (metamophic variety)
Hornblende (blue-green	*muscovite* and biotite
variety)	
Kyanite	Feldspars (acid plagioclase)
Sillimanite	Epidote
Andalusite	Zoisite
Staurolite	*Magnetite*
Acid igneous	
Apatite	*Zircon*, euhedra
Biotite	*Quartz* (igneous variety)
Hornblende	Microcline

Table 4.2 Detrital mineral suites characteristic of source rock types

Monazite	Magetite
Muscovite	*Tourmaline*, small pink
Sphene	euhedra
Basic igneous	
Anatase	*Leucoxene*
Augite	Olivine
Brookite	*Rutile*
Hypersthene	Plagioclase, intermediate
Ilmenite and Magnetite	Serpentine
Chromite	
Pegmatite	
Fluorite	*Muscovite*
Tourmaline, typically blue	
(indicolite)	*Topaz*
Garnet	Albite
Monazite	Microline

– Pettijohn (1975)

of source rock can be made from this table by noting the highest concentration of heavy minerals observed in this study within a particular source rock type. Based on this assumption a concentration of observed heavy minerals is noticed in the High-low rank metamorphic - Acid igneous - Metaporphic source rock types (Table 4.2).

4.4 PEBBLE MORPHOMETRY

4.4.1 Introduction

The purpose of pebble morphometry is to serve as an aid in environmental diagnosis (Nwajide and Hoque, 1982). The sandstone siltstone and clay units of Bida and Enagi Formations contain pebbles of feldspars and quartz. Pebbles occur in two distinct modes, as pebbles of poorly sorted basal sandstone units and as slightly pebbly sandstones and siltstone, with sharply defined lower parts, with indistinct upper boundaries as pebbles become less frequent in an increasingly sandy groundmass. The thickness of pebble beds ranges between 5 cm and 15 cm averaging 10 cm. The pebbles show neither imbrication nor preferred orientation of their long axes. In the second mode of occurence, pebbles constitute part of a conglomeratic sandstone, with little sandstone matrix. Feldspar and quartz pebbles are both extrabasinal. Feldspar pebbles are infrequent, occuring occasionally as large phenoclasts, mostly tabular in shape. Feldspar pebbles have been discarded in morphometric study because they are too soft to be sampled and are not sufficiently abundant. Quartz (vein quartz) pebbles appear to be the most amenable to morphometric studies; they are most abundant and their original shapes and forms are likely to have been modified only by attrition (Nwajide and Hoque,

1982) rather than feldspars that are easily weathered. A requiremtnt of grain size analysis, which should be met by any measurement technique is that since there may be a relationship between size and mineral species, the technique should be applied to one mineral only (Griffiths, 1967). In the present study, the choice of quartz seems justified.

4.4.2 Method of Study

A total of 134 pebbles were collected. Twenty (20) each from 1FR3, 1FR4, 3FR2, 4FR1, 4FR4, 4Fr6 while fourteen (14) were picked from 4FR3 due to insuficiency of quartz. Pebbles were not picked from 7FR1 because the pebbles ocfuring in this unit are made up of decomposed feldspars.

The pebbles in each batch were washed and numbered serially. The Long (L), Intermediate (I) and Short (S), pebble axes were measured using a Vernier Calipers based on the method recommended by Folk (1980, P. 10), and the roundness of each pebble was estimated using the chart of Shepard and Young (1961) showin in Fig 13. The values of each of the L, I, and S and roudness for the pebbbles were averaged, (Table 4.3).

From these values the following parameters were computed:

(1) Flatness ratio = S/L Sames (1966)

(2) Elongation ratio = 1/L Sames (1966)

(3) Maximum Projection Sphericity = $(S/LI)^{1/3}$

Sneed and Folk (1958).

Table 4.3 Morphometric Analysis of Pebbles

Sample No	S	I	L	S/L	I/L	(L-I)/(L-S)	$(S^2/LI)^{1/3}$	OP Index	Roundness
IFR_5A	0.800	1.300	2.400	0.333	0.542	0.687	0.590	5.624	5
IFR_5B	1.000	1.250	2.100	0.476	0.595	0.773	0.725	5.731	5
IFR_5C	1.600	1.700	3.500	0.457	0.486	0.947	0.755	9.781	5
IFR_5D	0.800	1.150	2.300	0.348	0.500	0.767	0.623	7.669	4
IFR_5E	1.000	1.300	2.300	0.435	0.565	0.769	0.694	6.189	3
IFR_5F	0.750	1.200	2.100	0.357	0.571	0.667	0.607	4.669	4
IFR_5G	1.550	1.900	3.400	0.456	0.559	0.811	0.719	6.821	4
IFR_5H	1.100	1.500	2.000	0.550	0.750	0.556	0.739	1.010	4
IFR_5I	0.700	1.050	2.000	0.350	0.525	0.731	0.616	6.600	4
IFR_5J	0.900	1.250	1.900	0.474	0.658	0.650	0.699	3.169	4
IFR_5K	1.300	1.700	2.350	0.553	0.723	0.619	0.751	2.155	4
IFR_5L	1.100	1.800	2.400	0.458	0.750	0.461	0.654	-0.841	3
IFR_5M	1.250	1.700	3.000	0.417	0.567	0.743	0.674	5.826	4
IFR_5N	1.100	1.400	1.900	0.579	0.737	0.625	0.769	2.159	5
IFR_5O	1.100	1.450	1.900	0.579	0.763	0.562	0.760	1.078	4
IFR_5P	1.100	1.550	2.250	0.489	0.689	0.609	0.703	2.222	4
IFR_5Q	1.100	1.300	2.250	0.489	0.578	0.826	0.745	6.662	3
IFR_5R	1.150	1.600	1.900	0.605	0.842	0.400	0.758	-1.653	6
IFR_5S	0.085	1.800	2.100	0.405	0.857	0.240	0.576	-6.420	6
IFR_5T	1.020	1.600	2.050	0.585	0.780	0.529	0.760	0.502	5
Mean	1.073	1.475	2.305	0.469	0.652	0.649	0.696	3.448	4.300
S.D	0.240	0.245	0.468	0.085	0.116	0.163	0.064	3.847	0.865

Table 4.3 Morphometric Analysis of Pebbles

Sample No	S	I	L	S/L	I/L	(L-I)/(L-S)	$(S^2/LI)^{-1/3}$	OP Index	Roundness
IFR_4A	1.400	2.100	2.650	0.528	0.792	0.440	0.706	-1.137	6
IFR_4B	1.300	2.050	2.650	0.491	0.774	0.444	0.678	-1.131	5
IFR_4C	1.600	3.400	3.800	0.421	0.895	0.182	0.583	-7.558	6
IFR_4D	1.600	2.050	2.500	0.640	0.820	0.500	0.793	0.000	6
IFR_4E	1.050	1.700	2.400	0.438	0.708	0.518	0.647	0.420	6
IFR_4F	1.450	1.850	2.850	0.509	0.649	0.714	0.736	4.210	4
IFR_4G	1.150	1.700	2.400	0.479	0.708	0.560	0.687	1.251	4
IFR_4H	1.450	2.150	2.800	0.518	0.768	0.481	0.704	-0.358	4
IFR_4I	1.500	2.000	2.150	0.698	0.930	0.231	0.806	-3.857	5
IFR_4J	1.550	2.400	3.050	0.508	0.787	0.433	0.690	-1.313	6
IFR_4K	1.450	2.400	3.100	0.468	0.774	0.424	0.656	-1.618	5
IFR_4L	1.600	2.300	3.250	0.492	0.708	0.576	0.700	1.539	4
IFR_4M	1.200	2.400	2.900	0.414	0.828	0.294	0.591	-4.973	4
IFR_4N	1.600	2.350	2.800	0.571	0.839	0.375	0.730	-2.190	4
IFR_4O	1.550	2.200	3.600	0.431	0.611	0.683	0.672	4.247	4
IFR_4P	1.150	2.250	3.000	0.383	0.750	0.405	0.581	-2.471	3
IFR_4Q	1.600	2.200	2.800	0.571	0.786	0.500	0.746	0.000	3
IFR_4R	2.150	2.250	3.400	0.632	0.662	0.920	0.845	6.645	6
IFR_4S	1.700	2.450	3.400	0.500	0.721	0.559	0.703	1.179	5
IFR_4T	2.250	3.100	3.900	0.577	0.795	0.485	0.748	-0.265	6
Mean	1.515	2.265	2.970	0.513	0.765	0.486	0.700	-0.369	4.800
S.D	0.297	0.404	0.474	0.082	0.079	0.166	0.070	3.224	1.056

Table 4.3 Morphometric Analysis of Pebbles

Sample No	S	I	L	S/L	I/L	(L-I)/(L-S)	$(S^2/LI)^{-1/3}$	DP Index	Roundness
$3FR_2A$	0.950	1.150	2.000	0.475	0.575	0.810	0.732	6.520	4
$3FR_2B$	0.950	1.300	1.900	0.500	0.684	0.632	0.715	2.634	5
$3FR_2C$	0.900	1.100	1.550	0.581	0.710	0.693	0.780	3.314	4
$3FR_2D$	0.750	1.000	1.550	0.484	0.645	0.687	0.713	3.870	4
$3FR_2E$	0.950	1.200	1.600	0.594	0.750	0.615	0.778	1.943	5
$3FR_2F$	0.950	1.300	2.000	0.475	0.650	0.667	0.703	3.509	4
$3FR_2G$	0.700	1.550	1.900	0.368	0.816	0.292	0.550	-5.662	4
$3FR_2H$	1.100	1.300	1.750	0.629	0.743	0.693	0.810	3.061	4
$3FR_2I$	0.600	0.850	1.500	0.400	0.567	0.722	0.656	5.551	3
$3FR_2J$	1.000	1.150	1.400	0.714	0.821	0.625	0.853	1.751	5
$3FR_2K$	0.700	1.200	1.600	0.438	0.750	0.444	0.634	-1.268	5
$3FR_2L$	0.900	1.250	1.550	0.581	0.806	0.461	0.748	-0.663	4
$3FR_2M$	0.750	1.050	1.400	0.536	0.750	0.539	0.726	0.718	5
$3FR_2N$	0.550	1.250	1.800	0.306	0.694	0.440	0.512	-1.963	4
$3FR_2O$	0.700	1.000	1.650	0.424	0.606	0.684	0.667	4.339	4
$3FR_2P$	0.600	1.100	1.650	0.364	0.667	0.524	0.583	0.655	4
$3FR_2Q$	0.800	1.050	1.450	0.552	0.724	0.615	0.749	2.090	4
$3FR_2R$	0.850	1.000	1.350	0.630	0.741	0.700	0.812	3.171	3
$3FR_2S$	0.650	1.050	1.500	0.433	0.700	0.529	0.645	0.679	3
$3FR_2T$	0.800	1.200	1.500	0.533	0.800	0.429	0.708	-1.339	4
Mean	0.808	1.153	1.630	0.501	0.710	0.590	0.704	1.646	4.100
S.D	0.152	0.153	0.199	0.104	0.075	0.128	0.089	2.856	0.641

Table 4.3 Morphometric Analysis of Pebbles

Sample No	S	I	L	S/L	I/L	(L-I)/(L-S)	$(S^2/LI)^{-1/3}$	OP Index	Roundness
$4FR_1A$	1.500	2.350	2.800	0.536	0.839	0.346	0.699	-2.871	5
$4FR_1B$	0.650	1.400	1.800	0.361	0.778	0.348	0.551	-4.215	4
$4FR_1C$	1.600	1.900	3.200	0.500	0.594	0.812	0.750	6.247	4
$4FR_1D$	1.450	2.200	2.700	0.537	0.815	0.400	0.707	-1.862	4
$4FR_1E$	1.200	1.550	2.300	0.522	0.674	0.682	0.739	3.480	5
$4FR_1F$	1.000	1.700	2.300	0.435	0.739	0.461	0.635	-0.886	4
$4FR_1G$	1.500	1.800	2.800	0.536	0.643	0.769	0.764	5.023	5
$4FR_1H$	1.200	1.250	2.350	0.511	0.532	0.957	0.788	8.942	4
$4FR_1I$	1.000	1.100	2.550	0.392	0.432	0.935	0.709	11.109	4
$4FR_1J$	0.900	1.200	1.850	0.486	0.649	0.694	0.715	3.786	3
$4FR_1K$	1.100	1.200	2.500	0.440	0.480	0.929	0.739	9.739	3
$4FR_1L$	1.200	1.700	2.250	0.533	0.756	0.524	0.722	0.447	4
$4FR_1M$	1.350	1.400	1.850	0.730	0.757	0.900	0.889	5.481	5
$4FR_1N$	1.250	1.800	2.700	0.463	0.667	0.621	0.685	2.608	4
$4FR_1O$	1.200	1.500	1.900	0.632	0.789	0.571	0.796	1.130	4
$4FR_1P$	1.000	1.800	2.300	0.435	0.783	0.385	0.623	-2.653	4
$4FR_1Q$	0.900	1.100	1.900	0.474	0.579	0.800	0.729	6.329	4
$4FR_1R$	1.200	1.700	2.200	0.545	0.773	0.500	0.727	0.000	3
$4FR_1S$	1.300	1.600	2.000	0.650	0.800	0.571	0.808	1.099	4
$4FR_1T$	1.600	2.200	2.600	0.615	0.846	0.400	0.765	-1.626	3
Mean	1.205	1.623	2.343	0.517	0.696	0.630	0.727	2.565	4.000
S.D	0.252	0.366	0.388	0.090	0.121	0.210	0.072	4.453	0.649

Table 4.3 Morphometric Analysis of Pebbles

Sample No	S	I	L	S/L	I/L	(L-I)/(L-S)	$(S^2/LI)^{1/3}$	DP Index	Roundness
$4FR_3A$	0.900	1.100	2.300	0.391	0.478	0.857	0.684	9.128	3
$4FR_3B$	0.600	1.100	1.800	0.333	0.611	0.583	0.567	2.505	3
$4FR_3C$	0.850	1.100	2.000	0.425	0.550	0.782	0.690	6.646	3
$4FR_3D$	1.150	1.550	1.850	0.622	0.838	0.429	0.773	-1.147	4
$4FR_3E$	1.100	1.250	1.750	0.629	0.714	0.769	0.821	4.280	2
$4FR_3F$	0.800	1.000	1.900	0.421	0.526	0.818	0.696	7.561	3
$4FR_3G$	0.700	1.000	1.400	0.500	0.714	0.571	0.705	1.429	4
$4FR_3H$	0.700	1.000	1.400	0.500	0.714	0.571	0.705	1.429	4
$4FR_3I$	0.950	1.150	1.600	0.531	0.719	0.600	0.732	1.881	3
$4FR_3J$	1.100	1.300	1.600	0.688	0.813	0.600	0.835	1.452	2
$4FR_3K$	0.800	1.200	1.550	0.516	0.774	0.467	0.701	-0.647	4
$4FR_3L$	0.700	0.800	1.300	0.538	0.615	0.833	0.778	6.196	3
$4FR_3M$	0.700	0.900	1.200	0.583	0.750	0.600	0.768	1.713	3
$4FR_3N$	0.700	1.200	1.400	0.500	0.857	0.286	0.663	-4.286	3
Mean	0.832	1.118	1.646	0.513	0.691	0.626	0.723	2.724	3.143
S.D.	0.174	0.185	0.305	0.098	0.118	0.168	0.069	3.685	0.663

Table 4.3 Morphometric Analysis of Pebbles

Sample No	S	I	L	S/L	I/L	(L-I)/(L-S)	$(S^2/LI)^{1/3}$	OP Index	Roundness
$4FR_4A$	1.100	1.700	2.100	0.524	0.810	0.400	0.697	-1.908	4
$4FR_4B$	1.200	1.400	2.000	0.600	0.700	0.750	0.801	4.167	4
$4FR_4C$	1.100	1.200	1.900	0.579	0.632	0.875	0.810	6.477	4
$4FR_4D$	1.350	1.450	2.100	0.643	0.690	0.867	0.843	5.708	4
$4FR_4E$	0.900	1.550	2.200	0.409	0.705	0.500	0.619	0.000	3
$4FR_4F$	1.250	1.300	2.200	0.568	0.591	0.947	0.817	7.870	3
$4FR_4G$	1.000	1.350	1.850	0.541	0.730	0.588	0.737	1.627	4
$4FR_4H$	1.100	1.600	1.900	0.579	0.842	0.375	0.341	-2.159	4
$4FR_4I$	1.000	1.200	1.900	0.526	0.632	0.778	0.760	5.285	4
$4FR_4J$	0.750	1.600	1.750	0.429	0.914	0.150	0.586	-8.159	3
$4FR_4K$	0.950	1.200	1.700	0.559	0.706	0.667	0.762	2.987	3
$4FR_4L$	0.700	1.200	1.800	0.389	0.667	0.545	0.610	1.157	3
$4FR_4M$	1.000	1.050	1.450	0.690	0.724	0.889	0.869	5.638	5
$4FR_4N$	0.900	1.100	1.650	0.545	0.667	0.733	0.764	4.275	3
$4FR_4O$	1.200	1.700	3.550	0.338	0.479	0.787	0.620	8.491	3
$4FR_4P$	1.100	1.600	1.800	0.611	0.889	0.286	0.749	-3.502	3
$4FR_4Q$	0.800	1.050	1.500	0.533	0.700	0.643	0.741	2.683	3
$4FR_4R$	1.000	1.500	1.700	0.588	0.882	0.286	0.732	-3.639	4
$4FR_4S$	0.850	1.200	1.500	0.567	0.800	0.462	0.738	-0.670	3
$4FR_4T$	0.850	1.100	1.650	0.515	0.667	0.688	0.736	3.650	4
Mean	1.005	1.353	1.910	0.537	0.721	0.611	0.717	1.999	3.550
S.D	0.172	0.221	0.445	0.087	0.108	0.228	0.118	4.342	0.605

Table 4.3 Morphometric Analysis of Pebbles

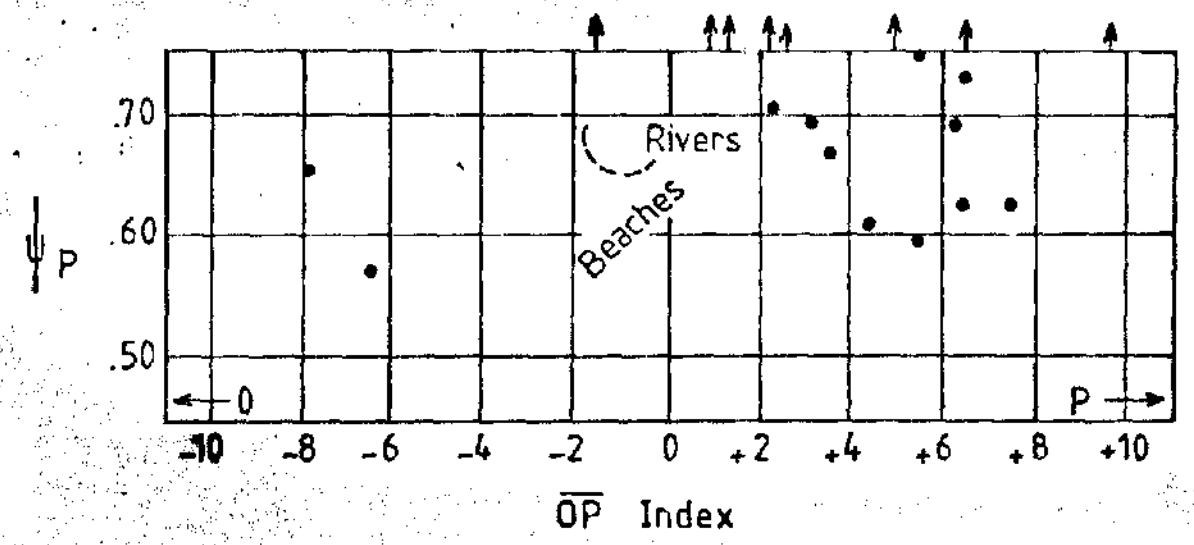
Sample No	S	I	L	S/L	I/L	(L-I)/(L-S)	$(S^2/LI)^{-1/3}$	OP Index	Roundness
4FR$_6$A	1.200	1.600	2.900	0.414	0.552	0.765	0.677	6.390	4
4FR$_6$B	1.500	1.550	2.700	0.556	0.574	0.959	0.813	8.251	5
4FR$_6$C	1.500	1.900	3.700	0.405	0.514	0.818	0.684	7.860	3
4FR$_6$D	1.100	1.900	2.900	0.379	0.655	0.556	0.603	1.466	4
4FR$_6$E	1.500	2.000	2.400	0.625	0.833	0.444	0.777	-0.889	5
4FR$_6$F	0.900	1.200	2.400	0.375	0.500	0.800	0.655	8.000	4
4FR$_6$G	1.200	1.800	2.100	0.571	0.857	0.333	0.725	-2.919	5
4FR$_6$H	1.050	1.500	2.100	0.500	0.714	0.571	0.705	1.429	4
4FR$_6$I	1.000	1.150	1.750	0.571	0.657	0.800	0.792	5.254	3
4FR$_6$J	1.000	1.450	2.250	0.444	0.644	0.640	0.674	3.149	4
4FR$_6$K	0.900	1.500	1.900	0.474	0.789	0.400	0.657	-2.110	5
4FR$_6$L	1.400	1.850	2.400	0.583	0.771	0.550	0.761	0.859	4
4FR$_6$M	0.900	1.450	2.100	0.429	0.690	0.542	0.643	0.972	3
4FR$_6$N	0.900	1.300	1.850	0.486	0.703	0.579	0.696	1.626	5
4FR$_6$O	1.100	1.600	1.800	0.611	0.889	0.286	0.749	-3.507	4
4FR$_6$P	0.950	1.300	2.150	0.442	0.605	0.708	0.686	4.711	3
4FR$_6$Q	0.900	1.600	1.900	0.563	0.842	0.300	0.643	-3.552	3
4FR$_6$R	1.050	1.250	2.100	0.514	0.595	0.810	0.749	6.194	4
4FR$_6$S	0.950	1.200	1.850	0.414	0.649	0.722	0.741	4.319	4
4FR$_6$T	1.000	1.150	1.700	0.588	0.676	0.786	0.800	4.856	3
Mean	1.100	1.513	2.248	0.502	0.685	0.618	0.712	2.618	3.950
S.D	0.214	0.270	0.494	0.079	0.115	0.194	0.059	3.874	0.759
Total				67.891	94.275		95.211	276.267	494.000

(4) Oblate - Prolate Index (OP) = $10 \frac{L - I}{L - S} - 0.5$

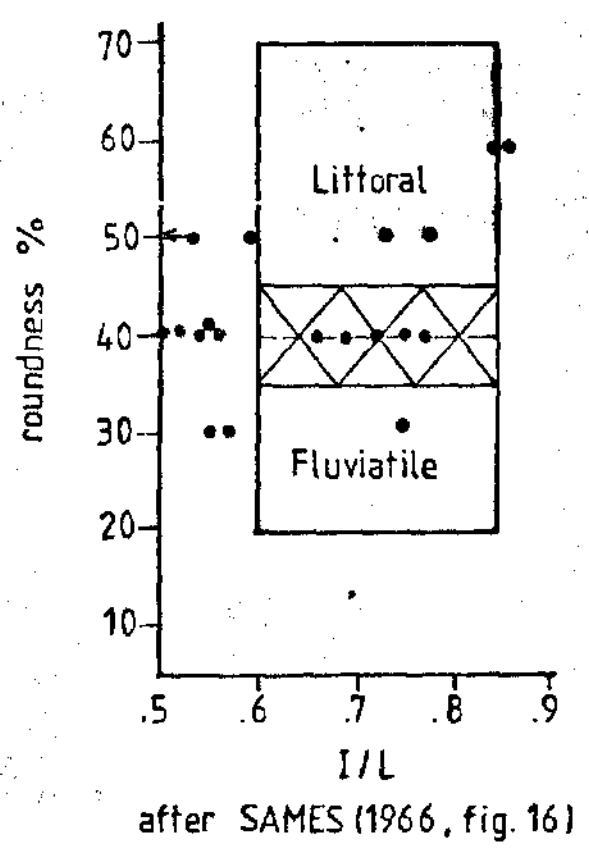
$\frac{L - S}{S/L}$

Dobkins and Folk (1970)

These parameters eventually becomes useful in environmental diagnosis (Fig 14, I - VII) and Table 4.4).



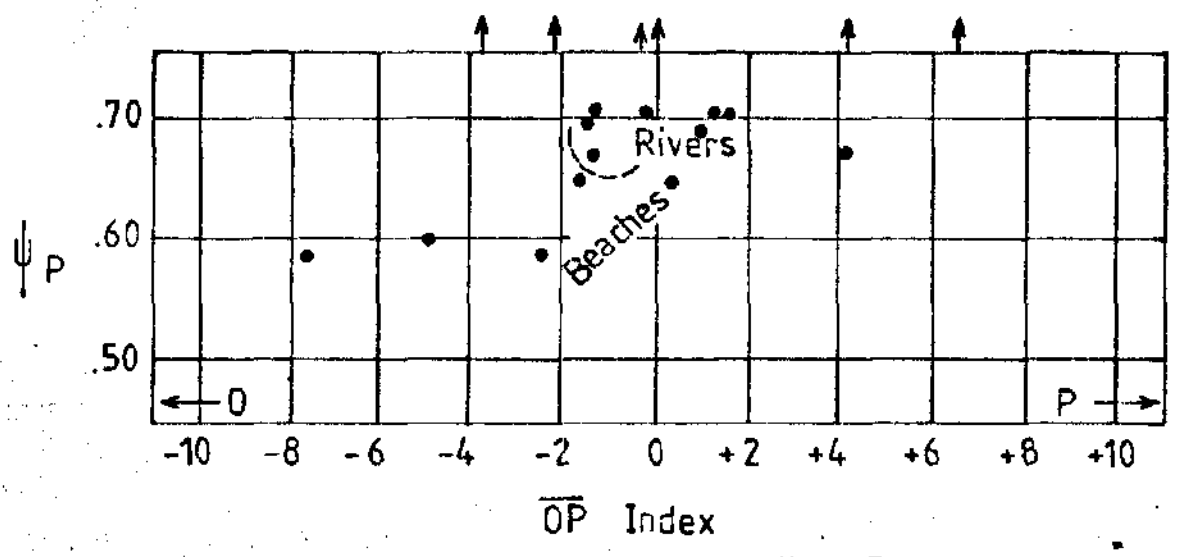
after Dobkins and Folk (1970)



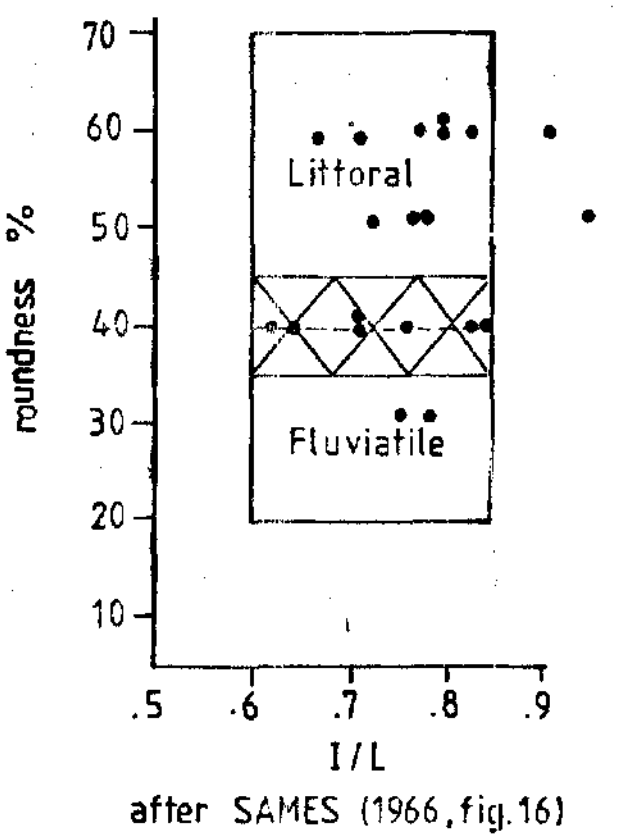
after SAMES (1966, fig. 16)

312571

Fig. 14 (I). Environmental Analysis of Pebbles $1FR_3$ (A-T)

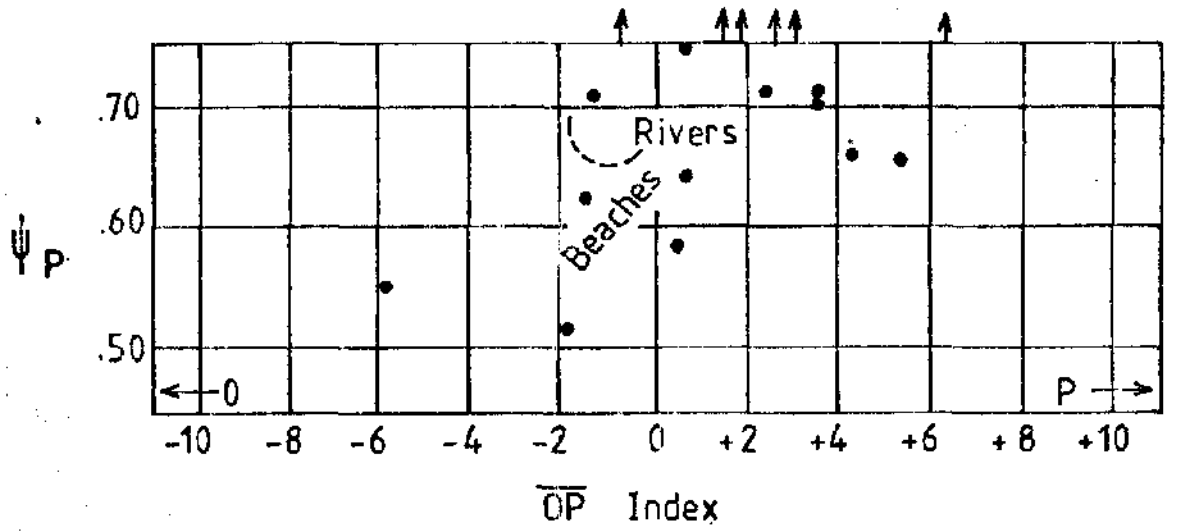


after Dobkins and Folk (1970)

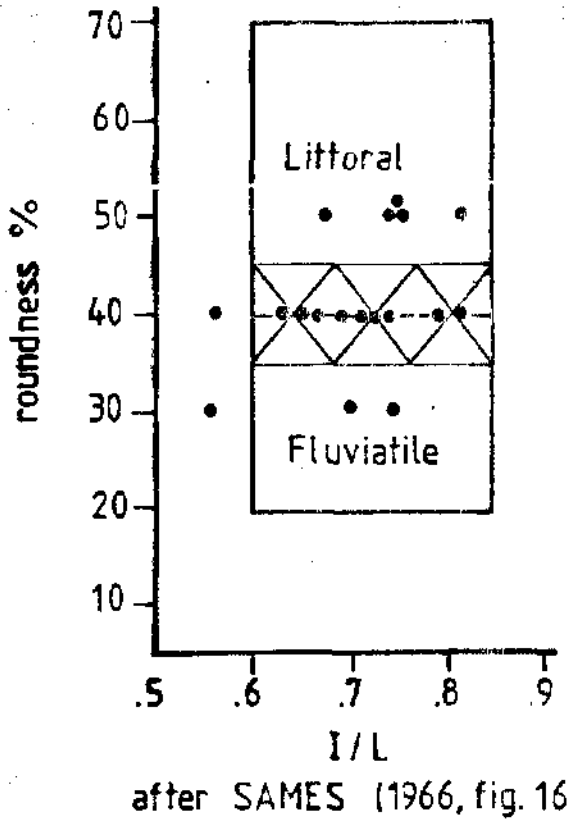


after SAMES (1966, fig. 16)

Fig. 14 (II). Environmental Analysis of Pebbles 1 FR_4 (A-T)

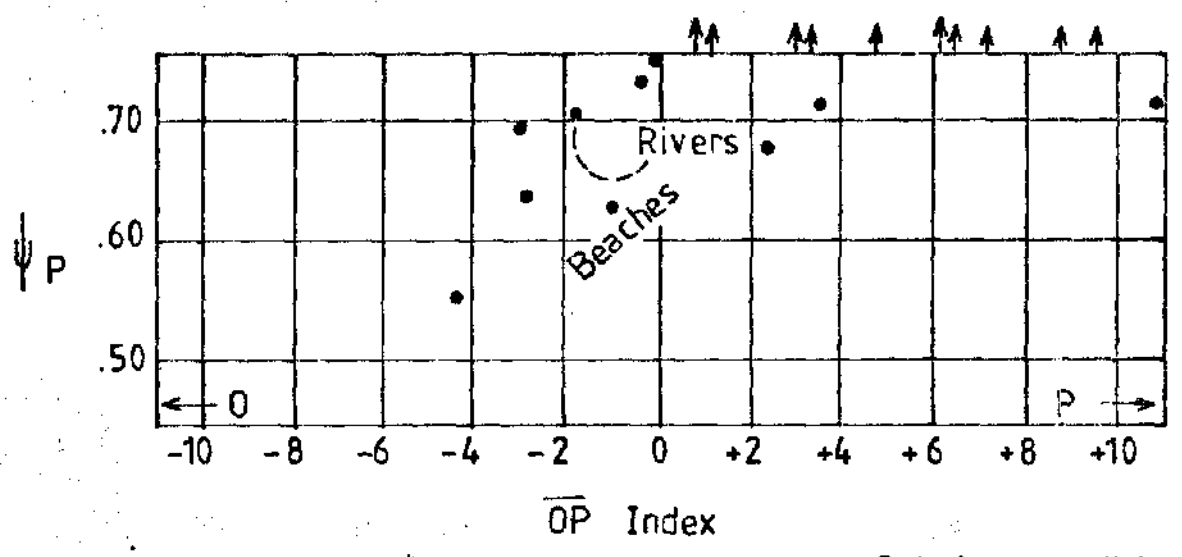


after Dobkins and Folk (1970)

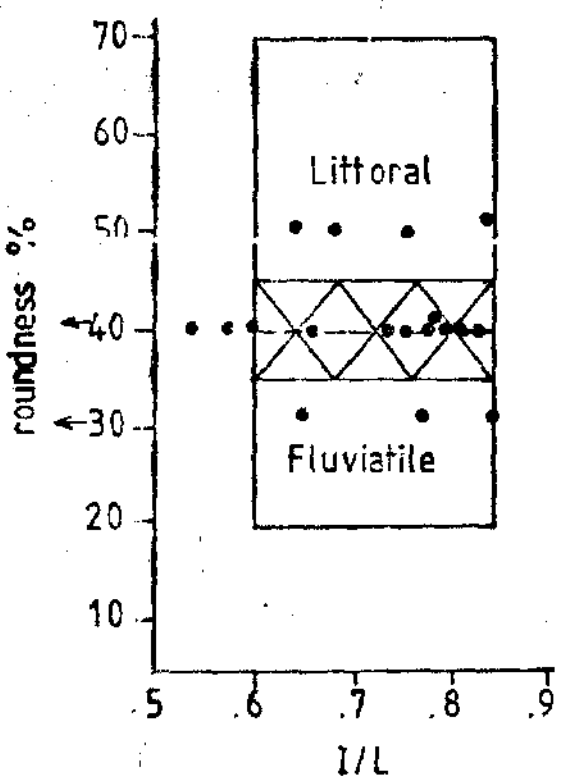


after SAMES (1966, fig. 16)

Fig. 14 (III). Environmental Analysis of Pebbles $3FR_2$ (A-T)

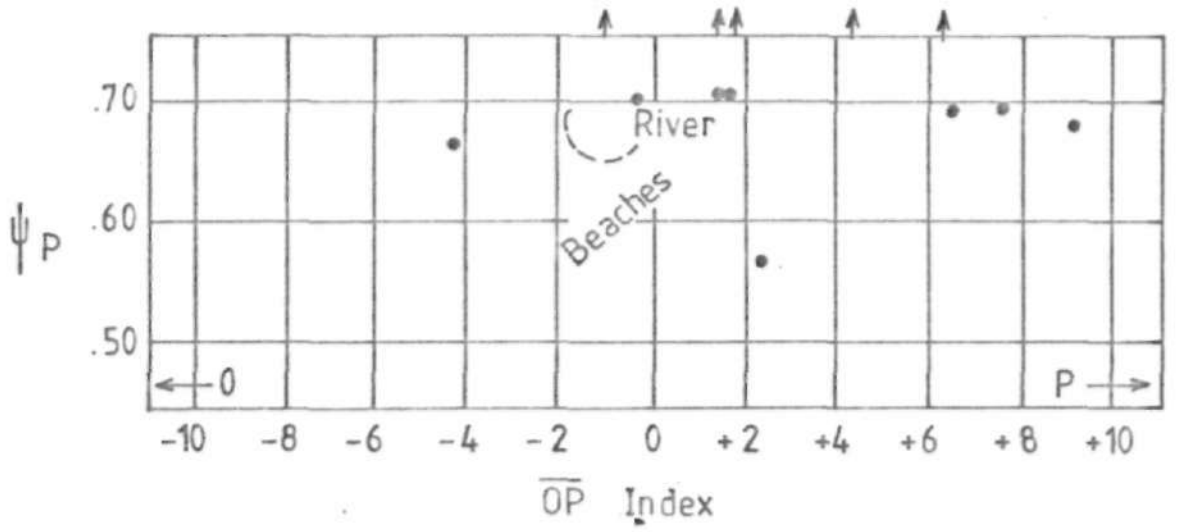


after Dobkins and Folk (1970)

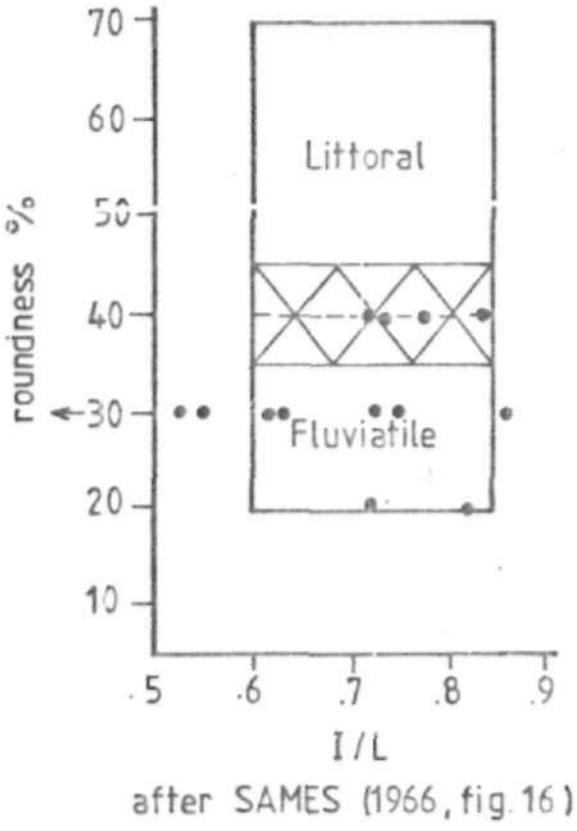


after SAMES (1966, fig. 16)

Fig. 14 (IV). Environmental Analysis of Pebbles $4FR_1$ (A-T)

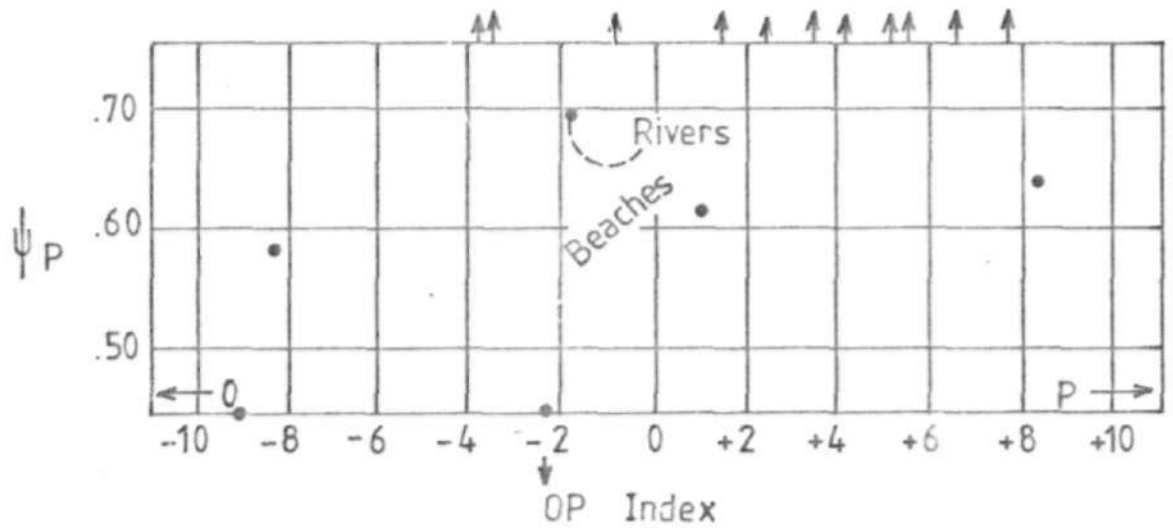


after Dobkins and Folk (1970)

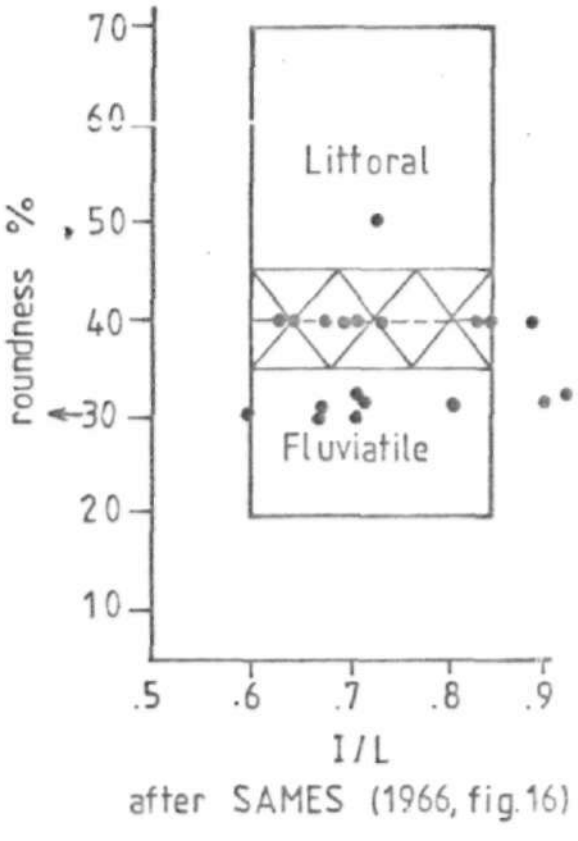


after SAMES (1966, fig. 16)

Fig. 14 (V). Environmental Analysis of Pebbles $4FR_3$(A-N)

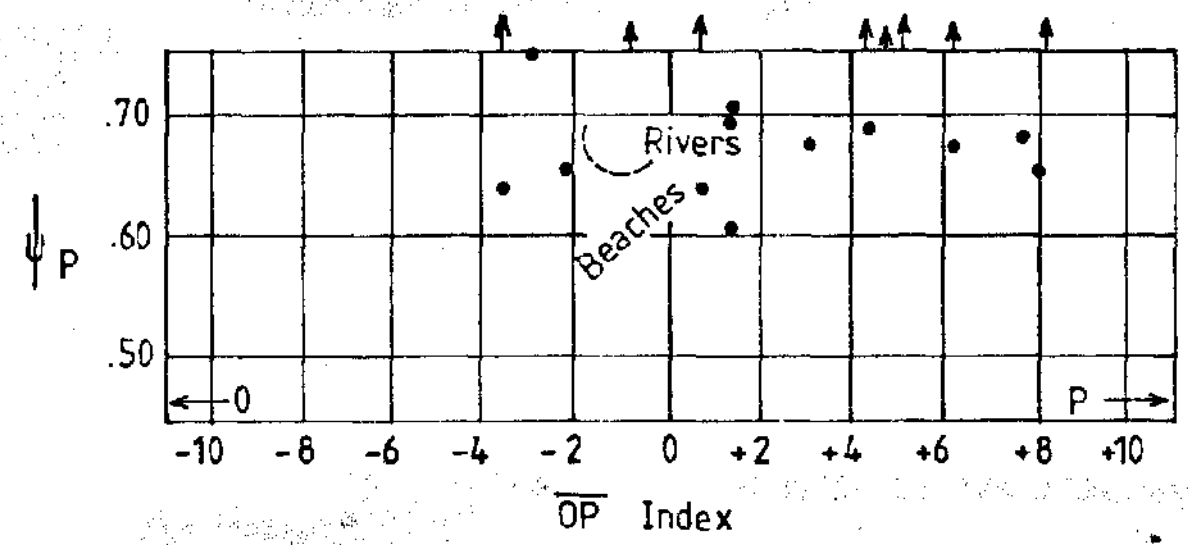


after Dobkins and Folk (1970)

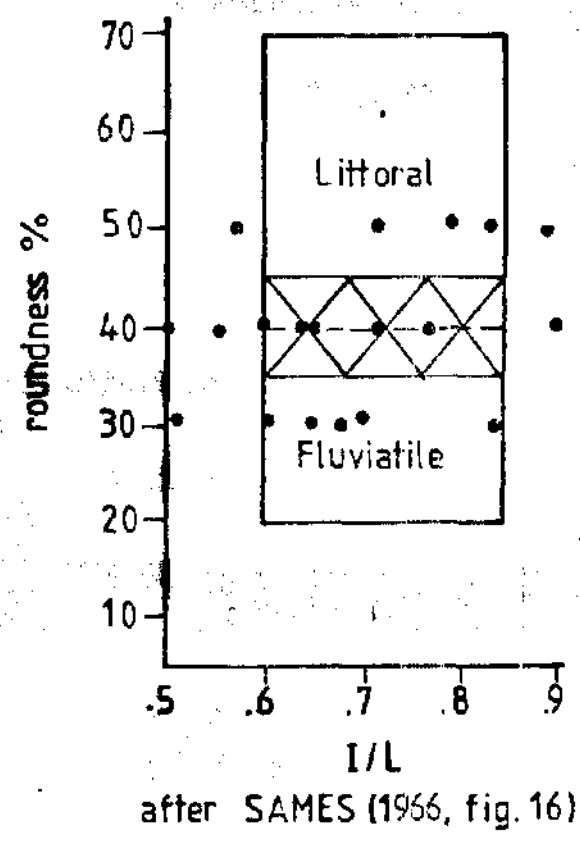


after SAMES (1966, fig. 16)

Fig. 14 (VI) - Environmental Analysis of Pebbles $4FR_4$ (A-T)



after Dobkins and Folk (1970)



after SAMES (1966, fig. 16)

Fig. 14 (VII) Environmental Analysis of Pebbles $4FR_6$ (A-T)

4.4.3 Results and Environmental implications

Flatness Ratio

The magnitude of grand mean flatness ratio for pebbles (0.507) is about the marine range (0.40-0.50) as sugested by Lutig, 1962) with a fluviatile range of 0.25-0.35 (Table 4.4).

Elongation Ratio

The grand mean elongation ratio obtained for pebbles (0.704) falls within Lutig's (1962) turrent type flowing water or in brooks and rivulets which, Lutig (1962) suggested accumulates with elongation values of 0.65-0.75 (Table 4.4).

Maximum Projection Sphericity (wp)

Dobkins and Folk (1970) reported that 0.66 sphericity line best separates beach and river pebbles, while lower values are typical of beaches, and higher values (> 0.66) suggest fluvial origin. Hence grand mean sphericity values for all pebbles fall within rivers (Fluvial) range, Table 4.4).

Oblate - Prolate Index (OP)

The OP index for pebbles under study has a grand mean value of 2.062 which is within the -1.00 to +5.00 range which Dobkins and Folk (1970, Fig. 21) classed as fluvial with 69 per cent certainty. Also following Dobkins and Folk (1970 Fig. 21), a bivariate plot of maximum projection sphericity index values against OP index has been drawn and plots indicate more of a fluvial environment of deposition for pebbles than littoral (Fig. 14, I - VII).

Table 4.4 Summary of Environmental diagnosis from Pebble Morphometry

	$1FR_3$		$1FR_4$		$3FR_2$	
MORPHOMETRIC	Characteristics	Environmental Indication	Characteristics	Environmental Indication	Characteristics	Environmental Indication
FLATNESS RATIO	Mean value = 0.469 ± 0.085	Marine Lutig (1962)	Mean value = 0.513 ± 0.082	Not diagnostic Lutig (1962)	Mean value = 0.501 ± 0.104	Marine Lutig (1962)
ELONGATION RATIO	Mean value = 0.652 ± 0.116	Fluviatile Lutig (1962)	Mean value = 0.785 ± 0.079	Non-fluviatile Lutig (1962)	Mean value = 0.710 ± 0.075	Fluviatile Lutig (1962)
MAX. PROJECTION SPHERICITY	Mean value = 0.696 ± 0.064	Fluviatile Dobkins and Folk (1970)	Mean value = 0.700 ± 0.070	Fluviatile Dobkins and Folk (1970)	Mean value = 0.704 ± 0.089	Fluviatile Dobkins and Folk (1970)
OBLATE PROLATE INDEX OP	Mean value = 3.448 ± 3.847	Fluviatile with 69% certainity Dobkins and Folk (1970)	Mean value = -0.369 ± 3.224	Fluviatile with 69% certainity Dobkins and Folk (1970)	Mean value = 1.646 ± 2.856	Fluviatile with 69% certainity Dobkins and Folk (1970)
PLOT OF ROUNDNESS AGAINST ELONGATION	15% Fluviatile 50% Transitional 35% Littoral	Transitional to Littoral Sames (1966, Fig 16)	10% Fluviatile 35% Transitional 55% Littoral	Littoral to Transitional Sames (1966, Fig 16)	15% Fluviatile 60% Transitional 25% Littoral	Transitional to Littoral (Sames 1966, Fig 16)
PLOT OF OP INDEX AGAINST SPHERICITY (Wp)	10% Beaches 90% Rivers	Fluviatile Dobkins and Folk (1970),	20% Beaches 80% Rivers 55% Littoral	Fluviatile Dobkins and Folk (1970)	15% Beaches 75% Rivers	Fluviatile Dobkins and Folk (1970)
Roundness (%)	Mean value = 43 Subrounded-Rounded	Non-marine Lutig (1962)	Mean value = 48 Subrounded-Rounded	Non-marine Lutig (1962)	Mean value = 41 Subrounded-Rounded	Non-marine Lutig (1962)

Table 4.4 Summary of Environmental diagnosis from Pebble Morphometry

	$4FR_1$		$4FR_3$		$4FR_4$	
MORPHOMETRIC	Characteristics	Environmental Indication	Characteristics	Environmental Indication	Characteristics	Environmental Indication
FLATNESS RATIO	Mean value = 0.517 ± 0.090	Not Diagnostic Lutig (1962)	Mean value = 0.513 ± 0.098	Not Diagnostic Lutig (1962)	Mean value = 0.537 ± 0.087	Not Diagnostic Lutig (1962)
ELONGATION RATIO	Mean value = 0.696 ± 0.121	Fluviatile Lutig (1962)	Mean value = 0.691 ± 0.118	Fluviatile Lutig (1962)	Mean value = 0.721 ± 0.108	Fluviatile Lutig (1962)
MAX. PROJECTION SPHERICITY	Mean value = 0.727 ± 0.072	Fluviatile Dobkins and Folk (1970)	Mean value = 0.723 ± 0.069	Fluviatile Dobkins and Folk (1970)	Mean value = 0.717 ± 0.118	Fluviatile Dobkins and Folk (1970)
ORLATE PROLATE INDEX OP	Mean value = 2.565 ± 4.453	Fluviatile Dobkins and Folk (1970)	Mean value = 2.724 ± 3.685	Fluviatile Dobkins and Folk (1970)	Mean value = 1.999 ± 4.342	Fluviatile Dobkins and Folk (1970)
PLOT OF ROUNDNESS AGAINST ELONGATION	20% Fluviatile 60% Transitional 20% Littoral	Transitional to Littoral Sames (1966, Fig 16)	71.4% Fluviatile 28.6% Transitional	Fluviatile Sames (1966, Fig 16)	50% Fluviatile 45% Transitional 5% Littoral	Fluviatile to Transitional Sames (1966, Fig 16)
PLOT OF OP - INDEX AGAINST SPHERICITY (Wp)	10% Beaches 90% Rivers	Fluviatile Dobkins and Folk (1970),	5% Beaches 95% Rivers	Fluviatile Dobkins and Folk (1970)	5% Beaches 95% Rivers	Fluviatile Dobkins and Folk (1970)
Roundness (%)	Mean value = 40 Subrounded	Non-marine Lutig (1962)	Mean value = 31.43 Subangular-subrounded	Non-marine Lutig (1962)	Mean value = 35.5 Subangular-Subrounded	Non-marine Lutig (1962)

Table 4.4 Summary of Environmental diagnosis from Pebble Morphometry

MORPHOMETRIC Characteristics		Environmental Indication		
		4FR$_a$		
FLATNESS RATIO	Mean value = 0.502 ± 0.079	Marine Lutig (1962)	Grand mean = 0.507	Marine Lutig (1962)
ELONGATION RATIO	Mean value = 0.685 ± 0.115	Fluviatile Lutig (1962)	Grand mean = 0.704	Fluviatile Lutig (1962)
MAX. PROJECTION SPHERICITY	Mean value = 0.712 ± 0.059	Fluviatile Dobkins and Folk (1970)	Grand mean = 0.711	Fluviatile Dobkins and Folk (1970)
OBLATE PROLATE INDEX OP	Mean value = 2.618 ± 3.874	Fluviatile Dobkins and Folk (1970)	Grand mean = 2.062	Fluviatile Dobkins and Folk (1970)
PLOT OF ROUNDNESS AGAINST ELONGATION	30% Fluviatile 45% Transitional 25% Littoral	Transitional to Littoral Sames (1966, Fig 16)	Total 211.4% Fluviatile 323.6% Transitional 165.0% Littoral	*Transitional to* Fluviatile Sames (1966, Fig 16)
PLOT OF OP INDEX AGAINST SPHERICITY (Wp)	10% Beaches 90% Rivers	Fluviatile Dobkins and Folk (1970),	75% Beaches 615% Rivers	Fluviatile Dobkins and Folk (1970)
Roundness (%)	Mean value = 39.5 Subangular-*subrounded*	Non-marine Lutig (1962)	Grand mean = 40.14 Subrounded	Non-marine Lutig (1962)

Roundness vs Elongation Ratio

Following Sames (1966, Fig. 16) a bivariate plot of roundness vs elongation ratio has been drwan (Fig. 14, I - VII) which shows a not too distinct environment for most of the pebbles, although grand total values in per cent (%) (Table 4.4) show more bias of pebbles to an environment that range between fluviatile and littoral than a completely fluviatile environment (that is, 211.4 per cent fluviatile, 323.6 per cent Transitional, 165 per cent Litoral).

Oblate-Prolate Index vs Sphericity

Following Dobkings and Folk (1970, Fig 12) a bivariate plot of the maximum projection sphericity values against the OP index has been drwan (Fig. 14, I - VII). The plots indicate more of a fluvial environment for pebbles and the grand mean total for all plebbles show this with 75 per cent of pebbles belonging to beaches and 615 per cent belonging to rivers (fluvial, Table 4.4).

Roundness

Roundness has been known to be a poor indicator of depositional environments because pebbles become rounded after only a short distance of transport (Pettijohn, 1975). Lutig (1962) has however suggested the 55 - 66 per cent roundness range as characteristic of fluviatile pebbles while 80-95 per cent range characterises marine pebbles. The very low roundness values obtained from pebbles in this study may thus be suggestive of closeness of the depositional site to source area. Also the choice of roundness scale by Shepard and Young (1961, Fig.1), as shown in 13, could be a factor since there are other charts or roundness

that have been proposed by differenct workers (Sames, 1966; Powers, 1953, Fig. 1, p. 118), and moreover the subjective nature in determining roundness values might cause variation with different workers. The grand mean roundness value obtained for all pebbles is 40.14 per cent (sub-rounded) and suggests a non-arine environment based on Lutig's (1962) classification.

4.5 Sieve Analysis

The Primary purpose of sieve analysis is to determine particle size distribution in sands. According to Friedman (1979) distribution of size relate to (1) the availability of different sizes of particles in parent material (2) processes operating where the sediments are deposited, particularly the competency of flow and (3) concentration of particles in suspension. Hencne differences in size frequency distributions among sand may correlate with their various origins, and their terminal depositional environments. With poorly cemented sandstones and unconsolidated sands, sieving is the most popular technique (Tucker, 1982). Once the grain size distribution has benn obtained then the sediment can be characterised by serveral parameters: mean grain size, mode, median grain size, sorting, skewness and kurtosis.

4.5.1 Method of Analysis

A total of 3 samples were collected from sandstone, siltstone and clay units logged from different locations. Indurated samples were disagregated to restore the grains to the condition they were in, at the moment when they were deposited with great care to avoid fabric destruction, by working the sediments in a large mortar with a rubber pestle.

Of each sample, 200 gm portion was weighed for sieving.....

at a mesh interval of 1/2 phi which is a recommended accurate interval, but in this study the 1/2 phi interval has a gap at 0-1.0 phi interval due to the non-availability of 0.5 phi or 0.71 mm mesh screen.

A sieving time of 15 min was adopted as adequate, and was consistently applied for all samples, though usually a range of between 10 and 20 min is considered accurate.

Appendix 1 shows sieve results obtained with columns of cumulative wt % and wt % respectively, and critical statistical parameters needed (ϕ5, ϕ16, ϕ25, ϕ50, ϕ75, ϕ84, ϕ95) obtained from cumulative frequency graphs plotted for each sample on a probability graph paper (Appendix 2). Also shown in Appendix 3 are smoothed frequency curves obtained by plotting gradients of cumulative frequency curves on an arithmetic scale graph, (Folk, 1980). This is to enable a visual interpretation of size distribution. Several size parameters of environmental significance have been calculated from phi values obtained from the cumulative frequency curve on probability paper. These size parameters (Table 4.5) below have been calculated by use of both graphic and moment measures. This is to enable comparison and because of the use of these parameters (derived by moment measures) in environmental discrimination by Friedman (1979),although moment measures is usually thought to be more accurate since they are more sensitive to environmental process than graphic measures (Friedman and Sanders, 1978).

Table 4.5 Size Parameter and their Formulas

Parameters	Moment Measures	Graphic Measures
Mean	$\frac{fm\phi}{100}$ *	$\frac{\phi16 + \phi50 + \phi84}{3}$ +
Standard Deviation OR (σ) Sorting	$\frac{f(Mo - X)^2)^{1/2}}{100}$ *	$\frac{\phi84-\phi16}{4} + \frac{\phi95 - \phi5}{6.6}$ +
Skewness	$\frac{f(mo-X)^3}{100\sigma^3}$ *	$\frac{\phi84+\phi16-\phi25}{2(\phi84-\phi16)} + \frac{\phi95+\phi5-2\phi50}{2(\phi95-\phi5)}$ +
Kurtosis	$\frac{f(mo - X)^4}{100\phi^4}$ *	$\frac{\phi95 - \phi5}{2.44(\phi75 - \phi25)}$ +
Mean cubed Deviation	$\frac{f(mo - X)^3}{100}$ *	
Simple skewness Measure (xs)		$\phi95 + \phi5 - 2(\phi50)$*
Simple sorting measure (SOS)		$\frac{\phi95 - \phi5}{2}$*
Median		50th percentile value+

* - Friedman and Sanders (1978)

+ - Folk and Ward (1957)

* - Friedman (1979)

Table 4.6 shows results (size parameters) obtained from sieve analysis byt both moment and graphic measures. Verbal sclaes and terms by Folk and Ward(1957) to described these size parameters obtained by graphic measures are presented below;

Sorting	Verbal term	
< 0.35	Very well sorted	(V.W.S)
0.35 - 0.50	Well sorted	(W.S.)
0.50 - 1.00	Moderately sorted	(M.S.)
1.00 - 2.00	Poorly sorted	(P.S.)
2.00 - 4.00	Very Poorly Sorted	(V.P.S.)
0.35 - 0.50	Well sorted	(W.S.)
> 4.00	Extremely Poorly sorted	(E.P.S)

Skewness	Verbal term	
-1.0 to -0.30	Very negatively skewed	(V.N.S.)
-0.30 to -0.10	Negatively skewed	(N.S)
-1.10 to 0.10	Nearly symetrical	(N.S)
-0.10 to 0.30	Positively skewed	(P.S.)
0.30 to 1.00	Very positively skewed	(V.P.S.)

Kurtosis	Verbal term	
< 0.67	Very platykurtic	(V.P)
0.67 - 0.90	Platykurtic	(P)
0.90 - 1.11	Mesokurtic	(M)
1.11 - 1.50	Leptokurtic	(L)
1.50 - 3.00	Very leptokurtic	(V.L)

> 3.00	Extremely leptokurtic	(E.P.)

In an attempt at environmental discrimination (diagnosis), bivariate plots of Friedman (1979) have been utilised. Six of his bivariate plots have been utilised as shown in Fig. 15 (I - VI). In all cases the paramters on the ordinate and abscissa axes of the bivariate plots are with reference to Table 4.6.

4.5.2 Results and Environmental Implications

A close inspection of Table 4.6 and a comparison of values obtained for both graphic and moment measures show variation which is especially pronounced for the higher moments and especially the mean-cubed deviation values obtained by moment measures are too large to be truly representative of the samples.

These anomalies could be explained as due to:

(1) Incomplete disaggregation of samples which gives room for coagulated, sand, silt, clay and iron minerals to be represented as monomineralic grains

(2) In using moment measures, it has been postulated that as higher moments are reached size parameters attain high values, Friedman (1979), hence this is relfected in the wide variation of values obtained from graphic and moment measures. Therefore for this work the values obtained by graphic measures are considered more reliable than those obtained by moment measures.

4.5.2.1 Mean Grain Size

The mean grain size obtained for all samples sieved from all different locations is 1.634 $\pm$ 0.613 phi (Table 4.6) which belongs to the medium sand sized class (Wentworth, 1922). Exactly 50 per cent of the 32 samples whose mean grain sizes were calculated by graphic measures have mean grain sizes within the medium sand sized class (1-2 phi).....

Table 4.6 Size Analysis Parameters(Derived from Sieving)

Sample Number	MOMENT MEASURES					INTERPRETATION (Folk and Ward, 1957)		
	Mean	Standard Deviation (3rd moment)	Mean Cubed Deviation	Skewness	Kurtosis	Sorting (S.D)	Skewness	Kurtosis
$1FR_1$	3.601	3.065	-29.600	-1.028	1.179	V.P.S	V.N.S	L
$1FR_2$	2.793	1.980	- 7.995	-1.030	1.353	P.S	V.N.S	L
$1FR_3$	1.312	1.388	- 0.650	-0.243	1.848	P.S	N.S	V.L
$2FR_1$	4.794	3.298	-29.630	-0.826	0.720	V.P.S	V.N.S	P
$2FR_2$	3.443	0.559	- 0.262	-1.498	10.377	M.S	?	E.L
$2FR_3$	3.495	2.224	-10.593	-0.963	1.076	V.P.S	V.N.S	M
$2FR_4$	4.241	2.727	-19.691	-0.971	1.068	V.P.S	V.N.S	M
$3FR_1$	3.608	2.601	-18.986	-1.079	1.336	V.P.S	V.N.S	L
$3FR_2$	2.044	1.733	- 5.236	-1.006	1.811	P.S	V.N.S	V.L
$4FR_1$	3.186	2.299	-13.998	-1.152	1.533	V.P.S	?	V.L
$4FR_2$	3.078	2.394	-14.297	-1.042	1.305	V.P.S	V.N.S	L
$4FR_3$	2.069	1.685	- 5.243	-1.096	1.579	P.S	V.N.S	V.L
$4FR_4$	1.842	1.485	- 3.520	-1.075	1.825	P.S	V.N.S	V.L
$4FR_5$	3.556	2.857	-23.833	-1.022	1.170	V.P.S	V.N.S	L
$4FR_6$	1.964	1.583	- 2.567	-0.647	1.500	P.S	V.N.S	V.L
$4FR_7$	2.710	1.664	- 4.437	-0.936	1.093	P.S	V.N.S	M
$4FR_8$	1.991	1.153	- 2.147	-1.401	2.293	P.S	?	V.L
$7FR_1$	2.025	2.093	- 6.143	-0.670	1.042	V.P.S	V.N.S	M
$7FR_2$	2.400	1.822	- 6.466	-1.069	1.378	P.S	V.N.S	L
$7FR_3$	3.731	2.973	-25.594	-0.974	1.052	V.P.S	V.N.S	M
$7FR_4$	1.400	1.392	- 1.840	-0.682	1.363	P.S	V.N.S	L
$7FR_5$	1.311	1.626	- 1.238	-0.288	1.387	P.S	N.S	L
$7FR_6$	4.116	3.416	-36.593	-0.918	0.916	V.P.S	V.N.S	M
$7FR_7$	2.799	2.399	-13.462	-0.975	1.156	V.P.S	V.N.S	L
$8FR_1$	3.689	2.715	-16.451	-0.822	0.731	V.P.S	V.N.S	P
$8FR_2$	1.724	1.408	- 1.340	-0.480	1.562	P.S	V.N.S	V.L
$8FR_3$	2.704	2.055	- 7.524	-0.867	1.049	V.P.S	V.N.S	M
$8FR_4$	3.646	3.017	-24.633	-0.897	0.903	V.P.S	V.N.S	M
$8FR_5$	1.874	1.712	- 3.653	-0.728	1.578	P.S	V.N.S	V.L
$9FR_1$	5.176	3.430	-38.578	-0.956	1.014	V.P.S	V.N.S	M
$9FR_2$	5.978	3.978	-50.297	-0.799	0.667	V.P.S	V.N.S	P
$9FR_3$	4.893	4.193	-64.356	-0.873	0.810	E.P.S	V.N.S	P
$9FR_4$	4.906	3.805	-40.821	-0.741	0.566	V.P.S	V.N.S	V.P
Average	3.094	2.325	-16.111	-0.902	1.522	V.P.S	V.N.S	V.L
S.D	1.217	0.880	16.022	0.258	1.635			
	102.099	16.729	-531.674	-29.781	50.240			

P = Platykurtic
V.P = Very platykurtic
M = Mesokurtic
L = Leptokurtic
V.L = Very Leptokurtic
E.L = Extremely Leptokurtic
N.S = Negatively skewed
V.N.S = Very negatively skewed
P.S = Poorly sorted
V.P.S = Very poorly sorted
E.P.S = Extremely poorly sorted

Table 4.6 Size Analysis Parameters(Derived from Sieving)

Sample Number	GRAPHIC MEASURES Mean	Sorting	Skewness	Kurtosis	1st Percentile	50th Percentile	Simple Skewness measure	Simple Sorting measure	INTERPRETATION (Folk and Ward, 1957) Sorting	Skewness	Kurtosis
$1FR_1$	1.817	1.575	0.190	0.356	?	1.600	0.900	2.350	P.S,	(P.S)	V.P
$1FR_2$	1.433	1.095	0.185	1.018	-0.900	1.300	0.600	1.800	P.S,	(P.S)	M
$1FR_3$	0.833	1.086	0.217	1.166	?	0.700	0.900	1.850	P.S,	(P.S)	L
$2FR_1$	2.367	0.907	0.028	1.105	0.300	2.350	0.100	1.550	M.S,	N.S	M
$2FR_2$	2.167	1.238	0.106	1.005	-0.200	2.050	0.300	1.900	P.S,	(P.S)	M
$2FR_3$	2.133	1.028	0.237	1.267	-0.150	1.950	0.700	1.700	P.S,	(P.S)	L
$2FR_4$	2.433	0.842	-0.017	1.197	0.000	2.400	-0.280	1.460	M.S,	N.S	L
$3FR_1$	2.100	1.433	0.088	0.868	-0.650	2.000	0.340	2.170	P.S,	N.S	P
$3FR_2$	0.967	?	?	?	?	0.900	?	?	?	?	?
$4FR_1$	1.717	1.186	-0.199	0.952	?	1.900	-0.650	1.975	P.S,	N.S	M
$4FR_2$	1.583	1.232	0.031	1.161	-0.950	1.600	0.350	2.125	P.S,	N.S	L
$4FR_3$	1.067	1.000	0.126	0.966	-0.250	1.000	0.500	1.650	M.P.S,	(P.S)	M
$4FR_4$	0.867	?	?	?	?	1.050	?	?	?	?	?
$4FR_5$	1.767	1.145	-0.180	0.843	?	1.900	-0.700	1.800	P.S,	N.S	P
$4FR_6$	0.997	1.015	0.141	1.353	-1.000	1.000	1.120	1.940	P.S,	(P.S)	L
$4FR_7$	1.550	0.573	0.087	1.571	0.000	1.550	0.400	1.150	M.W.S	N.S	V.L
$4FR_8$	1.433	0.822	-0.328	1.343	?	1.600	-0.950	1.475	M.S,	V.N.S	L
$7FR_1$	0.733	?	?	?	?	0.650	?	?	?	?	?
$7FR_2$	1.383	0.814	-0.024	0.944	-0.400	1.400	-0.150	1.325	M.S,	N.S	M
$7FR_3$	1.933	1.234	0.014	0.934	-0.600	1.950	0.200	2.050	P.S,	N.S	M
$7FR_4$	0.700	0.867	0.215	1.480	?	0.600	0.750	1.625	M.S,	(P.S)	L
$7FR_5$	0.750	1.229	0.226	1.266	?	0.650	1.420	2.240	P.S,	(P.S)	L
$7FR_6$	1.967	1.264	0.106	0.784	-0.400	1.900	0.250	2.025	P.S,	(P.S)	P
$7FR_7$	1.433	1.230	-0.050	1.063	-0.850	1.500	-0.100	1.750	P.S,	N.S	M
$8FR_1$	1.783	0.659	0.235	1.844	0.200	1.750	1.000	1.350	M.W.S,	(P.S)	V.L
$8FR_2$	1.050	0.927	0.458	1.018	-0.500	0.750	1.320	1.490	M.S,	V.P.S	M
$8FR_3$	1.400	1.023	0.310	1.472	-0.300	1.300	1.750	1.975	P.S,	V.P.S	L
$8FR_4$	1.733	1.073	-0.059	1.408	-1.000	1.800	-0.050	1.975	P.S,	N.S	L
$8FR_5$	?	?	?	?	?	0.800	?	?	?	?	?
$9FR_1$	2.817	1.196	-0.035	0.902	?	2.800	-0.350	1.925	P.S,	N.S	M
$9FR_2$	3.067	0.754	0.327	0.976	1.500	2.900	0.800	1.250	M.S,	V.P.S	M
$9FR_3$	2.150	1.264	0.323	0.708	?	1.800	1.000	1.900	P.S,	V.P.S	P
$9FR_4$	2.150	0.591	0.383	1.419	?	2.050	1.050	1.125	M.W.S	V.P.S)	L
Average	1.634	1.045	0.108	1.117	-0.324	1.559	0.432	1.755	P.S,	(P.S)	L
S.D	0.613	0.242	0.181	0.301	0.596	0.617	0.664	0.327			
	52.280	30.302	3.141	32.389	-6.150	51.450	12.520	50.900			

P.S = Poorly Sorted
(P.S) = Positively Skewed
V.P.S = Very Positively Skewed
N.S = Negatively Skewed
? = Not available

N.S = Nearly Symmetrical
M.P.S = Moderately Poorly Sorted
M.W.S = Moderately Well Sorted
M.S = Moderately Sorted

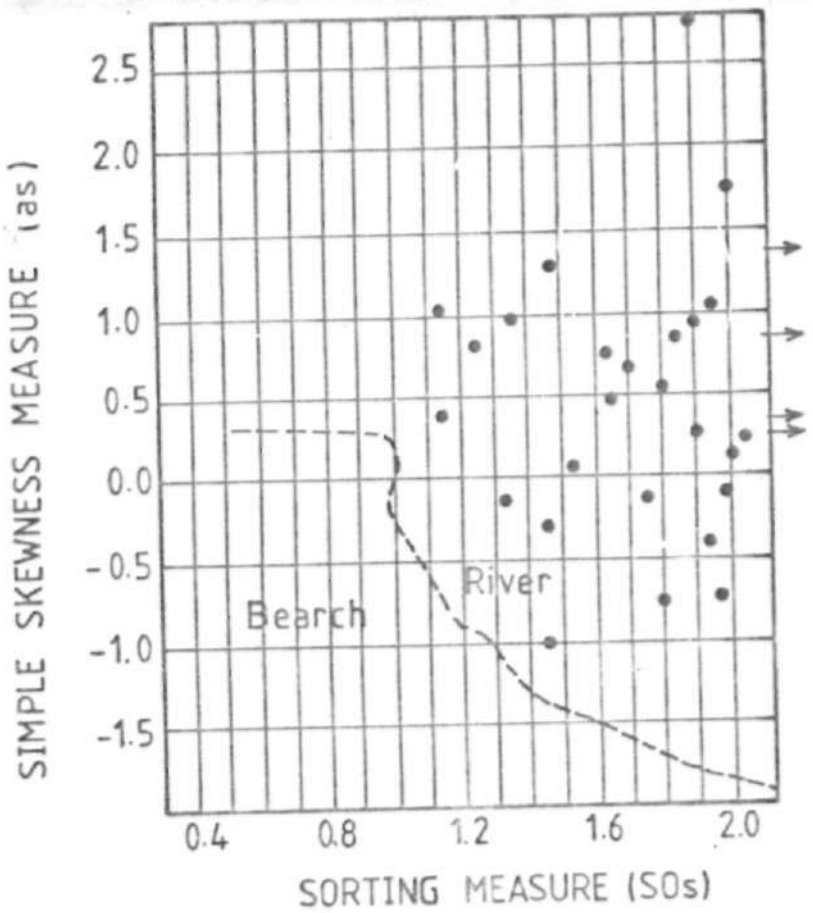


Fig. 15 (I) Scatter plot, Simple Skewness Measure versus Simple Sorting Measure;
(G.M. Friedman, 1967, Fig. 18, P. 342)

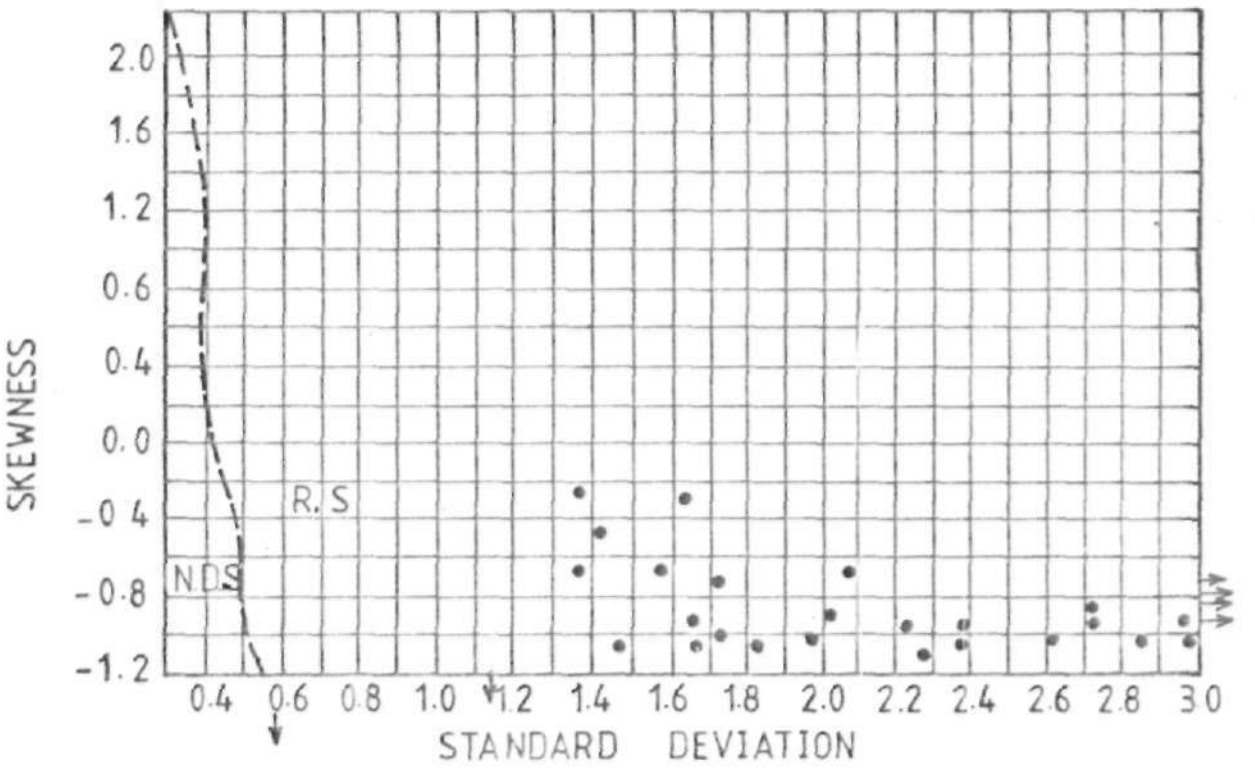


Fig. 15(II) Plot of Skewness and Standard Deviation for Nearshore Dune (N.D.S.) and River Sands (R.S.)
Friedman (1979)

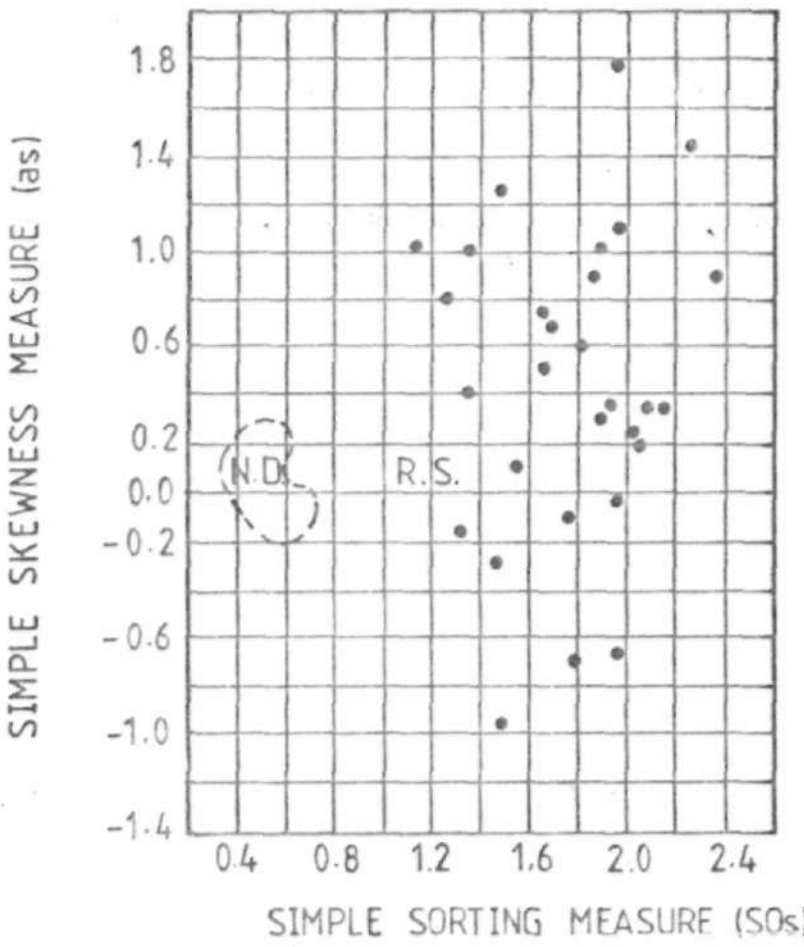


Fig. 15(III) Plot of Simple Skewness Measure and Simple Sorting Measure, for Nearshore Dune (N.D.) and River Sands (R.S.) Friedman (1979)

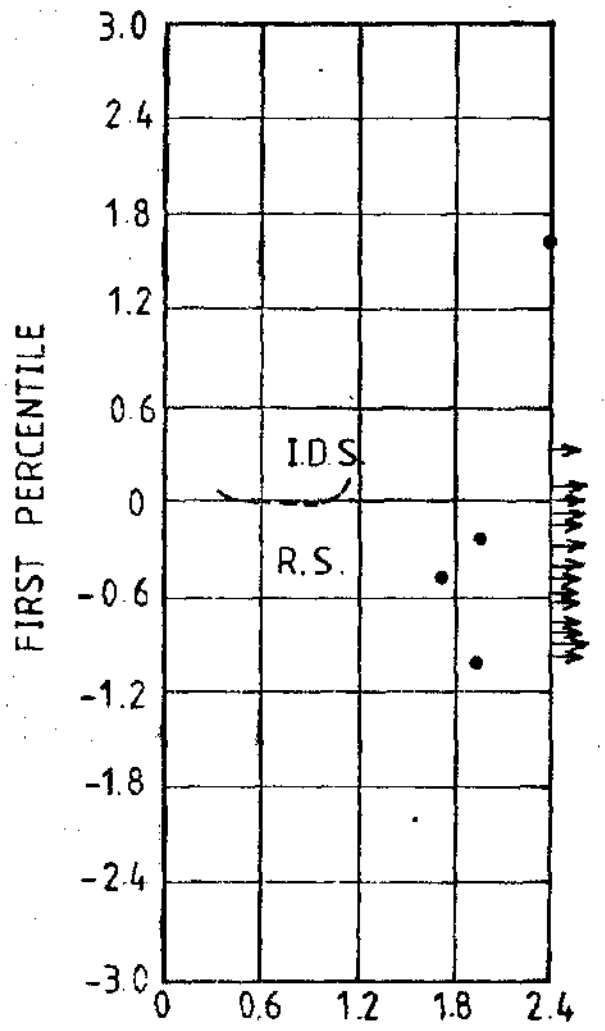


Fig. 15 (IV) Plot of 1st Percentile and Standard Deviation, for Inland Dune (I.D.S.) and River Sands (R.S.) Friedman (1979)

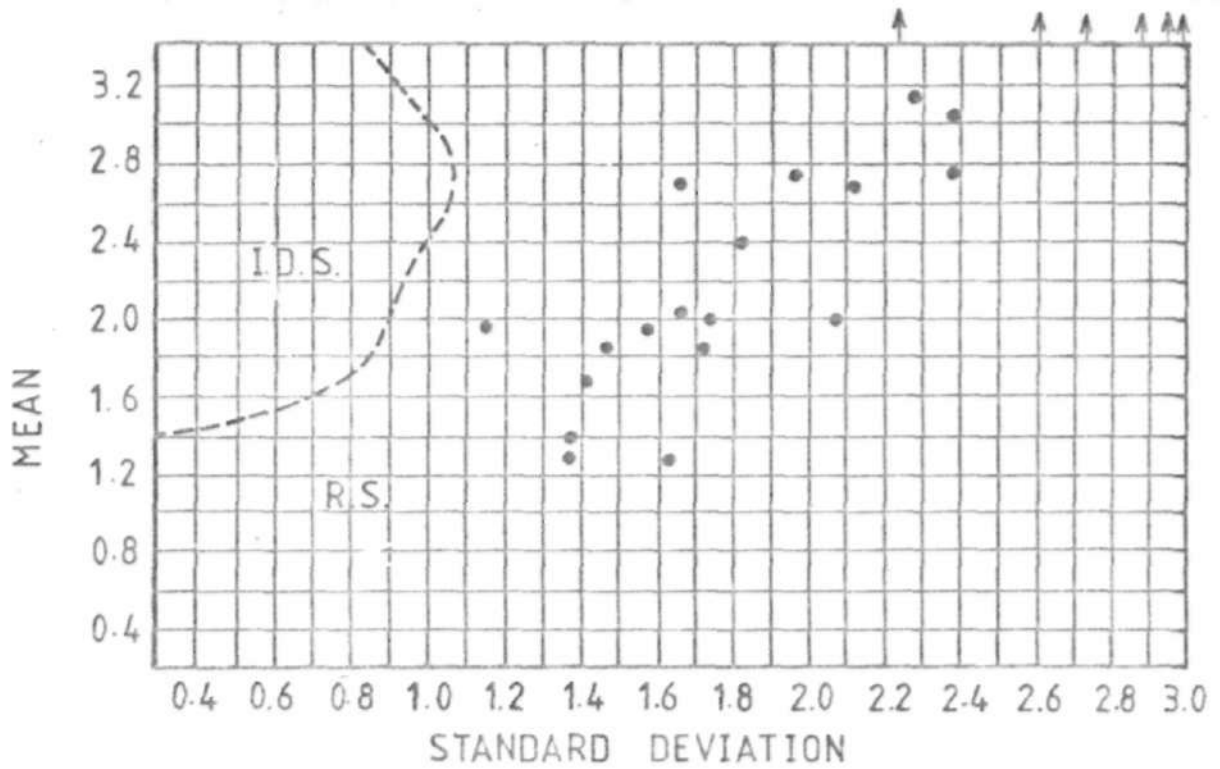


Fig. 15(V) Plot of Mean and Standard Deviation for Inland Dune (I.D.S.) and River Sands (R.S.) Friedman (1979)

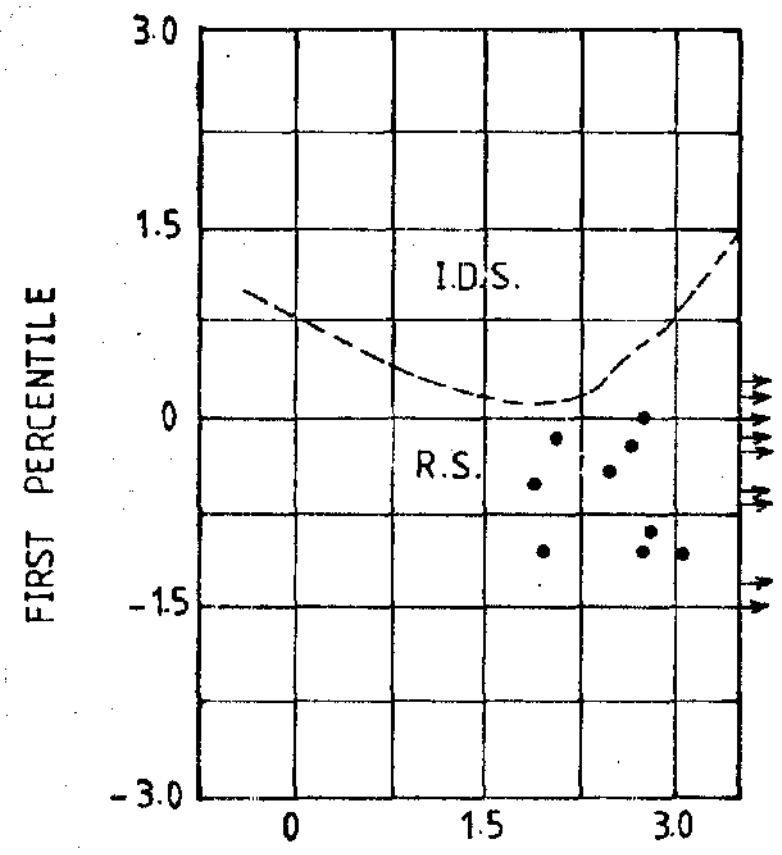


Fig 15(VI) Plot of 1st Percentile and Mean, for Inland Dune (I.D.S) and River Sands (R.S.) Friedman (1979)

while 25 per cent belongs to the fine sand class (2-3 phi), 21.88 per cent belongs to the coarse sand class (0-1 phi) while 3.12 per cent belongs to the very fine sand grade (3-4 phi). This suggests that in the real grain size sense by graphic measures there are no silt and clay units which have been classified into the argillaceous facies in the previous chapter (2), by visual inspection. But the grain size ranges (0-1, 1-2, 2-3 phi) within which mean grain size of sieved samples occur, appears normal because Pettijohn et al., (1972) postulated that there occurs a deficiency in the -2 to -1 phi (granule), -1 to 0 phi (Very coarse sand) and 3 to 4 phi (Very fine sand) grain sizes classes in not only fluvial sediments but also wind-blown, off-shore and beach environment.

Different reasons for such deficiencies have been attributed to different factors ranging from hydrodynamic, transportational, insufficient supply at source and mechanical instability of grain sizes within the deficient ranges. The low occurrence (3.12%) of mean grain size in the deficient range cannot be considered signi-ficant nor can the occurrence of mean grain size in the popular ranges be used as diagnostic of any environment.

4.5.2.2 Standard Deviation or Sorting

This represent the spread of grain size distribution and gives an indication of the effectiveness of the depositional medium in separating grains into classes, types of sediment source, and grain size distribution during transportation. Mean value of sorting by grahic measures is 1.045 ± 0.242 which according to Folk and Ward (1957) is poor sorting. Of the 29 samples whose degree of sorting were calculated by graphic measures (Table 4.6), 18 (62.07%) belongs to the

poorly sorted class, 7 (24.14%) are moderately sorted, 3 (10.34%) are moderately well sorted, while only one (1) (3.45%) is moderate to poorly sorted. The general poor sorting is an indication of the incompetency of depositional medium in separating grains into classes, or a reflection of grain size distribution as released at sediment source or uneven sorting during transportation. According to Tucker (1982) sediments which were deposited quickly such as storm beds, or were deposited from viscous flows, such as mud flows, are generally poorly sorted; sediments which have been worked and reworked by wind or water, the sandy deposits of deserts, beaches and shallow shelf seas are much better sorted. Based on these assumptions sediments analysed have not been much worked or reworked, that is, desert, beach or shallow shelf environment of deposition are not strongly favoured by this parameter.

4.5.2.3 Skewness

This is a measure of the symmetry of distribution, which apart from calculated value can best be visualised from the smoothed frequency curve (Appendix 3). If the distribution has a coarse "tail" that is, excess coarse material, then the sediment is negatively skewed, if there is a fine "tail" then the skewness is positive. If the distribution is symmetrical, then there is no skewness. Based on the mean skewness value obtained by graphic measures (Table 4.6) which is 0.108 ± 0.181, positive skewness values can be inferred (Folk and Ward, 1957). Of the 29 samples whose skewness values were calculated, 11 (37.93 per cent) are positively skewed, 3 (10.34 per cent) are negatively skewed and 1 (3.45 per cent) is very negatively skewed. The conclusion is that there is a tendency towards positive skewness to nearly symmetrical.

According to Friedman (1979) by further reasoning, distribution of particles in sandswill be influenced greatly by condition that determine what happens to the fine particles forming suspended load in river (sand), and that analysis of size frequency distribution of sand revealed that sands deposited by rivers almost invariably contain fine particles from the suspended load. The presence of these fine particles is shown by the stretching out or "trailing off" of the size frequency curve to the right of the mean, which indicates positive skewness. Also, despite many exceptions the frequency distributions of most river sands display positive numerical values for skewness. This results largely from the presence of the fine-grained fraction (Friedman, 1961, 1962b, 1967), by contrast, sands deposited on the parts of beaches, where the breaking waves continuously wash thin sheets of water back - and forth, invariably lack admixture of fine-grained particles, having symmetrical, negatively skewed or slightly positively skewed distribution. Hence, it can be inferred that sediments analysed are of river (fluvial) origin.

4.5.2.4 Kurtosis

This is a measure of the peakedness of size distribution on a frequency curve. It has little geological significance (Tucker, 1982). The mean kurtosis value obtained by graphic measures for the 29 samples is 1.117 ± 0.301 which can be classified as Leptokurtic (Folk and Ward, 1957). Of the 29 samples, 11 (37.93 per cent) are leptokurtic, 11 (37.93 per cent) are mesokurtic, 4 (13.79 per cent) are platykurtic, 2 (6.89 per cent) are very leptokurtic and 1 (3.45 per cent) is very platykurtic. Thus, there is a general tendency for sediments towards leptokurtic to

mesokurtic, that is, grain size distribution is neither widely spread nor narrow in range, that is, neither completely flat nor very peaked.

4.6 Bivariate Plots

Several bivariate plots have been invented by different workers, but those of Friedman (1961, 1962b, 1967, and 1979) have been of great success in attempts to discriminate environments. He attempted to define the relationship between textural para-meters and depositional processes for beach, dune and river sands based on scatter plots for sands of various origins. These have been used in the present study in an attempt to infer paleo-environments of sediments in the area of study. Figure 15 (I-VI) shows six bivariate plots which all indicate fluvial (river) setting as depositional environment(s) for sediments analysed. All size parameters employed in the bivariate plots are values derived by moment measures (Table 4.6) except for Simple sorting measure (SDs) and Simple skewness measure (xs) and of course first percentile which is obtained from cumulative frequency curve on probability graph paper.

4.7 Classification and Maturity

The method of classification of sandstone proposed by Pettijohn *et al.*, (1972), modified from Dott, (1964) presented in Fig 16 below is utilised in the classification of sandstone units studied. This classification is based on mineralo-gical composition (Quartz, feldspars and Rock fragments) and percentage of matrix. Based on this classification system, of the 24 sandstone units recognised in the field, 16 (66.67 per cent) are Quartz arenites, while 8 (33.33 per cent) belong to the Arkosic Arenite family.

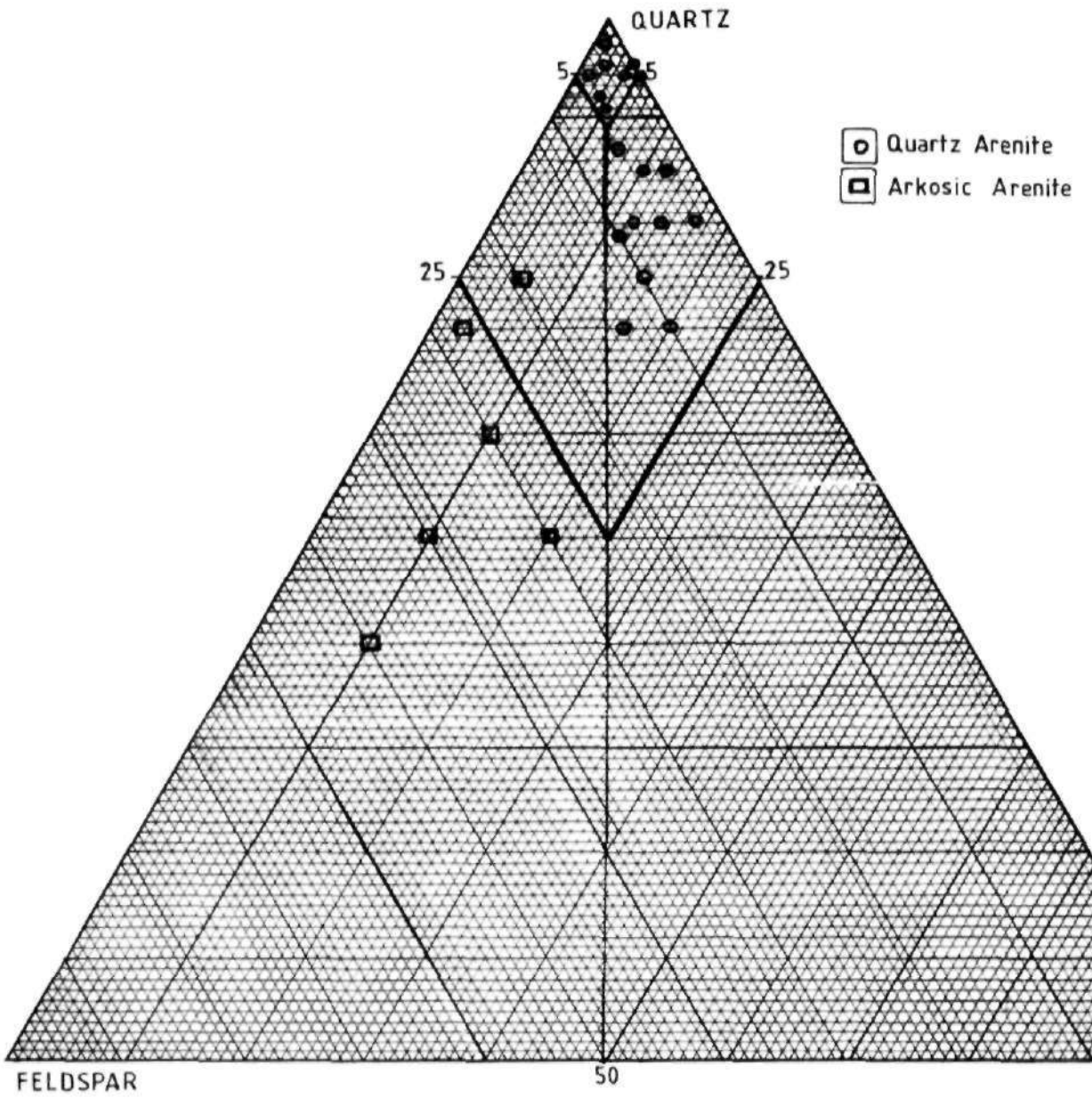


FIG. 16 CLASSIFICATION OF SANDSTONES IN THE STUDY AREA.

Olugbemiro, (1989)

This is shown in Table 4.7 while the siltstone, clay-shale units remain unclassified.

On maturity, Folk (1951) described four distinct stages of textural maturity of sandstones (immature, submature, mature and supermature) in terms of removal of clay content, degree of sorting, and increase in roundness of grains. Table 4.7 shows degree of maturity attained based on factors stated above for sandstone, siltstone and claystone units and show a varia-tion from immature to mature. The proportion of undulose quartz in total quartz population of a sandstone is often used as an index of maturity (Nwajide and Hoque, 1985). Undulosity in quartz indicates a high stress state of the grain resulting in thermo-dynamic and mechanical instability (Baltt, 1967), these grains are therefore more susceptible to fracturing or to solution. As there are still abundant recognizable amounts of strained quartz particles preserved an incompleteness of the textural maturation process is suggested, except where maturity has been inferred by consideration of other factors e.g. percentage of matrix (clay content) in which case abundance of undulose quartz can be explained as due to nearness of source or the dilution of the orignal detritus from source by undulatory quartz during transportation or even at deposition.

Because of the mechanical and thermodynamic instability of polycrystalline quartz grains, the amount of polycrystalline quartz in a sandstone has been used to evaluate the maturity of sandstones (Blatt and Christie 1963, Conolly 1965, and Blatt 1967). The high incidence of polycrystalline quartz is indicative of a low textural maturity stage of the sandstones, hence reworked sediments become progressively more mature as the proportion of polycrystalline quartz grains decreases in successive cycles or in a down-current

direction. From Table 4.7 it is clear that there is a consistent abundance of moncrystalline over polycrystalline quartz grains with monocrystalline: polycrystalline ratio ranging from as high as 20:1 to 10:1, hence maturity can be inferred based on this factor.

Reference to Table 4.7, shows majority of the sandstone units to be Quartz Arenites, except where other factors like percentage matrix (clay) negates such interpretation, although according to Nwajide and Hoque, (1985) care should be taken in assigning textural maturity stage based solely on clay content since the presence of clay matrix may be due to post-depositonal enrichment. Thus Bida sandstone falls into two groups (Table 4.7), Quartz arenites and Arkosic Arenites (due mainly to matrix content). The last column on Table 4.7 is a final judgement (maturity stage) based on the several factors that affect maturity and observation in thin section studied.

Table 4.7 Results of the Microscopic Examination of Aranaceous and Argillaceous facies Units (in area of study)

Sample NO.	Grain Shape (Mean) Shephard and Young (1961, Fig 1)	Roundness (Mean)	Modal Percentage of Quartz	Feldspars	Mica/Rock fragments	Matrix	Cement	Ratio of Monocrystalline to Polycrystalline quartz	Ratio of undulose to non-undulose quartz	Sand type	Maturity
$1FR_1$	Subangular-subrounded	2-3	5	< 1	< 30	< 60	< 2	20:1	20:1	Clay-	Immature
$1FR_2$	Subrounded-rounded	3-4	95	< 1.5	< 4	< 10	< 5	12:1	20:1	Quartz Arenite	Mature
$1FR_3$	Subangular-Subrounded	3-4	50	< 30	< 20	< 15	< 5	18:1	20:1	Arkosic Arenite	Immature
$2FR_1$	Angular-subangular	2-3	10	Nil	< 20	< 60	< 8	20:1	20:1	Silt-Stone	Mature
$2FR_2$	Subangular-Subrounded	2-3	2	Nil	< 20	< 70	< 10	20:1	20:1	Clay (ferruginized)	Immature
$2FR_3$	Subangular-Subrounded	3-4	5	< 5	< 20	< 65	< 10	20:1	20:1	Silt-stone	Mature
$2FR_4$	Subangular-Subrounded	3-4	< 2	< 5	< 15	< 75	< 5	15:1	20:1	Clay-	Immature
$3FR_1$	Subangular-subrounded	3-4	< 2	2	< 20	< 75	< 2	10:1	20:1	Clay-	Immature
$3FR_2$	Subangular-Subrounded	3-4	40	50	< 10	< 10	< 2	10:1	20:1	Arkosic Arenite	Immature
$4FR_1$	Angular-Subangular	2-3	60	30	< 10	< 10	< 5	12:1	20:1	Arkosic Arenite	Immature
$4FR_2$	Subangular-Subangular	2-3	93	5	< 3	< 10	< 5	20:1	20:1	Quartz Arenite	Mature
$4FR_3$	Subangular-Subrounded	3-4	96	Nil	< 4	< 2	< 10	10:1	20:1	Quartz Arenite	Immature
$4FR_4$	Subangular-Subrounded	3-4	91	< 5	< 4	< 5	< 15	20:1	20:1	Quartz Arenite	Mature
$4FR_5$	Subrounded-Subangular	2-3	2	3	< 20	< 75	< 15	20:1	20:1	Clay-Silt	Immature
$4FR_6$	Subangular-Subrounded	3-4	98	Nil	< 2	< 5	< 10	15:1	20:1	Quartz Arenite	Mature
$4FR_7$	Subrounded-Rounded	3-4	5	3	< 20	< 70	< 10	20:1	20:1	Silt-Stone	Mature

4FR$_6$	Subangular-Subrounded	3-4	95	Nil	< 5	< 10	< 10	20:1	20:1	Quartz-Arenite Mature
7FR$_1$	Angular-Subangular	2-3	70	< 25	< 3	< 10	< 5	18:1	20:1	Arkosic Arenite Immature
7FR$_2$	Subangular-Subrounded	3-4	85	Nil	< 5	< 10	< 5	20:1	20:1	Quartz Arenite (ferruginized) Mature
7FR$_3$	Subangular-Subrounded	3-4	75	Nil	<10	< 15	< 20	20:1	20:1	Quartz Arenite (ferruginized) Immature
7FR$_4$	Rounded-Subrounded	3-4	80	Nil	< 8	< 10	< 10	20:1	20:1	Quartz Arenite Mature
7FR$_5$	Subangular-Subrounded	3-4	70	Nil	<14	< 5	< 8	20:1	20:1	Siltstone Mature
7FR$_6$	Subangular-Subrounded	3-4	75	Nil	<10	< 10	< 10	10:1	20:1	Quartz Arenite Mature
7FR$_7$	Subangular-Subrounded	3-4	87	Nil	< 6	< 5	< 20	20:1	20:1	Quartz Arenite (feruginized) Mature
8FR$_1$	Subangular-Subrounded	3-4	93	6	< 1	< 10	< 5	12:1	20:1	Arkosic Arenite Immature
8FR$_2$	Subangular-Subrounded	3-4	95	4	1	< 10	< 10	20:1	20:1	Quartz Arenite Mature
8FR$_3$	Angular-Subrounded	3-4	75	20	< 5	< 15	< 5	20:1	20:1	Arkosic Arenite Immature
8FR$_4$	Subangular Subrounded	3-4	2	5	20	< 15	< 10	20:1	20:1	Silt-Stone Mature
8FR$_5$	Subangular Subrounded	3-4	50	40	<10	< 10	< 15	20:1	20:1	Arkosic Arenite Mature
9FR$_1$	Subangular Subrounded	3-4	80	Nil	6	< 5	< 10	20:1	20:1	Quartz Arenite Immature
9FR$_2$	Angular-Subangular	3-4	85	Nil	< 15	< 5	< 5	20:1	20:1	Quartz Arenite Mature
9FR$_3$	Subangular-Subrounded	3-4	90	Nil	< 5	< 5	< 5	20:1	20:1	Quartz Arenite Mature
9FR$_4$	Subangular-Subrounded	3-4	70	Nil	< 25	< 5	< 6	20:1	20:1	Quartz Arenite Mature

CHAPTER FIVE

BASIN SYNTHESIS

5.1 Depositional Environments

As a follow up to investigations carried out in earlier chapters, where stratigrahy, mineralogy and size analysis and sedimentary structures observed were discussed, a synthesis of these paramters is now attempted to determine depositional environments, mode of transport and paleogeology of sediments in the Bida Basin, by inferrence from studied area.

5.1.1 Stratigraphy of the area of study.

This is highly significant in interpreting conditions and environments of deposition of sedimentary fill of the Bida Basin. Stratigraphic successions observed in the area of study (Chapter 2) follow two general patterns,

(1) Cyclic fining upward (Locations 2, 4, 7, 8 and 9)

(2) Coarsening upward (Locations 1 and 3).

Although the first case is more common and infact predominates, there appear to be four major types of sequences.

(1) Fine sandstone --- Very fine sandstone --- Conglomerates --- Pebbly sandstone --- Medium sandstone --- Coarse sandstone.

(2) Coarse sandstone --- Pebbly sandstone --- Medium sandstone --- Coarse sandstone.

(3) Conglomerate --- Pebbly sandstone --- Medium sandstone --- Coarse sandstone

(4) Coarse sandstone --- Medium sandstone --- Pebbly sandstone.

Whether or not the cycle patterns are distinct is not very clear, however Allen (1970) and Pettijohn (1975) ascribed these fining-upward sequences to a fluviatile (meandering river) origin by analogy with deposits of modern streams.

Coarse members represent deposits of the channel and point bars, fine grained members represent flood plain deposits, while cycles with abundant calcareous matter (calcrete in Location 3) formed under arid to semi-arid conditions (Allen, 1970 and Pettijohn, 1975). Additionally the occurrence in the area of study of sharp and locally erosion based sandstones (Location 4) passing upwards into finer sandstones and silt is characteristic of fining upward alluvial sequences (Allen, 1970).

The cases of coarsening upward sequences (Locations1 and 3) can be explained as representing a prograding delta sequence which Pettijohn (1975) postulated is characterized by fine grained dark shales, at the base and end with coarse grained and locally gravelly sandstones, which is the situation observed in Location 1, although the importance of facies transition from coarse sandstone to conglomerate (as in Location 1) was discarded by Miall (1973), as due to debris flood flow interrupting quieter surface run-off processes. Also the coarsening upward section identified in Location 1 could be a fraction of a whole sequence (which is not observable) that may not necessarily be coarsening upward. The occurence of pebbly sandstones may or may not be of different genetic origin to the conglomerates, while conglomerates are results of debris flood, pebbly sandstones represent non-violent run-off, the pebbles being carried as a traction load rather than in suspension, Miall (1973). On the other hand, the siltstone unit which are often inter-

bedded with thin, relativity fine grained sandstones, could be interpreted as floodplain top stratum deposits representing, levee, backswamp and crevasse splay environments, (Allen, (1965).

Based on these theories, the cyclic sedimentation recorded (Locations 2, 4, 7, 8 and 9) are interpreted as due to:

(1) Simple wandering of rivers of deposition

(2) Varying base levels of deposition or

(3) Varying tectonic activity in the source area leading to increased sediment supply. It is also possible that the above stated factors operated simultaneously. While the coarsening upward sequences recorded (Location 1and 3) are indicative of a prograding deltaic environment or one similar to it with intermittent quiet run-off and debris flood operating alternatively.

5.1.2 Mineralogy and Size Analysis

The mineralogical composition and size analysis parameters of the sedimentary rocks studied, are factors dependent on not only environment of deposition but also of source area geology and transportational history of sediments.

The result of pebble morphometry and thin section study of roundness indicate a high degree of roundness of pebbles, where they occur in pebbly sandstones or as conglomerates, depicting a high energy medium of deposition, possibly debris flow medium while the non-pebbly sandstones, siltstone, and clay-stone units studied in thin section showing a low degree of roundness of quartz grains,especially, is indicative of nearness of source, or a preservation of grain roundness distribution at source or even contamination by more angular grains during transportation or at

deposition. This is supported by the view of Blatt *et al.*, (1980).

Packing of framework grains in the aranaceous and argillaceous facies units, is more compact in the basal unit and less compact at higher levels. This could be explained as due to the higher energy levels responsible for the deposition of basal units, hence the removal of much of the intervening clay matrix or the higher degree of weathering at higher levels which easily converts labile feldspars into matrix clay. Another possible factor is post-depositional disruption which might result in original packing of grains being disrupted by the sudden change in energy regime of depositional medium giving rise to a less compact arrangement of framework grains. This is expected especially in a fluvial regime, where fluid medium of transportation features frequent changes in energy. Such post-depositional disruption might lead to further introduction of clay matrix (Nwajide and Hoque, 1985).

The ironstone facies record a higher grain roundness values, although in a more cement (iron-oxide) dominated groundmass. Also the occurence of well rounded spherical to subspherical oolites is strongly comparable with those of the recent calcareous oolites of the Trucial coastlines, as described by Shearman *et al.*, (1970). The predominance of goethite in association with the iron-oxide cement suggest that the sources of the ironstone facies were rich in iron, since Porrenga (1967) have shown that goethite is probably the most stable clay mineral under very shallow subtidal conditions in tropical seas. Perhaps the goethite is in association with primary ferruginous materials derived from the same sources as the underlying formation, where iron-oxide also occur although not in equal amounts. The

occurrence of kaolinite is also compatible with the above deductions, since according to Rateev *et al.*, (1969), recent kaolinitic sediments are almost exclusively restricted to the tropical and sub-tropical zones of the world. Also the similarity between the detrital quatrz grains in the facies and those of the underlying aranaceous and argillaceous units and the occurrence of zircon and tourmaline, suggest a common source for the underlying facies and the ironstone facies, which makes it easier to explain the source of the ferruginous matter as being of primary origin rather than authigenic. Although it is conceivable that parts of the ferruginous materials were secondarily derived through leaching by the penecontemporaneous ground water of underlying formations. The presence of clay in the groundmass is evidence of a fair supply of argillacceous ferruginous clasts, while the size of the clasts suggest that the sediments reached the depositional site through the agency of weak currents. Such streams would be comparable with those of the very mature modern flood plains. This is supported by the fact that the ironstones sit on facies with argillaceous content. By analogy, therefore, it appears that the ironstone facies were deposited under acquatic conditions of marine affinity, possibly open lagoonal tidal deltas, tidal inlets and channels (Adeleye, 1973).

On size analysis, the use of statistical measures to discriminate between sands of various origin has been undertaken. Friedman (1979) consider mean-cubed deviation as one of the most effective of these measures followed by standard deviation. While the standard deviation has been used in this project, the values obtained for the mean-cubed deviation are too high to be considered as realistic (Table 4.6) and thus discarded, other parameters are skewness, first

percentile and mean.

However, Friedman does use two graphic measures - the Simple Sorting Measures (SOs) and Simple Skewness Measure (S and S) introduced for simplicity in computation and also to "assign to the tails of the distribution the importance which they deserve in environmental analysis". The various combination of these parameters have been utilised in this project, and a consistent pattern of a fluvial (river) environment of deposition is shown (Chapter 4), for the aranaceous and argillaceous facies units in the areas of study. Likewise, bivariate plots based on pebble size parameters - Flatness ratio, Elongation ratio, Maximum projection Sphericity Index, Oblate - Prolate Index, and roundness plotted after several workers (Dobkins and Folk, 1970, and Sames 1966, Fig 1) depcit pebble environments that ranges from fluviatile to transitional.

Futher by sieve analysis, cumulative frequency curves obtained (Appendix 3) show modality of the aranaceous and argillaceous facies. Unimodality and bimodality are the predominant curve patterns, except for $3FR_1$ and $8FR_2$ where more than two modes were displayed (polymodality).

Shapes of frequency curves have been used to deduce environment of depositions (Pettijohn, 1975). Unimodality is usually ascribed to fluvial sands, while bimodality is attributed to vigorous current action in tidal (beach) environments, although fluvial sands displaying bimodal distribution are also known (Pettijohn, 1975). Polymodality is a reflection of the mixtures of two or three grain population related to differing modes of sediment transport due to the awareness that many distributions are composites of two or three subpopulations.

Although Bagnold (1941) thinks that these bimodal

distributions could result from the sampling procedure in which materials collected are from distinct beds each with its own population, but according to Pettijohn (1975), there are many bimodal distributions produced within single layers which seem to be two populations deposited in the same episode of deposition. The bimodality displayed by most sediments in this study can thus be attributed to the co-existence of two grain population related to not necessarily differing modes of sediment transport but differences in energy of transportation and deposition, while unimodal distribution is ascribed to be a result of deposition in a fluvial environment with a single grain population. However, polymodality is interpreted as being due to mixtures of different sediment population existing together.

5.1.3 Sedimentary Structures and Paleocurrents

Sedimentary structures observed in the area of study are widely varied and highly significant. They are particularly important because their presence helps to establish the conditions prevailing at the time of deposition, or after deposition.

Cross bedding is the most prominent of all sedimentary structures observed. The mechanism that produces most cross-bedding is encroachment by avalanching down the lee slope of dunes, ripples, bars, fans, or small deltas and sorting of grains is also produced by the avalanching process. Although cross bedding may also be formed by the other mechanisms of deposition, (Allen, 1968). Cross bedding on a very large scale, with beds inclined at angles of only a few degrees is formed by accretion of sands on point bars during the migration of meanders (Blatt *et al.*, 1980). Cross bedding is especially a product of changing flow regime as observed in

this work. According to Blatt *et al.*, (1980) in fine to medium sands a waning current might deposit a bed or beds with the following sequence: lenticular, low-angle lamination (formed by antidunes), plane lamination (upper-regime flat bed), large scale trough and planar cross-bedding (formed by dunes and sand waves), small-scale cross-lamination (formed by ripples). Cross-bedding is not random but tends to show a strong preferred orientation in a given formation, this is in the form of the strike, dip and azimuth orientation, although so far no particular style or scale of cross bedding is characteristic of any particular agent and/or environment, but very large scale (which is not observed in this work) is probably either eolian or marine rather than fluvial (Potter and Pettijohn, 1977). Cross-bedding azimuth readings plotted on current roses for all the 7 locations in Fig 12, display a mean northerly paleoflow directions. All locations except 2 and 8 display unimodal current direction. Location 2 is strongly bimodal, while 8 is weakly bimodal, such bimodal patterns are suggestive of beach environments (Potter and Pettijohn, 1977). Of importance however is the mean azimuthal paleoflow direction which is northerly, further confirming that the sediments under study (in the Bida Basin) are derived from the igneous and metamorphic basement complex of southwestern Nigeria.

Mudcracks and load casts are essentially post depositionally (or diagenetic) formed physical sedimentary structures. While mud cracks are formed as a result of subaerial exposure of sediments, load casts are produced by gravitational instability of a denser layer overlying a less dense one. Mudcracks originate by dessication and compaction of water saturated muddy (or shale) sediments (or subaqueously by synaresis (Jungst, 1934)) signifying intermittent subaerial

exposure of surfaces of dried up ponds, coastal and inland sabkas, lakes and lagoons, abandoned river channels, flood plains and intertidal zones, (Reineck and Singh, 1978). Although the problem remains to determine if observed mud-cracks are ancient or modern. Load casts are a pointer towards the occurence of a denser medium on a less dense one, meaning that a stronger regime of deposition was responsible for the upper dense layer.

Graded bedding is thought to originate by a waning turbidity current. According to Pettijohn (1975), it is a feature primarily of sandstone and principally of graywackes in the paleozoic and older sequences, though it is not confined to these classesof sands or sandstone alone. Several workers have explained graded beds in several ways, (Coleman 1926, Bailey 1930, Pettijohn 1936, Kuenen and Migliorini 1950). But most importantly graded beds record a single short lived episode of deep water sedimentation beyond the reach of normal bottom currents and waves, by a dense turbidity flow which may be product of marine slump triggered by a violent mechanism. Also significant is the fact that graded beds are usually a record of a waning current (Reineck and Singh, 1978). Occurrence of graded bedding in the area of study therefore represent a gradual decrease in energy of a fluid medium (with reducing competence) responsible for the deposition of the graded beds. This is most especially common in fluvial environments where occasional turbidity currents develop.

Another sedimentary structure, though pedogenic is calcrete which has been reported worldwide (Goudie, 1973; Steel, 1974; Allen, 1974; Arakel, 1982, etc) is a nodular carbonate accumulation that forms in neither too arid nor too humid region, hence uncharacteristic of a climatic regime,

although Gile, *et al.*, (1966) postulated the common occurrence of such authigenic carbonate in soils of arid regions. The oocurence of calcrete (or caliche) in Location 3, precisely could as explained in Chapter 3, be favoured by low relief, alternating wet and dry climate and moderate moisture. The occurence of the calcrete in a clay-shale unit is however significant, since Pettijohn (1975) reported the occurence of such calcrete accumulation among fine-grained members of a fining upward sequence produced by a meandering river, representing flood plain deposit. The presence of such calcareous accumulation in Location 3, could be explained as authigenic in origin, within a clay-shale unit of a flood plain deposit (or alluvial fan) in an alternating arid and humid environment.

Consideration of ichnofossils is necessary in any discussion of sedimentary structures, since ichnofossils (or trace fossils) are records of conditions and events prevalent during deposition. As mentioned earlier in Chapter 3, Study of common trace fossils occuring in study area show that they are essentially feeding, resting and dwelling traces especially in situations where pellet remains are observed. These are common in the ironstone facies units, and based on bathymetry a shallow water environment is favoured over deep water environment of deposition for the ironstone units which have more vertical and branching burrows predominating. Characteristic Thalassinoides and Skolithos assemblage are observed especially in ironsstone units, while the Skolithos and Ophiomorpha assemblages are well displayed in the aranaceous facies units. Cruziana and Zoophycos assemblages are more common in the argillaceous facies units. The tapering nature, combined with the concentric "shells" of the burrows in the ironstone units reflect variations in the

chemical and/or physical states of the environment in which the burrowers lived. Such changes are salinity, temperature, fluctuations in the water table (Dodd and Stanton, 1981). During unfavourable conditions, the organisms might have retreated far down into their holes, while under succeeding favourable conditions, they would come up pushing aside, the newly derived debris partially filling their holes - hence the geometry of burrows. Also the occurrence of flat bedding within the ironstones units suggest that the kinetic energy levels of the depositional environments may have been fairly high, as above. Such variations of physical and chemical states, high kinetic energy, and trough shaped cross-bedding, is consistent with the interpretation of a beach, tidal inlet, lagoon or barrier island for the ironstones. This is consistent with the various environments of deposition that have been postulated for ironstones. Cayeux (1909, 1922), concluded that the ironstone of Armorica and Lovraine were deposited under certain environmental conditions somewhat similar to those of calcareous oolites. Taylor (1949, p. 79) concluded that the Northampton Sand Ironstone might have been deposited in "a shallow epi-continental sea, gulf or lagoon freely connected with the open sea and subject to considerable wave and current action. James (1954), presented a theoretical model of ironstone facies, different from those of Cayeux (1909, 1922) and Taylor (1949). Although James (1954) agreed that the ironstones represent shallow water accumulations, he thought that their deposition, at least those of Precambrian ironstones of Lake Superior region, were in restricted basins separated from the open sea by thres-holds. The work of Yanitsky (1961) has shown that fresh water oolitic ironstones could occur.

Another school of thought believes that some oolitic and

pisolitic ironstones have evolved from the concretionary action in gel (Pulfrey, 1933). Adeleye (1973) reported that a similar mechanism of conretionary action, in lateritic soils has also been advanced for some vague parts of the ironstones of the Middle Niger Valley of Nigeria by Du Preez (1949, 1952), Jones (1955, 1958), and that their deduction arose from the inability of the authors to find any fossil debris within the Nigerian ironstones. The paucity of fossil occurrence in the ironstone facies is indicative of an unstable (highly fluctuating) environment which is not conducive for survival of living organisms.

As for the aranaceous and argillaceous facies, pattern and extent of occurence of ichnofacies depicts a rather shallow water environment of moderate energy, where physical and chemical conditions are more stable. A coastal alluvial plain, flood plain, prograding deltaic environment is inferred.

5.2 Provenance

The provenance of the sedimentary fill of the Bida Basin has been discussed by several authors and has inevitably led to the postulation for the possible origin (mode of formation) of the basin itself (Adeleye 1971, Ojo and Ajakaiye 1974, Shekwolo, 1983). The two - provenance and basin origin seem intertwined. Based on the evidence of heavy minerals and sedimentary structures Adeleye, (1971) suggests that the depositional medium of the Nupe group of sediments has its source in the Igneous and Metamorphic basement of South-Western Nigeria. Ojo and Ajakaiye (1974b), in an attempt at investigating the maximum thickness of the sedimentary strata and general shape and origin of the basin suggested a maximum possible thickness for the Cretaceous sediments of not more

than 2 km (of the order of 1 km). They went further to attribute positive residual anomalies over parts of the basin to high density Metamorphic basement and to masses which are probably of schist composition, without any trace of deep fractures or faults. They drew a conclusion that the basin originated as a result of local subsidence associated with the adjacent Younger Granite Province tectonic activities in the Jurassic time and to a lesser extent the Benue valley, thus causing thining and subsidence of the basin. Shekwolo (1983) discarded a rift origin for the basin based on the arguments of Holmes (1965). Holmes (1965) believes that basins formed by rifts are produced by differential warping on a regional scale and are usually accompanied by marginal and interior faults, other effects are associated volcanisms, igneous activities and intermittent uplift. Also typical rift valleys have widths of about 50 ± 13 kms. None of the above observations occur in the Bida Basin which is, gently downwarped with width of about 165 kms (Shekwolo, 1983) and no evidence of volcanism or igneous activity. The isostatic subsidence hypothesis seems more plausible, although associ-ated with tectonic activities within adjacent basement areas - the Younger Granite Complex, and the Basement Complex of southwestern Nigeria.

Evidences from heavy minerals, types and mode of occurence of quartz and paleocurrents in this project are in support of the derivation of the clastic components of the Bida Basin from the igneous and metamorphic basement complex of southwestern Nigeria. This is clear from the subequant, slight to strongly undulose, composite (with two or more sub-individuals) and elongate quartz predominant in the aranaceous and argillaceous facies. Folk (1980), interprets such properties as having a metamorphic provenance especially by

the rather straight boundaries of composite quartz grains. Quartz in ironstones are monocrystalline, strongly undulose, non-composite with vacuoles. The rather low occurrence of polycrystalline and composite quartz in the ironstone facies is attributable to the high energy state of depositional environment which splits poly and composite grains into individuals. No evidence of volcanic quartz can be found in any of the facies.

Heavy mineral assemblage (Chapter 4) are distinctive of igneous (plutonic) and metamorphic provenance (Pettijohn, 1975), while the evidence of cross-bedding azimuth is in favour of a northerly direction of paleoflow of the medium of deposition of sedimentary rocks studied. Contributions towards the basin fill by the Younger Granite Complexes which are plutonic cannot be completely ruled out especially based on evidences of heavy mineral assemblages and properties of quartz, hence the subsidence of the Bida Basin seems related to tectonic activities in the Younger Granite region. Likewise contribution towards the Bida basin fill by the Benue Valley, is even more remote, due to associated igneous activities in the Benue trough, because no volcanic property of quartz or any other mineral is observed. Most importantly the northerly direction of paleoflow makes such contribution not easily conceivable.

CHAPTER SIX

DISCUSSION AND CONCLUSIONS

The geology of the part of the Bida Basin under investigation, is rather monotonous. It comprises mainly the Nupe group of sediments, the alluvium and the laterite capped hills. The Bida Sandstone Formation consists of massive and flat bedded sandstones, subsiduary claystones, fine conglomerates and siltstones. The sandstones have grains that are generally angular to subangular, well to poorly sorted, fine to very coarse and pebbly. The basal beds are succeeded by dominatly goethitic oolitic and pisolitic ironstones with iron-oxide cement forming a prominent break of slope along the mesa-walls in the Bida area and is referred to s the Sakpe Ironstone Formation.

The Sakpe (Lower Ironstone) Formation may or may not overlie the basal Bida Formation. Hence the argillaceous Enagi Formation can overlie either the basal sandstone or the Lower Ironstone. The Enagi Formation is fine grained sandstone, siltstone and claystones, commonly laminated or massive. On top of the Enagi Formation is the Batati (Upper Ironstone) Formation, forming capping of mesas under a lyer of laterite of variable thickness. The beds are dominatly oolitic, with subsidiary claystones, and shelly beds, generally massive with thin to thick flat-bedding and lamination.

The study of the mineralogy and investigation of textural paramters by size analysis of sedimentary rocks within the area of study has been valuable in not only determining environment of deposition but also in provenance determination. Pebble morphometry, sieve analysis, thin section.....

studies and heavy mineral analysis are especially valuable in this respect. Roundness was used for environmental discrimination by bivariate plots of Sames (1966, Fig 1) and in interpretation of environment after Lutig (1962). A predominantly fluviatile to transitional environment of deposition was deduced for not less than 90 per cent pebbles studied. Likewise, by the bivariate plot of Dobkins and Folk (1970), where Oblate - Prolate Index was plotted against Maximum Projection Sphericity (Yp), majority of pebbles though at a lower percentage were interpreted as having a river environment of deposition.

Sieve analysis on the other hand, despite the incomplete intervals of mesh, aided in determining size parameters like skewness, kurtosis, sorting, and mean grain sizes. Results show most sands in the Bida Basin to be poorly sorted, positively skewed and leptokurtic in distribution (Table 4.6), with grain size frequency distribution curve showing bimodality of grain sizes. The use of varied combinations of these parameters in environmental diagnosis after Friedman (1979), as shown in Fig 15, indicates a consistently fluviatile (river) environment of deposition. While the study of rocks by thin section has been especially useful in sandstone classification and determining degree of maturity. Majority of sands belong to the Quartz Arenite group, while others belong to the Arkosic Arenite group. Siltstone, Claystones and Ironstones are not classified. Heavy mineral analysis resulted in an assemblage of heavy minerals that clearly excluded a volcanic provenance for clastic grains, but an assemblage related to an igneous (plutonic) and metamorphic terrain provenance.

Sedimentary structures, hence paleocurrent analysis has been very useful too. Although ichnofacies may not be very

distinctive due to limitations of extent of study, a Zoophycos, Cruziana, Glossifungites and occasionally Nereites assemblages can be delineated. Paleocurrent analysis is however distinctive of sediment source of the Igneous and Metamorphic terrains of South-western Nigeria, because of the direction of azimuths of cross-beddings which is predominantly northerly in orientation. Although the ironstone facies environment of deposition could be rather shallow and high energy, Adeleye (1973) however suggested that environment of deposition of ironstone facies could be closely linked to the Tethys transgression in the Tertiary (Fig 17).

Finally, further work need be done in this area especially on the concentration of mesa-capped (lateritic) inselbergs in this area. Their mode of formation and the geomorphologic agents responsible need to be investigated, due to their near perfect geometry.

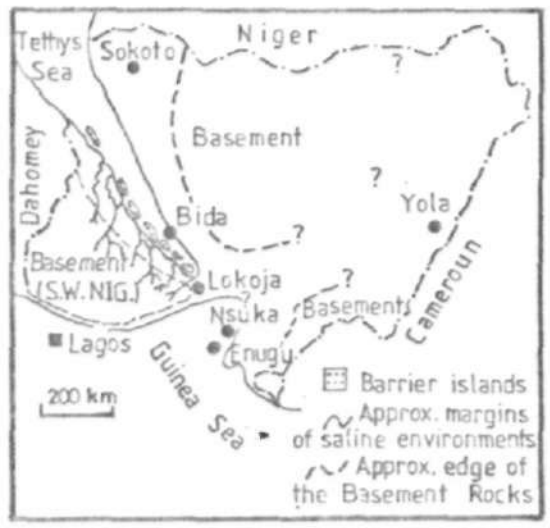


Fig. 17. Palaeogeographical map of Nigeria during the depositional phase of the Lower Ironstones. The pisolitic facies may have been deposited on the seaward side of the barrier islands, while the oolitic facies may have been deposited on the landward side.
After Adeleye (1973)

REFERENCES

Adeleye, D.R. (1971). Stratigraphy and Sedimentation ofthe Upper Cretaceous Strata around Bida, Nigeria: *Unpublished Ph.D. Thesis*, University of Ibadan, Nigeria, 297p.

Adeleye, D.R. (1973). Origin of Ironstones, an example from the Middle Niger Valley, Nigeria. *Jour. Sed. Petrol.* 43, 709-727.

Adeleye, D.R. (1974a). Sedimentology of the fluvial Bida Sandstone (Cretaceous), Nigeria. *Sedimentary Geology* 12, 1-24.

Adeleye, D.R. (1974b). The Geology of the Middle Niger Basin In: C.A. Kogbe (Ed); *Geology of Nigeria*, Elizabethan Publishing Co. Lagos (1976), pp. 283-287.

Adeleye, D.R. and Dessauvagie, T.F.J. (1972). Stratigraphy of the Niger Embayment. In: T.F.J. Dessauvagie and A.J. Whiteman (Eds); *African Geology*. Ibadan University Press pp 181-186.

Allen, J.R.L. (1965). A Review of the Origin and Characteristics of Recent Alluvial Sediments. *Sedimentology*, 5, 89-191.

Allen, J.R.L. (1968). On bed forms and paleocurrents. *Sedimentology*, 6, 153-190.

Allen, J.R.L. (1970). *Physical Processes of Sedimentation*. George Allen and Unwin Ltd, London, 248p.

Allen, J.R.L. (1974). Studies in fluviatile sedimentation: Implications of pedogenic carbonate units, Lower Old Red Sandstone, Anglo-Welsh outcrop. *Geological Jour.* 9, 181-208.

Allen, J.R.L. (1982). *Sedimentary structures: their character and physical basis*, Vol II. Elsevier Science Publishing Company, Amsterdam, 663p.

American Commission on Stratigraphic Nomenculature (1961). *Amer. Assoc. Petrol. Geol. Bull.* 45, 645-655.

Arakel, A.V. (1982). Genesis of calcrete in Quarternary soil profiles, Hutt and Leeman Lagoons, Western Australia. *Jour. Sed. Petrol.* 52, 109-125.

Bagnold, R.A. (1941). The Physics of Blown Sand and Desert Dunes. In: Blatt,H., Middleton, G. and Murray, R; *Origin of Sedimentary Rocks.* Prentice-Hall Inc., Englewood Cliffs, New Jersey, 07632, 728p.

Bagnold, R.A. (1956). The flow of cohesionless grains in fluids. In: Reineck, H.E and Singh, I.B; *Depositional Sedimentary Environments.* Springer-Verlag, Berlin. Heidelberg. New York. 1978, 439p.

Bailey, E.B. (1930). New light on sedimentation and tectonics. *Geol. Mag.* 67, 77-92.

Blatt, H. (1967). "Original Characteristics of Clastic Quartz Grains". *Jour. Sed. Petrol.* 37, 401-424.

Blatt, H. and Christie, J.M. (1963). "Undulatory Extinction in Quartz of Igneous and Metamorphic Rocks and its Significance in Prvenace studies of Sedimentary Rocks" *Jour. Sed. Petrol.* 33, 559-579.

Blatt, H., Middleton, G., and Murray, R. (1980). *Origin of Sedimentary Rocks.* Prentice-Hall, Inc., Englewood Cliffs, New Jersey, 07632, 782p.

Carr, T.R. (1982). Log-linear models, Markov Chains and Cyclic Sedimentation. *Jour. Sed. Petrol.* 52, 905-912.

Carr, T.R., Horowitz, a., Ridge, K.F., Straw, W.T., Webb, W., and Potter, P.E. (1966). Stratigraphic sections, bedding sequences, and random processes. *Science*, 1162-1164.

Cayeux, L. (1909). Les minerais de fer oolithique de France: *Fasc. I. Minerais de fer secondaires.* Paris.

Cayeux, L. (1922). Les minerais de fer oolithique de France: *Fasc. II. Minerais de fer secondaires.* Paris.

Coleman, A.P. (1926). *Ice ages, recent and ancient.* MacMillan, Inc. New York, 296p.

Collinson, J.D. and Thompson, D.B. (1982). *Sedimentary Structures.* George Allen and Unwin, London, 194p.

Conolly, J.R. (1965). The occurrence of polycrystallinity and undulatory extinction in quartz in sandstones *Jour. Sed. Petrol.* 35, 116-135.

Dobkins, J.E. and Folk R.L. (1970). Shape development on Tahiti-Nui. *Jour. Sed. Petrol.* 40, 1167-1203.

Dodd, J.R. and Stanton, J.R., Jr. (1981). *Paleoecology, Concepts and Applications.* John Wiley and Sons, Inc. Toronto, 559p.

Du Preez, J.W. (1949). Origin, Classification and Distribution of Nigerian Laterites. *Proceedings of the 3rd West African Conference*, Ibadan, 223-234.

Du Preez, J.W. (1952). Notes on the occurrence of Dolites and Pisolites in Nigerian Laterites. *Geol. Surv. Nigeria Rept.* No. 1027.

Ethier, V.G. (1975). Application of Markov Analysis to the Banff Formation (Mississippian), Alberta. *Math. Geol* 7, 47-61.

Fairchild, I.J. (1979). Sedimentation and origin of a Late Precambrian dolomite from Scotland. *Jour. Sed. Petrol* 50, 423-446.

Falconer, J.D. (1911). *The Geology and Geography of Northern Nigeria.* MacMillan, London.

Folk, R.L. (1951). Stages of textural maturity in sedimentary rocks. *Jour. Sed. Petrol.* 21, 127-130.

Folk, R.L. (1980). *Petrology of Sedimentary Rocks.* Hemphill Publishing Company, Austin, Texas, 182p.

Folk, R.L and Ward, W.C. (1980). *Brazos River Bar: A study in the significance of grain size parameters. Jour. Sed. Petrol.* 27, 3-27.

Fournier, F. (1962). *Carte du danger d'erosion en Afrique* au Sud du Sahara. In: Thomas, M.F; *Tropical Geomorphology.* MacMillan Press Ltd, 1974, 332p.

Friedman, G.M. (1961). Distinction between Dune, Beach and River Sands from their textural characteristics. *Jour. Sed. Petrol.* 31, 514-529.

Friedman, G.M. (1962b). On sorting, sorting coefficients and the lognormality of the grain size distribution of sandstones. *Jour. Geol.* 70, 737-753.

Friedman, G.M. (1967). Dynamic processes and statistical parameters compared for size frequency distribution of beach and river sands. *Jour. Sed. Petrol.* 37, 327-354

Friedman, G.M. (1979). Differences in size distributions of populations of particles among sands of various origins *Sedimentology.* 26, 3-32.

Friedman, G.M. and Sanders, J.E. (1978). *Principles of Sedimentology.* John Wiley and Sons. New York, Chichester. Brisbane. Toronto. 792p

Gary, M., McAfee Jr, R. and Wolf, C.L. (Eds), 1974. *Glossary of Geology.* American Geological Institute, 5205 Leesburg Pike, Falls Church, Va. 22041. 805p

Gingerich, P.D. (1969). Markov Analysis of cyclic alluvial sediments. *Jour. Sed. Petrol.* 39, 330-332.

Goudie, A. (1973). *Duricrusts in tropical and subtropical landscapes.* Clarendon Press, Oxford, 174p.

Greensmith, J.T. (1978). *Petrology of The Sedimentary Rocks* George Allen and Unwin, London, 241p.

Griffiths, J.C. (1967). *Scientific methods in analysis of sediments.* MacGraw-Hill Book Company. New York 508p

Harms, J.C, and Fahnestock, R.K. (1965). Stratification, bedforms, and flow phenomena (with an example from the Rio Grande), In: Middleton, G.V. (Ed). Primary sedimentary structures and their hydrodynamic interpretation - a symposium. *Soc. Econ. Pal. Min. Spec. Pub.* No. 12, 265p.

Holmes, A. (1965). *Principles of Geology.* Thomas Nelson Nigeria Ltd. Lagos, 287-289.

Hoque, M. and Nwajide, C.S. (1985). Application of Markov Chain and Entropy Analysis to lithologic successions: An example fromthe cretaceous of the Benue Trough (Nigeria). *Geologische Rundschau*, Stuggart, 74 (1), 165-177.

Iosifescu, M. (1980). *Finite Markov Processes and their Application.* John wiley and Company. New York, 295p.

James, H.L. (1954). Sedimentary Facies of iron Formation. *Econ. Geol.* 49, 235-293.

James, N.P. (1972). Holocene and Pleistocene calcareous crust (caliche) profiles: criteria for subaerial exposure. *Jour. Sed. Petrol.* 42, 817-836.

Jan Du Chene, R., Adegoke, O.S., Adediran, S.A. and Petters, S.W. (1978). Palynology and foraminifera of the Lokoja sandstone (Maastrichian), Bida Basin, *Nigeria Rev. Esp. Micropal.* 10(3), 379-393.

Jones, D.G. (1953). Report on a water supply for Bida town, Niger Province. *Geol. Surv. Nig. Rept.* No. 1113.

Jones, H.A. (1955). The occurrence of Oolitic Ironstones in Nigeria: Their Origin, Geological History and Petrology. *Unpublished, Ph.D. Thesis*, Oxford University, England. 207p.

Jones, H.A. (1958). The Oolitic Ironstones of Agbaja Plateau Kabba Province. *Record of the Geol. Surv*, Nigeria 20-43.

Jungst, H. (1934). Zur geologischen Bedentung der synarese *Geol. Rundschau.* 15, 312-325.

Kehinde, M.O. (1988). Groundwater studies in the Bida Basin, Nigeria. In Press; Proc. German-Afr. Geoscientists, Hanover, F.R.G.

Krumbein, W.C., and Dacey,M.F. (1969). Markov Chains and Embedded Markov Chains in Geology. *Math. Geol.* 1, 79-97

Kuenen, Ph. H., and Migliorini, C.I. (1950). Turbidity currents as a cause of graded bedding. *Jour. Geol.* 58, 91-127.

Leeder, M.R. (1982). *Sedimentology.* George Allen and Unwin, London. 344p.

Lutig, G. (1962). The shape of pebbles in the continental, fluviatile and marine facies. *Intern. Assoc. Scientific Hydrology, Publ.* No. 59, 235-258.

Maxlock Group Nig. Ltd. (1979). Niger State Regional Plan. *New Nigerian Newspapers Ltd*, Kaduna, pg 3.5.6.

McKee,L.D, and Weir, G.W. (1953). Terminology for stratification and cross-stratification in sedimentary rocks. *Bull. Geol. Soc. Am.* 64, 381-390.

Miall, A.D. (1973). Markov Chain Analysis applied to an ancient alluvial plain succession. *Sedimentology*, 20, 347-364.

Nwajide, C.S. (1987). Irregular sedimentary structures of the Makurdi Sandstones: Genesis and diagnostic utility. *Records of Geol.surv.*, Nigeria, vol. 10.

Nwajide, C.S. and Hoque, M. (1982). Pebble morphometry as an aid in environmental diagnosis: An example from the Middle Benue Trough. *Jour. Min. Geol.* 19(1), 114-120

Nwajide, C.S. and Hoque, M. (1985). Problems of classification and maturity evaluation of a diagenetically altered fluvial sandstone. *Geologie en Mijnbouw.* 64, 69-77.

Nye, P.H. (1954). Some soil forming processes in the humid tropics, Part I: A field study of a catena in the West African forest. *Jour. Soil Sci.* 5, 7-27.

Ojo, S.B., and Ajakaiye, D.E. (1974). Preliminary interpretation of gravity measurements in the Middle Niger Basin Area: In; Kogbe, C.A. (Ed); *Geology of Nigeria* Elizabethan Publ. Co., Lagos (1976), 295-306.

Pettijohn, F.J. (1936). Early Precambian varved state in northwestern Ontario. *Bull. Geol. Soc. Amer.* 47, 621-628.

Pettijohn, F.J. (1975). *Sedimentary Rocks.* Harper and Row, Publishers. New York, Evanston, San Francisco and London. 628p.

Pettijohn, F.J., Potter, P.E.,and Siever, R. (1972). *Sand and Sandstone.* Springer-Verlag, New York, Heidelberg, Berlin. 618p.

Porrenga, D.R. (1967). Glauconite and Chamosite as depth indicators in the marine environments. *Marine Geology.* 5, 495-501.

Potter, P.E., and Pettijohn, F.J. (1977). *Paleocurrent and Basin Analysis.* 2nd ed, Academic Press, New York 425p

Powers, M.C. (1953). A new roundness scale for sedimentary particles. *Jour. Sed. Petrol.* 23, 117-119.

Powers, D.W., and Easterling, R.G. (1982). Improved methodology for using Embedded Markov Chains to describe cyclic sediments. *Jour. Sed. Petrol.* 52, 913-923.

Pulfrey, W. (1933). The Iron Ore Oolites and Pisolites of North Wales. *Quartz. Jour. Geol. Soc. Lond.* 89, 401-430.

Pullan, R.A. (1967). A Morphological Classificatin of lateritic ironstones and ferruginized rocks in Northern Nigeria. *Nig. Jour. Sci.* 1, 161-173.

Rateev, M.A., Gorbunova, Z.N., Lisitzyn, A.P., and Nosov, G.L (196). The distribution of clay minerals in the oceans *Sedimentology.* 13, 21-43.

Read, W.A. (1969). *Analysis and solution of Namurian sediments in central Scotland using a Markov - process model. Math. Geol.* 1, 199-219.

Rees, A.I. (1966). Some flume experiments with a fine silt. *Sedimentology.* 1, 209-240.

Reeves, Jr., C.C. (1970). Origin, classification and geologic history of caliche on the Southern High Plains, Texas and Eastern New Mexico. *Jour. Geol.* 78, 352-362.

Reineck, H.E,and Singh, I.B. (1978). *Depositional Sedimentary Environments.* Springer-Verlag, Berlin, Heidelberg New York. 1978, 439p.

Richter, R. (1936). Marken und Spuren im Hunsru Kschiefer I. In: Reineck, H.E., and Singh, I.B; *Depositional Sedimentary Environments.* Springer-Verlag, Berlin, Heidelberg, New York. 1978, 439p.

Richter, R. (1937). Marken und Spuren aus allen Zeiten. I.II. In: Reineck, H.E., and Singh, I.B; *Depositional Sedimentary Environments.* Springer-Verlag, Berlin, Heidelberg, New York. 1978, 439p.

Richter, R. (1952). Fludial-Textur in Sediment-Gesteinen und uber Sedifluktion uberhaupt. In: Reineck, H.E., and Singh, I.B; *Depositional Sedimentary Environments.* Springer-Verlag, Berlin, Heidelberg, New York. 1978, 439p.

Royce Jr, C,F. (1970). An Introduction to Sediment Analysis. *Sediment Analysis.* Tempe, Arizona. 180p.

Russ, W. (1957). The Geology of Parts of Niger, Zaria and Sokoto Provinces. *Geol. Surv. Nig. Bull.* No. 27.

Sames, C.W. (1966). Morphometric data of some recent pebble associations and their application to ancient deposits. *Jour. Sed. Petrol.* 36, 126-142.

Seilacher, A. (1953). Studien zur Palichnologie. Neues Jahrnb. *Geol. Paleontology.* 96, 421-452.

Seilacher, A. (1964). Biogenic Sedimentary Structures. In: Imbrie, J., and Newell, N. (eds); *Approaches to Paleoecology.* Wiley and Sons, New York, 296-316.

Seilacher, A. (1967). Bathymetry of Trace Fossils. *Marine Geol.* 5, 413-428.

Shearman, D.J., Twyman, J., and Karimi, M.Z. (1970). The *Genesis and Diagnosis of Oolites.* *Proc. Geol. Assoc.* 81, 561-575.

Shekwolo, P.D. (1983). *Hydrogeology of Gbako River Basin, Niger State.* Unpublished M.Sc. Thesis, Ahmadu Bello University, Zaria. 138p.

Shepard, F.P., and Young, R. (1961). Distinguishing between beach and dune sands. *Jour. Sed. Petrol.* 31, 196-214

Simons, D.B., Richardson, E.V., and Nordin, C.F. (1965). Sedimentary structures generated by flow in alluvial channels. In: Middleton, G.V. (ed); Primary Sedimentary Structures and their hydrodynamic interpretation. *Soc. Econ. Paleon. Mineral. Spec. Publ.* 12, 34-52.

Sneed, E.D., and Folk, R.L. (1958). Pebbles in the lower Colorado River, Texas; a study in particle morphogenesis. *Jour. Geol.* 66, 114-150.

Steel, J.R. (1974). *Cornerstone (fossil caliche)* - its origin, stratigraphic and sedimentological importance in the New Red Sandstone, Western Scotland. *Jour. Geol.* 82, 251-269.

Taylor, J.H. (1949). Petrology of the Northampton Sand Ironstone Formation. *Memo. Geol. Surv. Great Britain.*

Thomas, M.F. (1966a). Some geomorphological implications of deep weathering patterns in crystalline rocks in Nigeria. In: Thomas, M.F; *Tropical Geomorphology.* MacMillan Press Ltd. London. 332p.

Thomas, M.F. (1974). *Tropical Geomorphology.* MacMillan Press Ltd. London. 332p.

Tucker, M.E. (1982). *Sedimentary Petrology:* An Introduction. Blackwell Scientific Publications, London. Vol. 3, 252p.

Udoh, R.K. (1978). *Geographical regions of Nigeria.* Heinemann Publishers, London. 212p.

Visher, G.S. (1965). Use of vertical profile in environmental reconstruction. *Am. Assoc. Petrol. Geol. Bull.* 49, 41-61.

Wentworth, C.K. (1922). A scale of grade and class terms for clastic sediments. *Jour. Geol.* 30, 377-392.

Yanitsky, A.L. (1961). Oolitic Ironstones of fresh water origin: (A Review of a Russian Monograph). Extract from the *Mining Magazine.* 104, 158-159.

APPENDIX 1 :

DATA SHEETS FOR SIEVE ANALYSIS .

APPENDIX 1

Report of Sieve Analysis

Sample No. $1FR_1$
Method of Analysis: (a) Screen type: Half-phi interval: ASTM
(b) Sieving time: 15 min.
Weight of sample: 200 gm
Note: To get cummulative weight percentage, divide each figure by the last number in the cummulative weight column and multiply by 100

Class Interval		Retained on sieve wt (gm)	Corrected wt (gm)	Cum. wt.	Cum wt %	Wt. %
mm	phi					
2.800–2.000	-1.50--1.00	0.00	0.000	0.000	0.000	0.000
2.000–1.400	-1.00--0.50	5.83	5.882	5.882	2.941	2.941
1.400–1.000	-0.50- 0.00	18.12	18.281	24.163	12.082	9.141
1.000–0.500	0.00- 1.00	51.12	51.574	75.737	37.869	25.787
0.500–0.355	1.00- 1.50	21.57	21.762	97.499	48.750	10.881
0.355–0.250	1.50- 2.00	21.04	21.227	118.726	59.363	10.614
0.250–0.180	2.00- 2.50	21.37	21.560	140.286	70.143	10.780
0.180–0.125	2.50- 3.00	15.36	15.496	155.782	77.891	7.748
0.125–0.106	3.00- 3.50	6.27	6.326	162.108	81.054	3.163
0.106–0.063	3.50- 4.00	15.44	15.577	177.685	88.843	7.789
0.063–0.045	4.00- 4.50	13.76	13.882	191.567	95.784	6.941
< 0.045	> 4.50	8.36	8.434	200.001	100.000	4.217
Sieve loss		1.76				
Total weight		198.24				

Statistical Parameters:
$\phi 5 = -0.30$; 016 = 0.20; 025 = 0.55; 050 = 1.60;
075 = 2.80; 084 = 3.65; 095 = 4.40

APPENDIX 1

Report of Sieve Analysis

Sample No. $1FR_2$
Method of Analysis: (a) Screen type: Half-phi interval: ASTM
(b) Sieving time: 15 min.
Weight of sample: 200 gm
Note: To get cummulative weight percentage, divide each figure by the last number in the cummulative weight column and multiply by 100

Class Interval		Retained on sieve wt (gm)	Corr-ected wt (gm)	Cum. wt.	Cum wt %	Wt. %
mm	phi					
2.800-2.000	-1.50--1.00	1.48	1.491	1.491	0.746	0.746
2.000-1.400	-1.00--0.50	3.96	3.991	5.482	2.741	1.996
1.400-1.000	-0.50- 0.00	9.51	9.583	15.065	7.533	4.792
1.000-0.500	0.00- 1.00	58.76	59.213	74.278	37.139	29.607
0.500-0.355	1.00- 1.50	38.50	38.797	113.075	56.538	19.399
0.355-0.250	1.50- 2.00	32.24	32.489	145.564	72.728	16.245
0.250-0.180	2.00- 2.50	17.58	17.716	163.280	81.640	8.858
0.180-0.125	2.50- 3.00	18.19	18.330	181.610	90.805	9.165
0.125-0.106	3.00- 3.50	9.80	9.876	191.486	95.743	4.938
0.106-0.063	3.50- 4.00	2.38	2.398	193.884	96.942	1.199
0.063-0.045	4.00- 4.50	2.60	2.620	196.504	98.252	1.310
< 0.045	> 4.50	3.47	3.497	200.001	100.000	1.749
Sieve loss		1.53				
Total weight		198.47				

Statistical Parameters:
05 = -0.20; 016 = 0.40; 025 = 0.70; 050 = 1.30;
075 = 2.15; 084 = 2.60; 095 = 3.40

APPENDIX 1

Report of Sieve Analysis

Sample No. IFR_5
Method of Analysis: (a) Screen type: Half-phi interval: ASTM
(b) Sieving time: 15 min.
Weight of sample: 200 gm
Note: To get cummulative weight percentage, divide each figure by the last number in the cummulative weight column and multiply by 100

Class Interval		Retained on sieve wt (gm)	Corr-ected wt (g)	Cum. wt.	Cum wt %	Wt. %
mm	phi					
2.800-2.000	-1.50--1.00	4.81	4.828	4.828	2.414	2.414
2.000-1.400	-1.00--0.50	10.49	10.529	15.357	7.679	5.265
1.400-1.000	-0.50- 0.00	25.25	25.344	40.701	20.351	12.672
1.000-0.500	0.00- 1.00	86.60	86.922	127.623	63.812	43.461
0.500-0.355	1.00- 1.50	24.94	25.034	152.656	76.328	12.517
0.355-0.250	1.50- 2.00	16.36	16.421	169.077	84.539	8.211
0.250-0.180	2.00- 2.25	9.26	9.294	178.371	89.186	4.647
0.180-0.125	2.50- 3.00	12.15	12.195	190.566	95.283	6.098
0.125-0.106	3.00- 3.50	0.13	0.130	190.696	95.348	0.065
0.106-0.063	3.50- 4.00	5.69	5.711	196.407	98.204	2.856
0.063-0.045	4.00- 4.50	0.88	0.883	197.290	98.645	0.442
< 0.045	> 4.50	2.70	2.710	200.000	100.000	1.355
Sieve loss		0.74				
Total weight		199.26				

Statistical Parameters:
05 = -0.70; 016 = -0.15; 025 = 0.10; 050 = 0.70;
075 = 1.40; 084 = 1.95; 095 = 3.10

APPENDIX 1

Report of Sieve Analysis

Sample No. $2FR_1$
Method of Analysis: (a) Screen type: Half-phi interval: ASTM
(b) Sieving time: 15 min.
Weight of sample: 200 gm
Note: To get cummulative weight percentage, divide each figure by the last number in the cummulative weight column and multiply by 100

Class Interval		Retained on sieve wt (gm)	Corrected wt (gm)	Cum. wt.	Cum wt %	Wt. %
mm	phi					
2.800-2.000	-1.50--1.00	0.000	0.000	0.000	0.000	0.000
2.000-1.400	-1.00--0.50	0.100	0.102	0.102	0.051	0.051
1.400-1.000	-0.50- 0.00	0.750	0.762	0.864	0.432	0.381
1.000-0.500	0.00- 1.00	13.840	14.070	14.934	7.467	7.035
0.500-0.355	1.00- 1.50	17.410	17.699	32.633	16.317	8.850
0.355-0.250	1.50- 2.00	36.490	37.097	69.730	34.865	18.549
0.250-0.180	2.00- 2.25	46.680	47.456	117.186	58.593	23.728
0.180-0.125	2.50- 3.00	37.110	37.727	154.913	77.457	18.864
0.125-0.106	3.00- 3.50	23.950	24.348	179.261	89.631	12.174
0.106-0.063	3.50- 4.00	11.710	11.905	191.166	95.583	5.953
0.063-0.045	4.00- 4.50	6.87	6.984	198.150	99.075	3.492
< 0.045	> 4.50	1.82	1.850	200.000	100.000	0.925
Sieve loss		3.27				
Total weight		196.73				

Statistical Parameters:
05 = 0.85; 016 = 1.50; 025 = 1.80; 050 = 2.35;
075 = 2.95; 084 = 3.25; 095 = 3.95

APPENDIX 1

Report of Sieve Analysis

Sample No. $2FR_2$
Method of Analysis: (a) Screen type: Half-phi interval: ASTM
(b) Sieving time: 15 min.
Weight of sample: 200 gm
Note: To get cummulative weight percentage, divide each figure by the last number in the cummulative weight column and multiply by 100

Class Interval		Retained on sieve wt (gm)	Corr-ected wt (gm)	Cum. wt.	Cum wt %	Wt. %
mm	phi					
2.800-2.000	-1.50--1.00	0.000	0.000	0.000	0.000	0.000
2.000-1.400	-1.00--0.50	0.290	0.290	0.290	0.145	0.145
1.400-1.000	-0.50- 0.00	4.730	4.732	5.022	2.511	2.366
1.000-0.500	0.00- 1.00	33.870	33.885	38.907	19.454	16.943
0.500-0.355	1.00- 1.50	25.310	25.321	64.228	32.114	12.661
0.355-0.250	1.50- 2.00	34.540	34.556	98.784	49.392	17.278
0.250-0.180	2.00- 2.25	30.550	30.564	129.348	64.674	15.222
0.180-0.125	2.50- 3.00	32.590	33.605	161.953	80.977	16.303
0.125-0.106	3.00- 3.50	3.560	3.562	165.515	82.758	1.781
0.106-0.063	3.50- 4.00	23.170	23.180	188.695	94.348	11.950
0.063-0.045	4.00- 4.50	7.84	7.844	196.539	98.270	3.922
< 0.045	> 4.50	3.46	3.462	200.001	100.001	1.731
Sieve loss		0.09				
Total weight		199.91				

Statistical Parameters:
05 = 0.30; 016 = 0.90; 025 = 1.25; 050 = 2.05;
075 = 2.80; 084 = 3.55; 095 = 4.10

APPENDIX 1

Report of Sieve Analysis

Sample No. $2FR_5$
Method of Analysis: (a) Screen type: Half-phi interval: ASTM
(b) Sieving time: 15 min.
Weight of sample: 200 gm
Note: To get cummulative weight percentage, divide each figure by the last number in the cummulative weight column and multiply by 100

Class Interval		Retained on sieve wt (gm)	Corr-ected wt (gm)	Cum. wt.	Cum wt %	Wt. %
mm	phi					
2.800-2.000	-1.50--1.00	0.000	0.000	0.000	0.000	0.000
2.000-1.400	-1.00--0.50	0.450	0.452	0.452	0.226	0.226
1.400-1.000	-0.50- 0.00	3.060	3.073	3.525	1.763	1.537
1.000-0.500	0.00- 1.00	15.880	15.946	19.471	9.736	7.973
0.500-0.355	1.00- 1.50	37.070	37.224	56.695	28.348	18.612
0.355-0.250	1.50- 2.00	47.240	47.437	104.132	52.066	23.719
0.250-0.180	2.00- 2.50	46.670	46.864	150.996	75.498	23.432
0.180-0.125	2.50- 3.00	8.720	8.756	159.752	79.876	4.378
0.125-0.106	3.00- 3.50	16.140	16.207	175.959	87.980	8.104
0.106-0.063	3.50- 4.00	13.980	14.038	189.997	94.999	7.019
0.063-0.045	4.00- 4.50	6.040	6.065	196.062	98.031	3.033
< 0.045	> 4.50	3.930	3.946	200.008	100.004	1.973
Sieve loss		0.830				
Total weight		199.170				

Statistical Parameters:
05 = 0.60; 016 = 1.20; 025 = 1.40; 050 = 1.95;
075 = 2.50; 084 = 3.25; 095 = 4.00

APPENDIX 1

Report of Sieve Analysis

Sample No. $2FR_4$
Method of Analysis: (a) Screen type: Half-phi interval: ASTM
(b) Sieving time: 15 min.
Weight of sample: 200 gm
Note: To get cummulative weight percentage, divide each figure by the last number in the cummulative weight column and multiply by 100

Class Interval		Retained on sieve wt (gm)	Corr-ected wt (gm)	Cum. wt.	Cum wt %	Wt. %
mm	phi					
2.800-2.000	-1.50--1.00	0.000	0.000	0.000	0.000	0.000
2.000-1.400	-1.00--0.50	0.120	0.120	0.120	0.060	0.060
1.400-1.000	-0.50- 0.00	1.810	1.813	1.933	0.967	0.907
1.000-0.500	0.00- 1.00	11.680	11.698	13.631	6.816	5.849
0.500-0.355	1.00- 1.50	10.950	10.966	24.597	12.299	5.483
0.355-0.250	1.50- 2.00	33.750	33.801	58.398	29.199	16.901
0.250-0.180	2.00- 2.50	47.770	47.842	106.240	53.120	23.921
0.180-0.125	2.50- 3.00	52.040	52.118	158.358	79.179	26.059
0.125-0.106	3.00- 3.50	18.110	18.137	176.495	88.248	9.069
0.106-0.063	3.50- 4.00	20.490	20.521	197.016	98.508	10.261
0.063-0.045	4.00- 4.50	2.050	2.053	199.069	99.535	1.027
< 0.045	> 4.50	0.930	0.931	200.000	100.000	0.466
Sieve loss		0.310				
Total weight		199.700				

Statistical Parameters:
05 = 0.80; 016 = 1.65; 025 = 1.90; 050 = 2.40;
075 = 2.90; 084 = 3.25; 095 = 3.75

APPENDIX 1

Report of Sieve Analysis

Sample No. 3FR$_1$
Method of Analysis: (a) Screen type: Half-phi interval: ASTM
(b) Sieving time: 15 min.
Weight of sample: 200 gm
Note: To get cummulative weight percentage, divide each figure by the last number in the cummulative weight column and multiply by 100

Class Interval		Retained on sieve wt (gm)	Corr-ected wt (gm)	Cum. wt.	Cum wt %	Wt. %
mm	phi					
2.800-2.000	-1.50--1.00	0.730	0.736	0.736	0.368	0.368
2.000-1.400	-1.00--0.50	2.340	2.359	3.095	1.548	1.180
1.400-1.000	-0.50- 0.00	7.560	7.620	10.715	5.358	3.810
1.000-0.500	0.00- 1.00	42.470	42.808	53.523	26.762	21.404
0.500-0.355	1.00- 1.50	20.170	20.331	73.854	36.927	10.166
0.355-0.250	1.50- 2.00	24.740	24.937	98.791	49.396	12.469
0.250-0.180	2.00- 2.25	26.860	27.074	125.865	62.933	13.537
0.180-0.125	2.50- 3.00	25.930	26.136	152.001	76.001	13.068
0.125-0.106	3.00- 3.50	7.150	7.207	159.208	79.604	3.604
0.106-0.063	3.50- 4.00	21.090	21.258	180.466	90.233	10.629
0.063-0.045	4.00- 4.50	12.050	12.146	192.612	96.306	6.073
< 0.045	> 4.50	7.330	7.388	200.000	100.000	3.694
Sieve loss		1.580				
Total weight		198.420				

Statistical Parameters:
05 = 0.00; 016 = 0.60; 025 = 0.90; 050 = 2.00;
075 = 2.95; 084 = 3.70; 095 = 4.34

APPENDIX 1

Report of Sieve Analysis

Sample No. $3FR_2$
Method of Analysis: (a) Screen type: Half-phi interval: ASTM
(b) Sieving time: 15 min.
Weight of sample: 200 gm
Note: To get cummulative weight percentage, divide each figure by the last number in the cummulative weight column and multiply by 100

Class Interval		Retained on sieve wt (gm)	Corr-ected wt (gm)	Cum. wt.	Cum wt %	Wt. %
mm	phi					
2.800-2.000	-1.50--1.00	20.000	20.145	20.145	10.073	10.073
2.000-1.400	-1.00--0.50	20.160	20.306	40.451	20.226	10.153
1.400-1.000	-0.50- 0.00	20.850	21.001	61.452	30.726	10.501
1.000-0.500	0.00- 1.00	42.060	42.365	103.817	51.909	21.183
0.500-0.355	1.00- 1.50	16.560	16.680	120.497	60.249	8.340
0.355-0.250	1.50- 2.00	20.380	20.528	141.025	70.573	10.264
0.250-0.180	2.00- 2.25	19.950	20.095	161.120	80.560	10.048
0.180-0.125	2.50- 3.00	18.020	18.151	179.271	89.636	9.076
0.125-0.106	3.00- 3.50	13.950	14.051	193.322	96.662	7.026
0.106-0.063	3.50- 4.00	3.100	3.123	196.445	98.223	1.562
0.063-0.045	4.00- 4.50	1.860	1.873	198.318	99.159	0.937
< 0.045	> 4.50	1.670	1.682	200.000	100.000	0.841
Sieve loss		1.440				
Total weight		198.560				

Statistical Parameters:
05 = ? ; 016 = -0.70; 025 = -0.25; 050 = 0.90;
075 = 2.20; 084 = 2.70; 095 = 3.35

APPENDIX 1

Report of Sieve Analysis

Sample No. $4FR_2$
Method of Analysis: (a) Screen type: Half-phi interval: ASTM
(b) Sieving time: 15 min.
Weight of sample: 200 gm
Note: To get cummulative weight percentage, divide each figure by the last number in the cummulative weight column and multiply by 100

Class Interval		Retained on sieve wt (gm)	Corr-ected wt (gm)	Cum. wt.	Cum wt %	Wt. %
mm	phi					
2.800–2.000	−1.50–−1.00	3.470	3.494	3.494	1.747	1.747
2.000–1.400	−1.00–−0.50	5.630	5.669	9.163	4.582	2.835
1.400–1.000	−0.50– 0.00	10.420	10.491	19.654	9.827	5.246
1.000–0.500	0.00– 1.00	32.680	32.904	52.558	26.279	16.452
0.500–0.355	1.00– 1.50	18.770	18.899	71.457	35.729	9.450
0.355–0.250	1.50– 2.00	37.160	37.414	108.871	54.436	18.707
0.250–0.180	2.00– 2.25	31.980	32.199	141.070	70.535	16.100
0.180–0.125	2.50– 3.00	40.520	40.797	181.867	90.934	20.399
0.125–0.106	3.00– 3.50	5.030	5.064	186.931	93.466	2.532
0.106–0.063	3.50– 4.00	12.460	12.545	199.476	99.738	6.273
0.063–0.045	4.00– 4.50	0.460	0.463	199.939	99.970	0.232
< 0.045	> 4.50	0.070	0.070	200.009	100.005	0.035
Sieve loss		1.360				
Total weight		198.640				

Statistical Parameters:
05 = −0.40; 016 = 0.45; 025 = 0.90; 050 = 1.90;
075 = 2.60; 084 = 2.80; 095 = 3.55

APPENDIX 1

Report of Sieve Analysis

Sample No. $4FR_2$
Method of Analysis: (a) Screen type: Half-phi interval: ASTM
(b) Sieving time: 15 min.
Weight of sample: 200 gm
Note: To get cummulative weight percentage, divide each figure by the last number in the cummulative weight column and multiply by 100

Class Interval		Retained on sieve wt (gm)	Corr-ected wt (gm)	Cum. wt.	Cum wt %	Wt. %
mm	phi					
2.800–2.000	−1.50–−1.00	1.780	1.781	1.781	0.891	0.891
2.000–1.400	−1.00–−0.50	6.810	6.814	8.595	4.298	3.407
1.400–1.000	−0.50– 0.00	10.900	10.907	19.502	9.751	5.454
1.000–0.500	0.00– 1.00	42.710	42.736	32.238	31.119	21.368
0.500–0.355	1.00– 1.50	32.800	32.820	95.058	47.529	16.410
0.355–0.250	1.50– 2.00	38.200	38.223	133.281	66.641	19.112
0.250–0.180	2.00– 2.50	25.660	25.675	158.956	79.478	12.838
0.180–0.125	2.50– 3.00	17.460	17.470	176.426	88.213	8.735
0.125–0.106	3.00– 3.50	3.210	3.212	179.638	89.819	1.606
0.106–0.063	3.50– 4.00	13.450	13.458	193.096	96.548	6.729
0.063–0.045	4.00– 4.50	3.760	3.762	196.858	98.429	1.881
< 0.045	> 4.50	3.140	3.142	200.000	100.000	1.571
Sieve loss		0.120				
Total weight		199.880				

Statistical Parameters:
05 = −0.35; 016 = 0.40; 025 = 0.80; 050 = 1.60;
075 = 2.30; 084 = 2.75; 095 = 3.90

APPENDIX 1

Report of Sieve Analysis

Sample No. $4FR_3$
Method of Analysis: (a) Screen type: Half-phi interval: ASTM
(b) Sieving time: 15 min.
Weight of sample: 200 gm
Note: To get cummulative weight percentage, divide each figure by the last number in the cummulative weight column and multiply by 100

Class Interval		Retained on sieve wt (gm)	Corr-ected wt (gm)	Cum. wt.	Cum wt %	Wt. %
mm	phi					
2.800–2.000	−1.50–−1.00	0.290	0.291	0.291	0.146	0.146
2.000–1.400	−1.00–−0.50	7.780	7.809	8.100	4.050	3.905
1.400–1.000	−0.50– 0.00	20.760	20.838	28.938	14.469	10.419
1.000–0.500	0.00– 1.00	72.240	72.512	101.450	50.725	36.256
0.500–0.355	1.00– 1.50	29.770	29.882	131.332	65.666	14.941
0.355–0.250	1.50– 2.00	34.790	34.921	166.253	83.127	17.461
0.250–0.180	2.00– 2.50	17.560	17.626	183.879	91.940	8.813
0.180–0.125	2.50– 3.00	7.410	7.438	191.317	95.659	3.719
0.125–0.106	3.00– 3.50	1.560	1.566	192.883	96.442	0.783
0.106–0.063	3.50– 4.00	3.080	3.092	195.975	97.988	1.546
0.063–0.045	4.00– 4.50	1.820	1.827	197.802	98.901	0.914
< 0.045	> 4.50	2.190	2.198	200.000	100.000	1.099
Sieve loss		0.750				
Total weight		199.250				

Statistical Parameters:
05 = −0.40; 016 = 0.10; 025 = 0.35; 050 = 1.00;
075 = 1.75; 084 = 2.10; 095 = 2.90

APPENDIX 1

Report of Sieve Analysis

Sample No. $4FR_4$
Method of Analysis: (a) Screen type: Half-phi interval: ASTM
(b) Sieving time: 15 min.
Weight of sample: 200 gm
Note: To get cummulative weight percentage, divide each figure by the last number in the cummulative weight column and multiply by 100

Class Interval		Retained on sieve wt (gm)	Corr-ected wt (gm)	Cum. wt.	Cum wt %	Wt. %
mm	phi					
2.800-2.000	-1.50--1.00	16.470	16.549	16.549	8.275	8.275
2.000-1.400	-1.00--0.50	11.470	11.525	28.074	14.037	5.763
1.400-1.000	-0.50- 0.00	16.790	16.871	44.945	22.473	8.436
1.000-0.500	0.00- 1.00	51.510	51.758	96.703	48.352	25.879
0.500-0.355	1.00- 1.50	32.340	32.496	129.199	64.600	16.248
0.355-0.250	1.50- 2.00	41.620	41.821	171.020	85.510	20.911
0.250-0.180	2.00- 2.25	16.500	16.580	187.600	93.800	8.290
0.180-0.125	2.50- 3.00	6.300	6.330	193.930	96.965	3.165
0.125-0.106	3.00- 3.50	4.020	4.039	197.969	98.985	2.020
0.106-0.063	3.50- 4.00	1.750	1.758	199.727	99.864	0.879
0.063-0.045	4.00- 4.50	0.190	0.201	199.928	99.964	0.101
< 0.045	> 4.50	0.080	0.080	200.008	100.004	0.040
Sieve loss		0.960				
Total weight		199.040				

Statistical Parameters:
05 = ? ; 016 = -0.40; 025 = 0.10; 050 = 1.05;
075 = 1.70; 084 = 1.95; 095 = 2.65

APPENDIX 1

Report of Sieve Analysis

Sample No. $4FR_6$
Method of Analysis: (a) Screen type: Half-phi interval: ASTM
(b) Sieving time: 15 min.
Weight of sample: 200 gm
Note: To get cummulative weight percentage, divide each figure by the last number in the cummulative weight column and multiply by 100

Class Interval		Retained on sieve wt (gm)	Corr-ected wt (g)	Cum. wt.	Cum wt %	Wt. %
mm	phi					
2.800-2.000	-1.50--1.00	0.000	0.000	0.000	0.000	0.000
2.000-1.400	-1.00--0.50	5.000	5.035	5.035	2.518	2.518
1.400-1.000	-0.50- 0.00	14.340	14.440	19.475	9.738	7.220
1.000-0.500	0.00- 1.00	31.800	32.023	51.498	25.749	16.012
0.500-0.355	1.00- 1.50	22.010	22.164	73.662	36.831	11.082
0.355-0.250	1.50- 2.00	33.010	33.241	106.903	53.452	16.621
0.250-0.180	2.00- 2.25	26.370	26.555	133.458	66.729	13.278
0.180-0.125	2.50- 3.00	41.460	41.750	175.208	87.604	20.875
0.125-0.106	3.00- 3.50	19.050	19.183	194.391	97.196	9.592
0.106-0.063	3.50- 4.00	4.930	4.965	199.356	99.678	2.483
0.063-0.045	4.00- 4.50	0.460	0.463	199.819	99.910	0.232
< 0.045	> 4.50	0.180	0.181	200.000	100.000	0.091
Sieve loss		1.390				
Total weight		198.610				

Statistical Parameters:
05 = -0.25; 016 = 0.50; 025 = 0.95; 050 = 1.90;
075 = 2.70; 084 = 2.90; 095 = 3.35

APPENDIX 1

Report of Sieve Analysis

Sample No. 4FR
Method of Analysis: (a) Screen type: Half-phi interval: ASTM
(b) Sieving time: 15 min.
Weight of sample: 200 gm
Note: To get cummulative weight percentage, divide each figure by the last number in the cummulative weight column and multiply by 100

Class Interval		Retained on sieve wt (gm)	Corrected wt (gm)	Cum. wt.	Cum wt %	Wt. %
mm	phi					
2.800-2.000	-1.50--1.00	1.900	1.922	1.922	0.961	0.961
2.000-1.400	-1.00--0.50	4.810	4.865	6.787	3.394	2.433
1.400-1.000	-0.50- 0.00	14.640	14.808	21.595	10.789	7.404
1.000-0.500	0.00- 1.00	76.820	77.702	99.297	49.649	38.851
0.500-0.355	1.00- 1.50	45.950	46.478	145.775	72.888	23.239
0.355-0.250	1.50- 2.00	28.370	26.696	174.471	87.236	14.348
0.250-0.180	2.00- 2.25	6.900	6.979	181.450	90.725	3.490
0.180-0.125	2.50- 3.00	7.490	7.576	189.026	94.513	3.788
0.125-0.106	3.00- 3.50	0.900	1.001	190.027	95.014	0.501
0.106-0.063	3.50- 4.00	4.810	4.865	194.892	97.446	2.433
0.063-0.045	4.00- 4.50	1.810	1.831	196.723	98.362	0.916
< 0.045	> 4.50	3.240	3.277	200.000	100.000	1.639
Sieve loss		2.270				
Total weight		197.730				

Statistical Parameters:
05 = -0.38; 016 = 0.14; 025 = 0.40; 050 = 1.00;
075 = 1.55; 084 = 1.85; 095 = 3.50

APPENDIX 1

Report of Sieve Analysis

Sample No. 4FR$_7$
Method of Analysis: (a) Screen type: Half-phi interval: ASTM
(b) Sieving time: 15 min.
Weight of sample: 200 gm
Note: To get cummulative weight percentage, divide each figure by the last number in the cummulative weight column and multiply by 100

Class Interval		Retained on sieve wt (gm)	Corr-ected wt (gm)	Cum. wt.	Cum wt %	Wt. %
mm	phi					
2.800-2.000	-1.50--1.00	0.010	0.010	0.010	0.005	0.005
2.000-1.400	-1.00--0.50	0.090	0.090	0.100	0.050	0.045
1.400-1.000	-0.50- 0.00	1.710	1.718	1.818	0.909	0.859
1.000-0.500	0.00- 1.00	22.070	22.170	23.988	11.994	11.085
0.500-0.355	1.00- 1.50	65.890	66.188	90.176	45.088	33.094
0.355-0.250	1.50- 2.00	79.080	79.437	169.613	84.807	39.719
0.250-0.180	2.00- 2.50	12.310	12.366	181.979	90.990	6.183
0.180-0.125	2.50- 3.00	10.420	10.467	192.446	96.223	5.234
0.125-0.106	3.00- 3.50	0.980	0.984	193.430	96.715	0.492
0.106-0.063	3.50- 4.00	3.120	3.134	196.564	98.282	1.567
0.063-0.045	4.00- 4.50	2.200	2.210	198.774	99.387	1.105
< 0.045	> 4.50	1.220	1.226	200.000	100.000	0.613
Sieve loss		0.900				
Total weight		199.100				

Statistical Parameters:
05 = 0.60; 016 = 1.10; 025 = 1.25; 050 = 1.55;
075 = 1.85; 084 = 2.00; 095 = 2.90

APPENDIX 1

Report of Sieve Analysis

Sample No. 4FR$_o$
Method of Analysis: (a) Screen type: Half-phi interval: ASTM
(b) Sieving time: 15 min.
Weight of sample: 200 gm
Note: To get cummulative weight percentage, divide each figure by the last number in the cummulative weight column and multiply by 100

Class Interval		Retained on sieve wt (gm)	Corr-ected wt (gm)	Cum. wt.	Cum wt %	Wt. %
mm	phi					
2.800-2.000	-1.50--1.00	3.720	3.746	3.746	1.873	1.873
2.000-1.400	-1.00--0.50	4.640	4.672	8.418	4.209	2.336
1.400-1.000	-0.50- 0.00	7.430	7.482	15.900	7.950	3.741
1.000-0.500	0.00- 1.00	34.650	34.891	50.791	25.396	17.446
0.500-0.355	1.00- 1.50	32.750	32.978	83.769	41.885	16.489
0.355-0.250	1.50- 2.00	76.510	77.042	160.811	80.406	38.521
0.250-0.180	2.00- 2.50	28.380	28.577	189.388	94.694	14.289
0.180-0.125	2.50- 3.00	7.340	7.391	196.779	98.390	3.696
0.125-0.106	3.00- 3.50	0.490	0.493	197.272	98.636	0.247
0.106-0.063	3.50- 4.00	1.260	1.269	198.541	99.271	0.635
0.063-0.045	4.00- 4.50	0.570	0.574	199.115	99.558	0.287
< 0.045	> 4.50	0.880	0.886	200.001	100.000	0.443
Sieve loss		1.380				
Total weight		198.620				

Statistical Parameters:
05 = -0.35; 016 = 0.60; 025 = 1.00; 050 = 1.60;
075 = 1.90; 084 = 2.10; 095 = 2.60

APPENDIX 1

Report of Sieve Analysis

Sample No. 7FR$_1$
Method of Analysis: (a) Screen type: Half-phi interval: ASTM
(b) Sieving time: 15 min.
Weight of sample: 200 gm
Note: To get cummulative weight percentage, divide each figure by the last number in the cummulative weight column and multiply by 100

Class Interval		Retained on sieve wt (gm)	Corr-ected wt (gm)	Cum. wt.	Cum wt %	Wt. %
mm	phi					
2.800-2.000	-1.50--1.00	23.060	23.170	23.170	11.585	11.585
2.000-1.400	-1.00--0.50	13.060	13.122	36.292	18.146	6.561
1.400-1.000	-0.50- 0.00	22.180	22.286	58.578	29.289	11.143
1.000-0.500	0.00- 1.00	65.420	65.732	124.310	62.155	32.866
0.500-0.355	1.00- 1.50	21.510	21.613	145.923	72.962	10.807
0.355-0.250	1.50- 2.00	17.510	17.594	163.517	81.759	8.797
0.250-0.180	2.00- 2.25	9.790	9.837	173.354	86.677	4.919
0.180-0.125	2.50- 3.00	10.860	10.912	184.266	92.133	5.456
0.125-0.106	3.00- 3.50	2.010	2.020	186.286	93.143	1.010
0.106-0.063	3.50- 4.00	8.780	8.822	195.108	97.554	4.411
0.063-0.045	4.00- 4.50	3.260	3.276	198.384	99.192	1.638
< 0.045	> 4.50	1.610	1.618	200.002	100.001	0.809
Sieve loss		0.950				
Total weight		199.050				

Statistical Parameters:
05 = ? ; 016 = -0.65; 025 = -0.20; 050 = 0.60;
075 = 1.60; 084 = 2.20; 095 = 3.70

APPENDIX 1

Report of Sieve Analysis

Sample No. $7FR_2$
Method of Analysis: (a) Screen type: Half-phi interval: ASTM
(b) Sieving time: 15 min.
Weight of sample: 200 gm
Note: To get cummulative weight percentage, divide each figure by the last number in the cummulative weight column and multiply by 100

Class Interval		Retained on sieve wt (gm)	Corr-ected wt (gm)	Cum. wt.	Cum wt %	Wt. %
mm	phi					
2.800-2.000	-1.50--1.00	0.260	0.262	0.262	0.131	0.131
2.000-1.400	-1.00--0.50	1.380	1.389	1.651	0.826	0.695
1.400-1.000	-0.50- 0.00	7.120	7.168	8.819	4.410	3.584
1.000-0.500	0.00- 1.00	59.120	59.516	68.335	34.168	29.758
0.500-0.355	1.00- 1.50	40.860	41.134	109.469	54.735	20.567
0.355-0.250	1.50- 2.00	45.080	45.382	154.851	77.426	22.691
0.250-0.180	2.00- 2.25	30.520	30.724	185.575	92.788	15.362
0.180-0.125	2.50- 3.00	9.180	9.241	194.816	97.408	4.621
0.125-0.106	3.00- 3.50	0.990	0.997	195.813	97.907	0.499
0.106-0.063	3.50- 4.00	3.810	3.836	199.649	99.825	1.918
0.063-0.045	4.00- 4.50	0.280	0.282	199.931	99.966	0.141
< 0.045	> 4.50	0.070	0.070	200.001	100.001	0.035
Sieve loss		1.330				
Total weight		198.670				

Statistical Parameters:
05 = 0.05; 016 = 0.55; 025 = 0.80; 050 = 1.40;
075 = 1.95; 084 = 2.20; 095 = 2.70

APPENDIX 1

Report of Sieve Analysis

Sample No. $7FR_S$
Method of Analysis: (a) Screen type: Half-phi interval: ASTM
(b) Sieving time: 15 min.
Weight of sample: 200 gm
Note: To get cummulative weight percentage, divide each figure by the last number in the cummulative weight column and multiply by 100

Class Interval		Retained on sieve wt (gm)	Corr-ected wt (gm)	Cum. wt.	Cum wt %	Wt. %
mm	phi					
2.800–2.000	-1.50--1.00	0.480	0.486	0.486	0.243	0.243
2.000–1.400	-1.00--0.50	2.560	2.594	3.080	1.540	1.297
1.400–1.000	-0.50- 0.00	6.840	6.930	10.010	5.005	3.465
1.000–0.500	0.00- 1.00	40.780	41.315	51.325	25.663	20.658
0.500–0.355	1.00- 1.50	23.160	23.464	74.789	37.395	11.732
0.355–0.250	1.50- 2.00	27.160	27.516	102.305	51.153	13.758
0.250–0.180	2.00- 2.25	25.850	26.189	128.494	64.247	13.095
0.180–0.125	2.50- 3.00	34.200	34.649	163.143	81.572	17.325
0.125–0.106	3.00- 3.50	16.270	16.483	179.627	89.814	8.242
0.106–0.063	3.50- 4.00	7.710	7.812	187.436	93.718	3.906
0.063–0.045	4.00- 4.50	11.080	11.225	198.662	99.331	5.613
< 0.045	> 4.50	1.320	1.337	200.000	100.000	0.669
Sieve loss		2.590				
Total weight		197.410				

Statistical Parameters:
05 = 0.00; 016 = 0.70; 025 = 1.00; 050 = 1.95;
075 = 2.80; 084 = 3.15; 095 = 4.10

APPENDIX 1

Report of Sieve Analysis

Sample No. $7FR_4$
Method of Analysis: (a) Screen type: Half-phi interval: ASTM
(b) Sieving time: 15 min.
Weight of sample: 200 gm
Note: To get cummulative weight percentage, divide each figure by the last number in the cummulative weight column and multiply by 100

Class Interval		Retained on sieve wt (gm)	Corr-ected wt (gm)	Cum. wt.	Cum wt %	Wt. %
mm	phi					
2.800-2.000	-1.50--1.00	4.410	4.526	4.526	2.263	2.263
2.000-1.400	-1.00--0.50	7.800	8.005	12.531	6.266	4.003
1.400-1.000	-0.50- 0.00	20.820	21.367	33.898	16.949	10.684
1.000-0.500	0.00- 1.00	106.410	109.206	143.104	71.552	54.603
0.500-0.355	1.00- 1.50	23.960	24.589	167.693	83.847	12.295
0.355-0.250	1.50- 2.00	9.650	9.904	177.597	88.799	4.952
0.250-0.180	2.00- 2.50	10.130	10.396	187.993	93.997	5.198
0.180-0.125	2.50- 3.00	6.990	7.174	195.167	97.584	3.587
0.125-0.106	3.00- 3.50	0.490	0.503	195.670	97.835	0.252
0.106-0.063	3.50- 4.00	3.760	3.859	199.529	99.765	1.930
0.063-0.045	4.00- 4.50	0.390	0.400	199.929	99.965	0.200
< 0.045	> 4.50	0.070	0.072	200.001	100.001	0.036
Sieve loss		5.120				
Total weight		194.880				

Statistical Parameters:
05 = -0.65; 016 = 0.00; 025 = 0.20; 050 = 0.60;
075 = 1.10; 084 = 1.50; 095 = 2.60

APPENDIX 1

Report of Sieve Analysis

Sample No. $7FR_6$
Method of Analysis: (a) Screen type: Half-phi interval: ASTM
(b) Sieving time: 15 min.
Weight of sample: 200 gm
Note: To get cummulative weight percentage, divide each figure by the last number in the cummulative weight column and multiply by 100

Class Interval		Retained on sieve wt (gm)	Corr-ected wt (gm)	Cum. wt.	Cum wt %	Wt. %
mm	phi					
2.800–2.000	−1.50–−1.00	6.910	6.912	6.912	3.456	3.456
2.000–1.400	−1.00–−0.50	16.500	16.504	23.416	11.708	8.252
1.400–1.000	−0.50– 0.00	30.000	30.008	53.424	26.712	15.004
1.000–0.500	0.00– 1.00	76.480	76.499	129.923	64.962	38.250
0.500–0.355	1.00– 1.50	26.580	26.587	156.510	78.255	13.294
0.355–0.250	1.50– 2.00	14.780	14.784	171.294	85.647	7.392
0.250–0.180	2.00– 2.50	7.070	7.072	178.366	89.183	3.536
0.180–0.125	2.50– 3.00	8.310	8.312	186.678	93.339	4.156
0.125–0.106	3.00– 3.50	1.360	1.360	188.038	94.019	0.680
0.106–0.063	3.50– 4.00	8.480	8.482	196.520	98.260	4.241
0.063–0.045	4.00– 4.50	1.380	1.380	197.900	98.950	0.690
< 0.045	> 4.50	2.100	2.101	200.001	100.001	1.051
Sieve loss		0.050				
Total weight		199.950				

Statistical Parameters:
05 = −0.88; 016 = −0.30; 025 = −0.05; 050 = 0.65;
075 = 1.40; 084 = 1.90; 095 = 3.60

APPENDIX 1

Report of Sieve Analysis

Sample No. 7FR4
Method of Analysis: (a) Screen type: Half-phi interval: ASTM
(b) Sieving time: 15 min.
Weight of sample: 200 gm
Note: To get cummulative weight percentage, divide each figure by the last number in the cummulative weight column and multiply by 100

Class Interval		Retained on sieve wt (gm)	Corr-ected wt (gm)	Cum. wt.	Cum wt %	Wt. %
mm	phi					
2.800-2.000	-1.50--1.00	0.220	0.222	0.222	0.111	0.111
2.000-1.400	-1.00--0.50	0.900	0.907	1.129	0.565	0.454
1.400-1.000	-0.50- 0.00	5.650	5.695	6.824	3.412	2.848
1.000-0.500	0.00- 1.00	44.210	44.562	51.386	25.693	22.281
0.500-0.355	1.00- 1.50	23.450	23.637	75.023	37.512	11.819
0.355-0.250	1.50- 2.00	28.490	28.717	103.740	51.870	14.359
0.250-0.180	2.00- 2.25	27.700	27.921	131.661	65.831	13.961
0.180-0.125	2.50- 3.00	23.670	23.858	155.519	77.760	11.929
0.125-0.106	3.00- 3.50	18.350	18.496	174.015	87.008	9.248
0.106-0.063	3.50- 4.00	10.150	10.231	184.246	92.123	5.116
0.063-0.045	4.00- 4.50	11.010	11.098	195.344	97.672	5.549
< 0.045	> 4.50	4.620	4.657	200.001	100.001	2.329
Sieve loss		1.580				
Total weight		198.420				

Statistical Parameters:
05 = 0.15 ; 016 = 0.70; 025 = 1.00; 050 = 1.90;

APPENDIX 1

Report of Sieve Analysis

Sample No. 7FR$_7$
Method of Analysis: (a) Screen type: Half-phi interval: ASTM
(b) Sieving time: 15 min.
Weight of sample: 200 gm
Note: To get cummulative weight percentage, divide each figure by the last number in the cummulative weight column and multiply by 100

Class Interval		Retained on sieve wt (gm)	Corr-ected wt (gm)	Cum. wt.	Cum wt %	Wt. %
mm	phi					
2.800-2.000	-1.50--1.00	1.190	1.192	1.192	0.596	0.596
2.000-1.400	-1.00--0.50	5.460	5.468	6.660	3.330	2.734
1.400-1.000	-0.50- 0.00	11.530	11.547	18.207	9.104	5.774
1.000-0.500	0.00- 1.00	50.370	50.443	68.650	34.325	25.222
0.500-0.355	1.00- 1.50	32.040	32.087	100.737	50.369	16.044
0.355-0.250	1.50- 2.00	46.290	46.357	147.094	73.547	23.179
0.250-0.180	2.00- 2.25	23.690	23.724	170.818	85.409	11.862
0.180-0.125	2.50- 3.00	17.400	17.425	188.243	94.122	8.713
0.125-0.106	3.00- 3.50	3.910	3.916	192.159	96.080	1.958
0.106-0.063	3.50- 4.00	4.390	4.396	196.555	98.278	2.198
0.063-0.045	4.00- 4.50	1.580	1.582	198.137	99.069	0.791
< 0.045	> 4.50	1.860	1.863	200.000	100.000	0.932
Sieve loss		0.290				
Total weight		199.710				

Statistical Parameters:
05 = -0.30; 016 = 0.35; 025 = 0.70; 050 = 1.50;
075 = 2.05; 084 = 2.45; 095 = 3.20

APPENDIX 1

Report of Sieve Analysis

Sample No. $8FR_1$
Method of Analysis: (a) Screen type: Half-phi interval: ASTM
(b) Sieving time: 15 min.
Weight of sample: 200 gm
Note: To get cummulative weight percentage, divide each figure by the last number in the cummulative weight column and multiply by 100

Class Interval		Retained on sieve wt (gm)	Corr-ected wt (gm)	Cum. wt.	Cum wt %	Wt. %
mm	phi					
2.800-2.000	-1.50--1.00	0.010	0.010	0.010	0.005	0.005
2.000-1.400	-1.00--0.50	0.010	0.010	0.020	0.010	0.005
1.400-1.000	-0.50- 0.00	1.010	1.045	1.065	0.533	0.523
1.000-0.500	0.00- 1.00	12.420	12.847	13.912	6.956	6.424
0.500-0.355	1.00- 1.50	40.650	42.048	55.960	27.980	21.024
0.355-0.250	1.50- 2.00	87.480	90.489	146.449	73.225	45.245
0.250-0.180	2.00- 2.25	29.970	31.001	177.450	88.725	15.501
0.180-0.125	2.50- 3.00	7.520	7.779	185.229	92.615	3.890
0.125-0.106	3.00- 3.50	1.610	1.665	186.894	93.447	0.833
0.106-0.063	3.50- 4.00	9.480	9.806	196.700	98.350	4.903
0.063-0.045	4.00- 4.50	1.530	1.583	198.283	99.142	0.792
< 0.045	> 4.50	1.660	1.717	200.000	100.000	0.859
Sieve loss		6.650				
Total weight		193.350				

Statistical Parameters:
05 = 0.90; 016 = 1.30; 025 = 1.45; 050 = 1.75;
075 = 2.05; 084 = 2.30; 095 = 3.60

APPENDIX 1

Report of Sieve Analysis

Sample No. $8FR_2$
Method of Analysis: (a) Screen type: Half-phi interval: ASTM
(b) Sieving time: 15 min.
Weight of sample: 200 gm
Note: To get cummulative weight percentage, divide each figure by the last number in the cummulative weight column and multiply by 100

Class Interval		Retained on sieve wt (gm)	Corr-ected wt (gm)	Cum. wt.	Cum wt %	Wt. %
mm	phi					
2.800-2.000	-1.50--1.00	0.400	0.400	0.400	0.200	0.200
2.000-1.400	-1.00--0.50	1.540	1.540	1.940	0.970	0.770
1.400-1.000	-0.50- 0.00	11.590	11.592	13.532	6.766	5.796
1.000-0.500	0.00- 1.00	125.340	125.359	138.891	69.446	62.680
0.500-0.355	1.00- 1.50	8.530	8.531	147.422	73.711	4.266
0.355-0.250	1.50- 2.00	15.290	15.292	162.714	81.357	7.646
0.250-0.180	2.00- 2.50	18.620	18.623	181.337	90.669	9.312
0.180-0.125	2.50- 3.00	10.870	10.872	192.209	96.105	5.436
0.125-0.106	3.00- 3.50	0.720	0.720	192.929	96.465	0.360
0.106-0.063	3.50- 4.00	4.050	4.051	196.980	98.490	2.026
0.063-0.045	4.00- 4.50	2.270	2.270	199.250	99.625	1.135
< 0.045	> 4.50	0.750	0.750	200.000	100.000	0.375
Sieve loss		0.030				
Total weight		199.970				

Statistical Parameters:
05 = -0.08; 016 = 0.25; 025 = 0.40; 050 = 0.75;
075 = 1.60; 084 = 2.15; 095 = 2.90

APPENDIX 1

Report of Sieve Analysis

Sample No. BFR_2
Method of Analysis: (a) Screen type: Half-phi interval: ASTM
(b) Sieving time: 15 min.
Weight of sample: 200 gm
Note: To get cummulative weight percentage, divide each figure by the last number in the cummulative weight column and multiply by 100

Class Interval		Retained on sieve wt (gm)	Corr-ected wt (gm)	Cum. wt.	Cum wt %	Wt. %
mm	phi					
2.800-2.000	-1.50--1.00	0.400	0.400	0.400	0.200	0.200
2.000-1.400	-1.00--0.50	1.540	1.540	1.940	0.970	0.770
1.400-1.000	-0.50- 0.00	11.590	11.592	13.532	6.766	5.796
1.000-0.500	0.00- 1.00	125.340	125.359	138.891	69.446	62.680
0.500-0.355	1.00- 1.50	8.530	8.531	147.422	73.711	4.266
0.355-0.250	1.50- 2.00	15.290	15.292	162.714	81.357	7.646
0.250-0.180	2.00- 2.50	18.620	18.623	181.337	90.669	9.312
0.180-0.125	2.50- 3.00	10.870	10.872	192.209	96.105	5.436
0.125-0.106	3.00- 3.50	0.720	0.720	192.929	96.465	0.360
0.106-0.063	3.50- 4.00	4.050	4.051	196.980	98.490	2.026
0.063-0.045	4.00- 4.50	2.270	2.270	199.250	99.625	1.135
< 0.045	> 4.50	0.750	0.750	200.000	100.000	0.375
Sieve loss		0.030				
Total weight		199.970				

Statistical Parameters:
05 = -0.08; 016 = 0.25; 025 = 0.40; 050 = 0.75;
075 = 1.60; 084 = 2.15; 095 = 2.90

APPENDIX 1

Report of Sieve Analysis

Sample No. $8FR_s$
Method of Analysis: (a) Screen type: Half-phi interval: ASTM
(b) Sieving time: 15 min.
Weight of sample: 200 gm
Note: To get cummulative weight percentage, divide each figure by the last number in the cummulative weight column and multiply by 100

Class Interval		Retained on sieve wt (gm)	Corr-ected wt (gm)	Cum. wt.	Cum wt %	Wt. %
mm	phi					
2.800-2.000	-1.50--1.00	0.130	0.130	0.130	0.065	0.065
2.000-1.400	-1.00--0.50	1.000	1.002	1.132	0.566	0.501
1.400-1.000	-0.50- 0.00	5.000	5.010	6.142	3.077	2.505
1.000-0.500	0.00- 1.00	65.830	65.962	72.104	36.052	32.981
0.500-0.355	1.00- 1.50	47.350	47.445	119.559	59.780	23.723
0.355-0.250	1.50- 2.00	37.830	37.906	157.455	78.728	18.953
0.250-0.180	2.00- 2.50	15.830	15.862	173.317	86.659	7.931
0.180-0.125	2.50- 3.00	9.380	9.399	182.716	91.358	4.700
0.125-0.106	3.00- 3.50	2.330	2.335	185.051	92.526	1.168
0.106-0.063	3.50- 4.00	1.500	1.503	186.554	93.277	0.752
0.063-0.045	4.00- 4.50	9.320	9.339	195.893	97.947	4.670
< 0.045	> 4.50	4.100	4.108	200.001	100.001	2.054
Sieve loss		0.410				
Total weight		199.600				

Statistical Parameters:
05 = 0.20; 016 = 0.60; 025 = 0.80; 050 = 1.30;
075 = 1.90; 084 = 2.30; 095 = 4.15

APPENDIX 1

Report of Sieve Analysis

Sample No. 8FR$_4$
Method of Analysis: (a) Screen type: Half-phi interval: ASTM
(b) Sieving time: 15 min.
Weight of sample: 200 gm
Note: To get cummulative weight percentage, divide each figure by the last number in the cummulative weight column and multiply by 100

Class Interval		Retained on sieve wt (gm)	Corr-ected wt (gm)	Cum. wt.	Cum wt %	Wt. %
mm	phi					
2.800-2.000	-1.50--1.00	1.990	1.992	1.992	0.996	0.996
2.000-1.400	-1.00--0.50	4.690	4.696	6.688	3.344	2.348
1.400-1.000	-0.50- 0.00	6.690	6.698	13.386	6.693	3.349
1.000-0.500	0.00- 1.00	27.070	27.103	40.489	20.245	13.552
0.500-0.355	1.00- 1.50	28.840	28.875	69.364	34.682	14.438
0.355-0.250	1.50- 2.00	57.150	57.219	126.583	63.292	28.610
0.250-0.180	2.00- 2.25	34.700	34.742	161.325	80.663	17.371
0.180-0.125	2.50- 3.00	18.560	18.582	179.907	89.954	9.291
0.125-0.106	3.00- 3.50	4.070	4.075	183.982	91.991	2.038
0.106-0.063	3.50- 4.00	10.550	10.563	194.545	97.273	5.282
0.063-0.045	4.00- 4.50	3.700	3.704	198.249	99.125	1.852
< 0.045	> 4.50	1.750	1.752	200.001	100.001	0.876
Sieve loss		0.240				
Total weight		199.760				

Statistical Parameters:
05 = -0.20; 016 = 0.75; 025 = 1.15; 050 = 1.80;
075 = 2.30; 084 = 2.65; 095 = 3.75

APPENDIX 1

Report of Sieve Analysis

Sample No. BFR_s
Method of Analysis: (a) Screen type: Half-phi interval: ASTM
(b) Sieving time: 15 min.
Weight of sample: 200 gm
Note: To get cummulative weight percentage, divide each figure by the last number in the cummulative weight column and multiply by 100

Class Interval		Retained on sieve wt (gm)	Corr-ected wt (gm)	Cum. wt.	Cum wt %	Wt. %
mm	phi					
2.800-2.000	-1.50--1.00	37.080	37.091	37.091	18.546	18.546
2.000-1.400	-1.00--0.50	14.600	14.604	51.695	25.848	7.302
1.400-1.000	-0.50- 0.00	13.910	13.914	65.609	32.805	6.957
1.000-0.500	0.00- 1.00	45.460	45.474	111.083	55.542	22.737
0.500-0.355	1.00- 1.50	25.370	25.378	136.461	68.231	12.689
0.355-0.250	1.50- 2.00	26.920	26.928	163.389	81.695	13.464
0.250-0.180	2.00- 2.25	12.070	12.074	175.463	87.732	6.037
0.180-0.125	2.50- 3.00	9.230	9.232	184.695	92.348	4.616
0.125-0.106	3.00- 3.50	2.320	2.321	187.016	93.508	1.161
0.106-0.063	3.50- 4.00	6.160	6.162	193.178	96.589	3.081
0.063-0.045	4.00- 4.50	3.050	3.051	196.229	98.115	1.526
< 0.045	> 4.50	3.770	3.771	200.000	100.000	1.886
Sieve loss		0.060				
Total weight		199.940				

Statistical Parameters:
05 = ? ; 016 = ? ; 025 = -0.60; 050 = 0.80;
075 = 1.75; 084 = 2.20; 095 = 3.70

APPENDIX 1

Report of Sieve Analysis

Sample No. $9FR_1$
Method of Analysis: (a) Screen type: Half-phi interval: ASTM
(b) Sieving time: 15 min.
Weight of sample: 200 gm
Note: To get cummulative weight percentage, divide each figure by the last number in the cummulative weight column and multiply by 100

Class Interval		Retained on sieve wt (gm)	Corr-ected wt (gm)	Cum. wt.	Cum wt %	Wt. %
mm	phi					
2.800–2.000	-1.50--1.00	0.000	0.000	0.000	0.000	0.000
2.000–1.400	-1.00--0.50	0.000	0.000	0.000	0.000	0.000
1.400–1.000	-0.50- 0.00	2.190	2.221	2.221	1.101	1.111
1.000–0.500	0.00- 1.00	15.570	15.792	18.013	9.007	7.896
0.500–0.355	1.00- 1.50	9.370	9.504	27.517	13.759	4.752
0.355–0.250	1.50- 2.00	24.610	24.961	52.478	26.239	12.481
0.250–0.180	2.00- 2.25	31.880	32.334	84.812	42.406	16.167
0.180–0.125	2.50- 3.00	25.620	25.985	110.797	55.399	12.993
0.125–0.106	3.00- 3.50	9.180	9.311	120.108	60.054	4.656
0.106–0.063	3.50- 4.00	44.620	45.256	165.364	82.682	22.628
0.063–0.045	4.00- 4.50	22.300	22.618	187.982	93.991	11.309
< 0.045	> 4.50	11.850	12.019	200.001	100.001	6.010
Sieve loss		2.810				
Total weight		197.190				

Statistical Parameters:
05 = 0.70; 016 = 1.60; 025 = 2.00; 050 = 2.80;
075 = 3.75; 084 = 4.05; 095 = 4.55

APPENDIX 1

Report of Sieve Analysis

Sample No. $9FR_2$
Method of Analysis: (a) Screen type: Half-phi interval: ASTM
(b) Sieving time: 15 min.
Weight of sample: 200 gm
Note: To get cummulative weight percentage, divide each figure by the last number in the cummulative weight column and multiply by 100

Class Interval		Retained on sieve wt (gm)	Corrected wt (gm)	Cum. wt.	Cum wt %	Wt. %
mm	phi					
2.800–2.000	-1.50--1.00	0.000	0.000	0.000	0.000	0.000
2.000–1.400	-1.00--0.50	0.000	0.000	0.000	0.000	0.000
1.400–1.000	-0.50- 0.00	0.000	0.000	0.000	0.000	0.000
1.000–0.500	0.00- 1.00	0.160	0.165	0.165	0.083	0.083
0.500–0.355	1.00- 1.50	2.160	2.230	2.395	1.198	1.115
0.355–0.250	1.50- 2.00	5.530	5.710	8.105	4.053	2.855
0.250–0.180	2.00- 2.50	31.160	32.173	40.278	20.139	16.087
0.180–0.125	2.50- 3.00	67.940	70.150	110.428	55.214	35.075
0.125–0.106	3.00- 3.50	25.760	26.598	137.026	68.513	13.299
0.106–0.063	3.50- 4.00	34.150	35.261	172.287	86.144	17.631
0.063–0.045	4.00- 4.50	12.980	13.402	185.689	92.845	6.701
< 0.045	> 4.50	13.860	14.311	200.000	100.000	7.156
Sieve loss		6.300				
Total weight		193.700				

Statistical Parameters:
05 = 2.05; 016 = 2.40; 025 = 2.60; 050 = 2.90;
075 = 3.65; 084 = 3.90; 095 = 4.55

APPENDIX 1

Report of Sieve Analysis

Sample No. $9FR_S$
Method of Analysis: (a) Screen type: Half-phi interval: ASTM
(b) Sieving time: 15 min.
Weight of sample: 200 gm
Note: To get cummulative weight percentage, divide each figure by the last number in the cummulative weight column and multiply by 100

Class Interval		Retained on sieve wt (gm)	Corr-ected wt (gm)	Cum. wt.	Cum wt %	Wt. %
mm	phi					
2.800–2.000	−1.50–−1.00	0.000	0.000	0.000	0.000	0.000
2.000–1.400	−1.00–−0.50	0.000	0.000	0.000	0.000	0.000
1.400–1.000	−0.50– 0.00	3.040	3.076	3.076	1.538	1.538
1.000–0.500	0.00– 1.00	31.570	31.942	35.018	17.509	15.971
0.500–0.355	1.00– 1.50	47.880	48.444	83.462	41.731	24.222
0.355–0.250	1.50– 2.00	24.420	24.708	108.170	54.085	12.354
0.250–0.180	2.00– 2.50	1.950	1.973	110.143	55.072	0.987
0.180–0.125	2.50– 3.00	19.570	19.801	129.944	64.972	9.901
0.125–0.106	3.00– 3.50	24.990	25.285	155.229	77.615	12.693
0.106–0.063	3.50– 4.00	25.090	25.386	180.615	90.308	17.631
0.063–0.045	4.00– 4.50	15.340	15.521	196.136	98.068	7.761
< 0.045	> 4.50	3.820	3.865	200.001	100.001	1.933
Sieve loss		2.330				
Total weight		197.670				

Statistical Parameters:
05 = 1.45; 016 = 1.70; 025 = 1.80; 050 = 2.05;
075 = 2.45; 084 = 2.70; 095 = 3.70

APPENDIX 1

Report of Sieve Analysis

Sample No. 9FR*
Method of Analysis: (a) Screen type: Half-phi interval: ASTM
(b) Sieving time: 15 min-
Uleight of sample: 200 gm
Note: To get cummulative weight percentage, divide each -figure by the last number in the cummulative weight column and multiply by 100

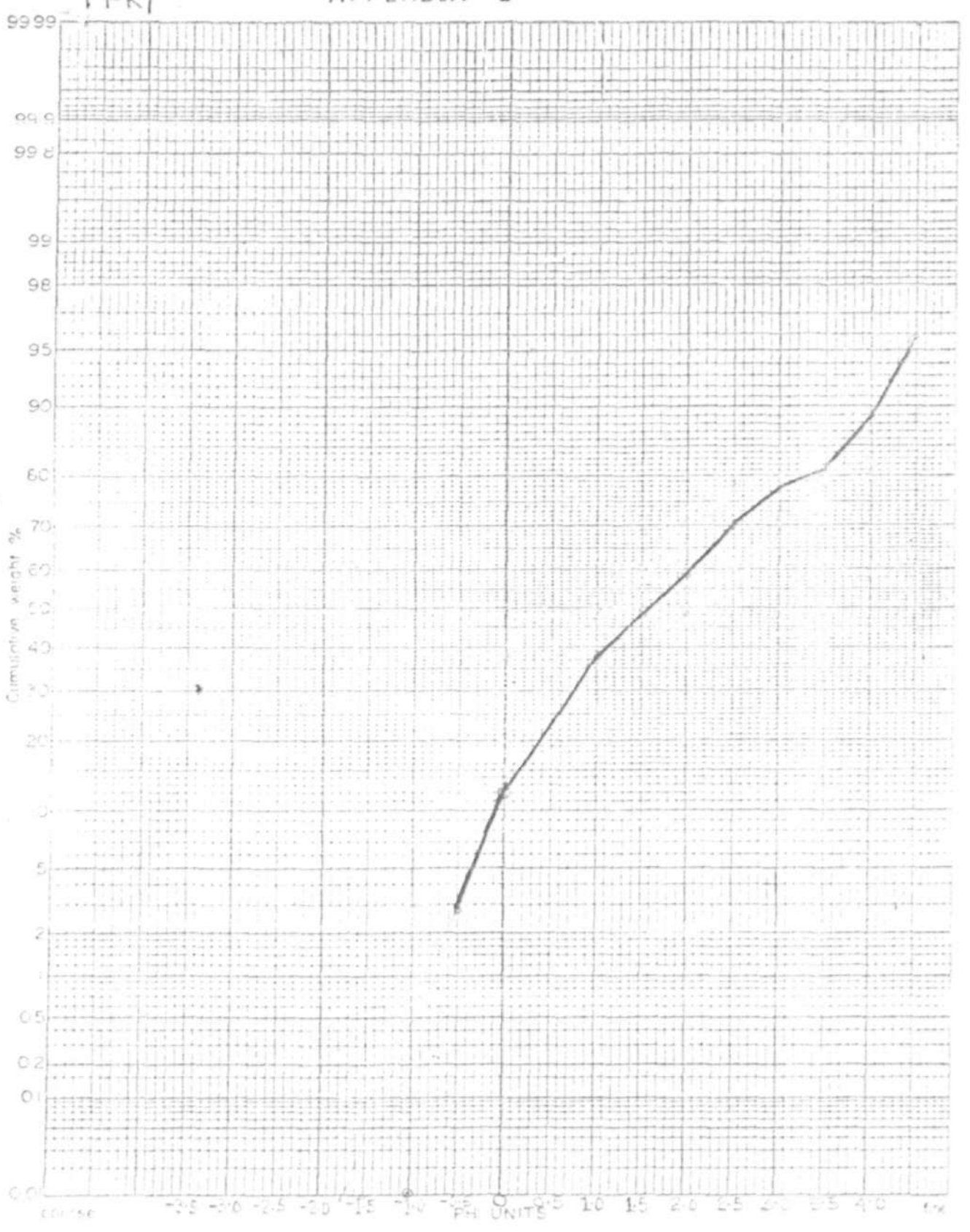
Class Interval		Retained on sieve wt (gm)	Corr— ected wt (gm)	Cum. wt.	Cum wt ⁒	Wt.
mm	phi					
2.800-2.000	-1.50—1.00	0.000	0.000	0.000	0.000	0.000
2.000-1.400	-1,00—0.50	0.000	0.000	0.000	0.000	0.000
1.400-1.000	-0.50- 0.00	0.000	0.000	0.000	0.000	0.000
1.000-0.500	0-00- 1.00	2.770	2.730	2.730	1.370	1.390
0.500-0.355	1.00- 1.50	8.410	8.439	11.219	5.610	4.220
0.355-0.250	1.50- 2.00	70.140	70.333	81.602	40.301	35.192
0.250-0.190	2.00- 2.50	76.330	76.594	153.196	79.093	33.297
0.180-0.125	2.50- 3.00	25.270	jt-t-l . owl/	183.553	91.777	12.^79
0.125-0.106	3.00- 3.50	3.S80	3.393	137.446	93.723	1-947
0.106-0.063	3.50- 4.00	6.080	6.101	193.547	96.774	3.051
0.063-0.045	4.00- 4.50	3.070	3.081	196.628	93.314	1.541
< 0.045	> 4.50	._-.-.-.t_»s_«	"T -T-T—t	200.000	100.000	x.o36
Sieve	loss	0.690				
Total	weight	199.310				

Statistical Parameters:
05 = 0.40; 016 = 0.95; 025 = 1.20; 050 = 1.30;
075 = 3.40; 084 = 3.70; 095 = 4.20

APPENDIX 2:

CUMULATIVE FREQUENCY CURVES ON A PROBABILITY GRAPH SCALE.

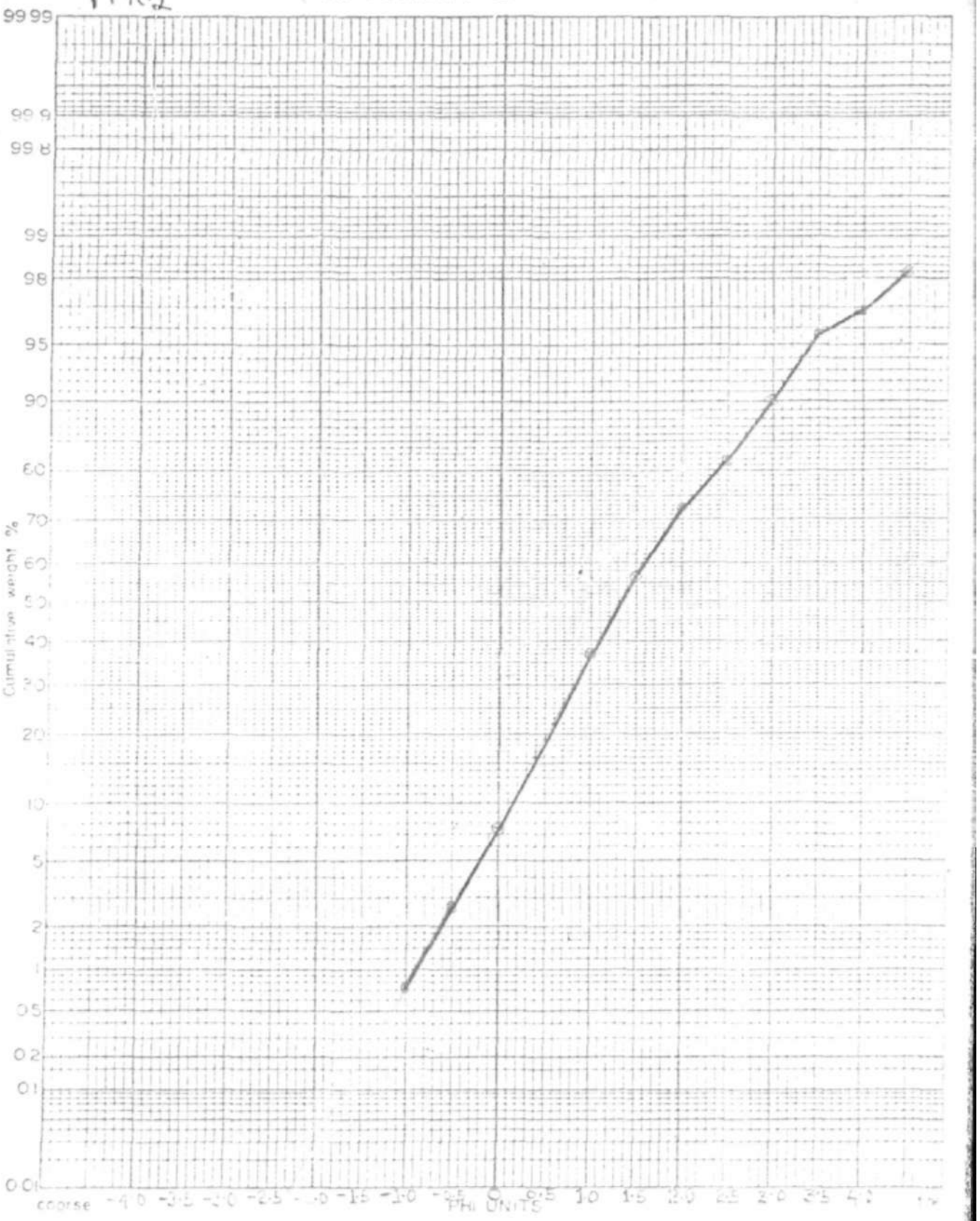
APPENDIX 2



Probability paper for plotting grain-size distributions.

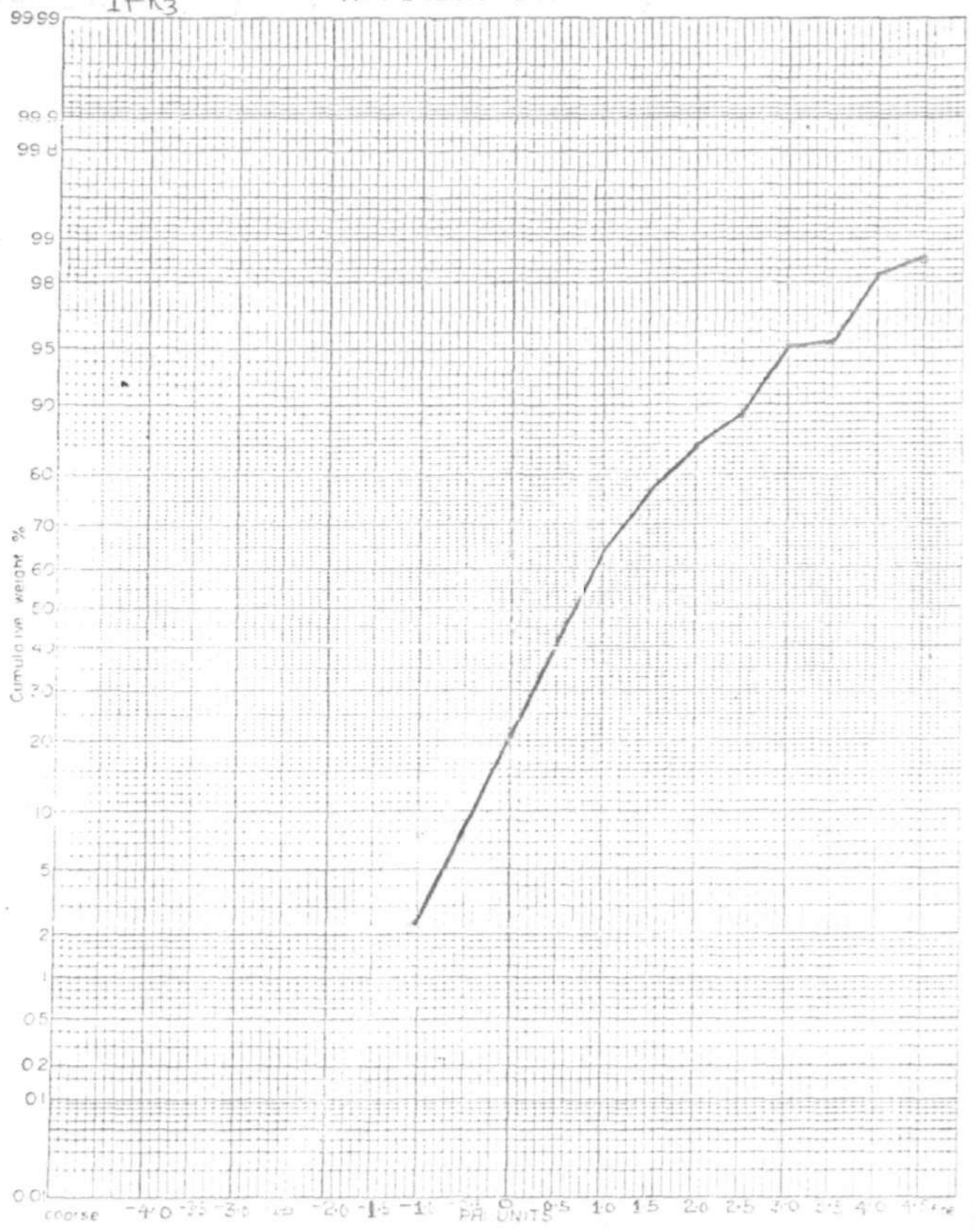
APPENDIX 2

1FR2



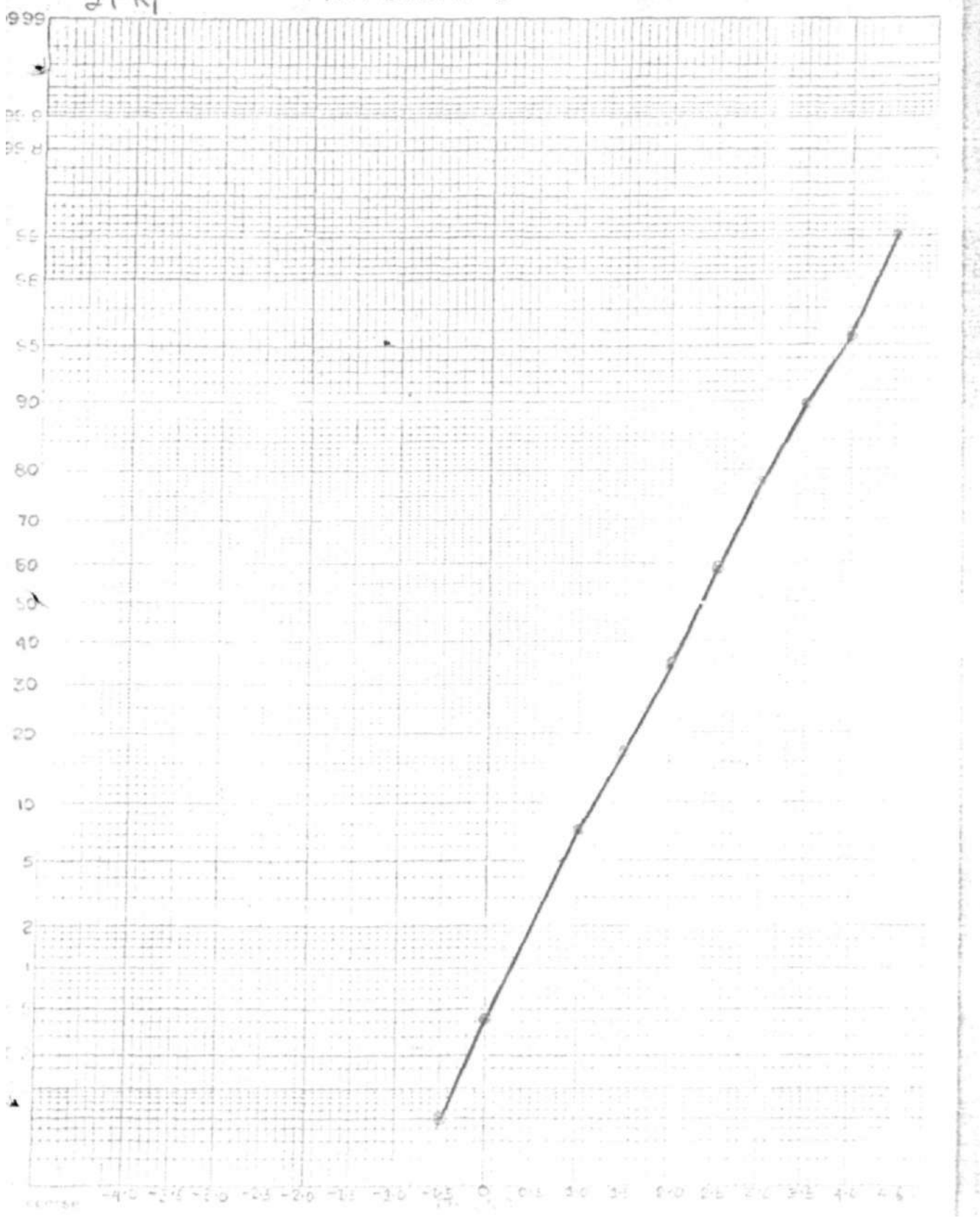
Probability paper for plotting grain-size distributions.

APPENDIX 2

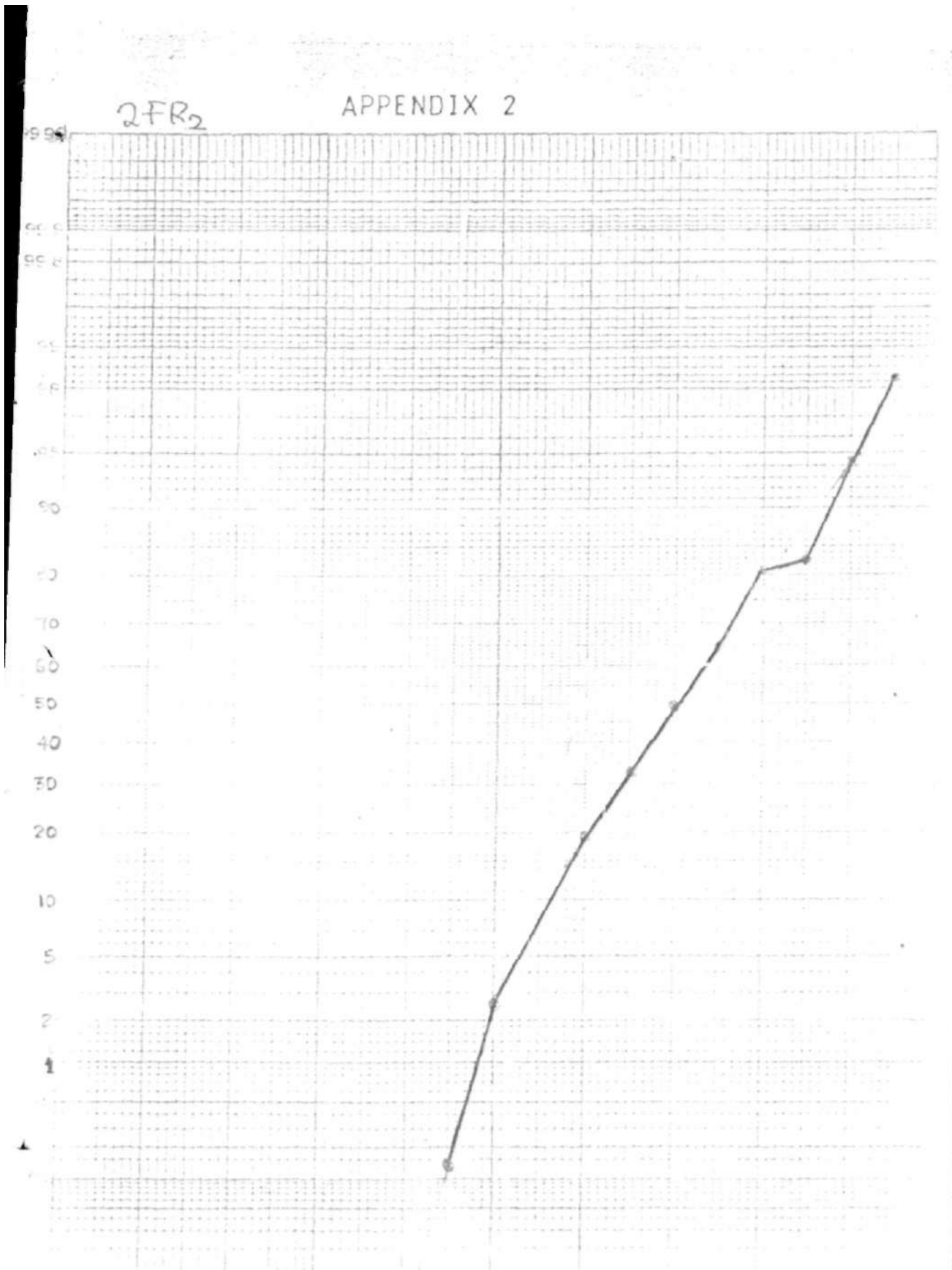


Probability paper for plotting grain-size distributions.

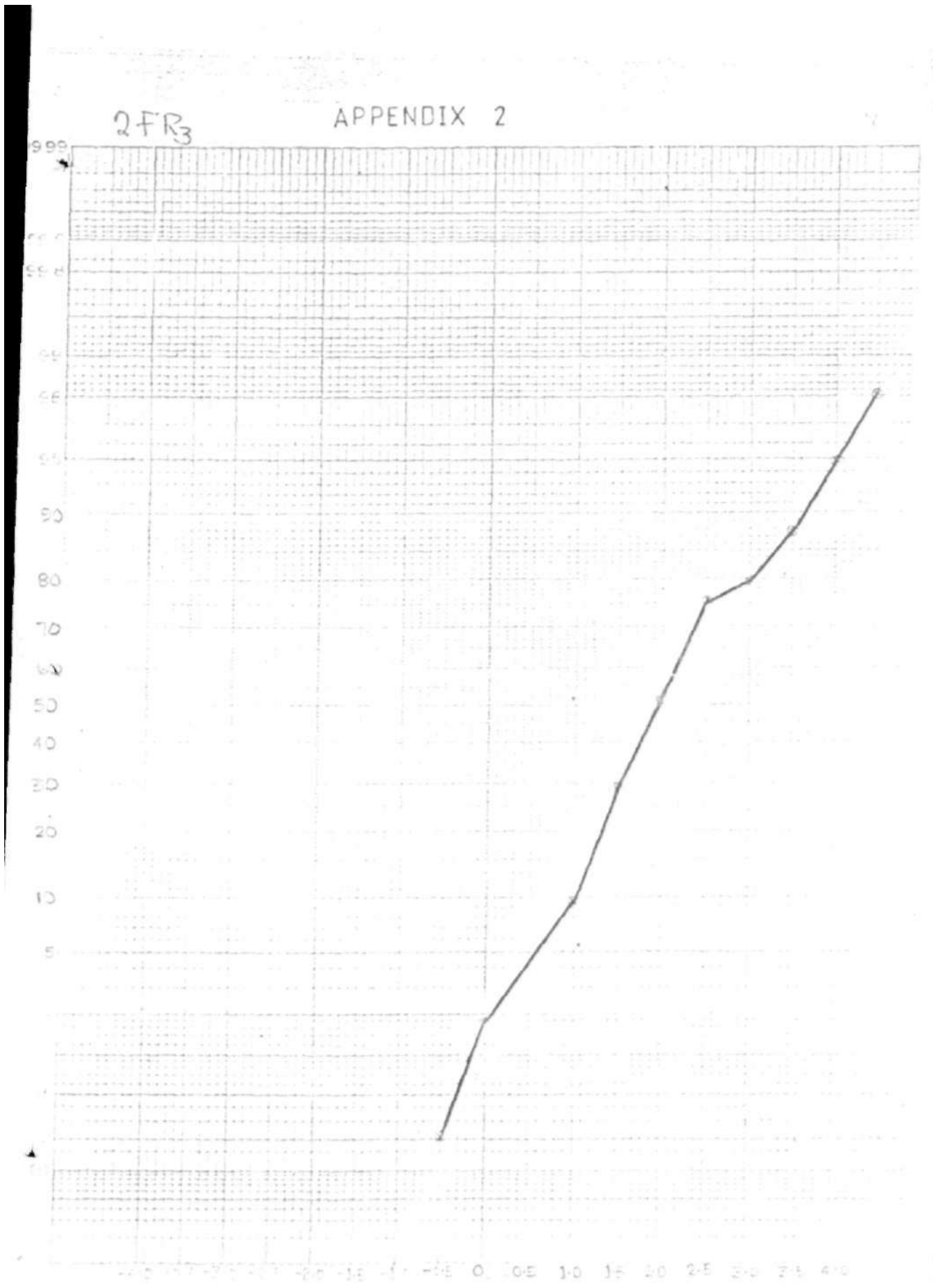
APPENDIX 2



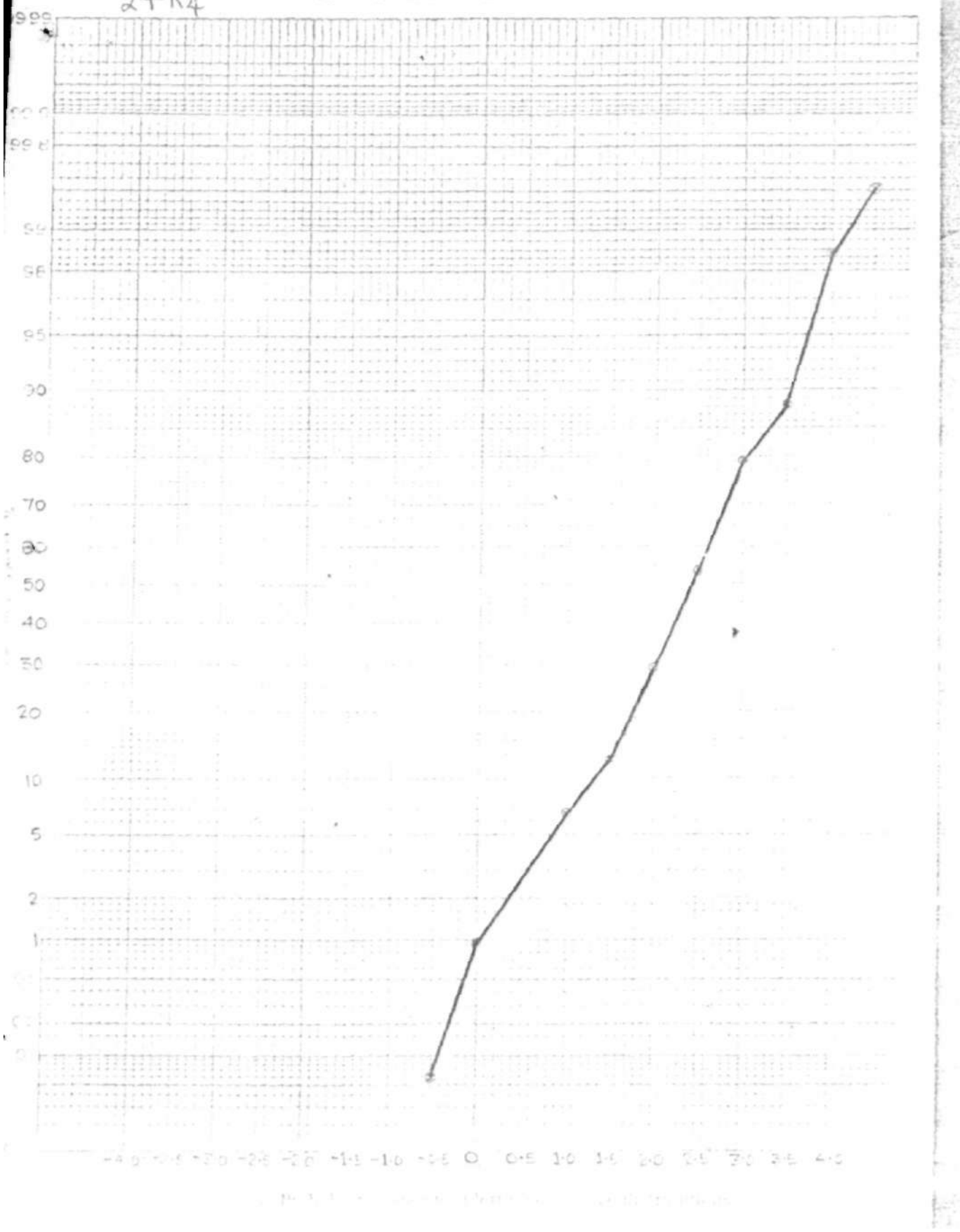
APPENDIX 2



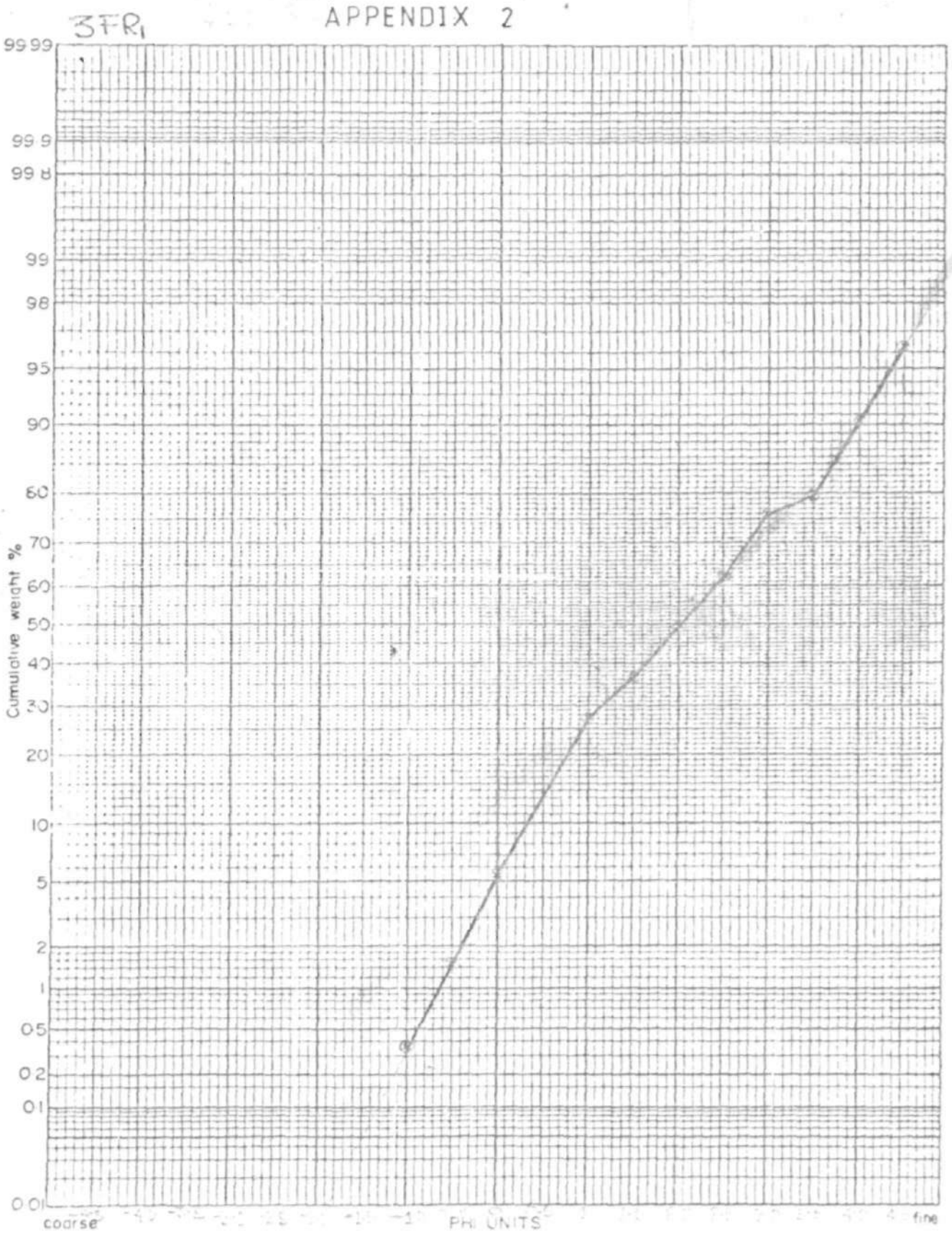
APPENDIX 2



APPENDIX 2


2FR4
99.9
99.8
99
95
90
80
70
60
50
40
30
20
10
5
2
1
0.5
0.2
0.1
-4.0
-3.5
-3.0
-2.5
-2.0
-1.5
-1.0
-0.5
0
0.5
1.0
1.5
2.0
2.5
3.0
3.5
4.0

APPENDIX 2



Probability paper for plotting grain-size distributions.

3FR2

APPENDIX 2

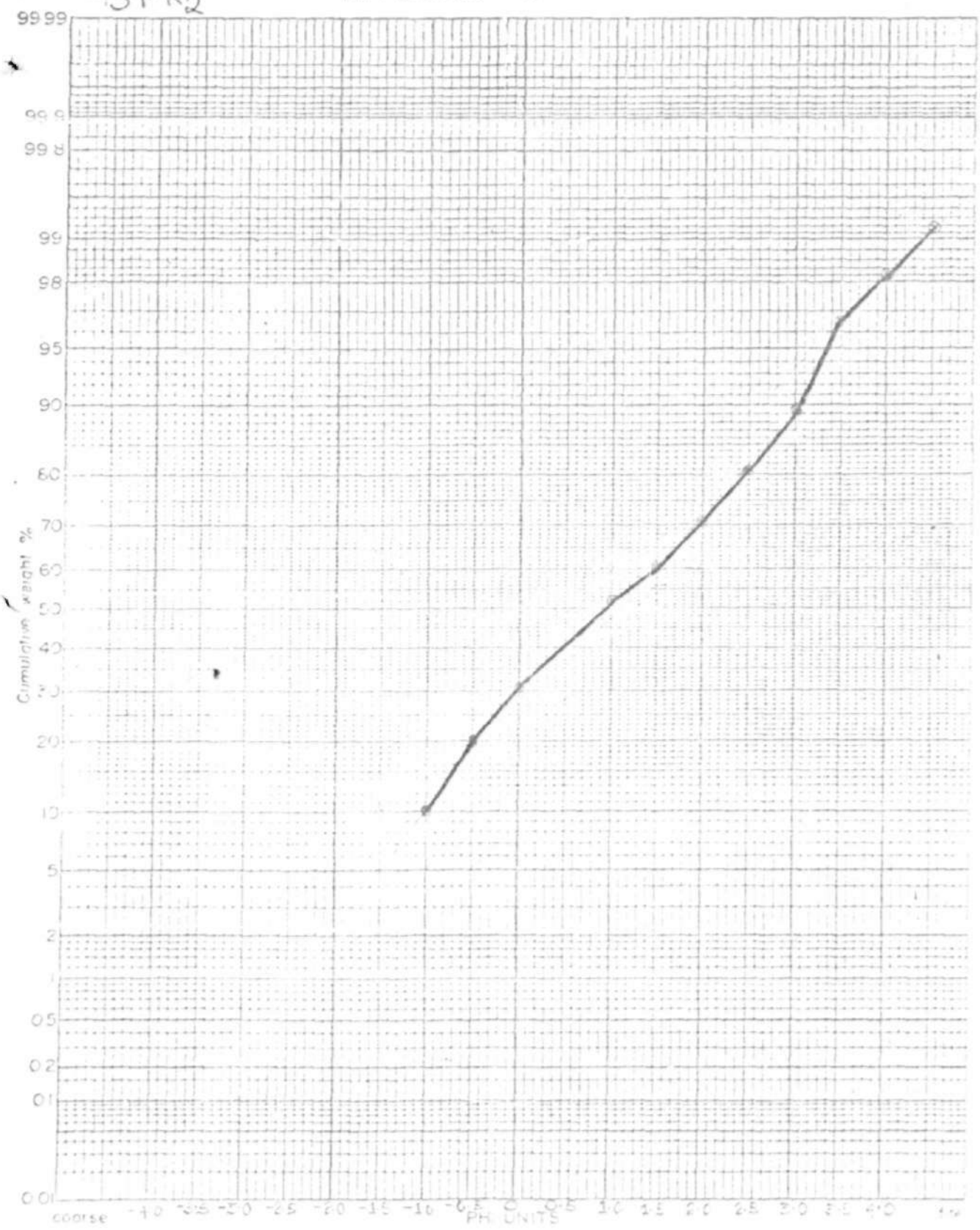
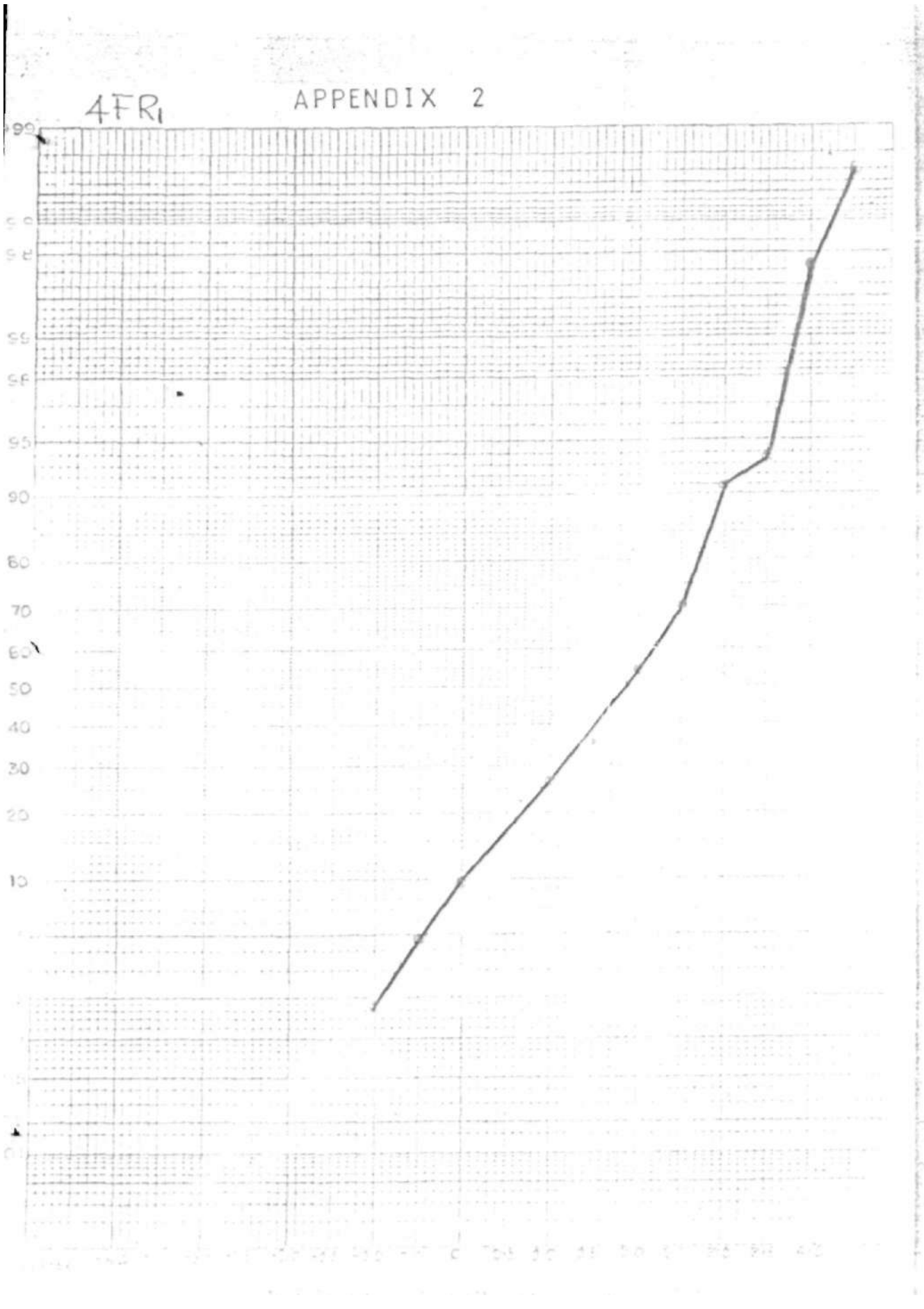
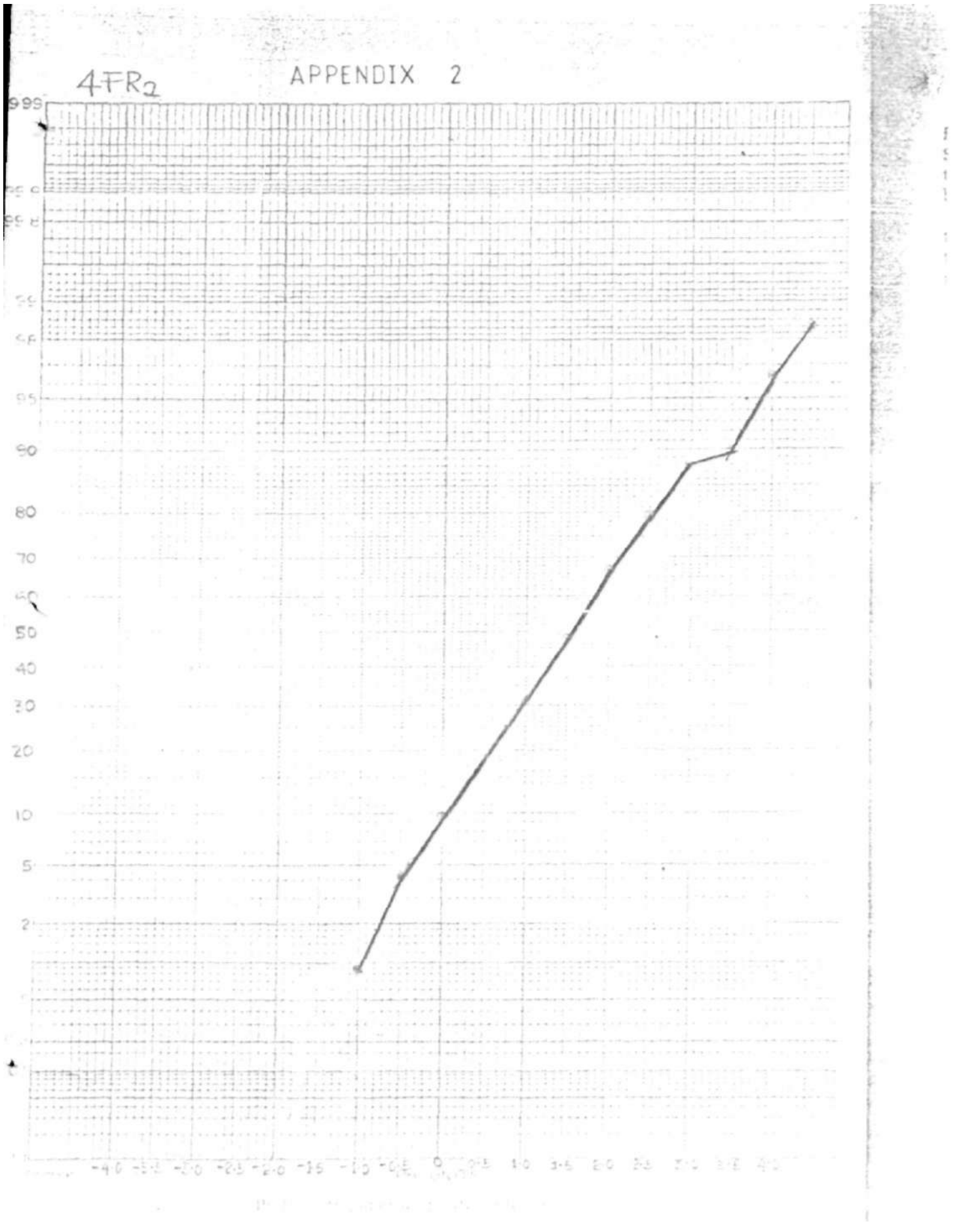


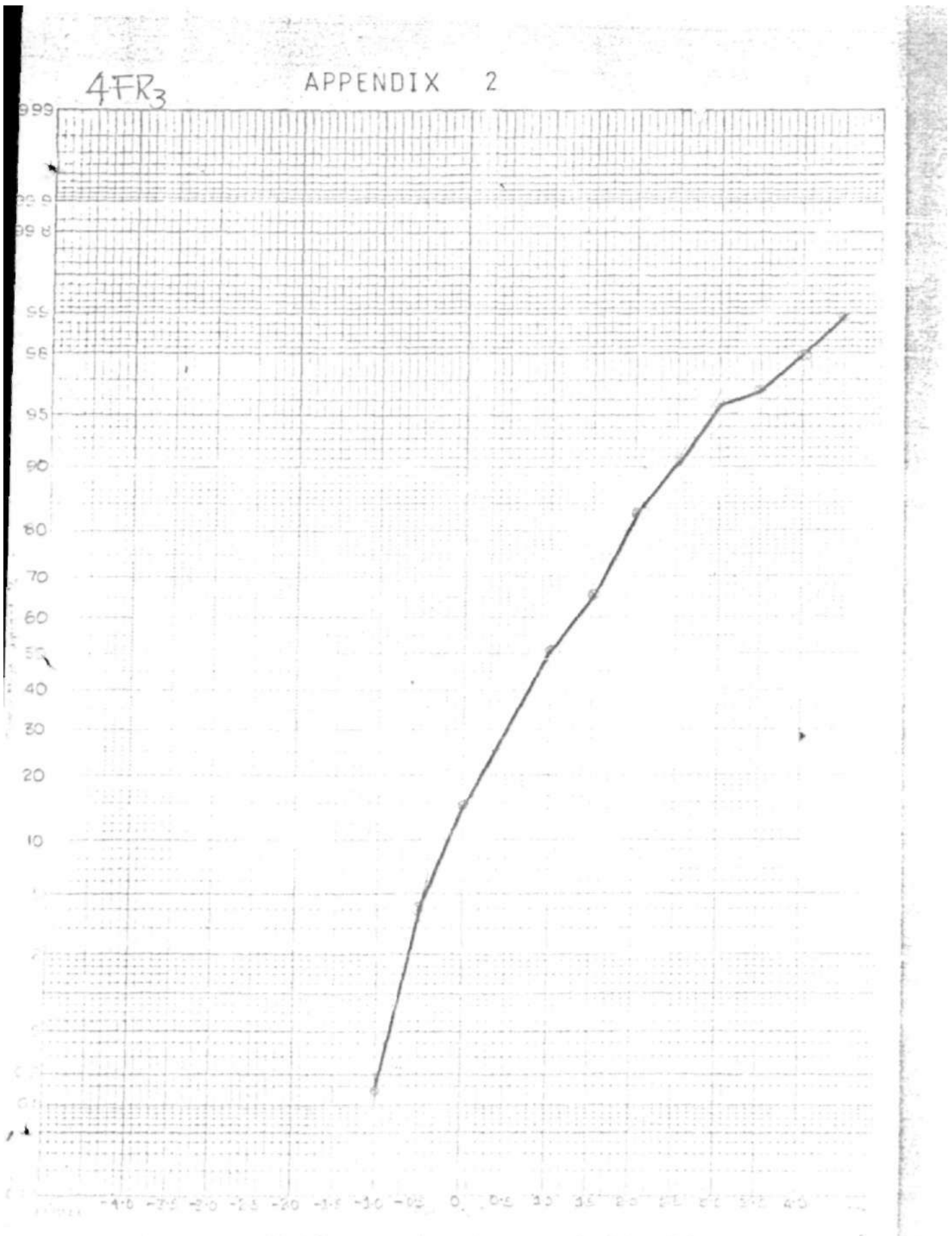
Fig. 1. Log-probability plot showing typical grain-size distributions.

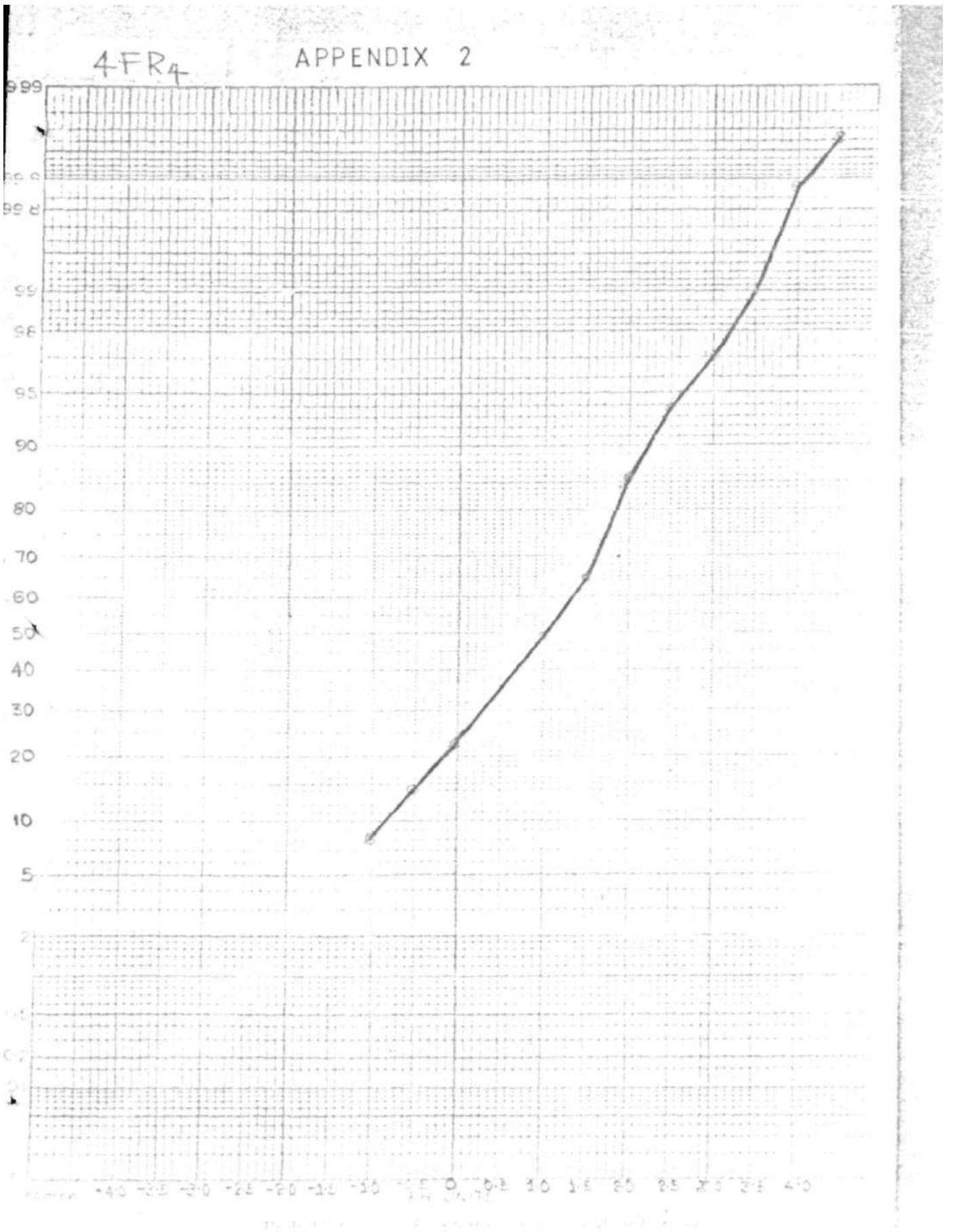
APPENDIX 2



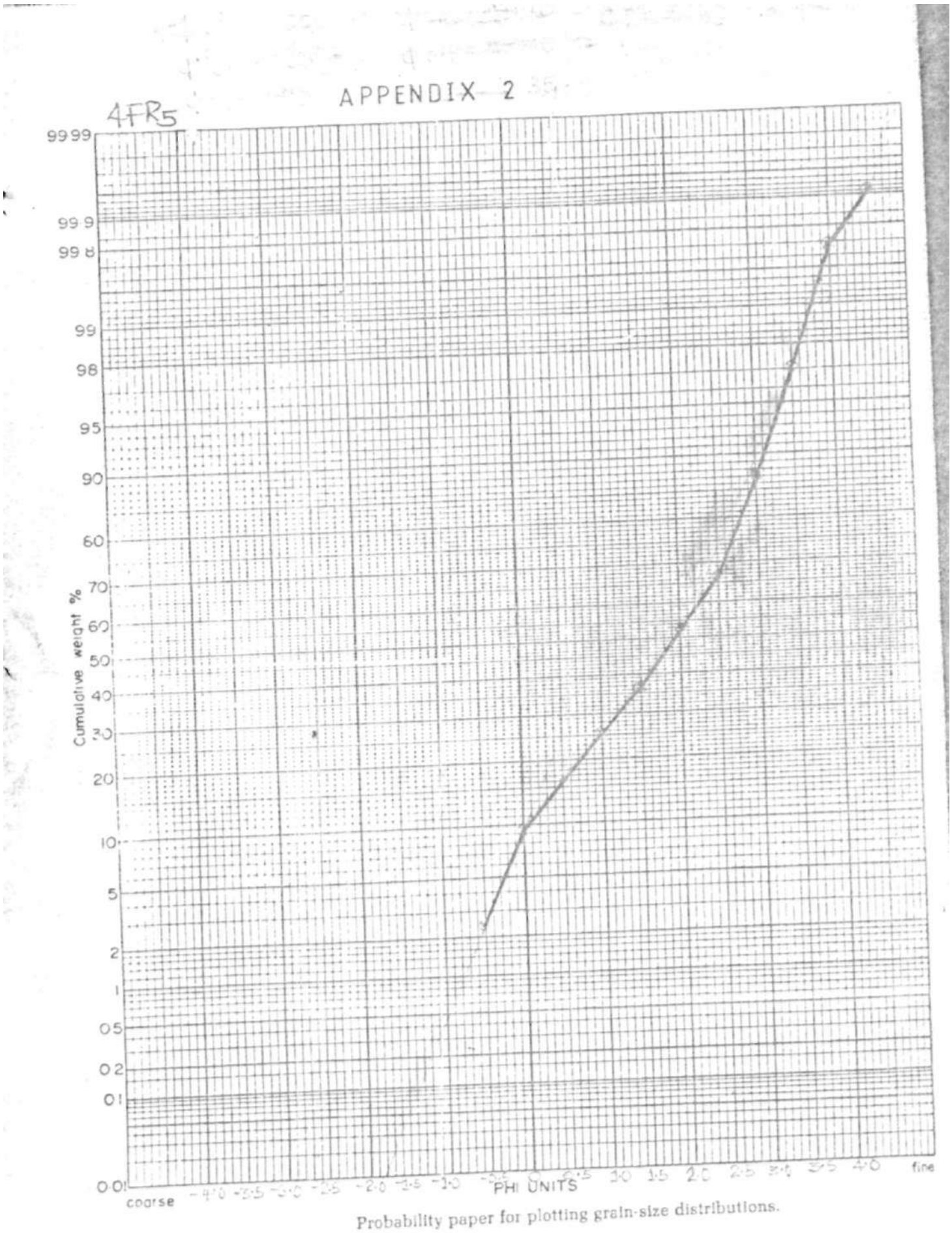
APPENDIX 2




4FR3
APPENDIX 2
999
99 8
95
90
80
70
60
40
30
20
10

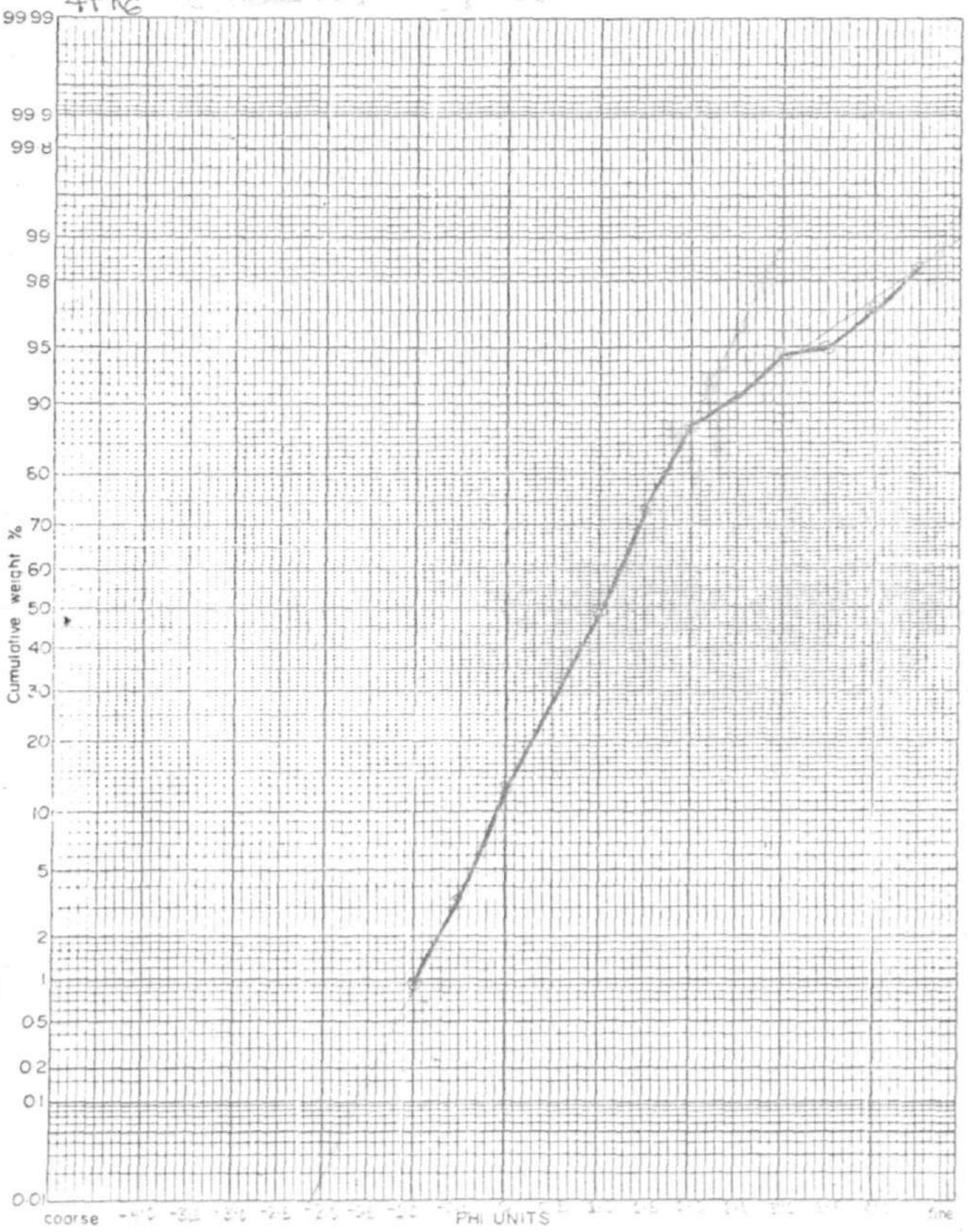

4FR4
APPENDIX 2
99
95
90
80
70
60
50
40
30
20
10
5

APPENDIX 2



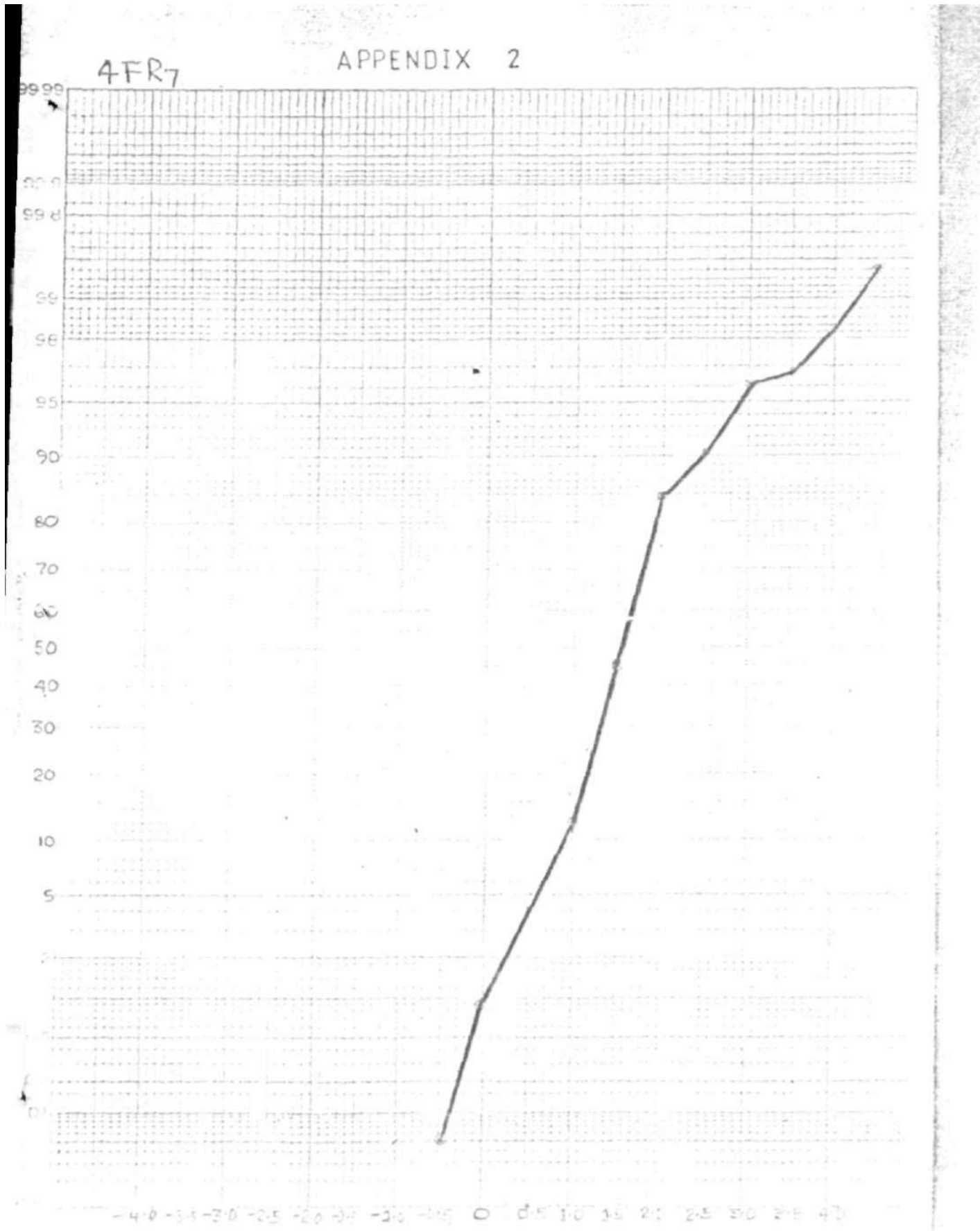
Probability paper for plotting grain-size distributions.

APPENDIX 2

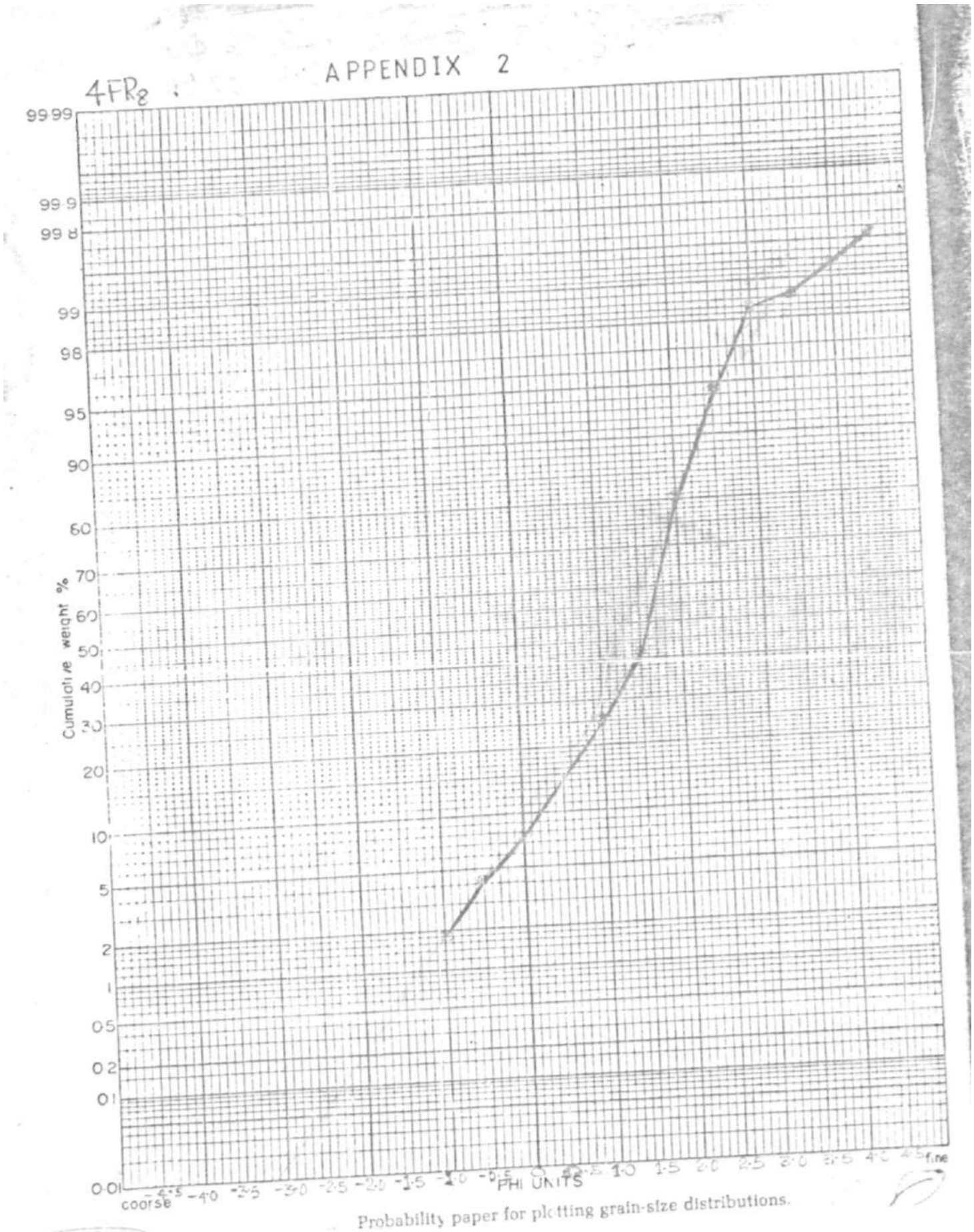


Probability paper for plotting grain-size distributions.

APPENDIX 2

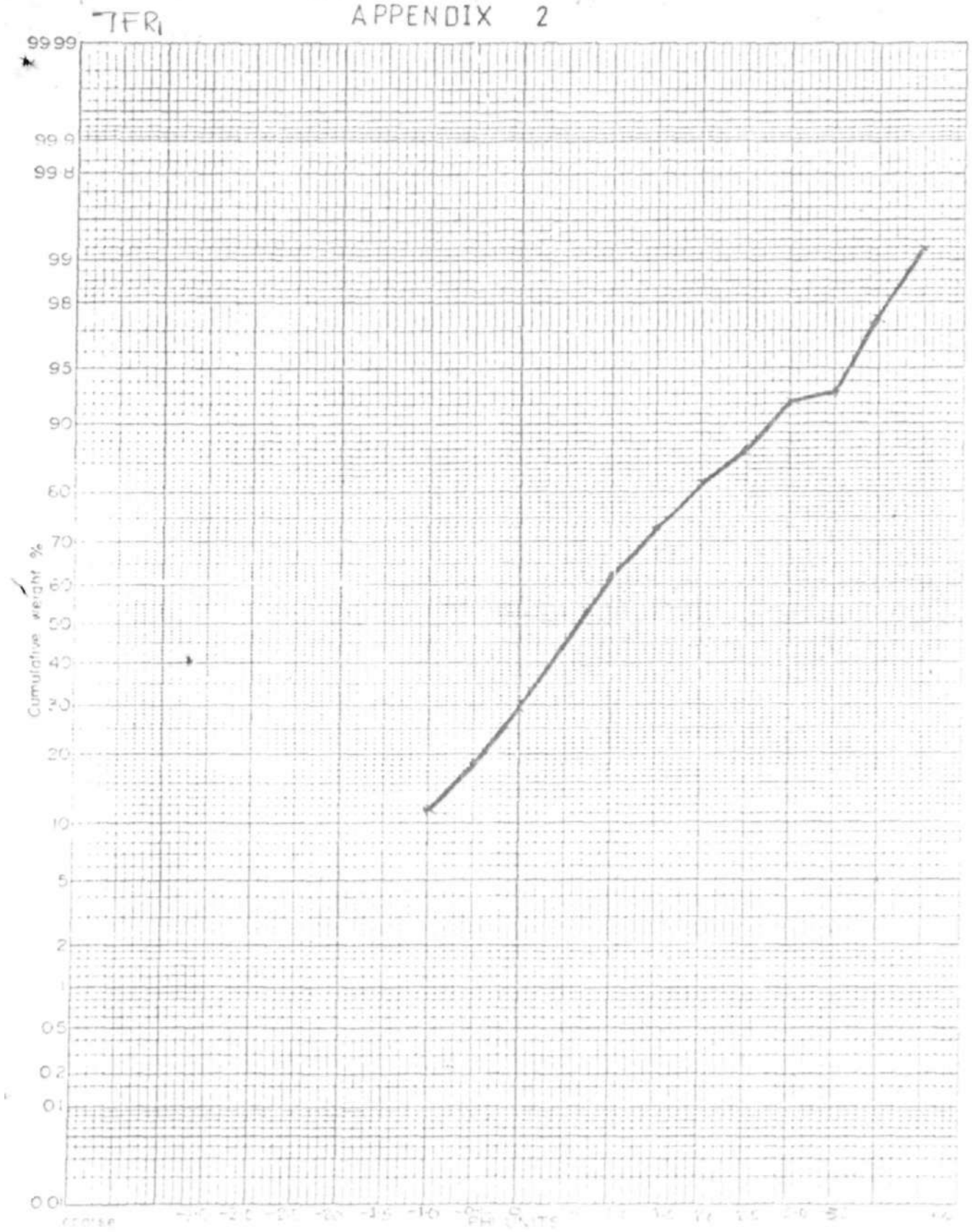

4FR7
99.99
99.9
99
95
90
80
70
60
50
40
30
20
10
5
1
0.1
-4.0 -3.5 -3.0 -2.5 -2.0 -1.5 -1.0 -0.5 0 0.5 1.0 1.5 2.0 2.5 3.0 3.5 4.0

APPENDIX 2



Probability paper for plotting grain-size distributions.

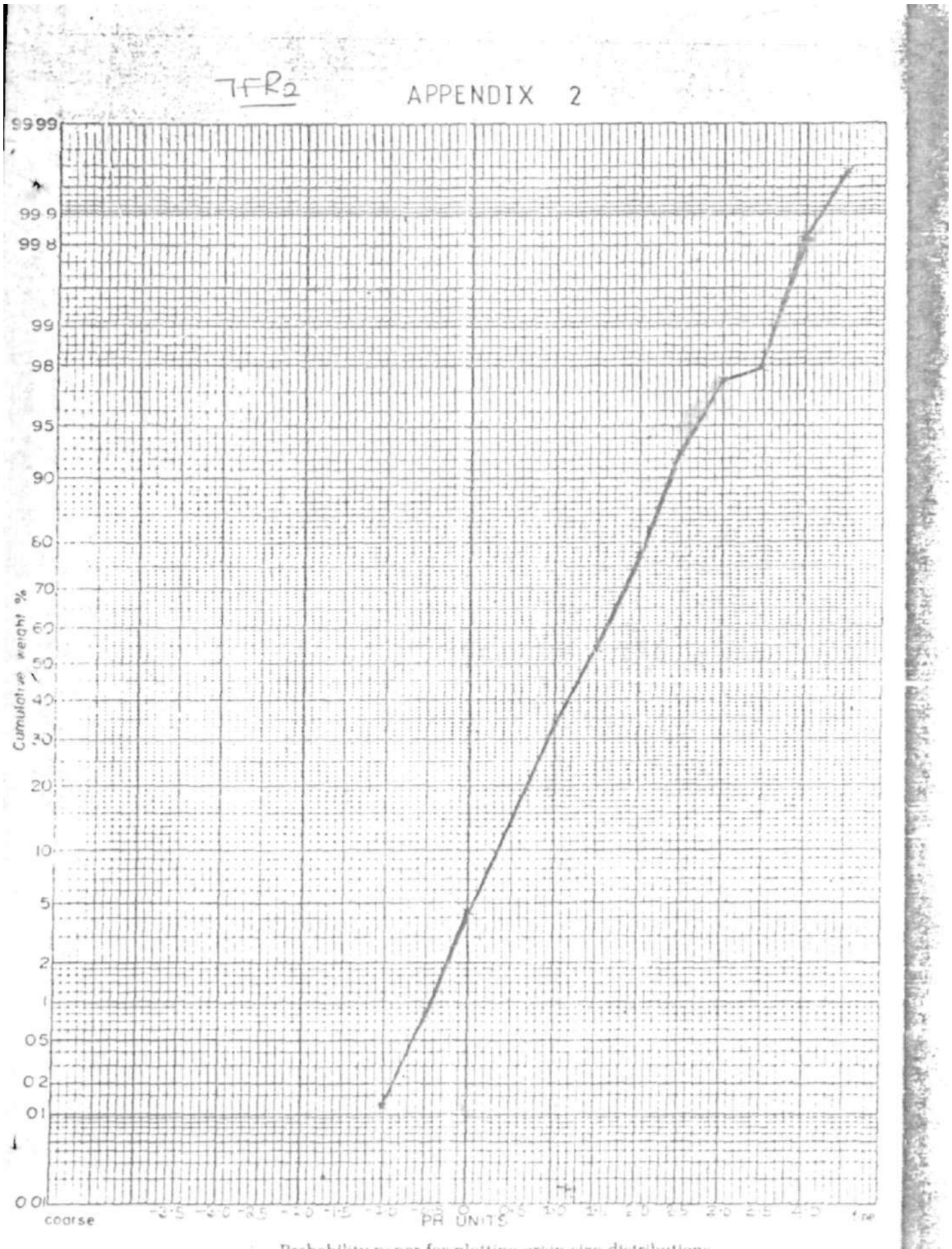
APPENDIX 2



Probability paper for plotting grain size distributions.

TFR2

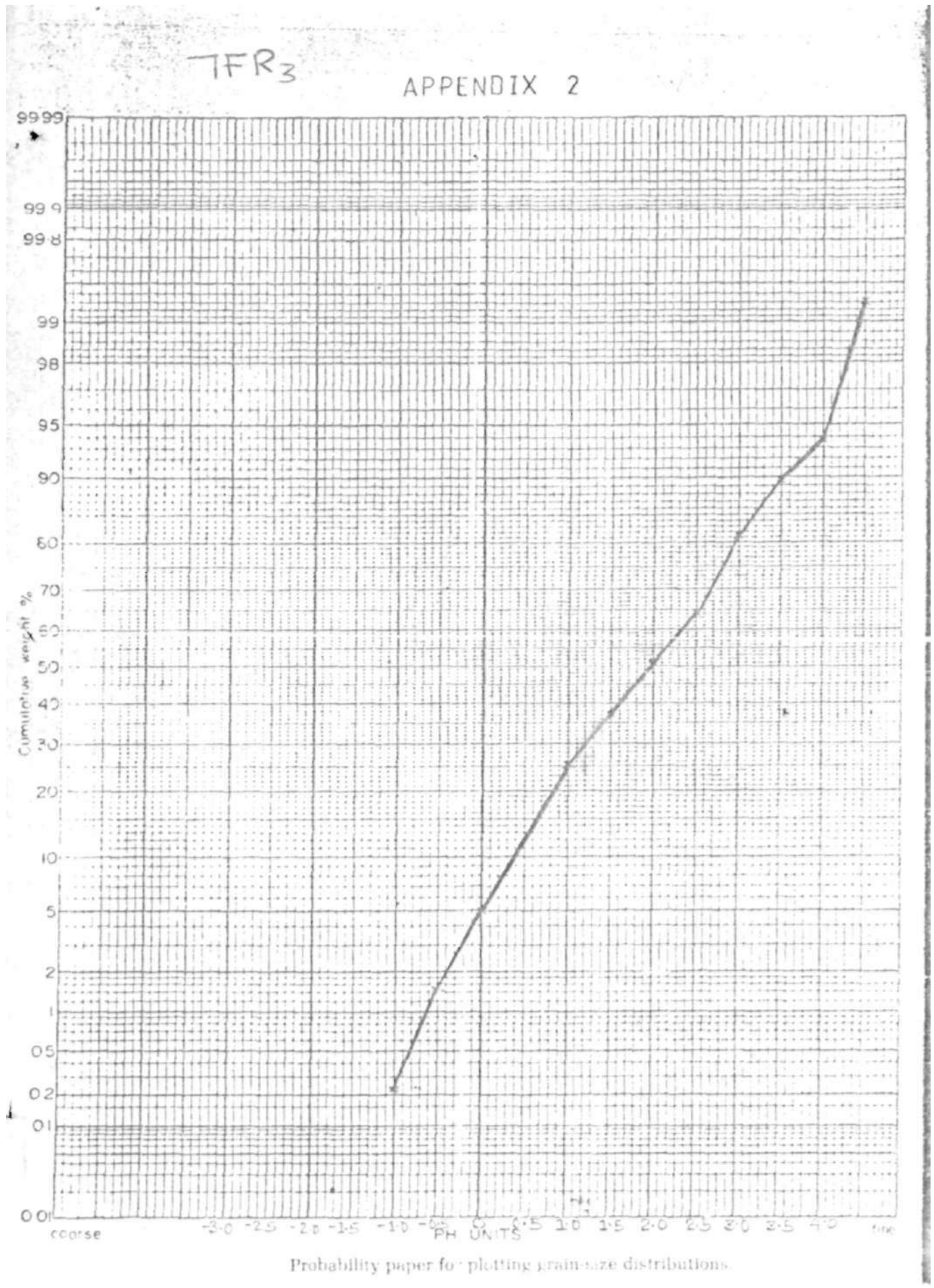
APPENDIX 2



Probability paper for plotting grain-size distributions.

TFR3

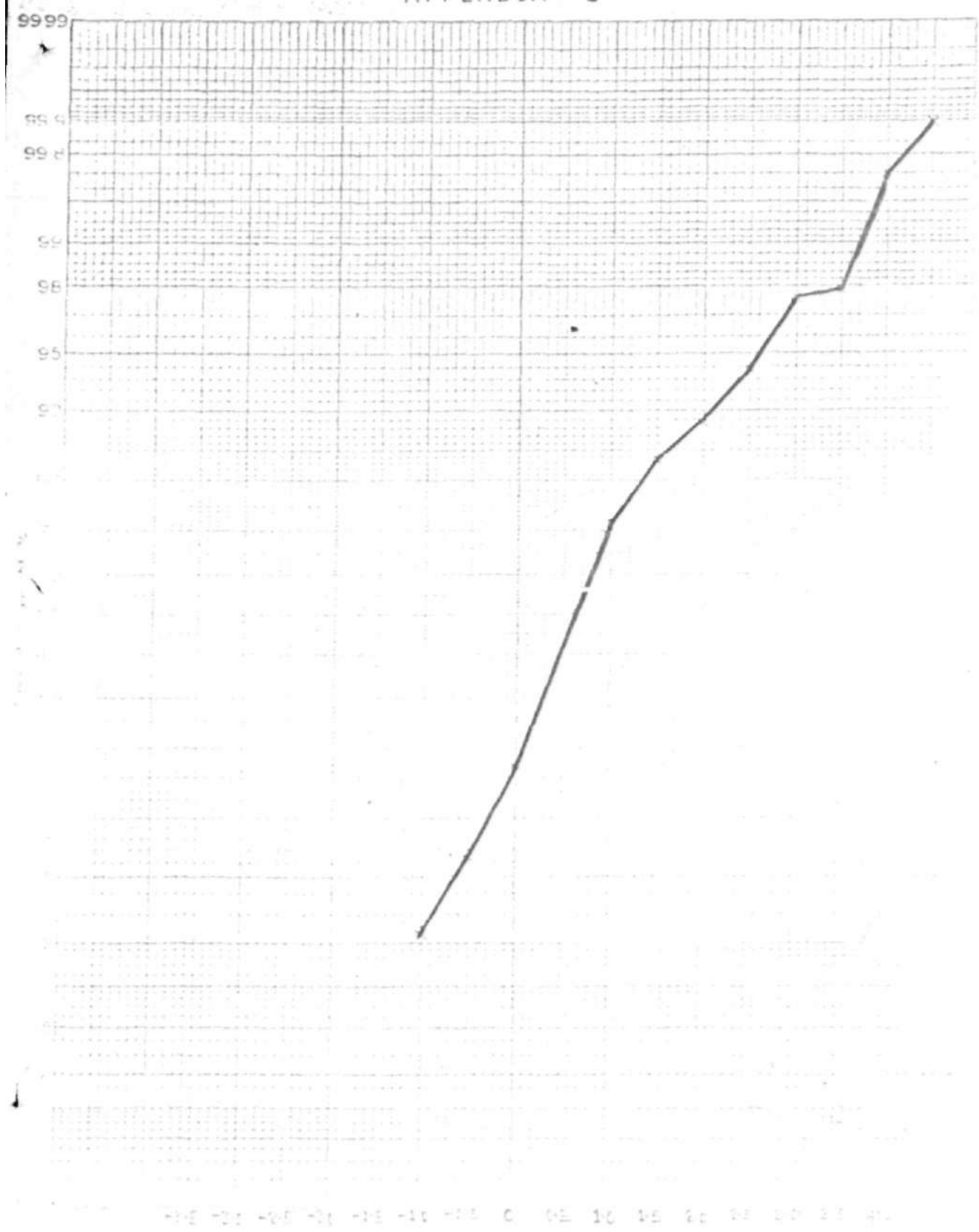
APPENDIX 2



Probability paper for plotting grain-size distributions

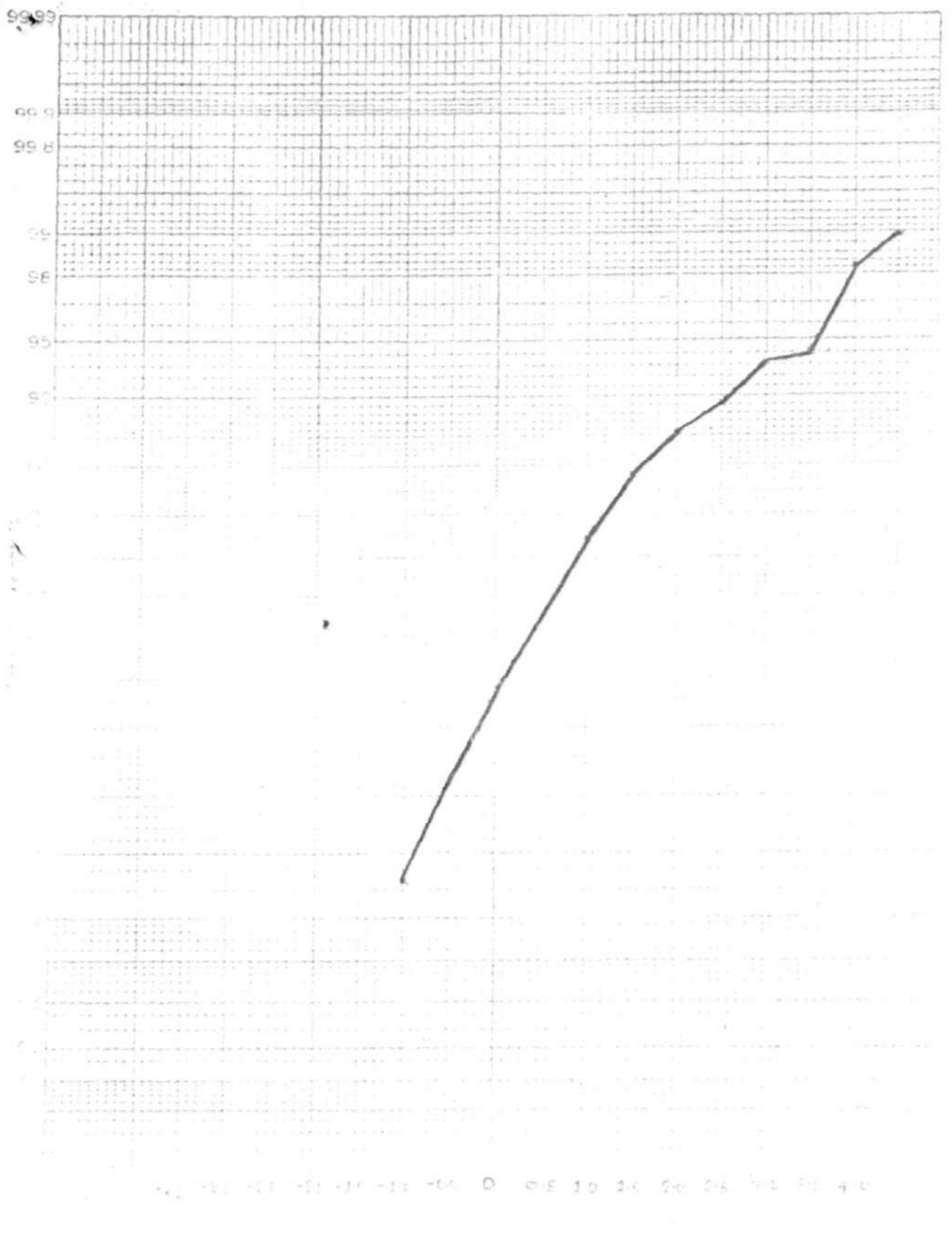
TFR4

APPENDIX '2



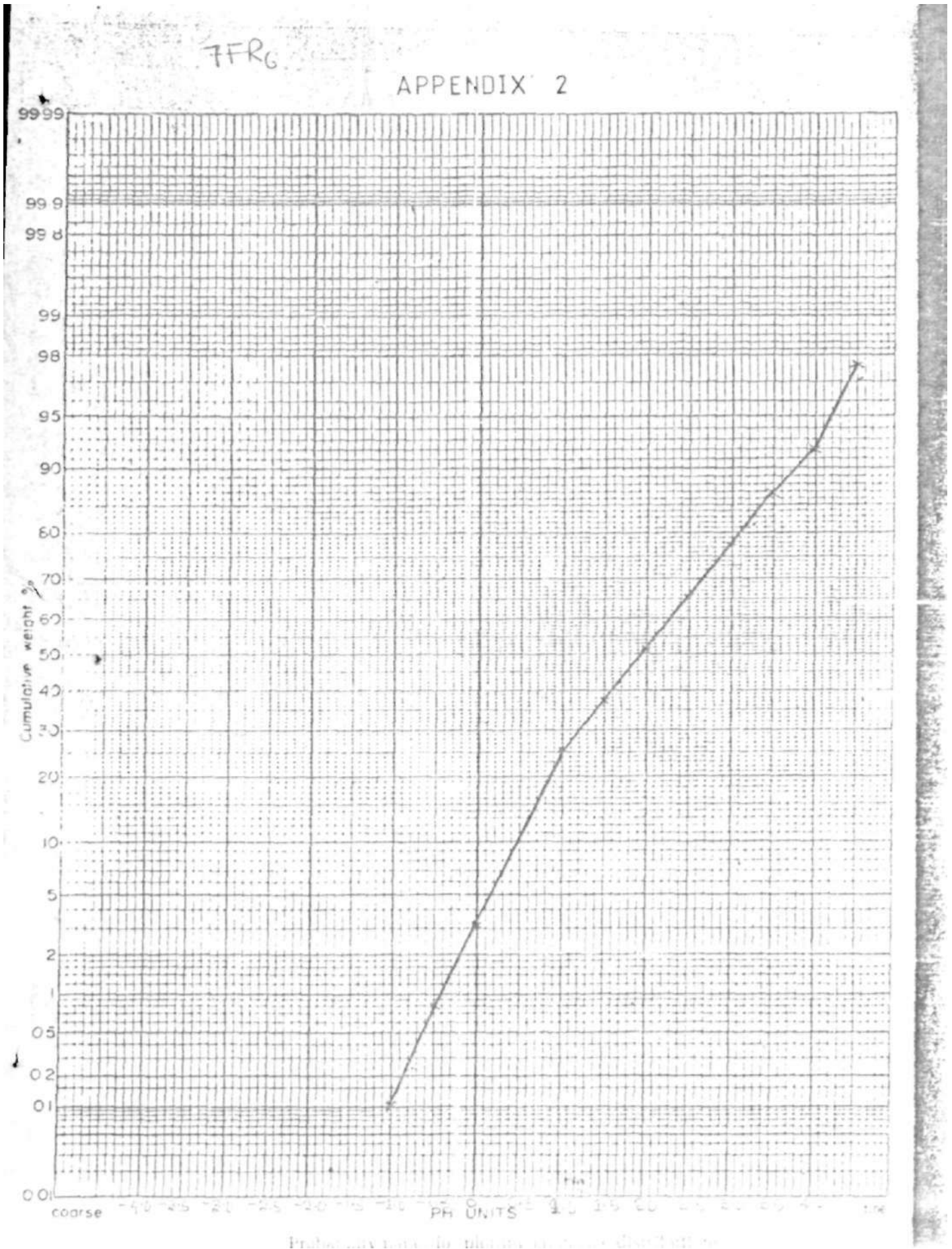
7Fls.

APPENDIX 2



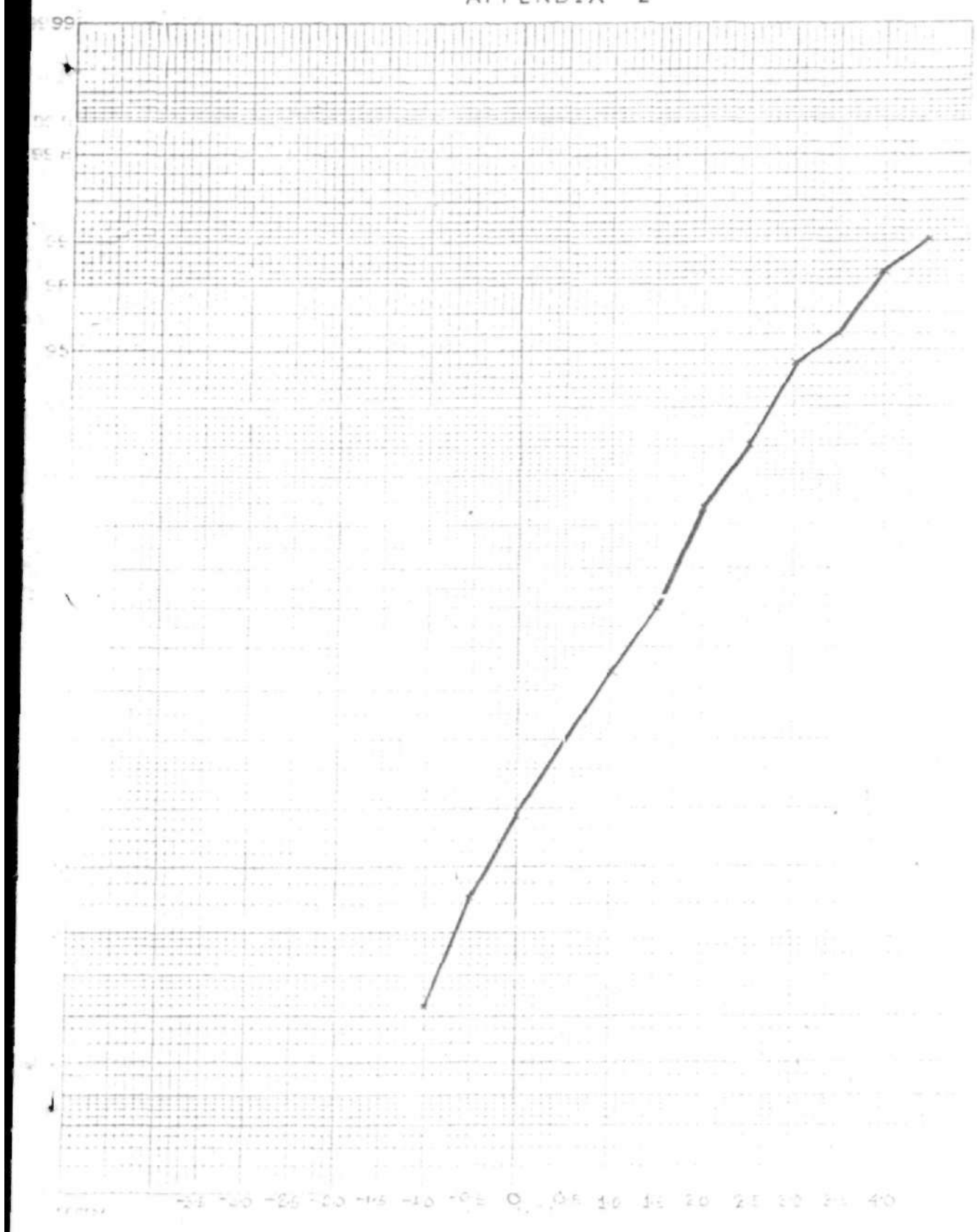
7FR6

APPENDIX 2



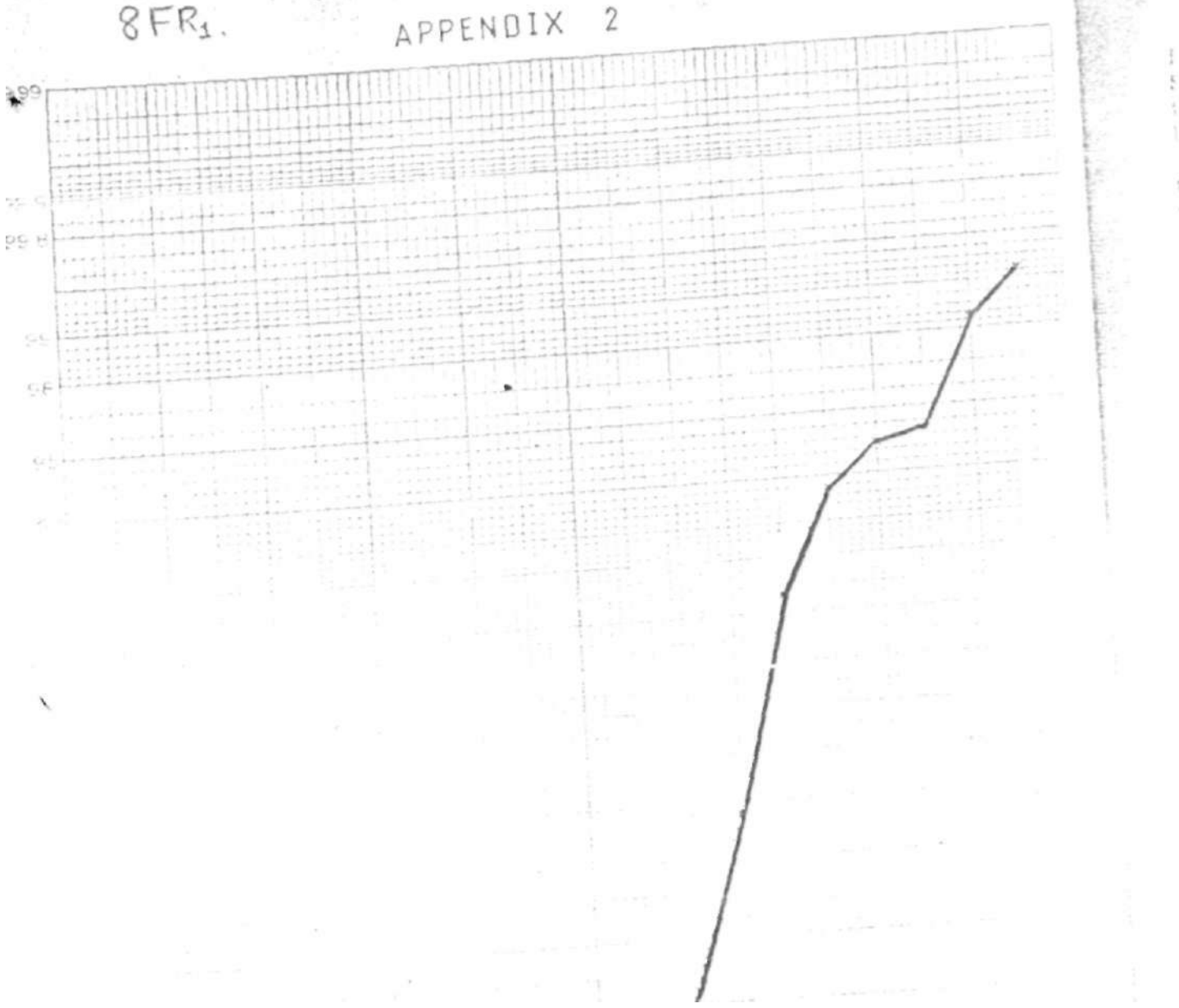
TFR7

APPENDIX 2



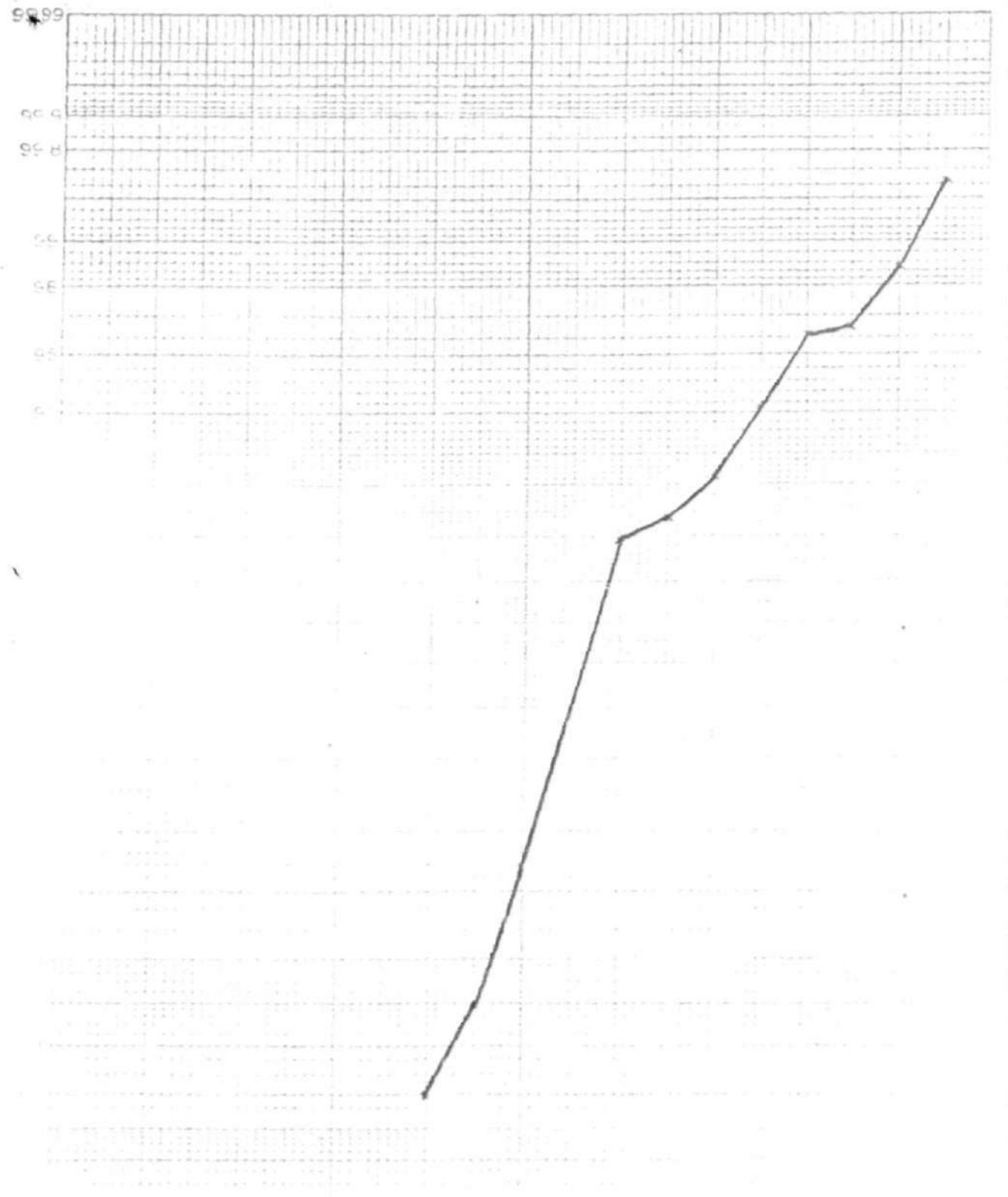
8FR1.

APPENDIX 2

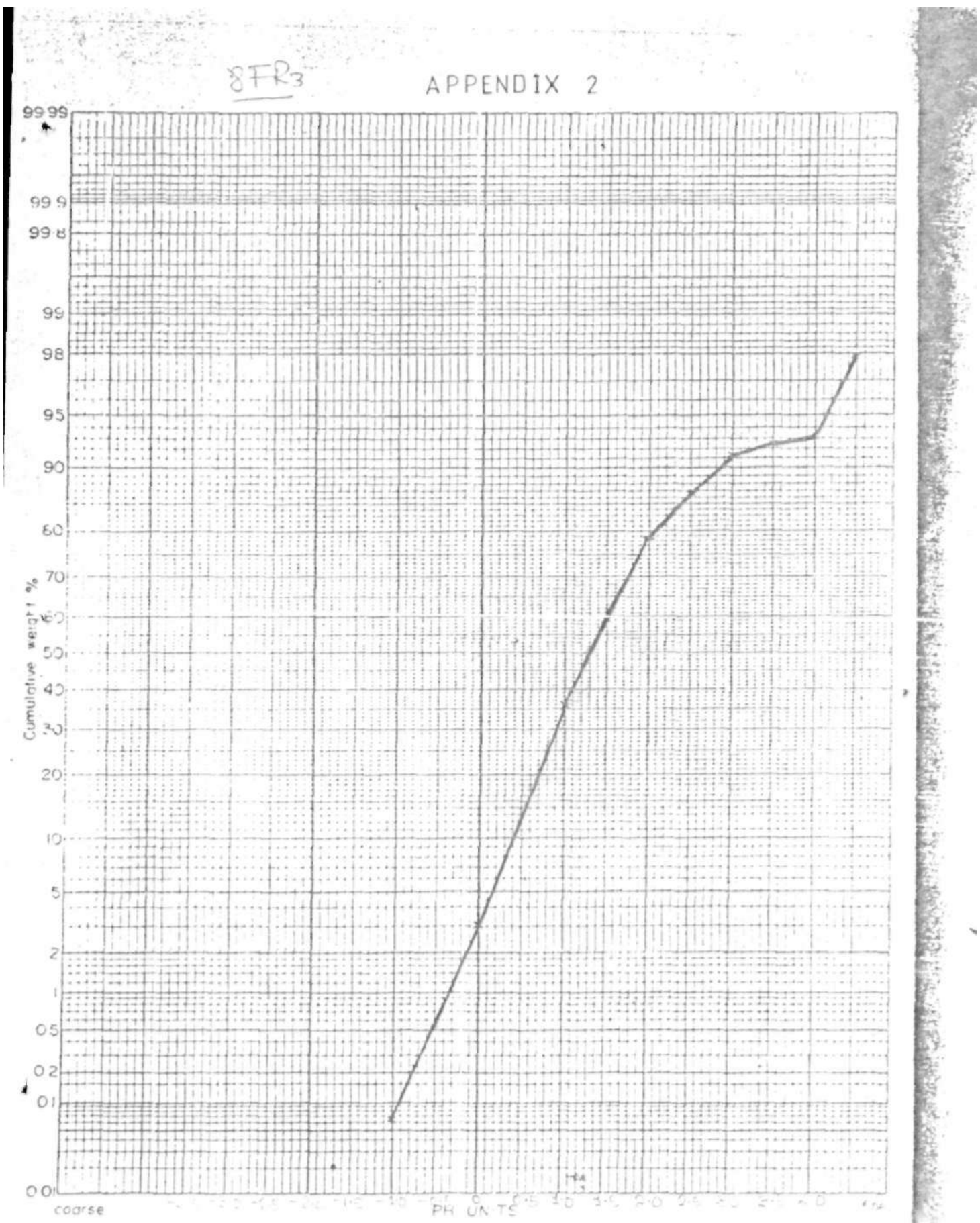


8FR2

APPENDIX 2



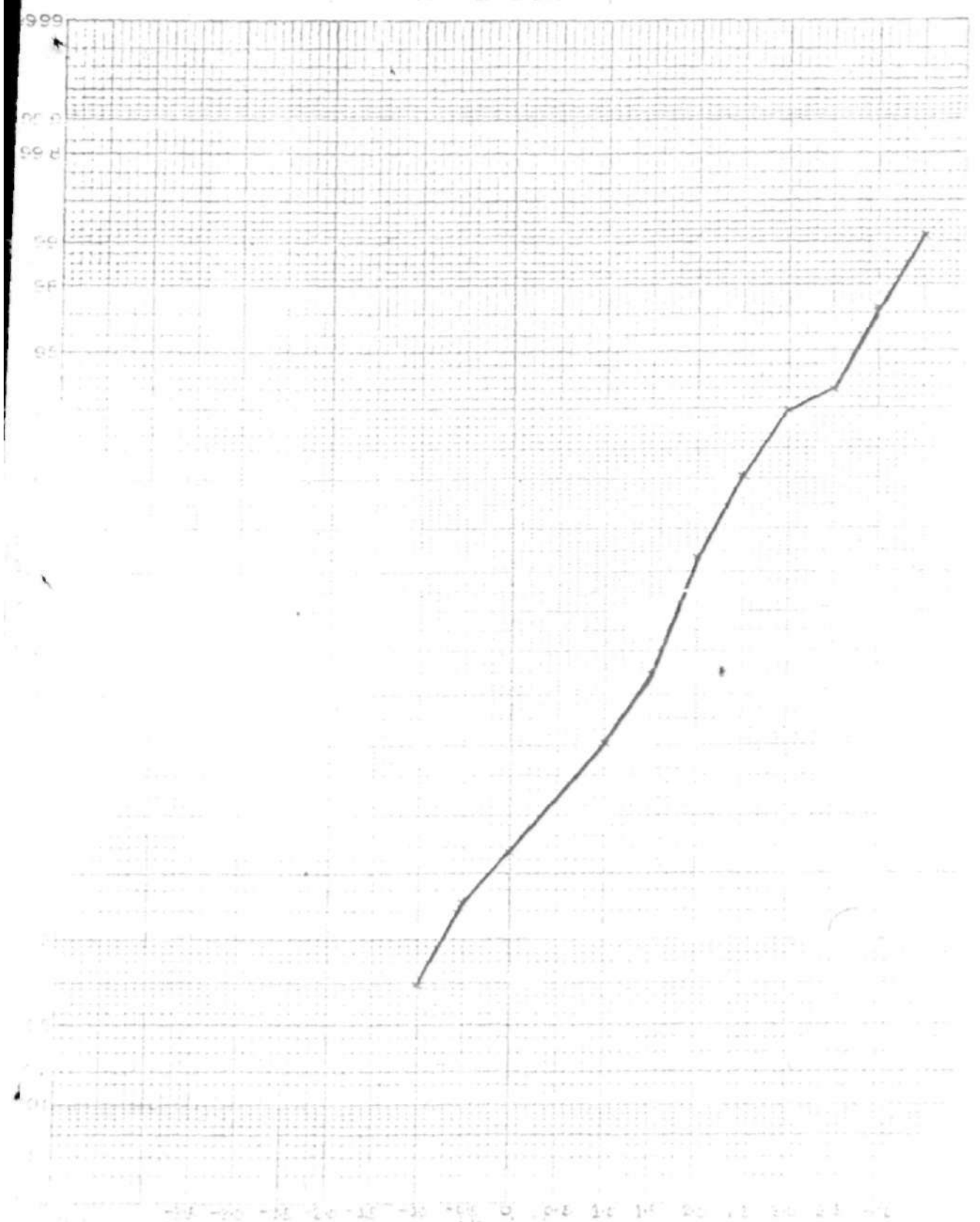
APPENDIX 2



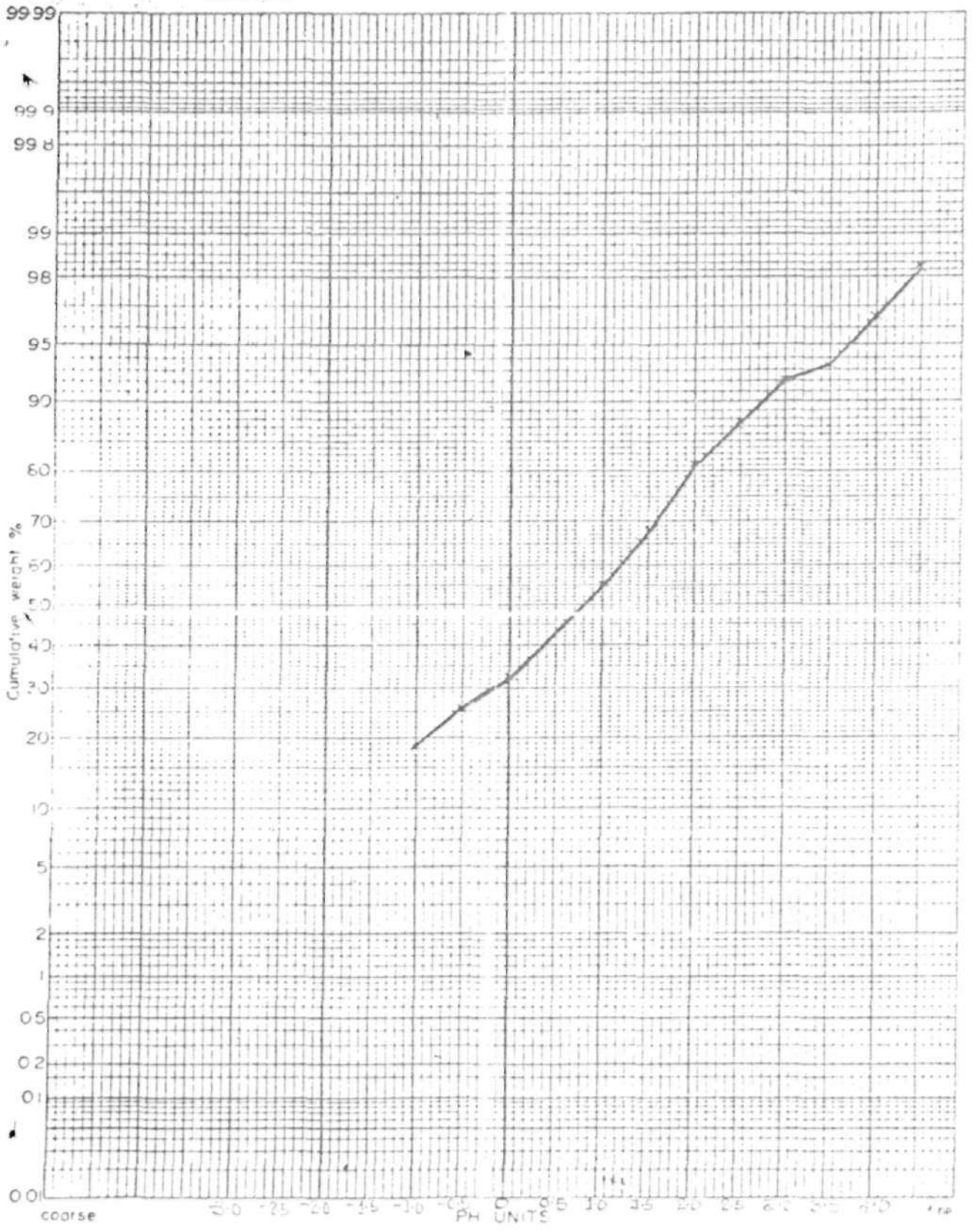
Probability paper for plotting grain-size distributions

8FR4

APPENDIX 2

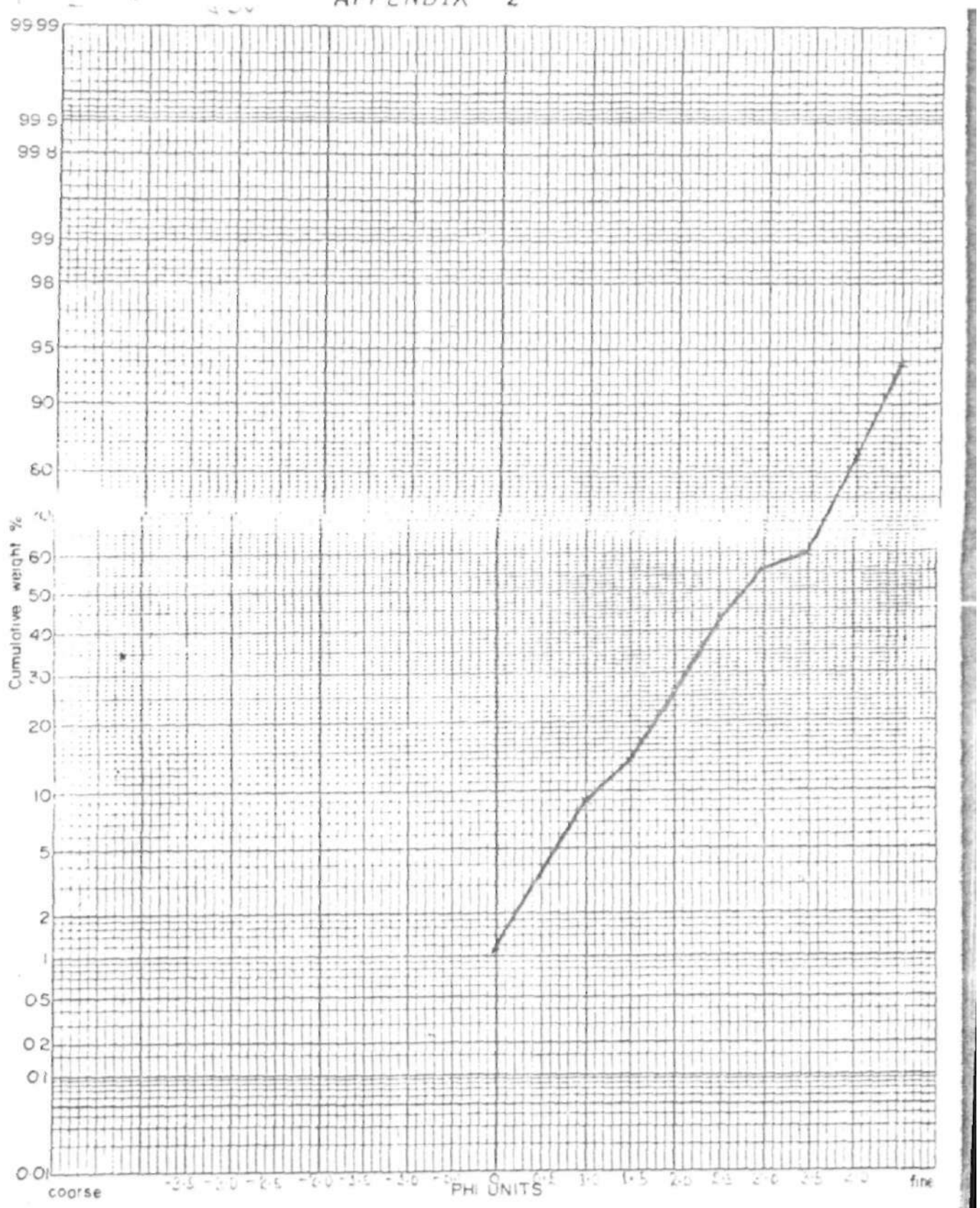


APPENDIX 2



Probability paper for plotting grain-size distributions

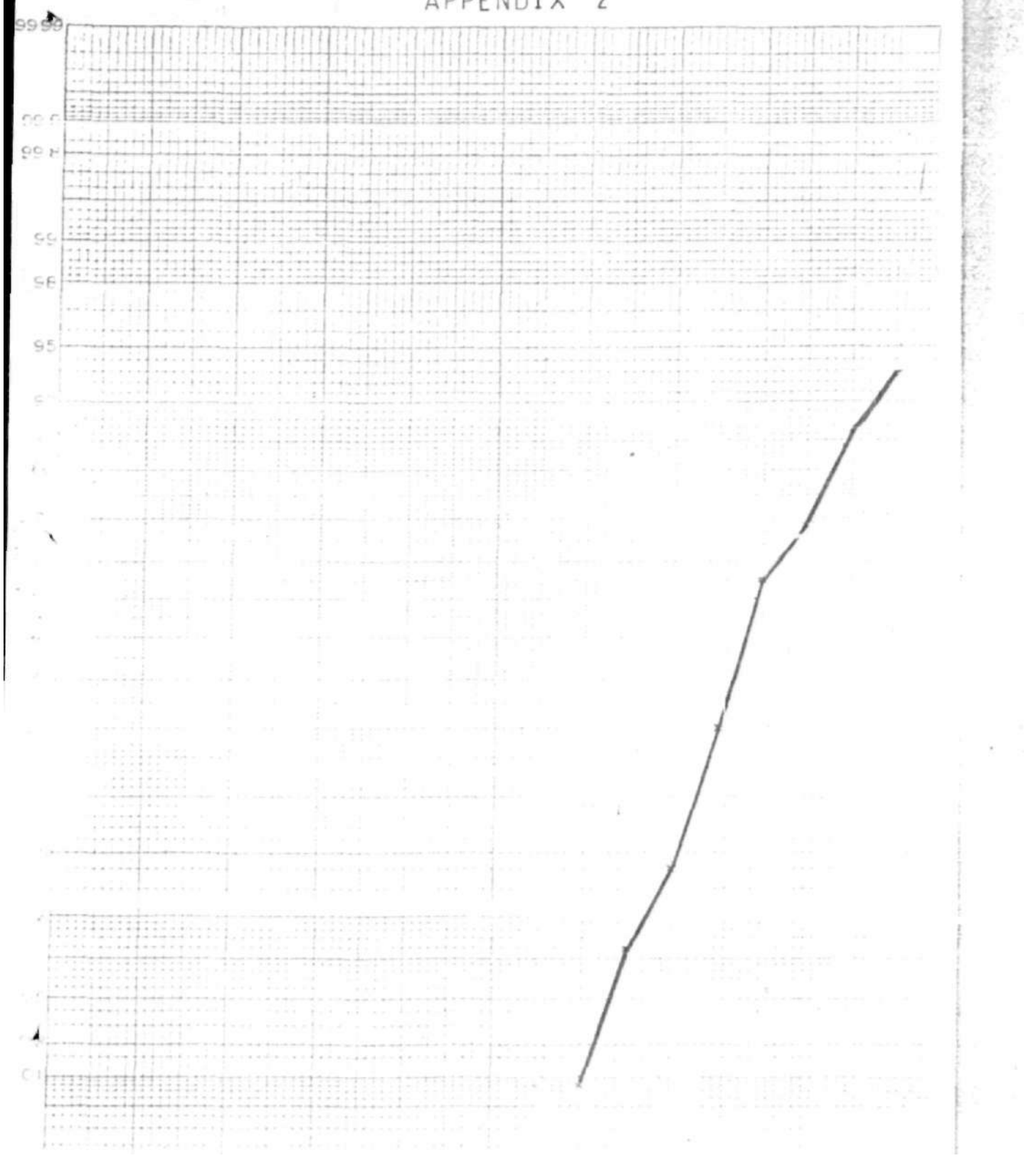
APPENDIX 2



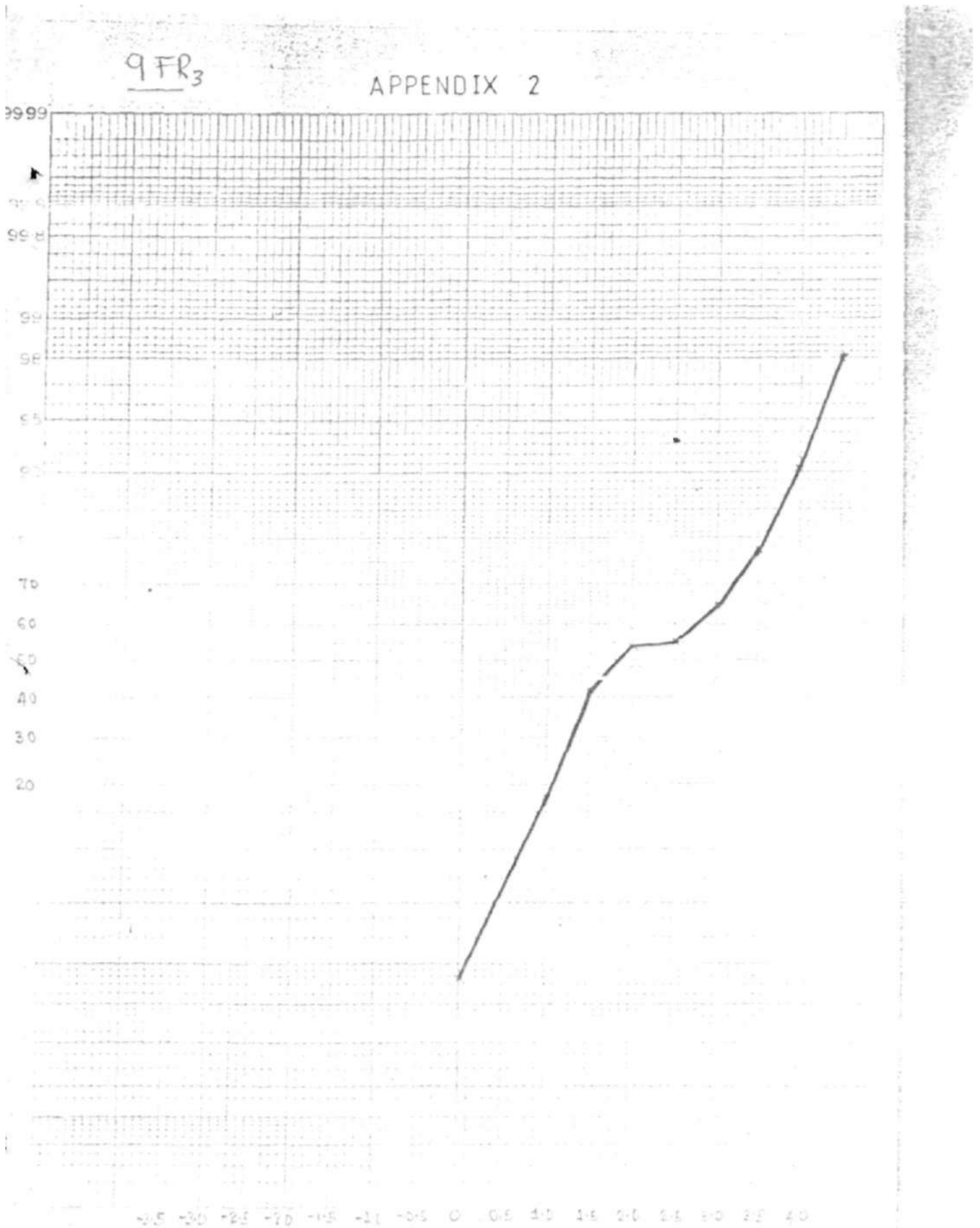
Probability paper for plotting grain-size distributions.

9FR2

APPENDIX 2

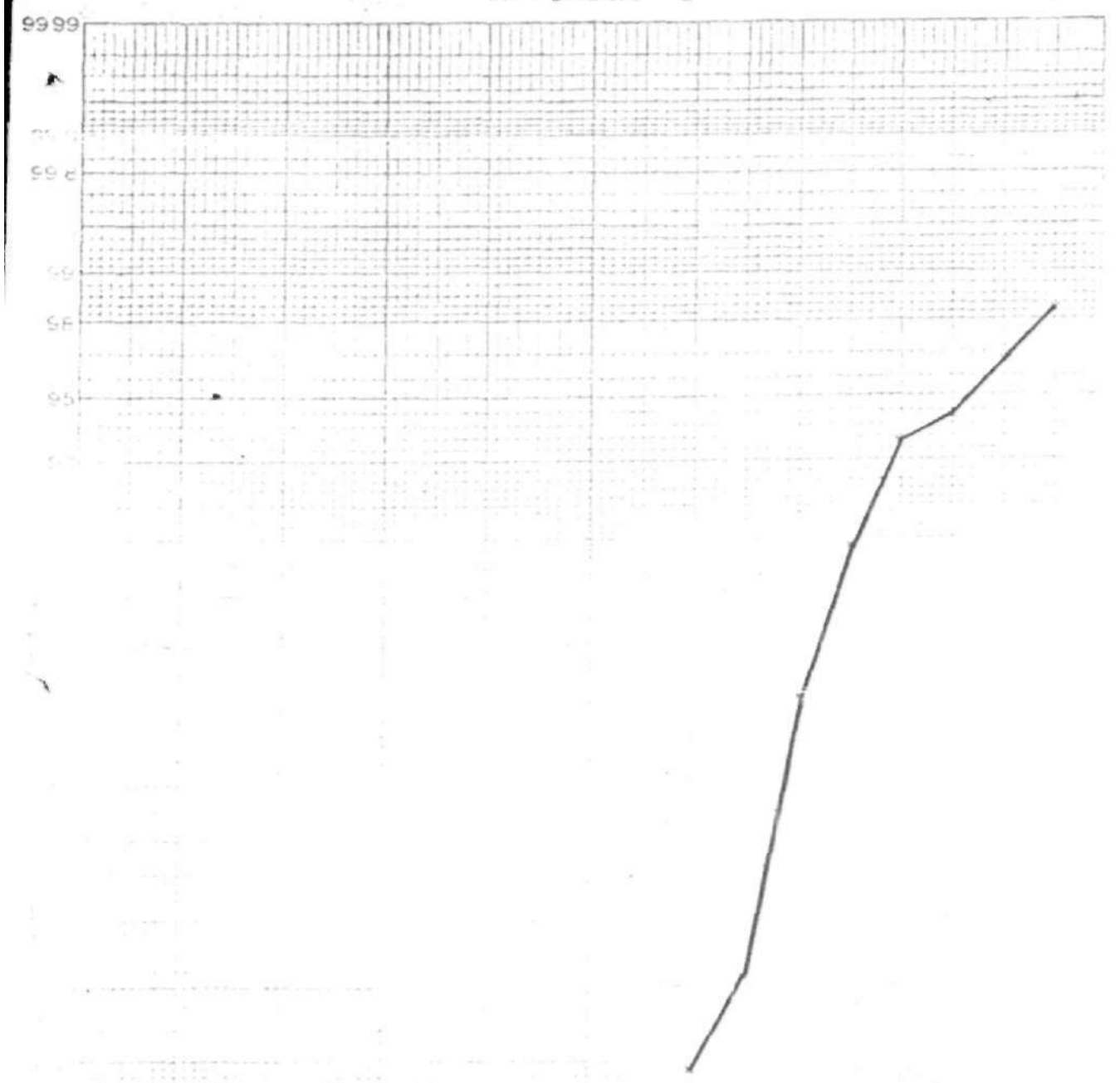


APPENDIX 2



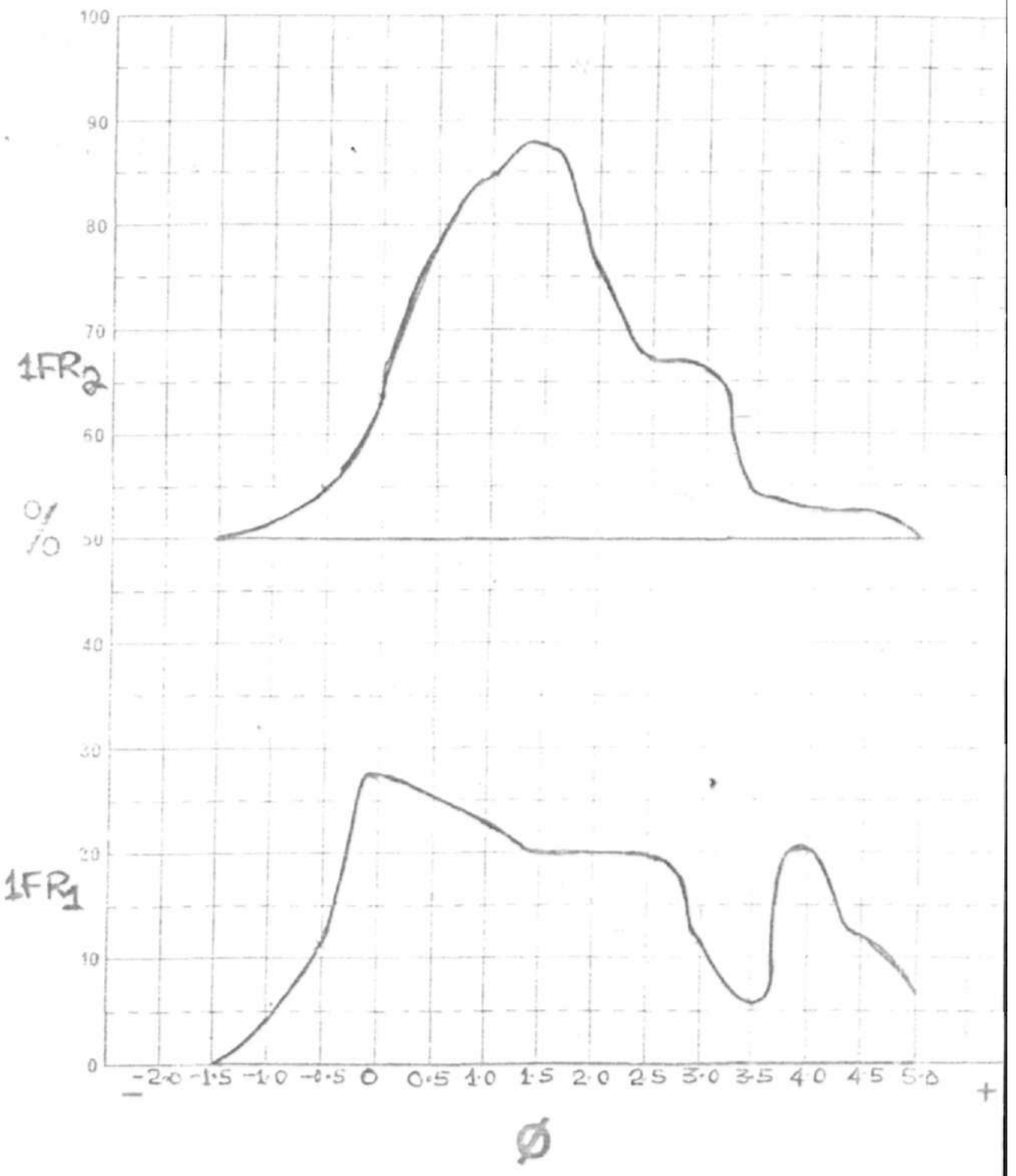
qFR_4

APPENDIX 2



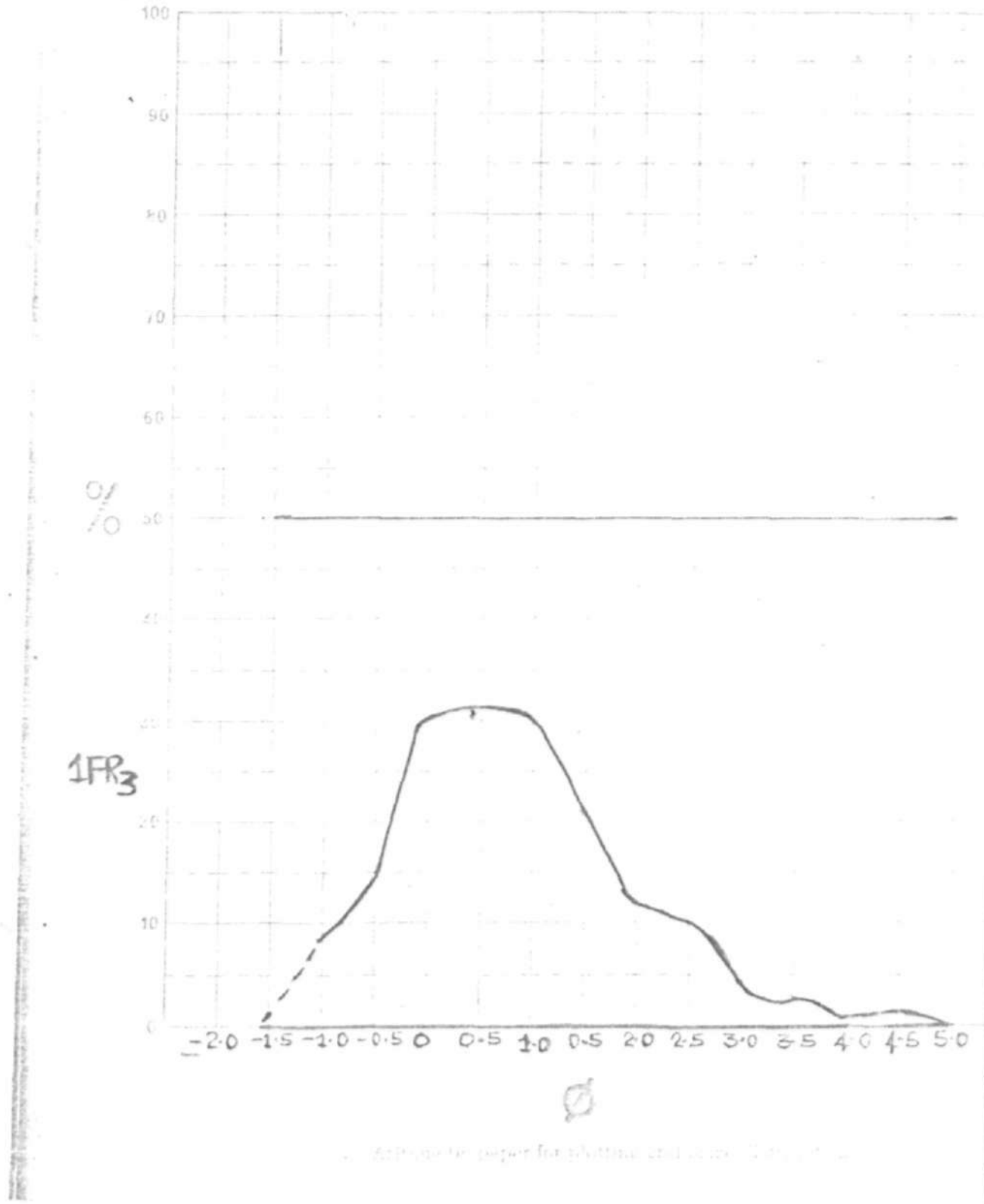
APPENDIX 3 :
SMOOTHED FREQUENCY CURVES ON AN ARITHMETIC GRAPH SCALE .

APPENDIX 3

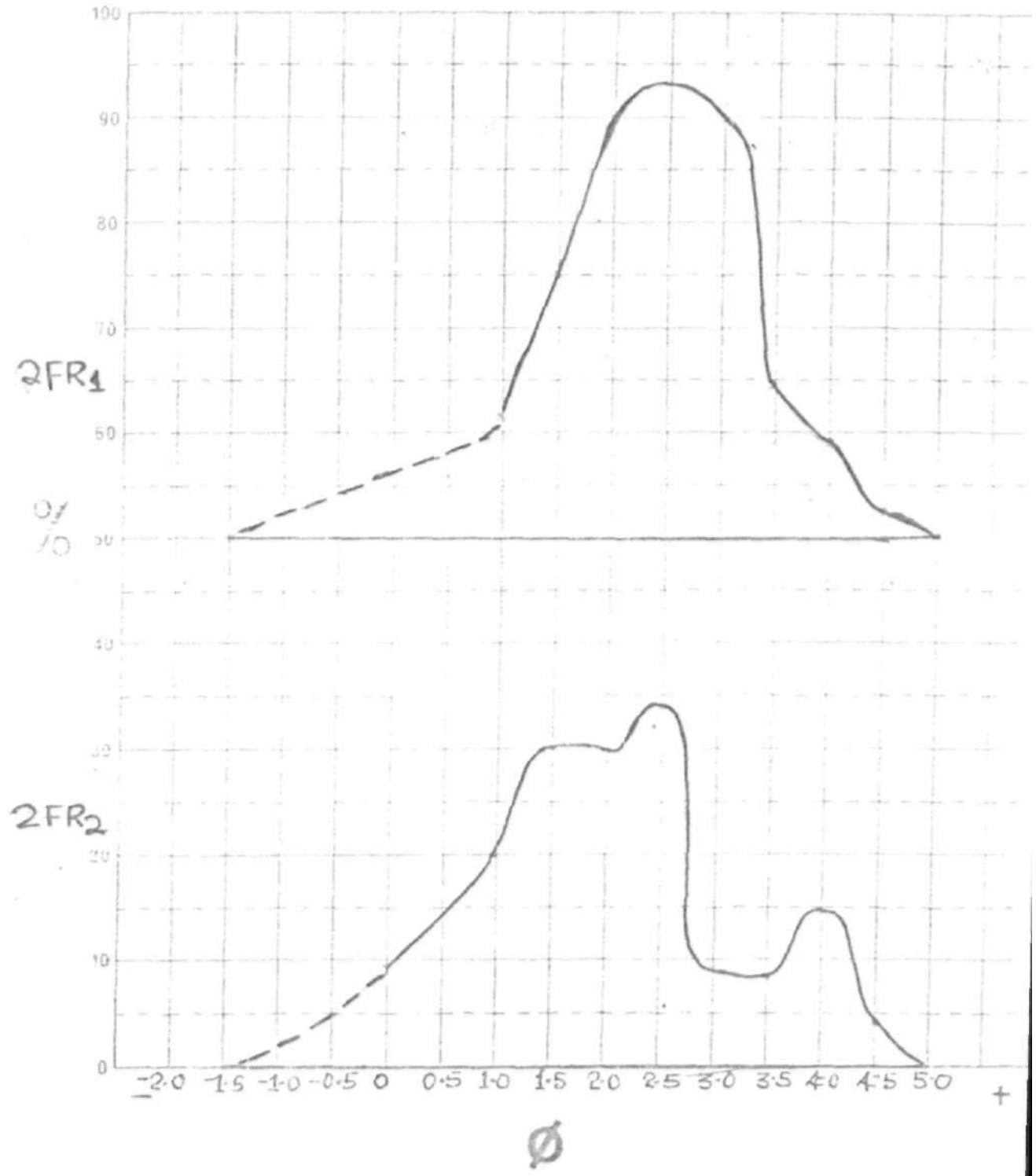


Arithmetic paper for plotting grain-size distributions.

APPENDIX 3

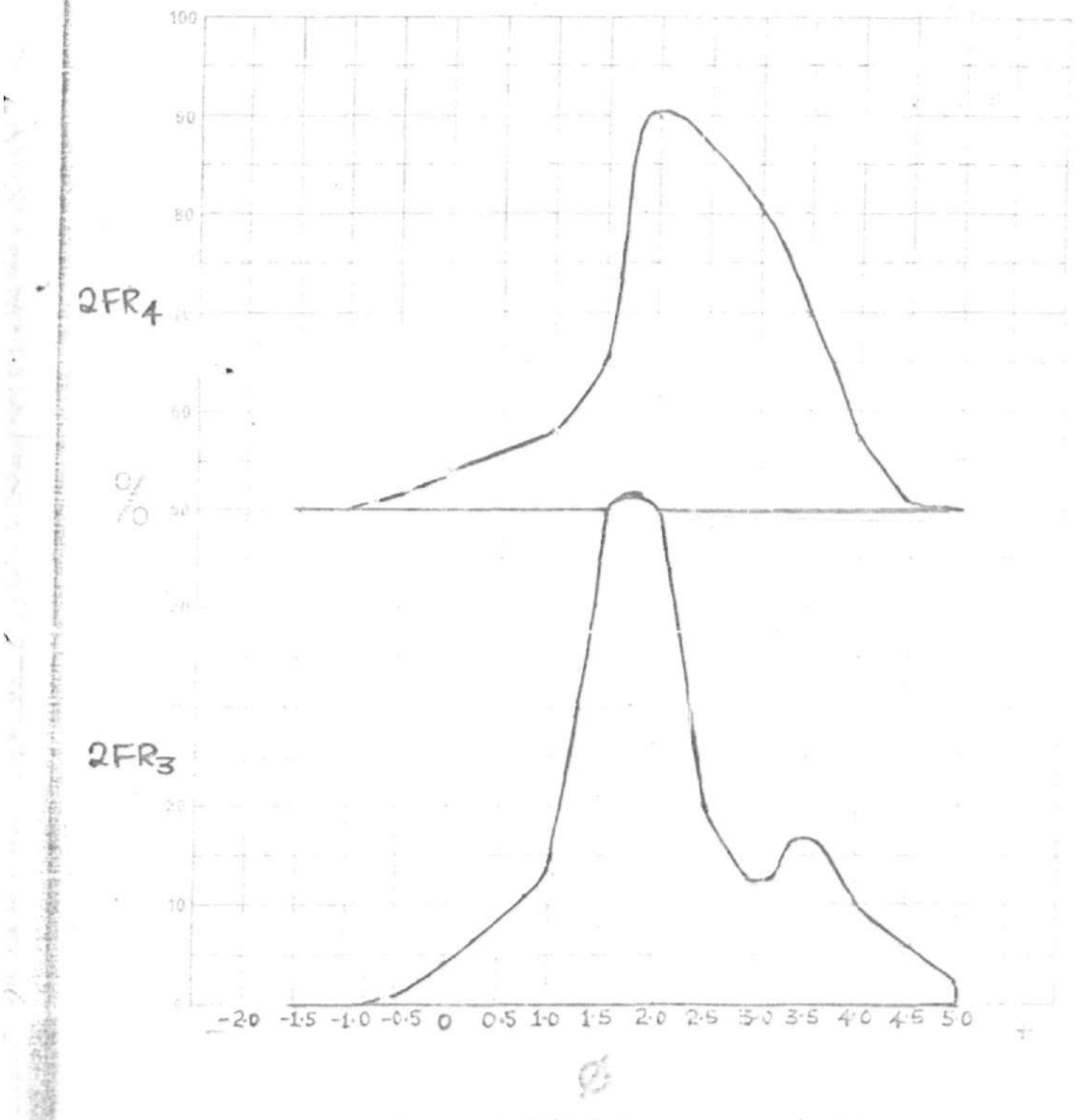

100
90
80
70
60
%
50
40
30
20
10
0
1FR3
-2·0 -1·5 -1·0 -0·5 0 0·5 1·0 0·5 2·0 2·5 3·0 3·5 4·0 4·5 5·0
Ø

APPENDIX 3

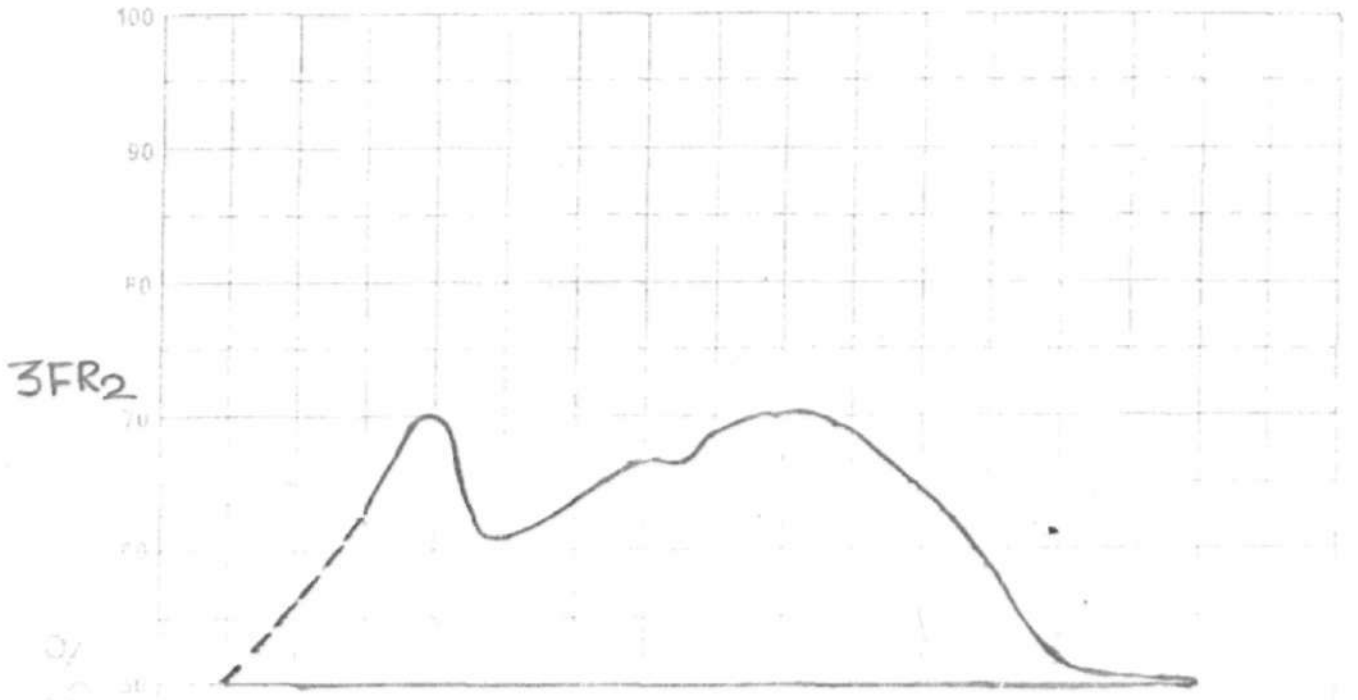


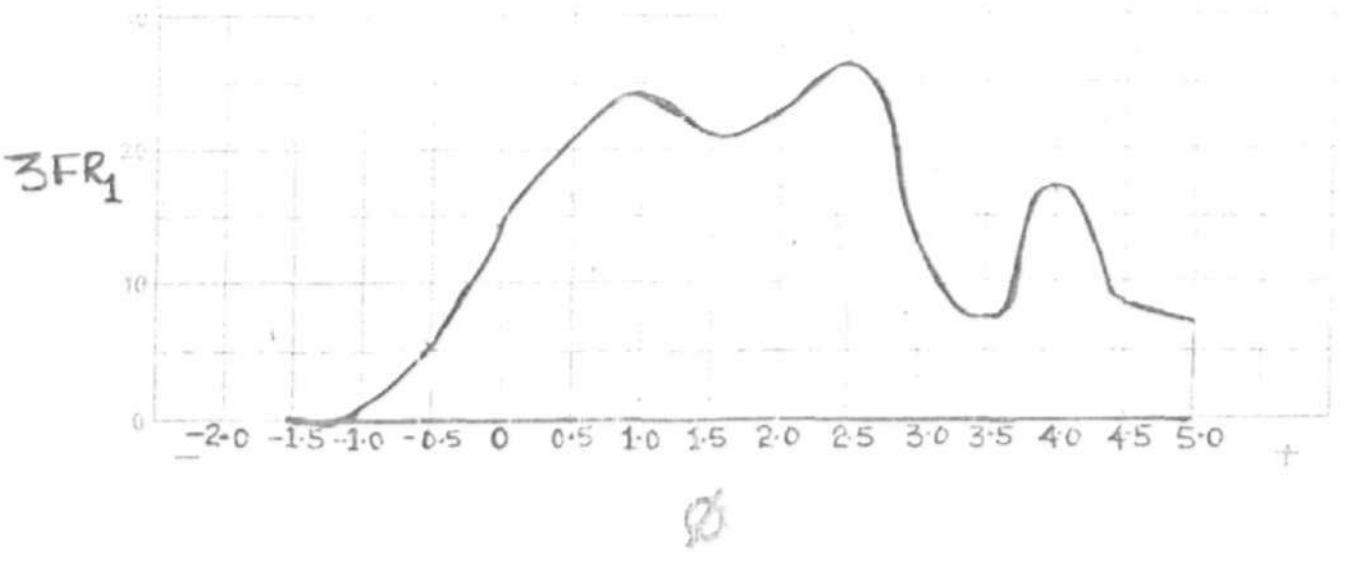
Arithmetic paper for plotting grain-size distributions.

APPENDIX 3

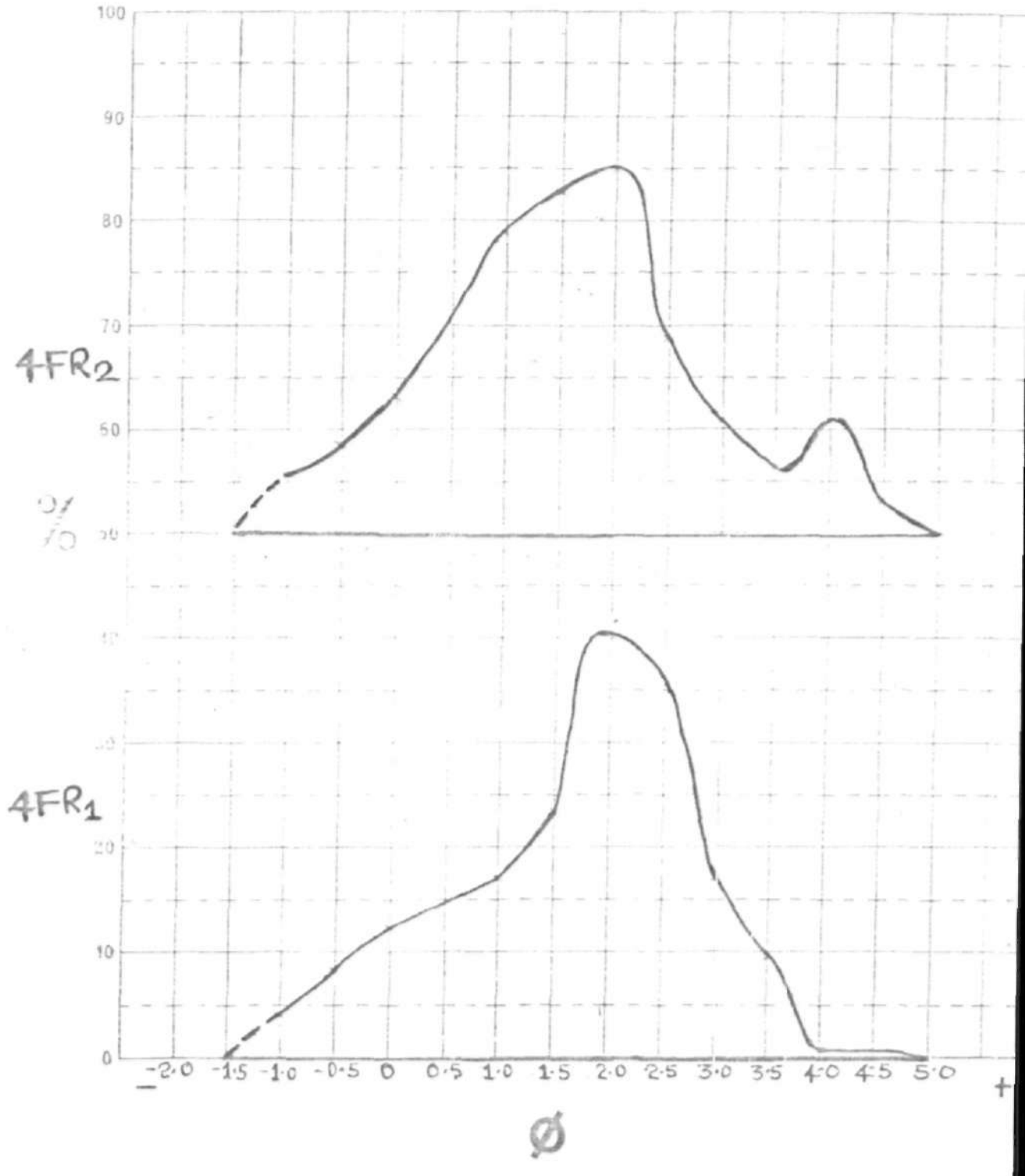


APPENDIX 3


100
90
80
70
3FR2

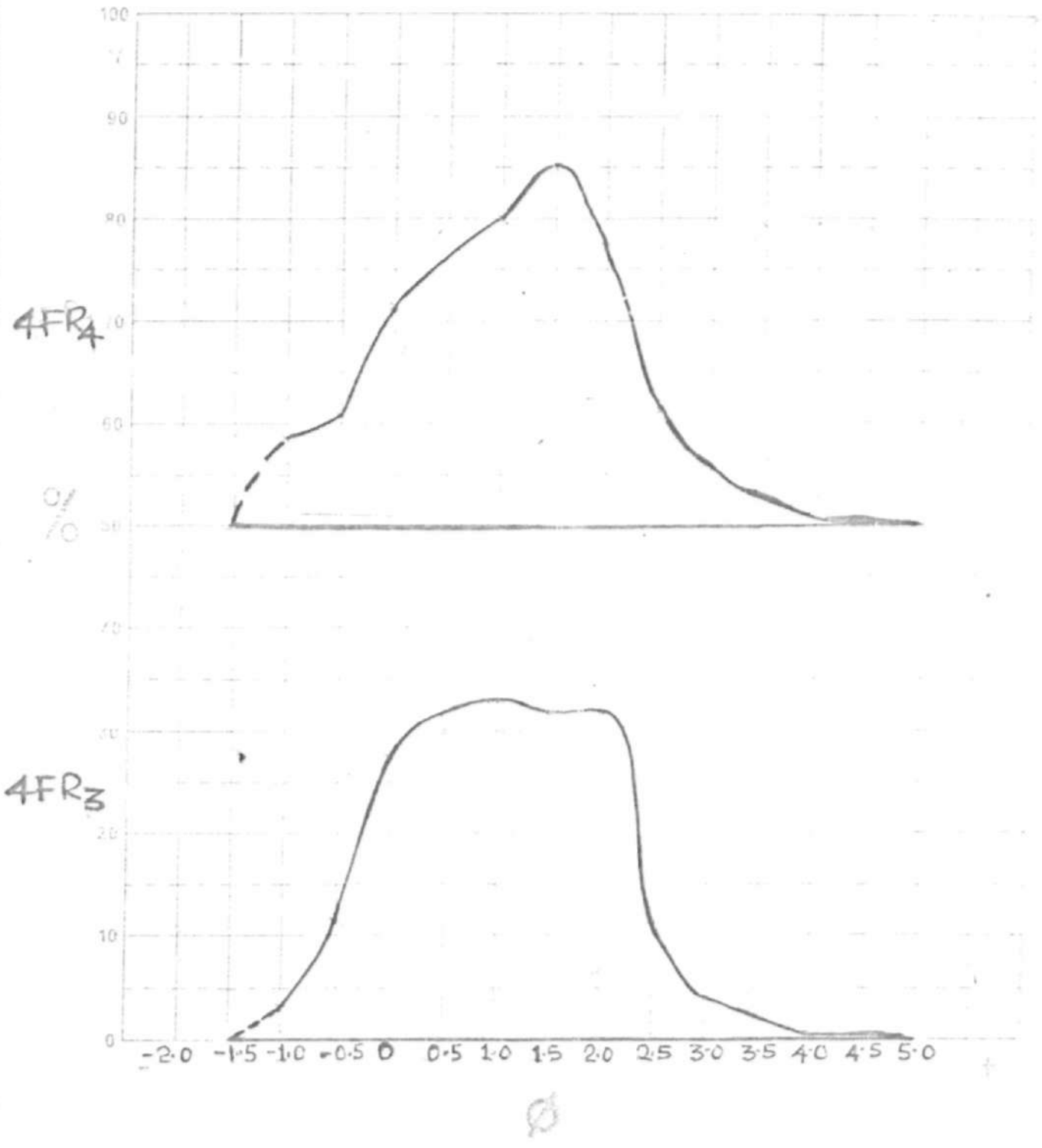

3FR1
20
10
0
-2·0 -1·5 -1·0 -0·5 0 0·5 1·0 1·5 2·0 2·5 3·0 3·5 4·0 4·5 5·0
Ø

APPENDIX 3

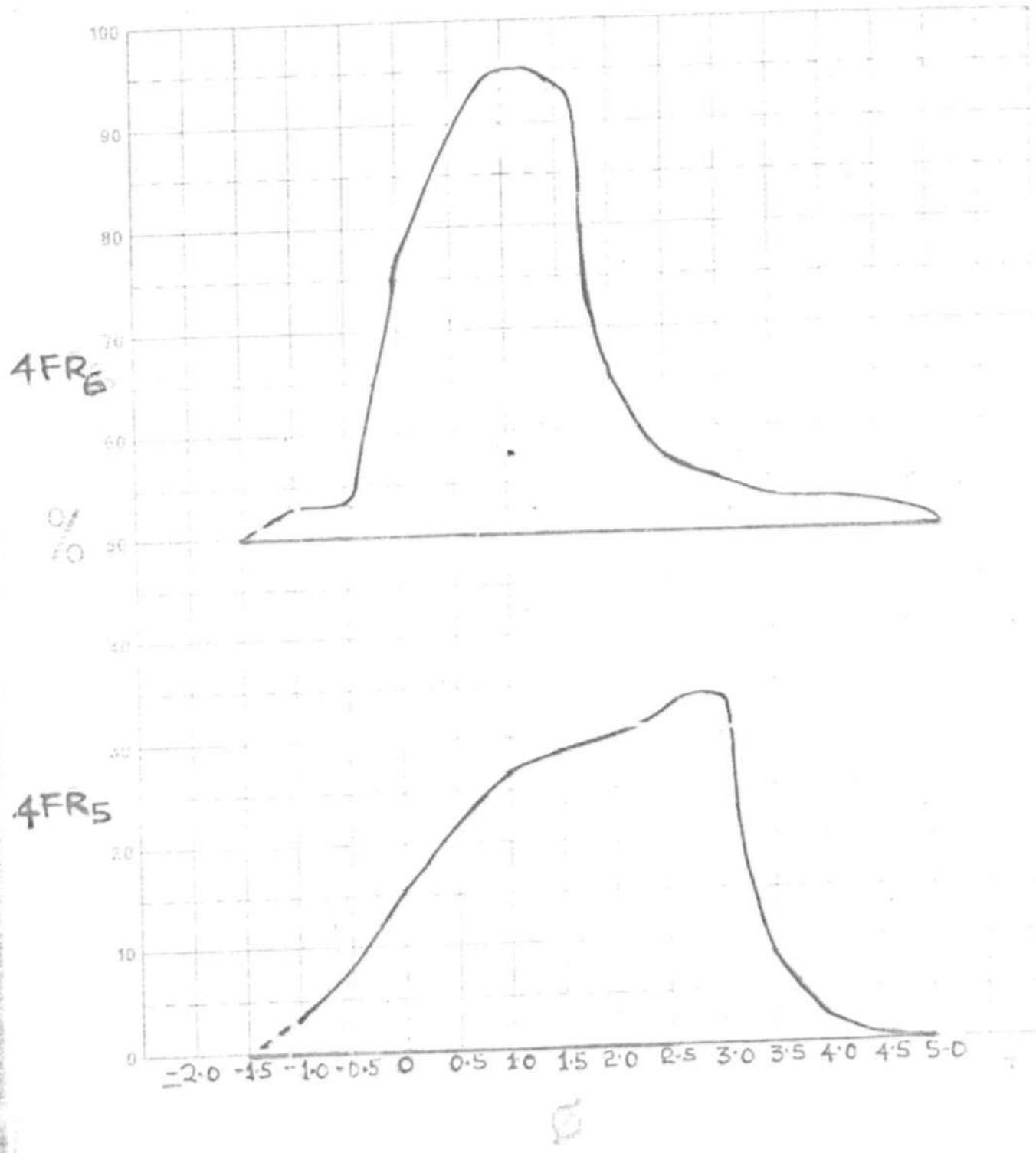


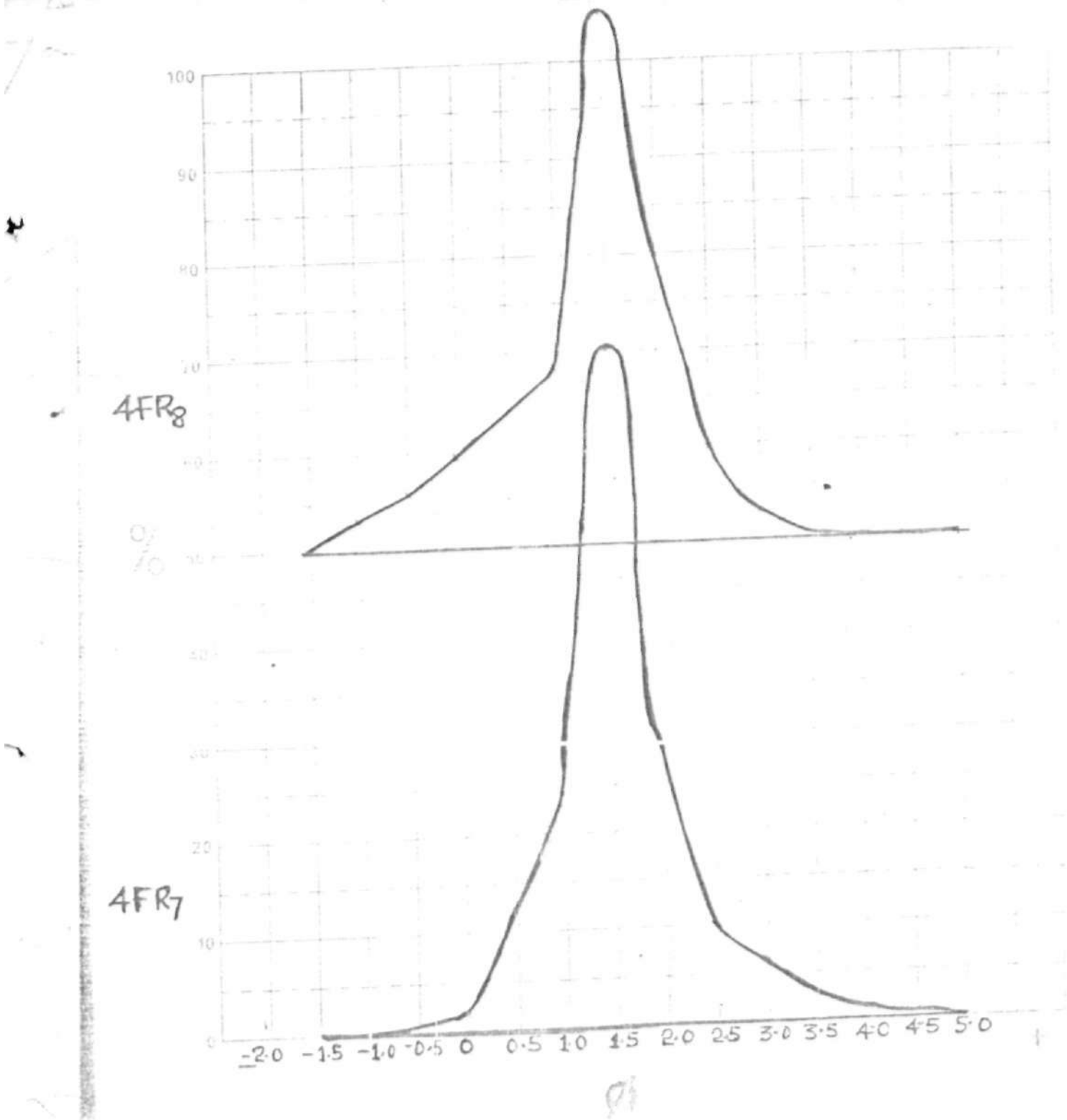
Arithmetic paper for plotting grain-size distributions.

APPENDIX 3

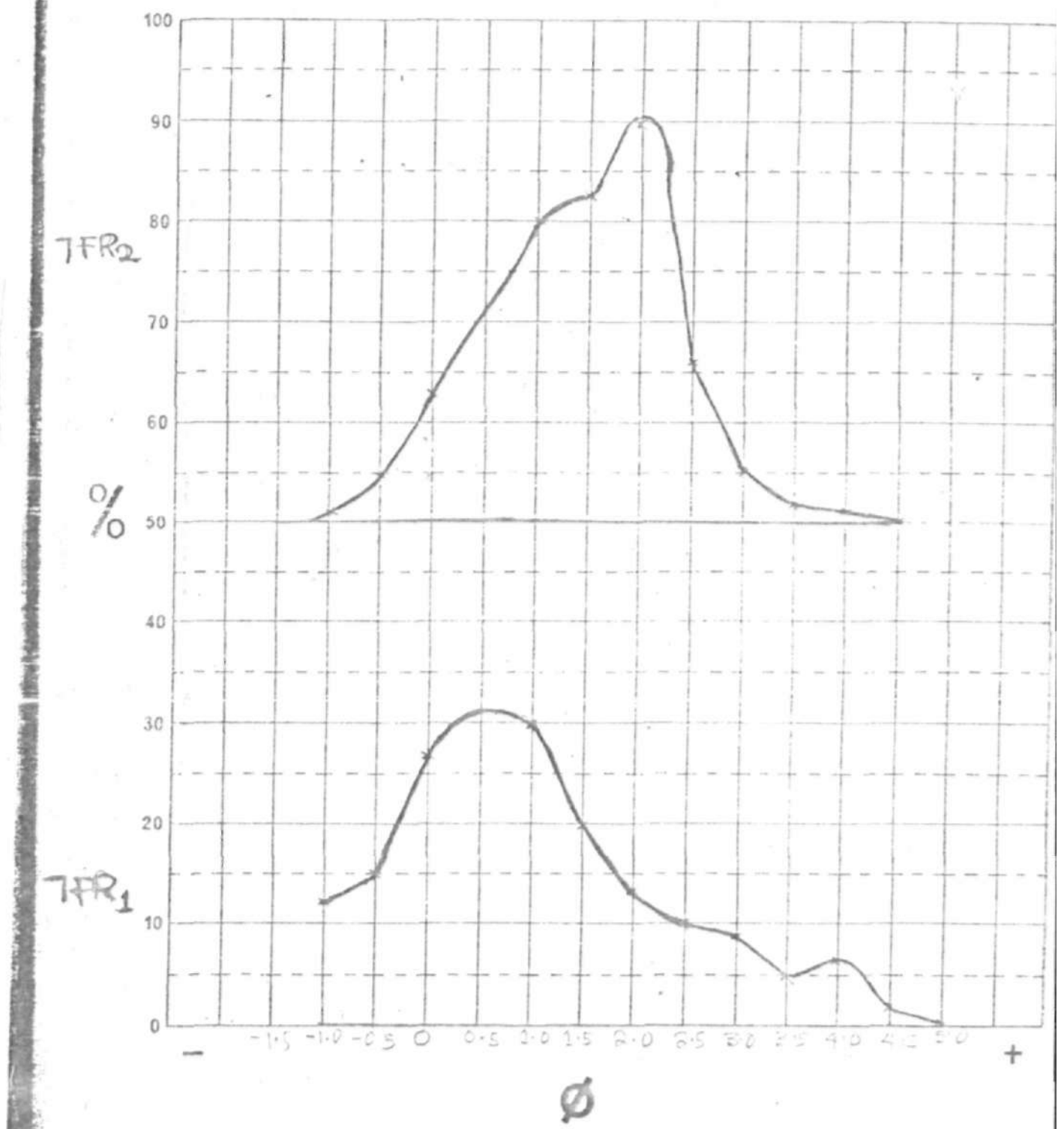

4FR4
%
100
90
80
70
60
50
4FR3
40
30
20
10
0
-2·0 -1·5 -1·0 -0·5 0 0·5 1·0 1·5 2·0 2·5 3·0 3·5 4·0 4·5 5·0
Ø

APPENDIX 3


100
90
80
70
60
50
40
30
20
10
0
% 4FR6
4FR5
-2·0 -1·5 -1·0 -0·5 0 0·5 1·0 1·5 2·0 2·5 3·0 3·5 4·0 4·5 5·0

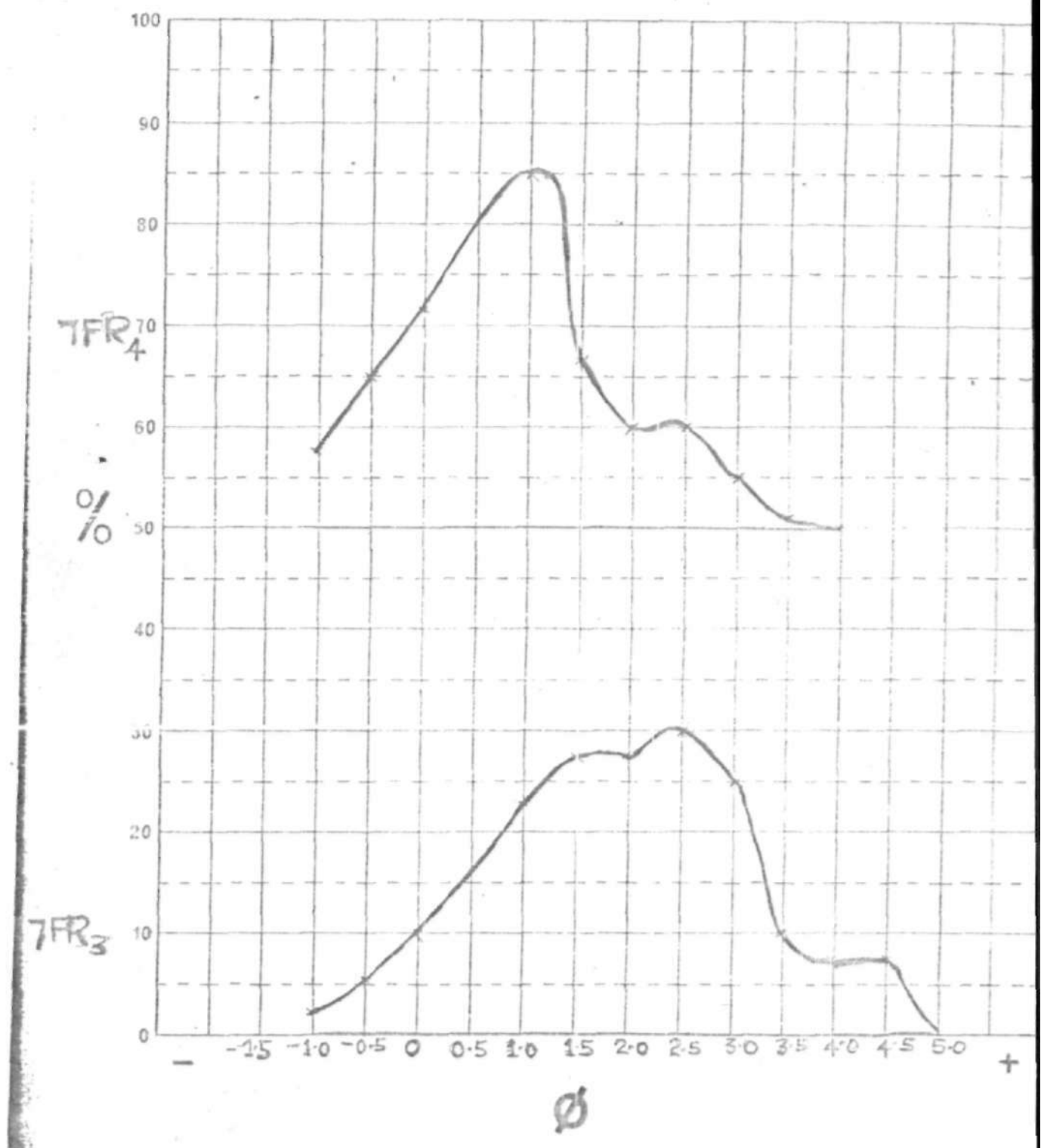

4FR8
4FR7
100
90
80
20
10
0
-2·0 -1·5 -1·0 -0·5 0 0·5 1·0 1·5 2·0 2·5 3·0 3·5 4·0 4·5 5·0

APPENDIX 3



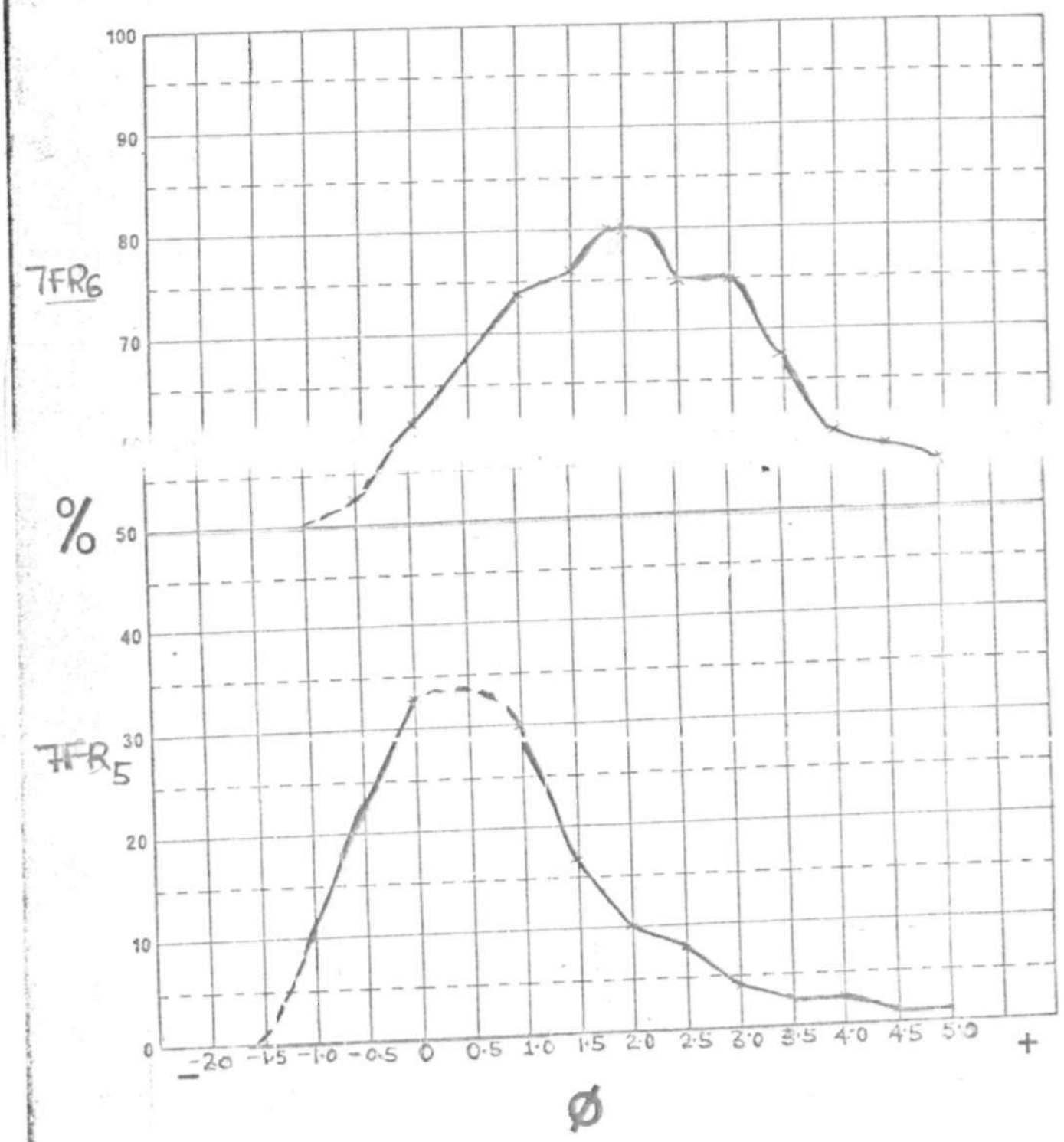
Arithmetic paper for plotting grain-size distributions.

APPENDIX 3



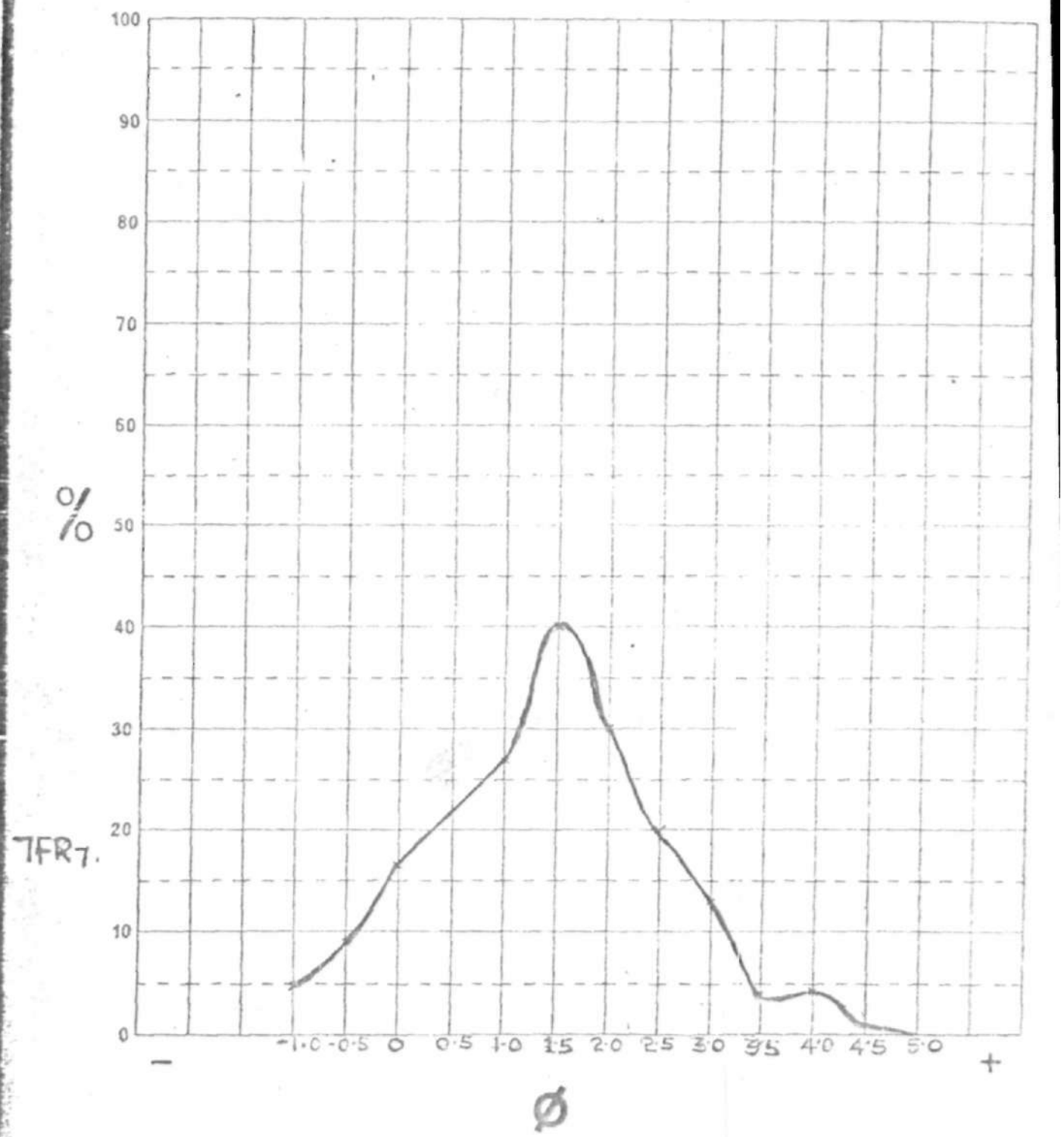
Arithmet c paper for plotting grain-size distributions.

APPENDIX 3



Arithmetic paper for plotting grain-size distributions.

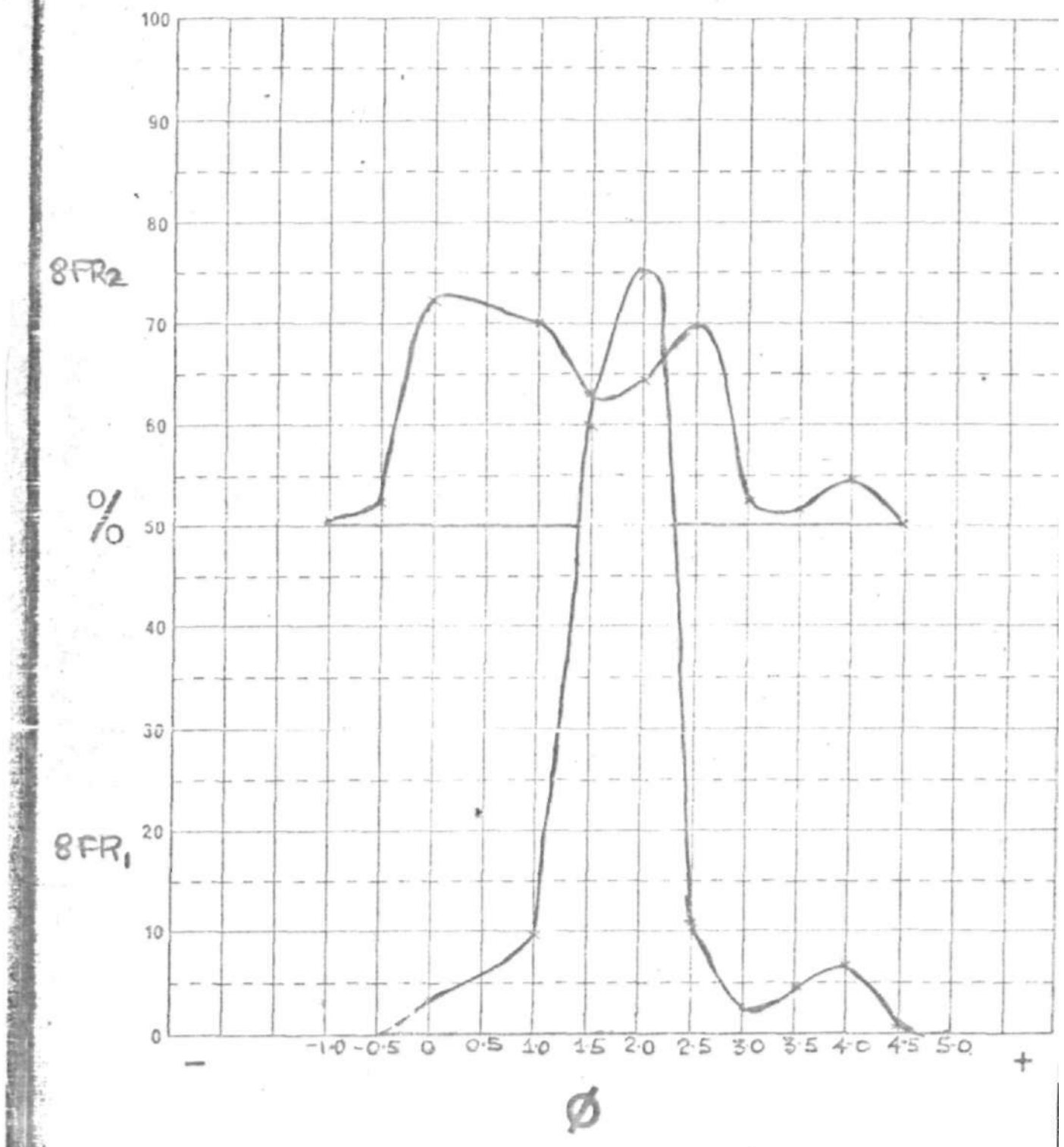
APPENDIX 3



TFR7.

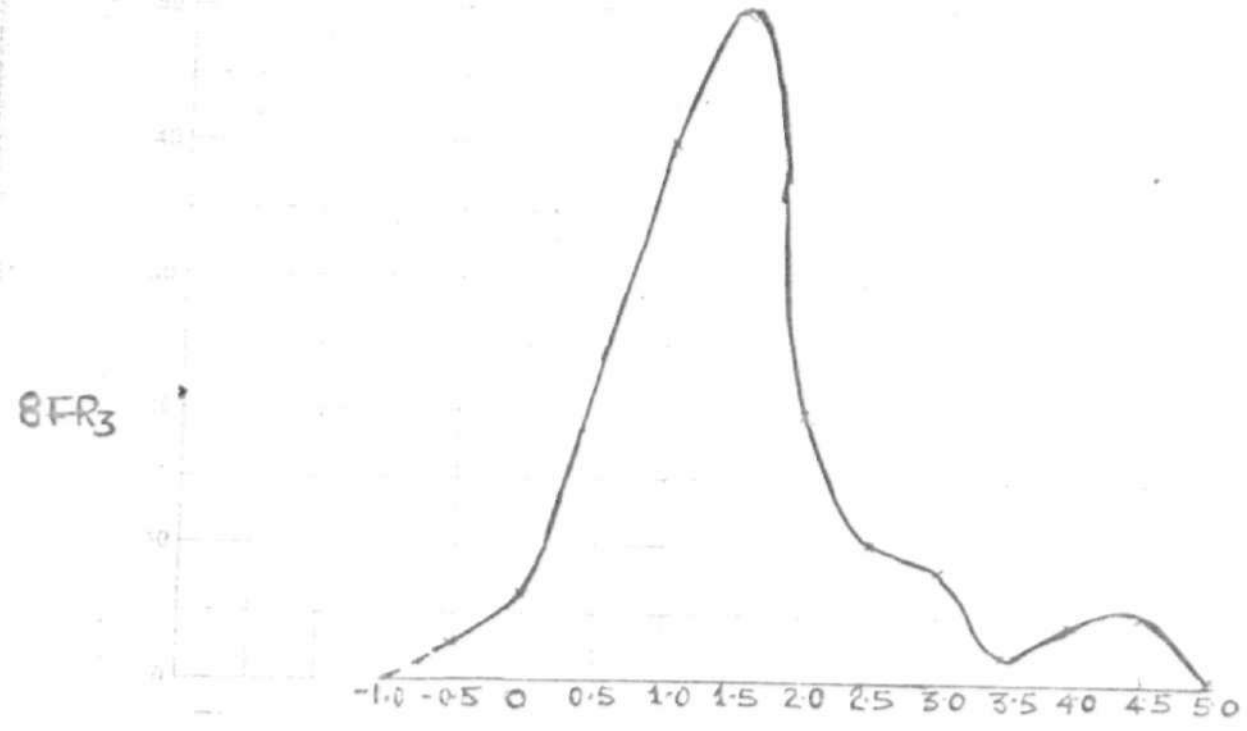
Arithmet c paper for plotting grain-size distributions.

APPENDIX 3

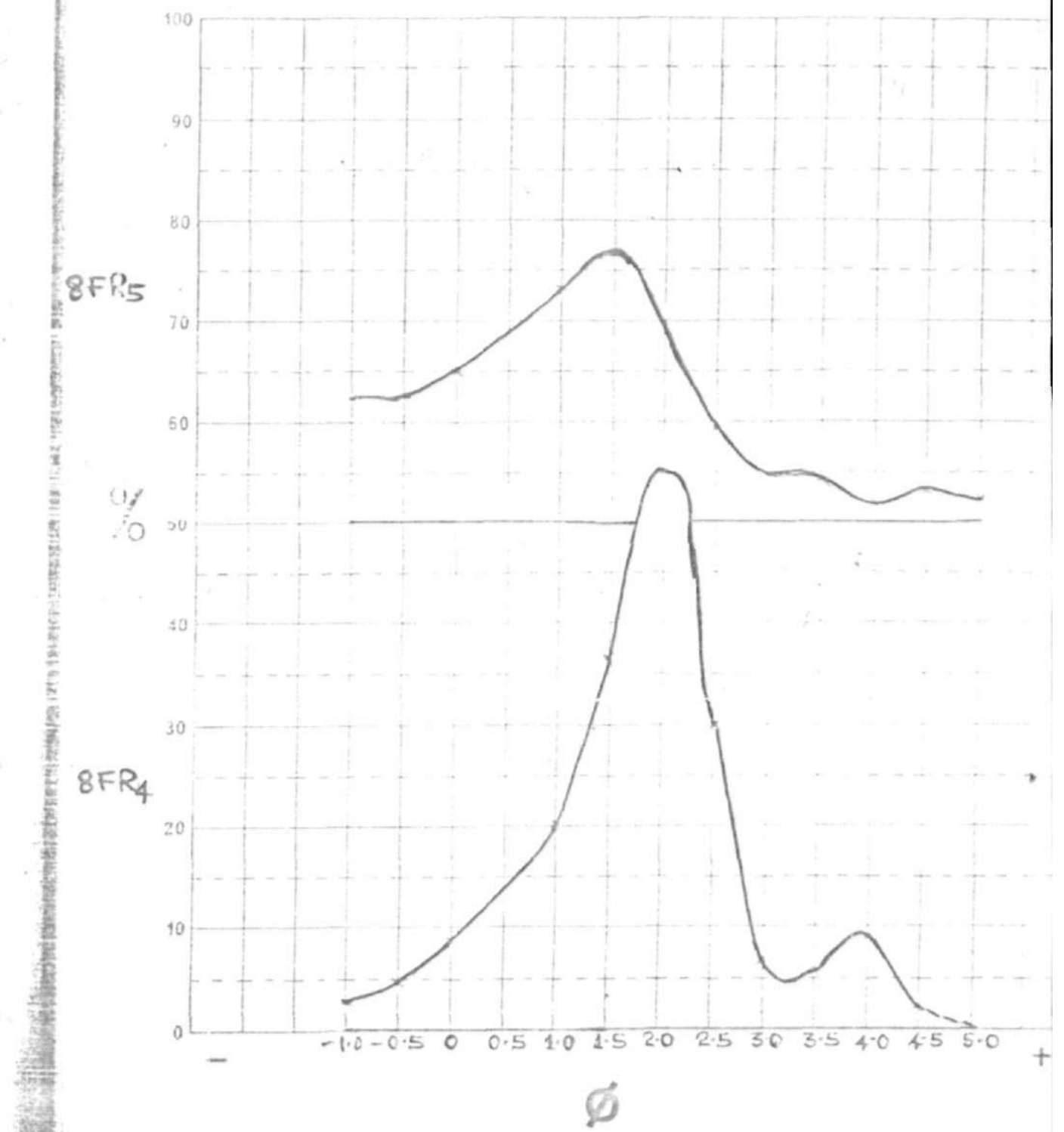


Arithmet c paper for plotting grain-size distributions.

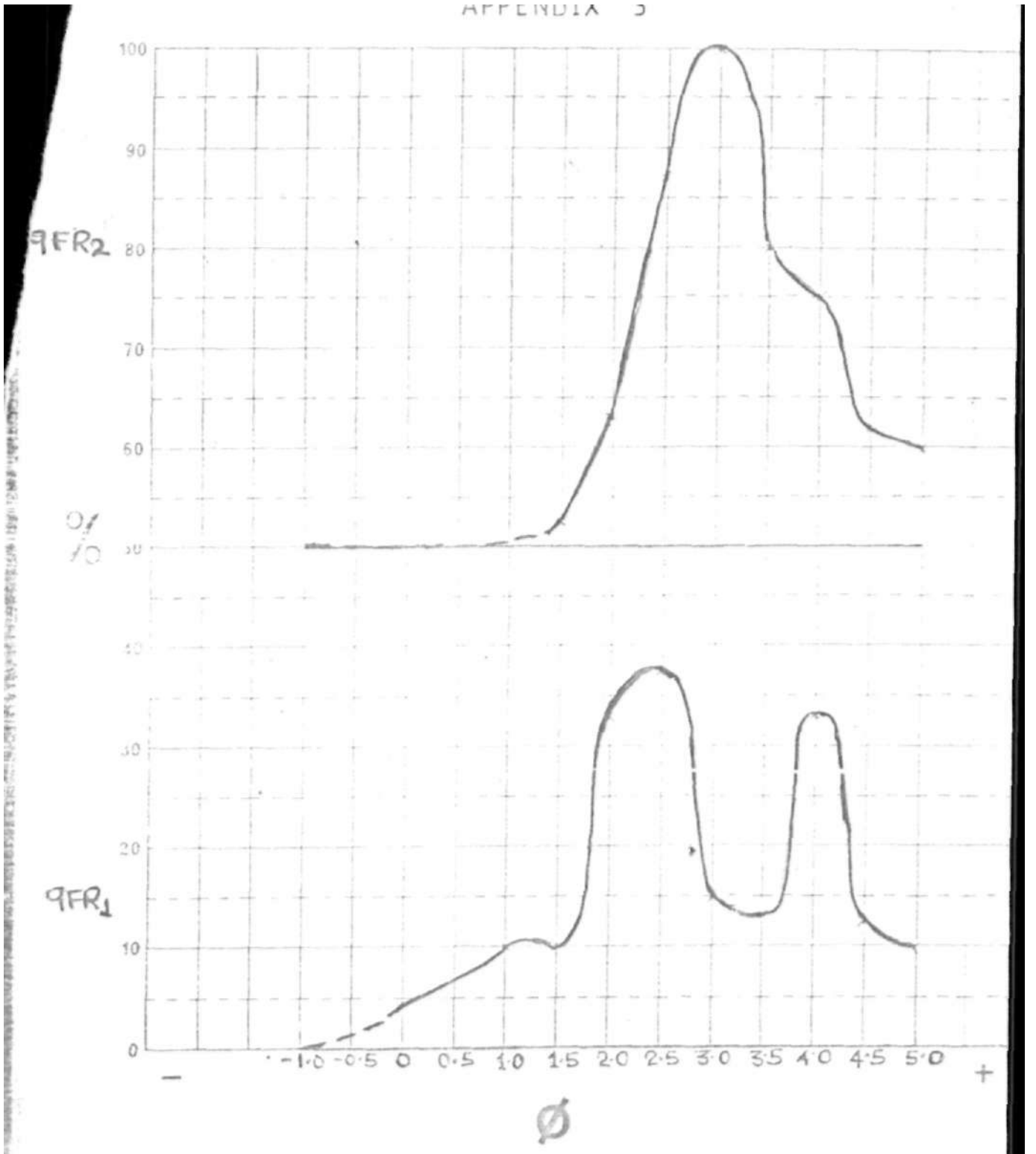
APPENDIX 3



APPENDIX 3

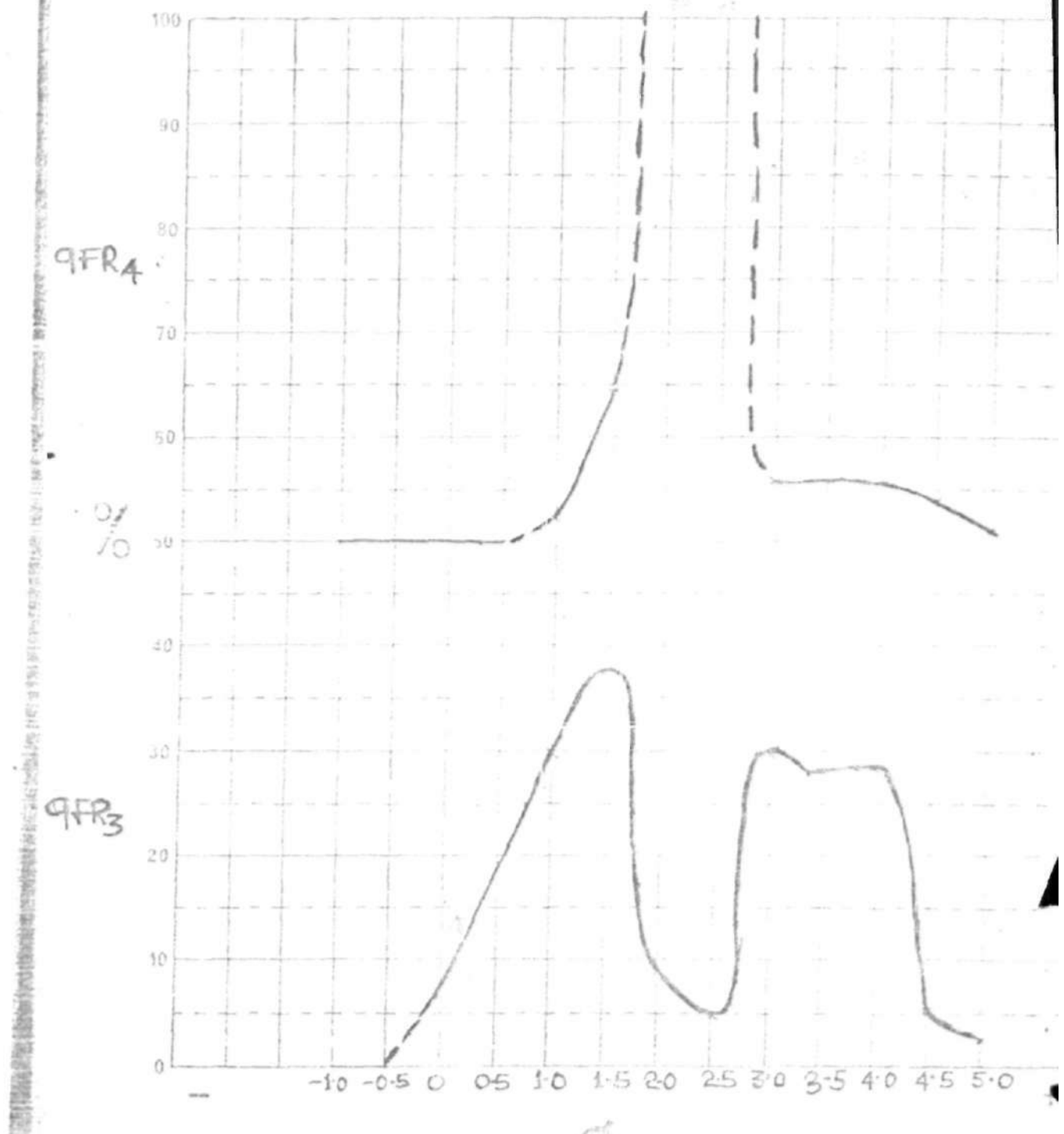


Arithmetic paper for plotting grain-size distributions.



Arithmetic paper for plotting grain size distributions.

APPENDIX 3



Arithmetic paper for plotting grain-size distributions.